Fall 2008

Ground motion sensitivity analyses for the greater St. Louis Metropolitan area

Ece Karadeniz

Department:

GROUND MOTION SENSITIVITY ANALYSES

FOR THE GREATER ST. LOUIS METROPOLITAN AREA

by

ECE KARADENIZ

A THESIS

Presented to the Faculty of the Graduate School of the

MISSOURI UNIVERSITY OF SCIENCE AND TECHNONOGY

In Partial Fulfillment of the Requirements for the Degree

MASTER OF SCIENCE IN GEOLOGICAL SCIENCE AND ENGINEERING

2008

Approved by

J. David Rogers, Advisor
Jeffrey D. Cawlfield
Yu-Ning Ge

This masters is dedicated to the people

Who lost their lives in

1992 Erzincan, 1995 Dinar, 1998 Adana-Ceyhan and 1999 Kocaeli-Duzce

Earthquakes that occurred in Turkey

ABSTRACT

Local site effects can play an important role in modifying the intensity of ground shaking and earthquake damage. The process of rock motion propagating through the soil column can be approximated using one-dimensional site response analyses. To evaluate the likely site response several input parameters are required. These include: thickness of the unconsolidated soil cap, shear wave velocity, unit density, dynamic soil properties, and acceleration time histories. Considerable uncertainty often exists in regards to these input parameters. In this study, the program Shake2000 was employed for site response analyses and sensitivity analyses were performed to determine how the uncertainties in soil cap thickness, shear wave velocity, and input ground motion affect predicted site response. These evaluations were made for PGA, 0.2 sec, and 1 sec period for spectral accelerations and amplifications.

The test results indicated considerable differences in spectral accelerations and amplifications due to the uncertainties of soil cap thickness, input ground motion, and shear wave velocity. When all three input parameters were compared, the most important parameter affecting spectral accelerations and amplifications appear to be the character of the input rock motion. The shear wave velocity and the thickness of the soil cap appear to be secondary and equally important parameters. When ground motion periods (PGA, 0.2 sec and 1 sec) are compared; the highest spectral accelerations were predicted at 0.2 sec period, which appears to be more sensitive to the various uncertainties. The peak spectral accelerations and site amplifications appear to be triggered by resonance of the soil cap. The peak periods increase with increasing thickness of the soil cap and decrease with increasing shear wave velocity.

ACKNOWLEDGMENTS

I would like to express my gratitude to my advisor; Dr. J. David Rogers for his encouragement, guidance, and financial support during the course of this study and reviewing this thesis patiently and carefully. I would also like to recognize my committee members and express my special thanks to Dr. Jeffrey D. Cawlfield and Dr. Yu-Ning Ge for serving on my committee and their guidance.

I sincerely would like to appreciate Dr. Deniz Karadeniz and Dr. Chris Cramer for their valuable recommendations and offering assistance throughout this thesis. I also owe a debt of thanks to the U.S. Geological Survey and the National Earthquake Hazard Reduction Program, for their financial support. I would also like to express my gratitude to my former professors and advisors who inspired me with their professional academic life style; Dr. Faruk Calapkulu, Dr. Talip Gungor, Dr. Erhan Akay, and Dr. Burhan Erdogan.

Special thanks go to my mother and uncle for their love, and motivation during my study and giving me the strength to accomplish my goals. And last, but most importantly, I would like to recognize my dearest life companion, Deniz, who lightened my life with his endless love and encouraged me to sustain when the path was craggy.

TABLE OF CONTENTS

LIST OF ILLUSTRATIONS

LIST OF TABLES

1. INTRODUCTION

1.1. PROBLEM STATEMENT

Damaging earthquakes have damaged and/or destroyed civilized infrastructure since the beginning of recorded history. It wasn't long before the contrasting impacts of earthquakes emanating from different areas came to the attention of those who survived these natural calamities. During the 1906 San Francisco and 1922 Tokyo earthquakes the controlling impact of site geology was recognized and described by those individuals who studied the events.

By the late 1920s American engineers began realizing the principal factors affecting structural response of buildings (Dewell, 1929a and 1929b; Freeman, 1930). Around this same time Huber (1930) penned the first article that described the impacts of directionality on observed damage, contrasting the impacts of the 1868 Hayward and 1906 San Francisco quakes on buildings in San Francisco. The 1933 Long Beach earthquake was the first to provide strong motion records, which provided valuable insights on spectral accelerations and amplification (Heck and Neumann, 1933). Strong motion records from the 1940 El Centro earthquake provided some early clues about the potentially deleterious impacts of long period motions on taller structures at considerable distance from the causative shaking. The influence of local geology on shaking intensity came to international prominence following the 1985 Michoacan earthquake, which devasted portions of Mexico City, located some 300 km from the epicenter (Romo and Seed, 1986). In 1969 Idriss and Seed published the first article that provided a methodology for deconvolution of seismic energy through surficial materials. This led to the development of the computer program SHAKE, which allowed simple one-dimensional analysis of shear wave energy through the softer sediments underlying most building sites.

SHAKE and its successor programs allow estimations of ground surface motions, provided that reliable geologic and geophysical data are incorporated into the model and appropriate input ground motions were fed into the program. The accuracy of the one-dimensional predictions depends on a number of variables, including:

a) Insufficient geologic data, with a random distribution of borehole data points. Many

times these data are simply lacking and the "data gaps" between adjacent borings or outcrops are estimated using statistical methods, such as kriging, and these estimates are provided with a standard error,

b) Physical properties within a designated stratigraphic unit are often variable, and

c) Educational and experimental differences often exist between subsurface investigations by different individuals, companies, agencies, etc.

Uncertainties in measuring and interpreting the variables described above are unavoidable. In order to understand the importance of these interpretations and the impact of each parameter on site response, sensitivity analysis can be undertaken.

The St. Louis metropolitan area is about 200 km to 340 km north of the New Madrid Seismic Zone. The area is underlain by a veneer of unconsolidated sediments, up to 55 m deep. There is a 25 to 40% probability of a Magnitude 6.0 or larger earthquake (M 6.0 to 6.8) emanating from the New Madrid Seismic Zone in the next 50 years (USGS). Numerous "data gaps" exist in the existing geodatabase for the Granite City Quadrangle, adjacent to downtown St. Louis, MO (Figure 1.1). As the distance between adjacent boreholes piercing the Paleozoic-age bedrock rocks increases, there exists greater uncertainties in stratigraphy and the predicted depth-to-bedrock beneath the existing ground surface. In a recent study seismic statistical analyses were undertaken which considered a number of variables, including geotechnical data (shear wave velocity, density) and geological data (respective thickness of mapped stratigraphic units). The uncertainties in predicted ground shaking intensity for the St Louis metropolitan area were estimated by Karadeniz (2007) using probabilistic Monte Carlo approach. The aim of this study is to estimate these uncertainties' effects on response spectra by applying conventional sensitivity analyses.

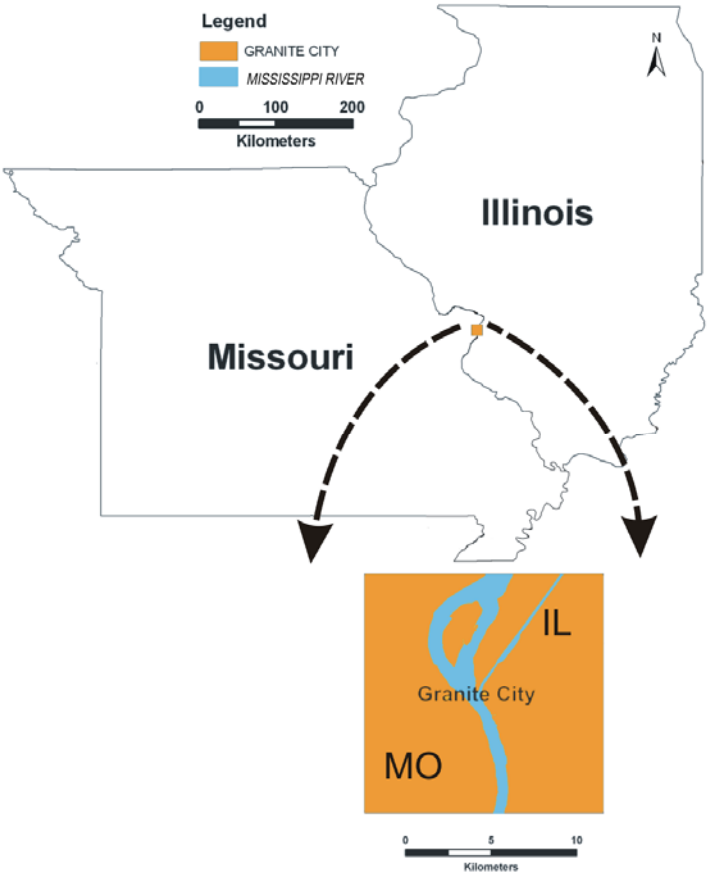

Figure 1.1. The location of Granite City Quadrangle.

1.2. RESEARCH OBJECTIVES

The following objectives were addressed as part of this study:

i. Perform site screening analyses for the three major input variables: 1) shear wave velocity; 2) depth-to-bedrock (thickness of the 'soil cap'); and, 3) rock acceleration (acceleration time history).

ii. Generate peak ground acceleration (PGA), 0.2 second, 1 second response spectrum, and maximum spectral acceleration, with their corresponding periods and define the differences between each.

iii. Identify the influence of uncertainties in the various input parameters (e.g. shear wave velocity, soil thickness and time history) on site response and highlight which factors appear to exert the most influence on site response,

even those situations utilizing seemingly small changes in the input values.

iv. Categorize the most important parameters affecting seismic site response in the St. Louis Metro area. This should help future researchers providing the information of which parameters are most useful to ascertain more reliable estimation of site response and which would not significantly alter the site response predictions. Thus, unnecessary expenditures of effort would be avoided.

v. Compare the results generated by deterministic approaches with those generated using probabilistic methods.

1.3. RESEARCH METHODOLOGY

To visualize the impacts of stated uncertainties, one typically inputs pessimistic, expected, and optimistic values for each of the uncertain variables, holding the other variable constant. Different scenarios are thereby created and a series of response analyses are performed. Sensitivity analyses were performed and the changes in response spectra due to different earthquake scenarios thereby examined. Figure 1.1 explains the course of study.

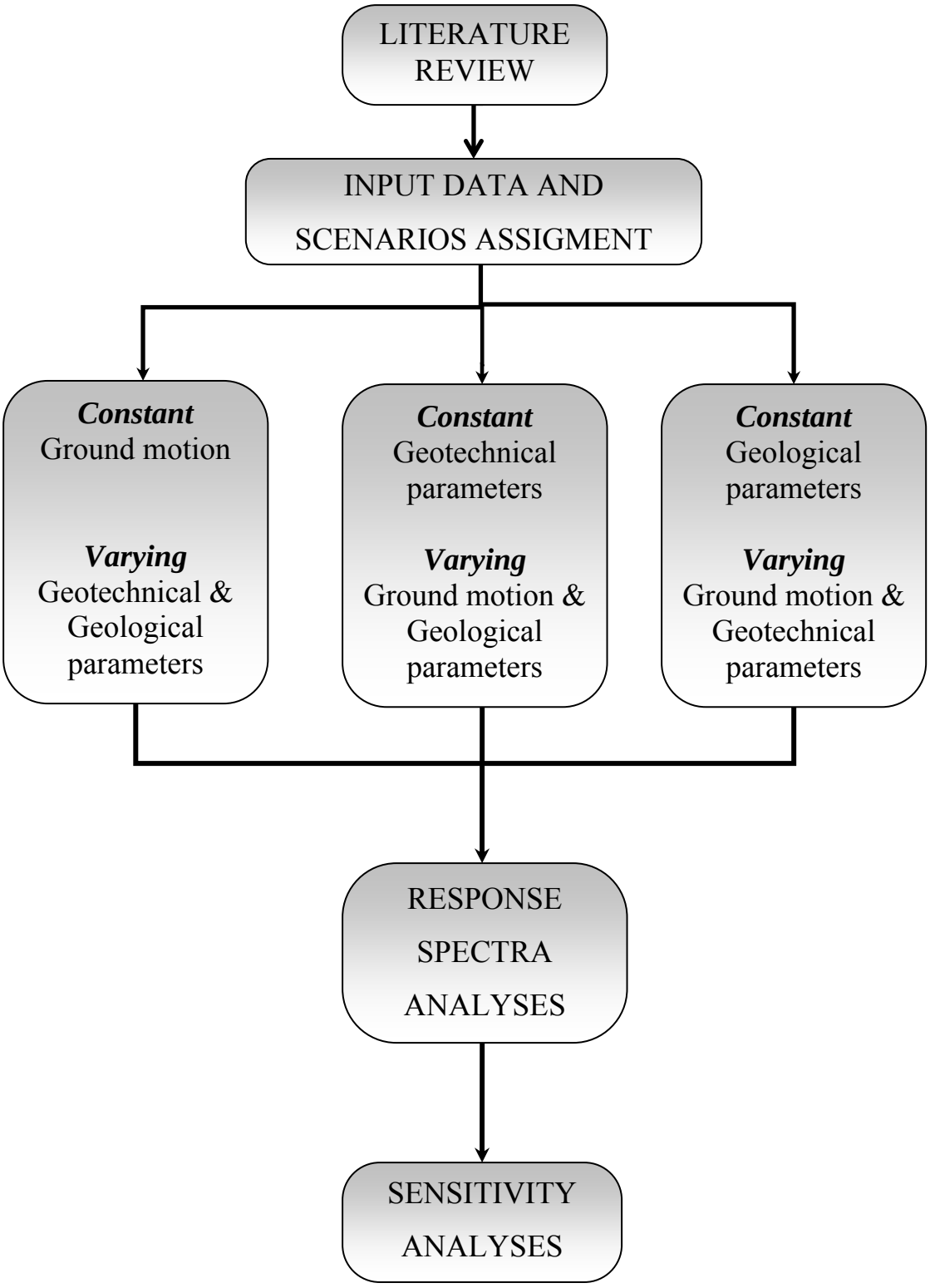

Figure 1.2. Flow chart illustrating the essential elements of this study

2. LITERATURE REVIEW

2.1. LOCAL SITE EFFECTS

Earthquake ground motions are influenced by three basic mechanisms: earthquake source, travel path, and site effects. Rupture type, magnitude of earthquake, and its location form the source effects. Propagation of stress waves from crustal rock through the overlying unconsolidated 'soil cap' is commonly described as 'path effects' and 'site effects,' defined by the type of soil, its thickness, and shear wave velocity (Seed and Idriss, 1982; Kramer, 1996). The local soil conditions are one of the most important factors affecting the 'free field motions' felt at any given site, at the earth's surface (Seed and Idriss, 1982). The controlling role of soil conditions on structural behavior during earthquakes has been demonstrated repeatedly, through evaluation of strong motion records recorded in such events as the 1957 Lake Merced, 1963 Nagoya, 1967 Caracas, 1985 Mexico City, 1989 Loma Prieta, and 1999 Kocaeli, Turkey (Seed and Idriss, 1969, 1982; Kramer 1996). Data collected from these earthquakes suggested that damage levels could be correlated with the thickness and consistency of unconsolidated soils underlying adjacent portions of major metropolitan cities, other factors being more-or-less equal. A brief review of these particular earthquakes follows.

2.1.1. San Francisco Earthquake. On 22 March 1957, a magnitude 5.3 earthquake injured about 40 people and caused property damage estimated at $1 million. The quake was centered on the San Andreas Fault at Lake Merced, just south of San Francisco. The intensity of shaking varied considerably, ranging from no observable damage to localized pockets of liquefaction (rare for such a small magnitude quake). Figure 2.1 presents three strong motion records from the San Francisco financial district, located close to one another (similar epicentral distance). These recordings were made on rock, ~80 m of unconsolidated soils, and ~100 m of unconsolidated soil, shown in Figure 2.1. Considerable differences in peak ground accelerations were recorded because of these contrasting site conditions, essentially controlled by the depth of the 'soil cap' (Seed and Idriss, 1969).

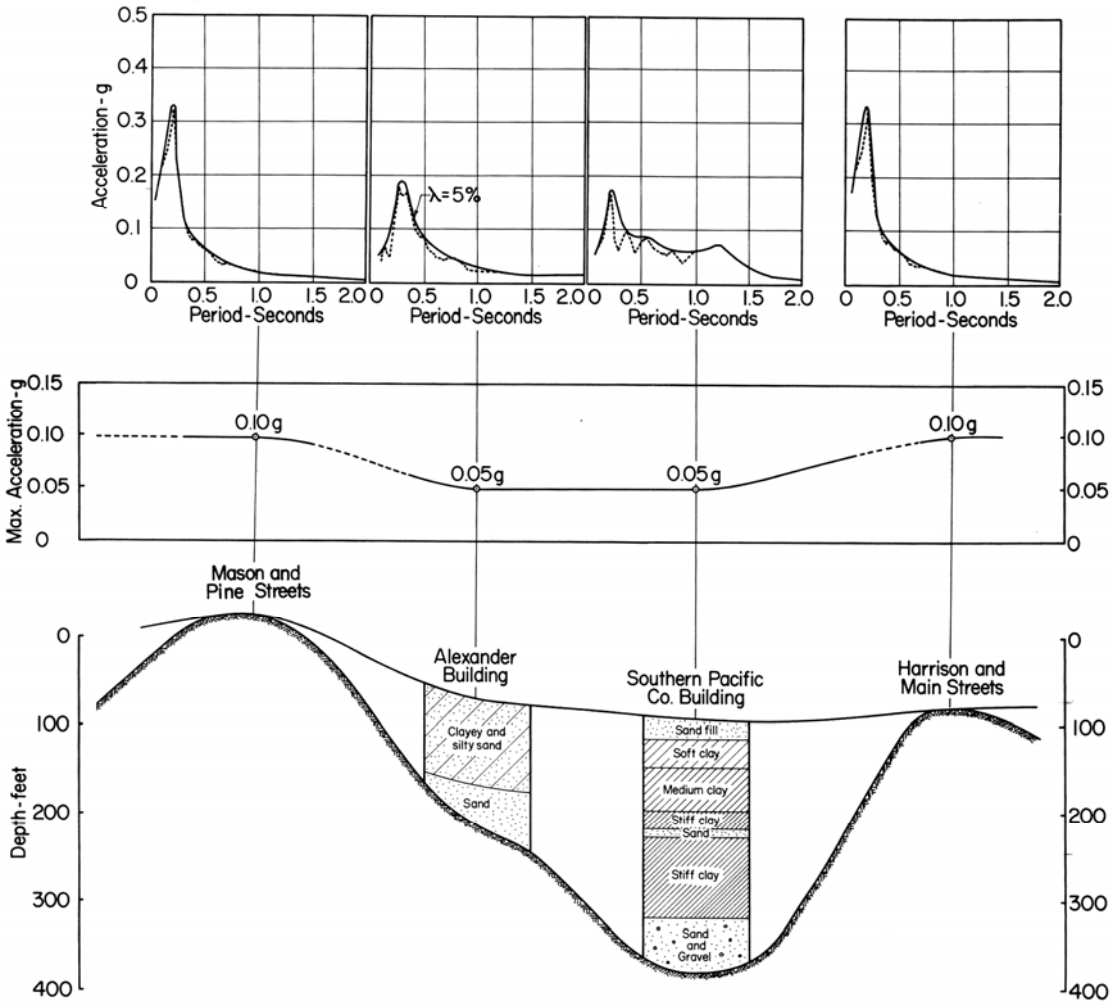

Figure 2.1. Comparison of three response spectra recorded at adjacent sites in downtown during the 1957 Lake Merced earthquake (adapted from Seed and Idriss, 1969)

The spectral accelerations recorded on the rocky ridgeline were high at low periods and lower at high periods. The soft cap of dominantly Holocene age (<11 ka) clayey and sandy soils exerted marked influence on site response, which was much lower at low periods and higher at longer periods. On the other hand, for stiffer soils (e.g. Colma formation, about 90 ka age), the observed spectral accelerations were found to be higher at low periods and low at longer periods (Kramer and Arduino, 2008).

2.1.2. Caracas Earthquake. The Magnitude 6.4 Caracas earthquake on July 29, 1967 was centered near the coast of Venezuela. It's epicenter was located about 35 miles north of Caracas. Four 10 to 12 story apartments collapsed and many structures suffered structural damage. 240 residents were killed and $100 million property damage was attributed to the quake, and 80,000 people were left homeless. Observers found that buildings of similar structural frames and heights behaved differently, depending ion the depth of unconsolidated soils upon which they were founded. Some of the data supporting these observations are reproduced herein as Figure 2.2, taken from Seed and Idriss (1982). These data suggest that damage intensity was most severe for three to five story structures founded on 30 to 50 m of soil, five to nine story high structures founded on 50 to 70 m of soil, and 10-plus story high structures founded on more than 100 m of soil.

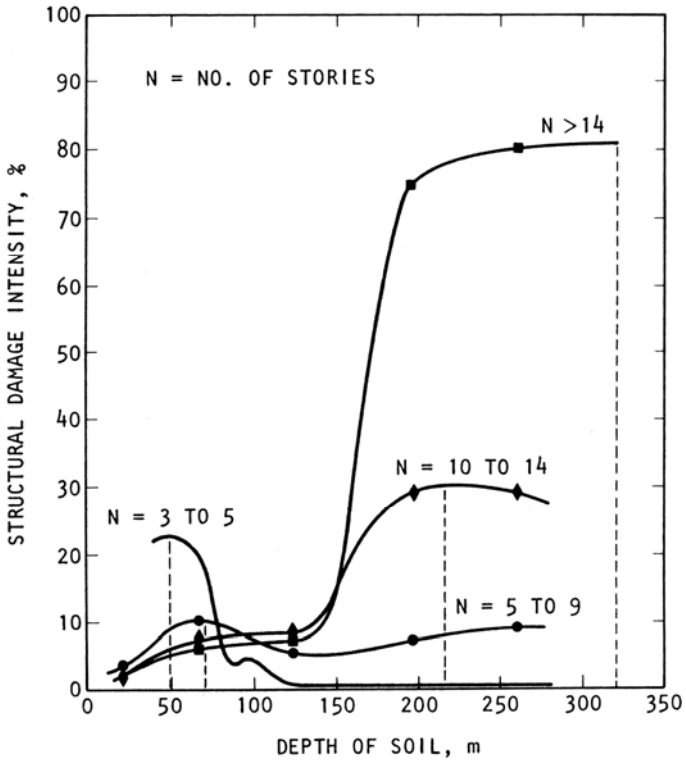

Figure 2.2. Relationship between intensity of structural damage and soil depth for Caracas Earthquake (adapted from Seed and Alonso, 1974)

2.1.3. Mexico City Earthquake. The Magnitude 8.1 Michoacan earthquake emanated from subduction movement along the East Pacific Rise off the west coast of Mexico on September 19, 1985. Shaking from this quake was magnified along a narrow belt running through the southern half of Mexico City, some ~300 km from the quake's epicenter. The magnified seismic wave train caused complete collapse of high rise structures, between 7 and 22 stories high, killing over 10,000 people and causing $6 billion in damages. Tall structures founded on 30 to 45 meters of soft lacustrine clay soils suffered the greatest damage (Seed et al., 1985). Interestingly, a swimming pool at the University of Arizona in Tucson which was located 2000 km away from the epicenter, lost water from a seiche triggered by this quake! Table 2.1 presents the considerable variances in recorded motions with soil conditions for strong motion recorders located in different parts of Mexico City.

Table 2.1. Site response summary of Michoacan Earthquake (Romo and Seed, 1986; Reither, 1990; Kramer and Arduino, 2008)

Soil conditions	**Rock and stiff soil sites**	**Medium depth clay deposits (~30-40 meters)**	**Deeper clay deposits (~45-57 meters)**
	$Vs_{(ROCK)}$ > 500 m/s	Vs = 75-80 m/s γ = 1.2 t/m^3	Vs = 65-75 m/s γ = 1.2 t/m^3
PGA	~0.04 g	~0.17 g	~0.09g
PSA	~0.11 g	~0.8 g	~0.35g
Predominant period	2 second	2 second	3.5 second
Damping	5%	5%	5%
Damage	Negligible	• Heavily damaged • Major amplifications occurred	Severe

Ground motions were amplified significantly at those sites underlain by clayey soils 30 to 40 m deep. Much less site amplification was noted where the thickness of these same soils exceeded 50 m. The soft clays amplified bedrock motions by as much as 745% (Seed et al., 1976). Higher spectral accelerations were also observed at long periods (e.g. ~3.5 seconds) for deep soil sites. It's clear that different soil conditions had a significant effect on shaking intensity in different parts of Mexico City (Whitman, 1986).

2.1.4. Loma Prieta Earthquake. The moderately large (Magnitude 7.1) Loma Prieta earthquake occurred on October 17, 1989 in the Santa Cruz Mountains of California, just south of San Francisco Bay. The quake took 63 lives, injured 3,757 people and damaged more than 27,000 structures. More than 80% of the fatal casualties and most of the major damage occurred 80 to 100 km north of the quake's epicenter (Rogers and Figuers, 1991). Severe ground shaking also caused secondary failures to develop, such as liquefaction and lateral spreading (Romero and Rix, 2005). Approximate correlations between underlying site conditions and site response are summarized in Table 2.2. The peak horizontal accelerations obtained on soft soil sites were about 3 times of rock sites.

Table 2.2. Response of deep soft soil sites in the October 1989 Loma Prieta Earthquake (Kramer, 1996; Seekins and Boatwright, 1994)

Soil conditions	Rock	Deep cohesive soft soil deposits
PGA	0.06 g	0.15 g
PSA	0.2 g	0.75 g
Damage	Negligible	• Amplification 2-3X @ up to 0.2 sec periods • Amplification 5-6X @ 1sec periods • Majority of damage occurred to taller, and/or longer period structures

2.1.5. Northridge Earthquake. The January 17, 1994 Northridge earthquake was the most costly temblor in United States history because of its proximity to densely populated portions of the Los Angeles metro area. It was assigned a magnitude of 6.7 (M = 6.7) and released energy along a sloping reverse fault, which dipped northerly, beneath the Santa Susana Mountains bordering the San Fernando Valley. The earthquake impacted people and structures at distances up to about 90 kilometers from the quake's epicenter in Northridge, with greater severity on the hanging wall (northern) side of the causative fault. Although the region closest to the quake was greatly impacted, pockets of increased ground disturbance and severe damage were noted at distant locations. Subsequent investigation revealed that seismic energy at most of these sites was magnified by a number of physical factors, including: infilled stream channels, areas of high groundwater, steep-sided ridges, colluvial and alluvial filled bedrock swales, and depth of fill. Fifty-seven people were killed and more than 9,000 were injured. Thousands of buildings were slightly damaged and more than 20,000 people were temporarily displaced from their homes (USGS). The most damage was observed on channel fills in alluvial deposits. The moderate size Northridge earthquake emphasized that near fault ground motions engender a distinct pulse-like characteristic, which was not represented in the lateral force provisions of then-existing building codes. As a result, engineers and policy makers were induced to rethink these building design criteria and these effects were incorporated into the 1997 Uniform Building Code, succeeded by International Building Code, which has since been adopted over much of the conterminous United States.

2.1.6. Dinar Earthquake. Magnitude 6.1, Dinar earthquake in Turkey took place on October 1995 causing extensive damage in the town of Dinar. The earthquake was associated with predominantly normal faulting killed 90 people, injured 260, and caused highly localized damage (Durakel, et al.1998). Despite the moderate size of the earthquake approximately 40% the buildings in Dinar was either collapsed or heavily damaged due to high lateral shear wave velocity contrast between the hill zone and the transition zone (geological inhomogeneities) and long duration of earthquake (Ansal et al 2001; Kanli et al 2006). Most four and five storey reinforced concrete apartment buildings locating in the valley were heavily damaged or totally collapsed. The buildings

located on the hills and slopes minor damaged. The PGA in Dinar was 0.33 g and amplification factor was up to 6.5. Mostly high amplifications were estimated in heavily damaged areas, but at 3 locations where 3-4 storey high structures highly damaged, lower spectral amplifications were observed due to a possible resonance effects (Ansal et al, 2001).

2.1.7. Kobe Earthquake. The Kobe earthquake which was one of the most devastating earthquakes ever to hit Japan occurred on January, 17 1995. Over 5,500 people died and 26,000 injured due to the 6.9 magnitude earthquake. Kobe was built on very soft uncompacted soil which is worst possible soil for an earthquake to produce liquefaction. Over 100,000 buildings were heavily damaged or destroyed and the total loss was estimated $200 billion (Bachman, 1995). Accelerations on soft soil were increased by two to three times and reached 0.82 g.

Table 2.3. Summary of damage and recorded PGA values for Northridge Earthquake (EQE, 1994)

Distance from the epicenter	**~6km (Tarzana)**	**10km**	**30km (Santa Monica)**
PGA	1g and *1.8g	0.3g - 1.2g	0.9g
Note	• Highest accelerations occurred on the top of a hill • Amplification @0.5sec	caused severe structural damage	buildings heavily damaged

*One of the highest accelerations ever recorded in an earthquake

2.1.8. Adana Earthquake. A moderate earthquake (M 6.2) produced by left lateral fault struck Turkey (Adana and Ceyhan) on June 28, 1998. The earthquake caused approximately 150 deaths, 1500 injuries, many thousands of people to left homeless, and around one billion US dollars economic loss (Adalier and Aydingun, 2001). Intensive damage occurred to old and modern reinforced concrete multistory buildings (Wenk et al., 1998; Celebi, 1998; Yalcinkaya and Alptekin, 2005). Celebi (1998) stated that the double resonance effect might have been one of the reasons of collapsed buildings which are the mid-rise (7-10 story buildings).

Table 2.4. Summarized damage and local site effects for Adana Earthquake (Wenk et al., 1998; Celebi, 1998; Yalcinkaya and Alptekin, 2005)

	Ceyhan (32 km from epicenter)	**Adana (30 km from epicenter)**
Soil conditions	Deeper than Adana	Shallower and stiff soil
Fundamental soil frequency	1.1 Hz.	between 3 and 6 Hz.
Damage	The most damage 7-10 story buildings	Most damage Low rise buildings
Notes	• Damage to new mid-rise buildings, especially in 5- and 6-story buildings • The peak frequency of the main shock, the fundamental frequency of the soil and the fundamental frequencies of the damaged buildings are close.	• The majority of mid-rise and taller buildings(5-15 stories) in Adana performed well • The maximum amplifications are seen at high frequencies

2.1.9. Kocaeli Earthquakes. The August 17, 1999 magnitude 7.4 Kocaeli Earthquake was one of the most catastrophic earthquakes in history of Turkey. More than 17,000 deaths have been confirmed and more another 20,000 people are declared missing and presumed dead. More than 12,000 housing units were heavily damaged or collapsed displacing more than 250,000 people. The total economic loss was estimated $15 to $20 billion (Bruneau et al, 2000). Thousands of four to seven stories height reinforced concrete buildings fully or partially collapsed and number of buildings overturned due to the seismic shaking dissipated from North Anatolian Fault Zone (Tezcan et al., 2002). Local soil conditions caused amplified rock accelerations to occur depending on the soil type and distance from the epicentral area. Table 2.7 represents these local site effects.

2.1.10. Bhuj Earthquake. One of the most damaging earthquakes in Bhuj, magnitude 7.7 Gujarat earthquake, occurred on January 2001 in India. Number of destroyed or damaged homes exceeded 1.1 million, 13,805 deaths, and 167,000 injured people reported. Extensive damage occurred about 300 km east of the epicenter in Ahmedabad city where no damage reported about the same distance northwest of the epicenter in the city Karachi. Extensive damage occurred due to the amplification of the ground where deep cohesionless soils presents. Four story and 10 story high residential buildings either collapsed or damaged (Govindaraju et al., 2004). Peak ground accelerations were recorded 0.064g fifteen meters below the ground surface and 0.106g at the ground floor of a building at a distance of 300 km from the epicenter (Govindaraju et al., 2004).

Table 2.5. Effect of local soil conditions during Kocaeli, Turkey Earthquake (Ergin et al., Tezcan et al., Bruneau et al, Cranswick et al., Erdik, 2000)

Place	**Sakarya**	**Yarimca**	**Istanbul (city)**	**Avcilar (town of Istanbul)**
Distance from the epicenter	~3.3 kilometers (2 miles)	~4.4 kilometers (2.7 miles)	~70 kilometers (43 miles)	~120 kilometers (56 miles)
PGA	0.4 g	0.32 g	0.04g	0.25g
Predominant Period (second)	0.3second	0.9 and 1.4 second		0.7, 1 and 1.6 second
Soil	Stiff	Soft		Clay, Stiff Sand
Damage	• 3-6 storey high buildings • Higher response @ shorter periods	• Taller structures • Higher response @ longer periods	NO heavy or moderate damage	• 5-8 storey high buildings • 60 buildings destroyed

2.2. GEOLOGIC CONDITIONS

One of the important input parameters needed for seismic site screening analyses is the thickness of the soil cover lying over the bedrock, often referred to as the 'soil cap' in earthquake seismology. Existence of hard rock, weathered rock, stiff soil, soft soil and depth to bedrock are the factors affecting the characteristics of seismic site response. The importance of the local site conditions was emphasized in Section 1 and the correlations between site effects and corresponding damage were summarized as well. This effect

especially was observed for Caracas Earthquake where the variations in soil thicknesses caused different structural damage (Seed and Idriss, 1982). Bedrock properties (density, fracture intensity, age of rock) are also important when evaluating the site response and this importance was stressed by different attenuations of seismic waves in Central and Eastern United States (CEUS) and Western United States (WUS). Due to contrasting bedrock properties in higher travel velocities and less path attenuation of surface waves are seen in CEUS compared to WUS. This also explains the fact that the earthquakes in CEUS can be felt over a large area than WUS (Cramer, 2007). For instance, the San Francisco, California, earthquake of 1906 (magnitude 7.8) was felt 350 miles away in the middle of Nevada, whereas the New Madrid earthquake of December 1811 (magnitude 8.0) rang church bells in Boston, Massachusetts, 1,000 miles away (Schweig, et al. 1995). The bedrock and surface geology for Granite City Quadrangle is summarized in the following paragraphs.

2.2.1. Bedrock Geology. The oldest bedrock unit underlying the surficial materials in the Granite City Quadrangle are St. Genevieve and St Louis Limestones (Mississippian age) as defined by (Denny, 2003; Denny and Devera, 2001; Harrison, R. W., 1994; Lutzen and Rockaway, 1987; Goodfield, 1965). These formations are composed mainly of limestone, dolostone, chert, and sandstone with occasional chert nodules and stringers. These limestones have almost horizontal dip and the entire formation is karstified with solution features developed down to 6 meters or more into the rock (Lutzen and Rockaway, 1987). Shales of Pennsylvanian age also overlie some portion of the limestone in the area (Grimley et al. 2001). Unfortunately, very few borings pierce the bedrock basement within the Missouri River flood plain and in the loess covered uplands bordering the floodplains, therefore the extent of the shale and weathering depth is not known.

2.2.2. Surficial Geology. The surficial geology of St. Louis is characterized by two geologic units in both of which different mechanisms dictated and controlled their deposition which was illustrated in Figure 2.4.

2.2.2.1 Lowland deposits. The lowland deposits are Missouri/Mississippi River stream deposits which are also classified as alluvial or floodplain deposits in the literature. In Granite City, lowland deposits are composed of two formations: Cahokia

Formation and Henry Formation. Cahokia Formation is Quaternary in age (less than 10,000 years before present) and is composed of soft/loose clay, silt and sand. Henry Formation underlies Cahokia Formation, it is Pleistocene in age (between 10,000 and 12,000 years before present), and is composed of sand at the top and more gravelly to the bottom. Henry Formation is deposited from the erosion and melting of the glaciers located north of the area in the upper Mississippi River basin (Willman and Frye, 1970; Grimley et al. 2001; Grimley and Lepley, 2005). Lowland deposits (alluvium) are bounded by the upland deposits (loess) on the western edge of the Granite City quadrangle (see Figure 2.3).

2.2.2.2 Upland Deposits: In Granite City, Glasford Till overlies the bedrock and contains unsorted mixtures of sand, gravel, silt. This deposit originates from the past glaciation activities which occurred in two stages; the first one about 450,000 years ago and the second one 130,000 years ago (Willman and Frye, 1970; Grimley et al. 2001). Glasford till is overlain by wind-blown loess deposits which are composed mainly of two texturally similar formations: Peoria Formation is younger than Roxana Formation and unlike pink colored Roxana, it is yellow brown in color. However, they both are composed of sand, coarse silt, and clay (Grimley and Lepley, 2005). The contact of till and loess deposits is highly variable and questionable due to limited number of borings in the area. Therefore, this study did not differentiate till and loess as separate units instead treated them as one formation (see Figure 2.3).

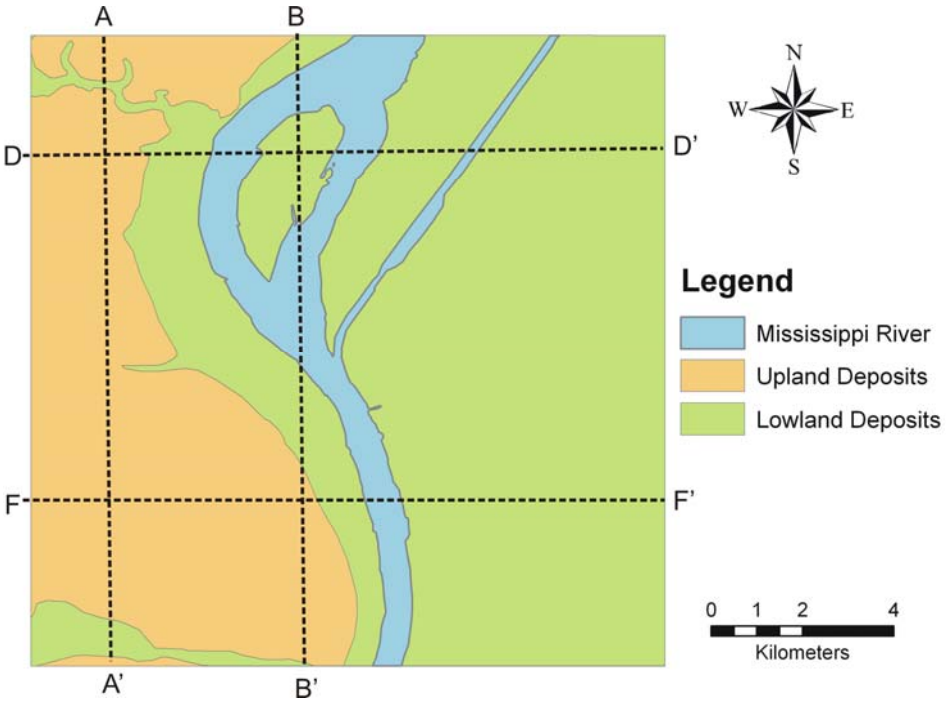

Figure 2.3. Generalized surficial geologic map of Granite City Quadrangle. In this map, Cahokia clay, Cahokia sand, Henry Formation and disturbed ground are combined into Lowland deposits, and Glasford till and Peoria and Roxana Formations are combined into Upland deposits (Grimley et al., 2007; Phillips et al., 2001).

2.2.3. Predicted Surficial Geology Thickness. Detailed depth-to-bedrock map has been prepared in a recent study by Karadeniz (2007) for Granite City, Monks Mount, and Colombia Bottom Quadrangles. In his study, he compared existing ground elevations with the top of the bedrock elevations following a four step procedure: First, data which were collected by Missouri and Illinois Departments of Transportation and Missouri and Illinois Geological Surveys, were gleaned and a database was created. Second, the collected data was digitized in ArcGIS (Figure 2.4). Third, ordinary kriging method was applied and top of bedrock surface was created with its associated standard prediction error values (Figure 2.5 and Figure 2.6). In the last step, top of bedrock prediction map was subtracted from the ground surface elevation map (Digital Elevation Model); hereby, soil thickness and its standard error prediction maps were created (Figure 2.7 and 2.8)

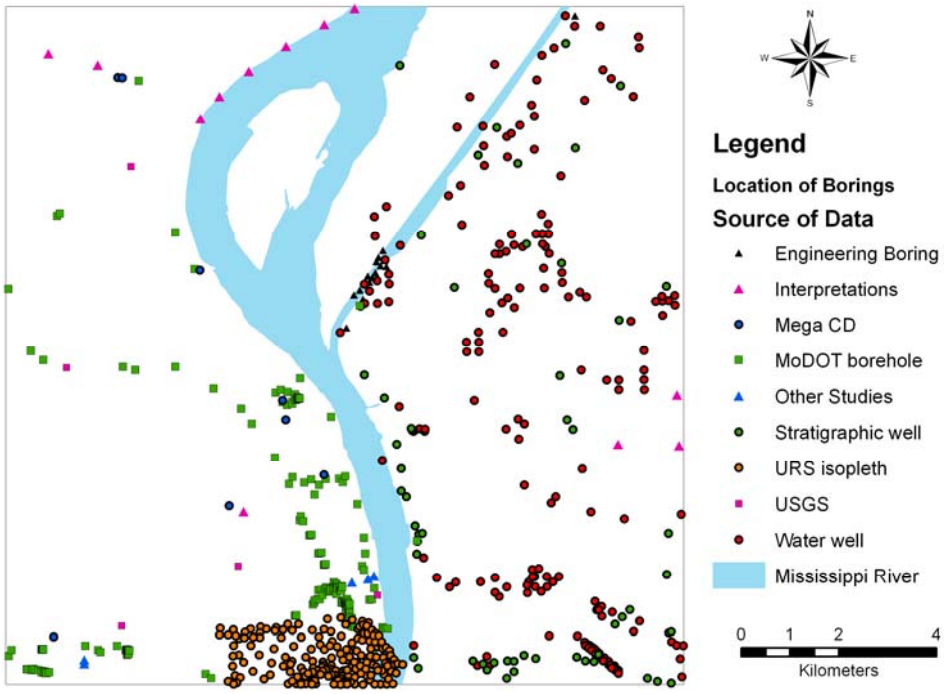

Figure 2.4. Location of borings and well logs of Granite City quadrangle (modified form Karadeniz, 2007)

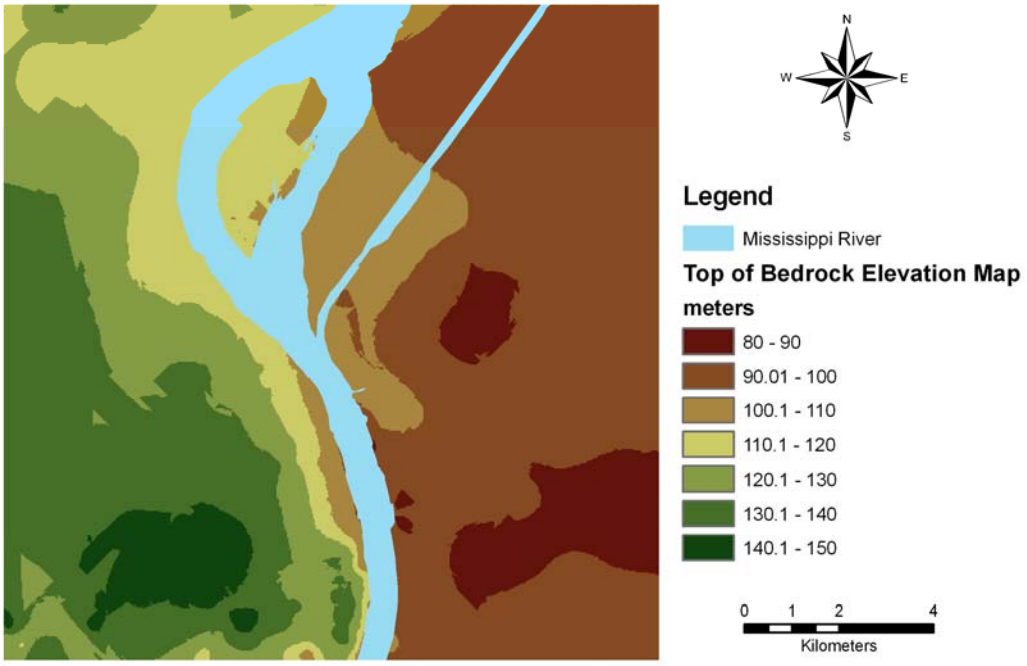

Figure 2.5. Top of bedrock elevation map of Granite City quadrangle (modified from Karadeniz, 2007)

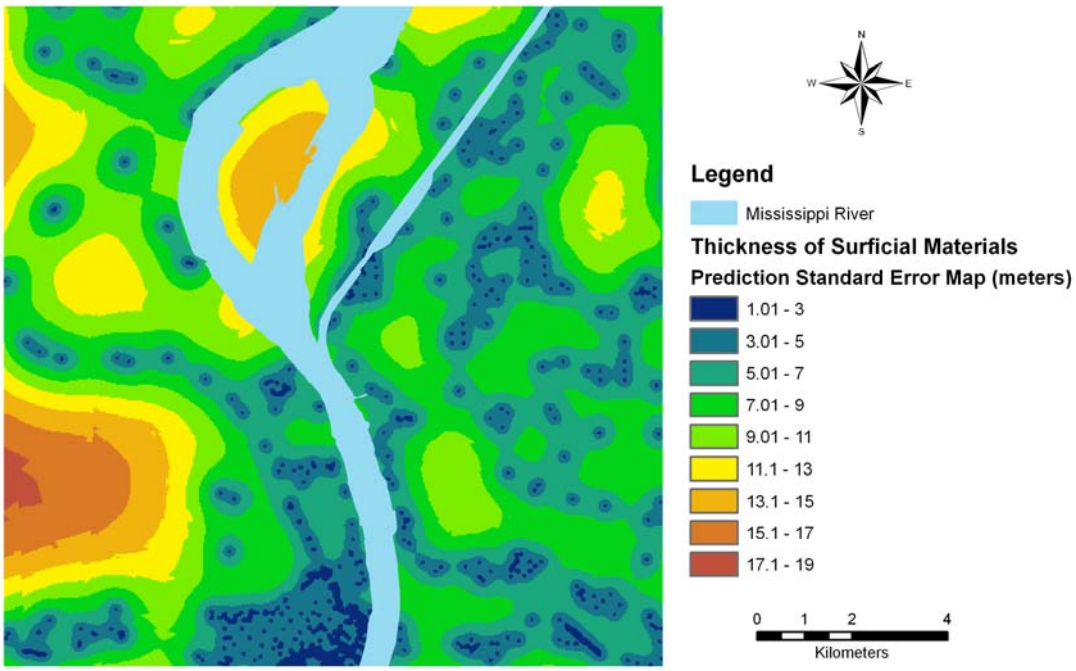

Figure 2.6. Predicted standard error map of top of bedrock map of Granite City quadrangle (modified from Karadeniz, 2007)

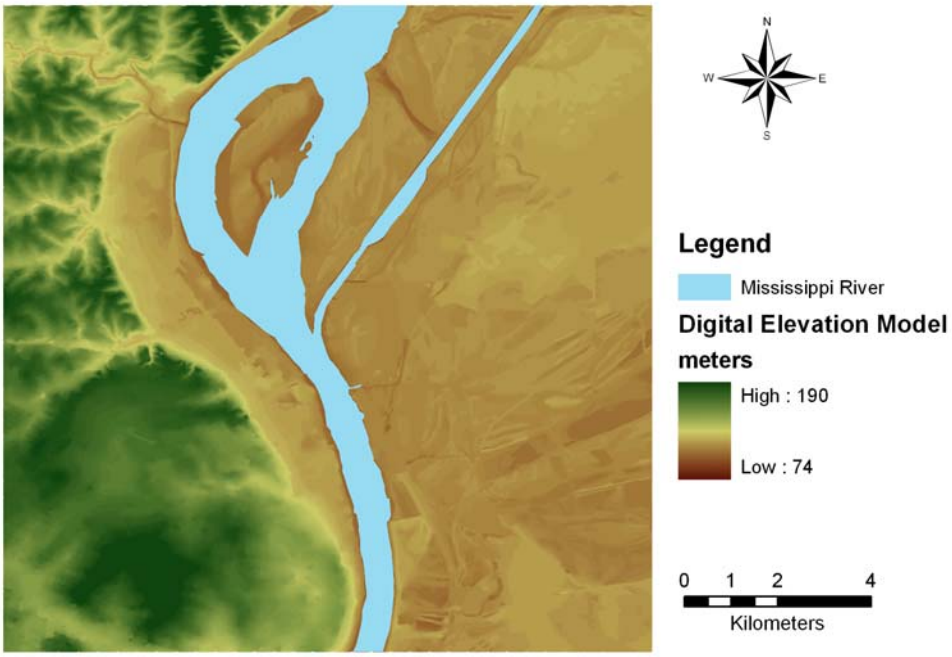

Figure 2.7. Ground surface elevation map of Granite City quadrangle (modified from Karadeniz 2007)

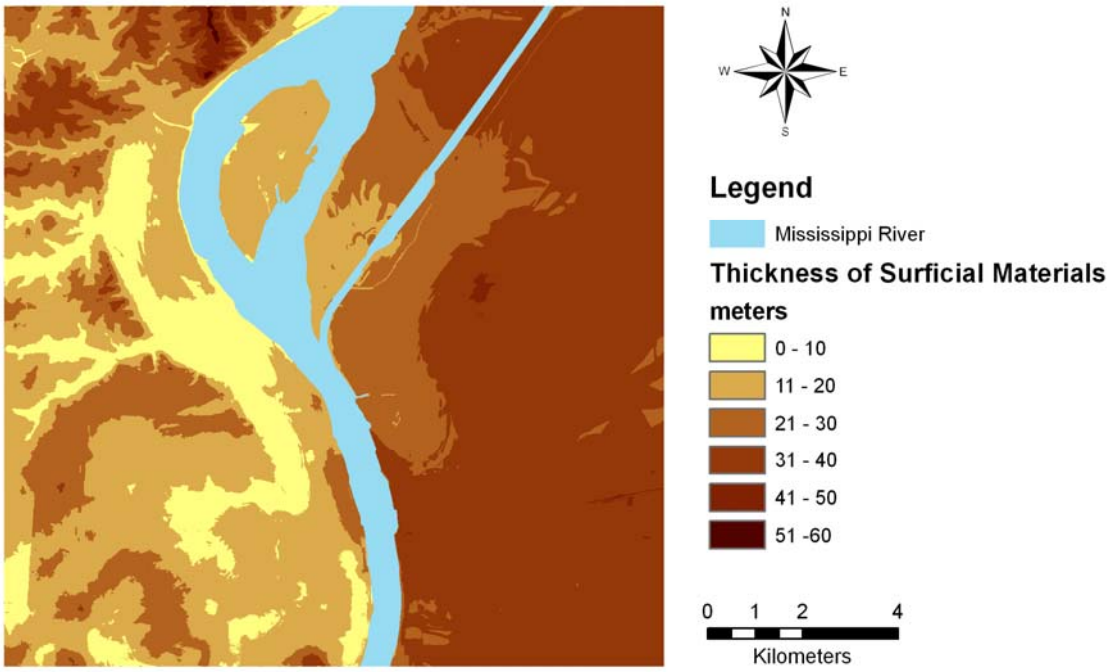

Figure 2.8. Predicted Soil thickness map of Granite City quadrangle (modified from Karadeniz, 2007)

The predicted thickness of the soil cap was determined to be between 30 to 40 meters for lowland (alluvial) deposits and 5 to 55 meters for upland (loess) deposits. The associated error ranges from 1.7 meters to as much as 18.4 meters. The west half of the quadrangle has much higher standard errors compared to the east half. This difference can be attributed to lack of data points on the western half and large variations in the data values (Karadeniz, 2007).

2.3. SEISMICITY

The central and eastern United States (CEUS) has older and rigid rocks which cause the seismic waves to spread laterally over much broader region. Due to the earth's crust in the region, earthquakes in the central and eastern U.S are typically felt over a large area. For instance, according to USGS (Stover and Coffman, 1993), a magnitude

4.0 earthquake could be felt 100 kilometers away from its epicenter and an affect of magnitude 5.5 earthquake could reach as far as 500 kilometers from it's epicenter. Two major seismic zones are accepted as source zones for medium to large magnitude earthquakes (M>6): New Madrid Seismic Zone (NMSZ) and Wabash Valley Seismic Zone (WVSZ).

The New Madrid Seismic Zone (NMSZ) is located at the intersection of the Missouri, Kentucky, Tennessee, and Arkansas borders. The NMSZ dominates Central U.S seismicity and has the highest seismic moment release rate of any seismic source zone in a stable continental region (Johnson and Nava 1990). NMSZ is also source of some of the largest historic earthquakes in Central and Eastern North America. Three historically important earthquakes occurred during the winter of 1811-1812. The first earthquake (16 December 1811) predicted to have occurred in Arkansas/Missouri border with a moment magnitude range between M7.2 and 8.0; the second earthquake (24 January 1812) predicted to have occurred in Missouri with a moment magnitude range between 6.8 to 7.8; the third earthquake (7 February 1812) predicted to have occurred in Tennessee/Missouri border with a moment magnitude range between 7.2 and 7.9 (Wheeler, 2003; Karadeniz, 2007). These earthquakes are believed to have originated from either or both strike slip and/or reverse fault movements.

The Wabash Valley Seismic zone, north of the more seismically active New Madrid seismic zone and 240 kilometers east of the St. Louis, is located in Southeastern Illinois and Southwestern Indiana. The fault system consists of normal faults dipping steeply both east and west. Geological and paleoseismic studies documented four main historical earthquakes occurred in the WVSZ which are: 1) Vincennes-Bridgeport earthquake (6011 ± 200 yr BP) with a magnitude range M7.1 and 7.8 (Obermeier, 1998); 2) Skelton-Mt Carmel earthquake (12,000 ± 1000 yr BP) with a magnitude range between M 6.7 and 7.4 (Munson et al., 1997 and Hajic et al., 1995); 3) Vallonia earthquake (3,900 ±250 yr BP) with a magnitude range between 6.3 and 7.1 (Munson et al, 1997); and 4) Martinsville-Waverly earthquake (8,500 and 3,500 yr BP) with magnitude estimated to be between M 6.2 and 6.9 (Munson et al, 1997).

Earthquakes of the New Madrid and Wabash Valley seismic zones are shown in Figure 2.9. The earthquakes which occurred earlier than the year 1974 are represented in

green color and the earthquakes from 1974 to 2002 are represented in red circles. The size of the circles symbolizes the earthquakes magnitude (USGS, 2007).

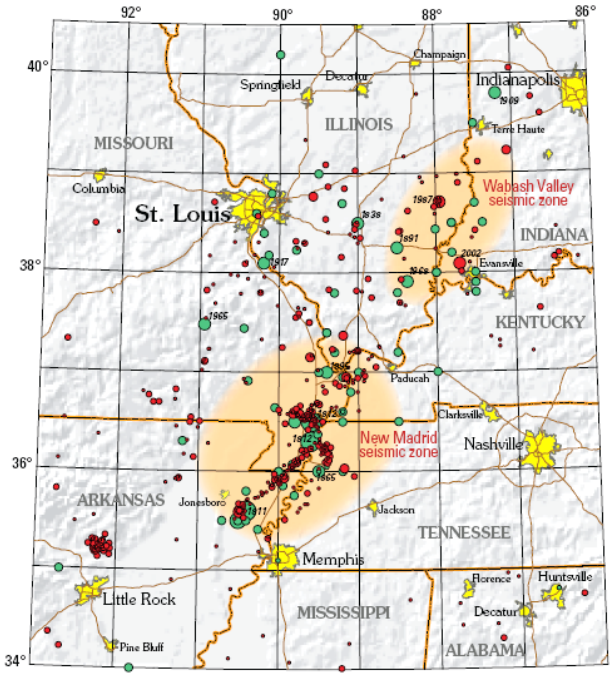

Figure 2.9. Earthquakes occurred in New Madrid and Wabash Valley seismic zones until 2002. In this figure, circles symbolize the earthquakes, orange patches represent the seismic zones, and yellow patches characterize large urban areas (adapted from USGS Fact Sheet 3073-508, 2007).

The most recent earthquake occurred on April 18, 2008. The magnitude was 5.2 and the epicenter was between Mt. Vernon and West Franklin in Posey County. The quake was felt also in St Louis causing minor damage, such as rattled windows, falling stuff from shelves, and concrete falling from the 72-year-old building (St Louis Today, 04/18/2008).

Maximum magnitude was predicted as M_{max}7.5 for both Wabash Valley and New

Madrid Seismic Zones based on the distribution of the paleoliquefaction features in the USGS National Seismic Hazard map study (Petersen et al., 2008). The zones of the selected maximum magnitudes are shown in Figure 2.9.

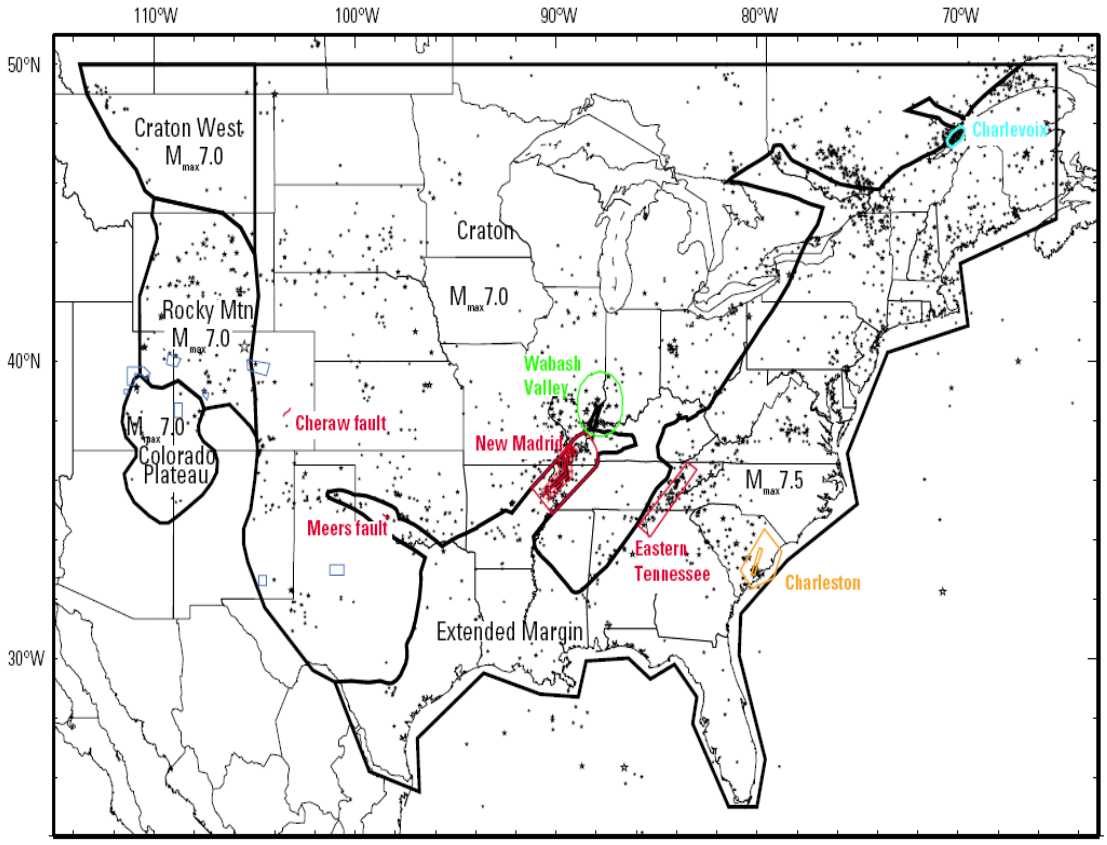

Figure 2.10. Map showing zones and maximum magnitudes assigned for each zone in preparation of USGS National Seismic Hazard Maps (adapted from Peterson et al., 2008)

2.4. RESPONSE SPECTRA

Seismic waves traveling away from a fault zone are reflected and refracted as they get further from the source in earthen structures. Rock motions are propagated through the soil column and finally reach the ground surface. The process of rock motion

propagating through the soil column can be modeled using a site response analyses. Site response analyses are usually performed with computer codes which applies one of two methods: equivalent linear analysis or nonlinear analyses (Kramer and Paulsen, 2004; Romero and Rix, 2005). Applicability, usage and capability of these methods were summarized in Table 2.6. Equivalent linear analyses assume soil stiffness and damping characteristics to be compatible with the level of strain induced in the soil. On the other hand, nonlinear analyses actually consider the nonlinear inelastic stress strain behavior of soils (Kramer, 1996).

Table 2.6. Site response analysis (Kramer and Paulsen, 2004; Kramer, 1996; Romero and Rix, 2005)

	Equivalent linear approach	Nonlinear approach
Use	An average shear modulus Total stress Soil stiffness and damping adjusted	Effective stress and total stress Nonlinear inelastic stress strain behavior
Applicable	For small strains (<1-2 %) Modest accelerations (<0.3-0.4 g) are expected	For large strains Displacements are expected Liquefaction hazard analysis
Capability	NOT capable modeling pore pressures NOT capable calculating permanent displacements	Predict permanent deformations develop stress Strain relationship Modeling pore pressure
Mostly used type/region	1-D Equivalent Linear North America	2-D/3-D nonlinear analyses Overseas

Commonly used computer codes for practice of site response analyses are

summarized in Table 2.7. These programs are categorized based on general soil model, and dimensions of the model (Kramer and Paulsen, 2004). Both equivalent linear and nonlinear models can be used for one, two or three dimensional problems. 1-D analyses are performed assuming the ground surface is level; all soil layers below ground surface are horizontal and extend to infinity (Govindaraju et al). 2-D and 3-D analyses are performed using dynamic finite element analyses for two- and three- dimensional earth structures such as earth dams and embankments (Kramer, 1996). 2-D and 3-D analyses are more complex compared to 1-D analyses. The validation of equivalent linear analyses and nonlinear analyses has been studied by Seed (1990) and EPRI (1993). When motions were between 0.05g to 0.5g, the differences in results of equivalent and nonlinear were very small (EPRI, 1993). When the rock motions were less than 0.2g, equivalent linear approach estimated the motion adequately (Seed, 1990; Idriss 1990).

1-D equivalent linear ground response analysis is performed using Shake2000 in this study due to; a) its simplicity and conservative results, b) the maximum accelerations around St Louis area is expected to be small (on the order of 0.05g to 0.2g), c) major liquefaction is not predicted.

Table 2.7. Common computer codes used in practice of site response analysis (modified from Kramer and Paulsen, 2004; Romero and Rix, 2005)

Dimensions	**Equivalent Linear**	**Nonlinear**
1-D	SHAKE	DESRA, DMOD, Deepsoil, FLAC
2-D/3-D	FLUSH, QUAD4	TARA, FLAC, PLAXIS

There major steps involved in 1-D equivalent linear deterministic ground response analysis. The first step is deciding the maximum magnitude, and the appropriate distance

of the site from the source. The second step is selecting appropriate rock motions. Natural time histories or synthetic motions could be used to represent the rock motion at the site. If selected histories are natural time histories, peak ground motion parameters, response spectra content and duration of shaking should be known (Govindaraju et al, 2004). In absence of natural motions, synthetic motions could be selected and their spectra should approximately fit design rock spectra (USACE, 1999). The third step is determining idealized soil profiles which characterize dynamic soil properties (e. g. shear wave velocity, damping and shear modulus and strain) for site of interest. The final step is performing the ground response analysis with a computer program. Using the rock motions and soil profiles as input motion, maximum force experienced by a mass on top of a rod (spectral acceleration) and particular natural vibration period could be computed (http://earthquake.usgs.gov). These resulting parameters are called response spectra and represent the maximum response of a single degree-of-freedom. The maximum amplitude of the ground acceleration time history which corresponds to the acceleration value at zero natural period is called PGA (peak acceleration) indicating what is experienced by a particle on the ground and spectral acceleration (SA) implies approximately what is experienced by a building.

During earthquakes soil acting like a filter and modifying the ground motion character as the ground motions reach the ground surface. This process is also known as soil amplification and can cause excessive ground shaking and greatest building damage (Govindaraju et al, 2004). Increased amplifications occur; a) When seismic wave energy period is equal to the natural site period (resonance), b) When the differences in shear wave velocities between the materials increases (Kramer, 1996 Romero and Rix, 2005).

When analyzing response spectrum of a site both spectral accelerations and amplifications and their corresponding periods should be statistically considered. These periods point approximately the height of the structures and the relationship is expressed

$$T = \frac{N}{10} \tag{1}$$

Where N is the number of stories and T is the period in second (Seed and Idriss,

1969: Kramer, 1996). In general, short natural periods (0.2-0.6 sec) indicate short buildings (less than 7 stories) where long natural periods (0.7 sec or longer), point out tall buildings (more than 7 stories). At different periods variable amounts of energy are produced by an earthquake, however particular periods (0, 0.2 second and 1 second) are accepted as index in seismic hazard maps for assigning a probabilistic spectral value for engineering design purposes. The spectral parameters guide engineers how a building will perform during an earthquake. In this process, uncertainties also play a major role, and they effect the decision on the design and planning.

3. SENSITIVITY ANALYSES

3.1. INTRODUCTION

Research about earthquakes has been done to mitigate seismic hazards for many years. Even with the advanced technology it is still impossible to determine the definite seismic site response. All these researches are approximate approaches due to the unknown or inaccurate information about; a) Magnitude of earthquake, b) Duration, c) Characteristics of ground motion, d) Seismic wave propagation in soil, e) Distance from the source, f) Geologic characteristics (such as soil type, and thickness), and g) Geotechnical characteristics (such as density, shear wave velocity, shear modulus, and damping ratio). Majority of the time, all these data has known with a range of uncertainty. The uncertainty of input data can be improved by gathering more data. However, gathering more data can be expensive, time consuming and may be not necessary. To overcome the problems of uncertainty sensitivity analyses can be performed which estimates the rate of change in the output model (response spectra) with respect to changes in model input parameters. The product of sensitivity analyses highlights the effects of uncertainties on response spectra; therefore, the most and least important input parameters could be ascertained. Consequently, effort to estimate more reliable input parameters could be come into question for site response predictions.

3.2. METHODOLOGY

This section describes the method and the input data procedures for the ground response analyses. Figure 3.1 represents the flow of this study. The scope of this study is to determine the effect of uncertainties of shear wave velocity, ground motion and surficial material thickness on site response with deterministic approach. In order to apply sensitivity analyses, first, two locations were selected; one test site on an alluvial flood plain and another on loess covered uplands. Second, a series of scenarios were created depending on variations in the input data and site response analyses were performed using Shake2000 for each scenario. Twenty-seven tests were performed for alluvial deposits and fifty four for loess deposits (with/without weathered rock). The total of eighty-one tests was completed. Third, site response analysis was applied to each of

these scenarios while considering each variable separately and keeping the other parameters constant. Eighty-one graphs of response spectra were provided in Appendix A. Fourth, the scenarios were interpreted related to the chosen input variables to find out how a change in one variable affected the accelerations and the results were compared for peak ground acceleration, 0.2 second period and 1 second period. These periods were considered due to their existence in national hazard maps.

Ninety-six various graphics were used to identify and clarify the differences in accelerations and amplifications. Consequently, the most significant parameters and factors influencing seismic site response in the St. Louis area were identified.

3.2.1. Shake2000. Shake2000 is windows based user friendly computer program for 1-D analysis which is used for evaluating the effects of earthquake on soil deposits. Ordonez (2006) categorized following four steps in order to run the analysis with Shake 2000.

Step 1: Collection of following information;

- Material properties (shear wave velocity, density, soil type, damping, depth to bedrock, soil layer distribution and thickness)
- Acceleration time history whose respond spectrum reasonably match the target respond spectrum.

Step 2: Creation of input file using below steps;

- Divide the soil profiles into layers
- Select the dynamic soil properties for each soil type
- Assign the specific data for each layer (density, layer thickness, shear wave velocity, damping)
- Select an input ground motion and define its layer number
- Define the number of iterations and strain ratio

Step 3: After the input parameters are created, desired seismic site response analysis output parameters should be assigned. Analysis option includes;

- Shear stress/strain preliminary information the following four procedures should be specified

- Obtain information for specific layers such as peak acceleration values, acceleration time histories, respond spectra and amplification spectrum

Step 4: After the interested options are filled in, the program could be run.

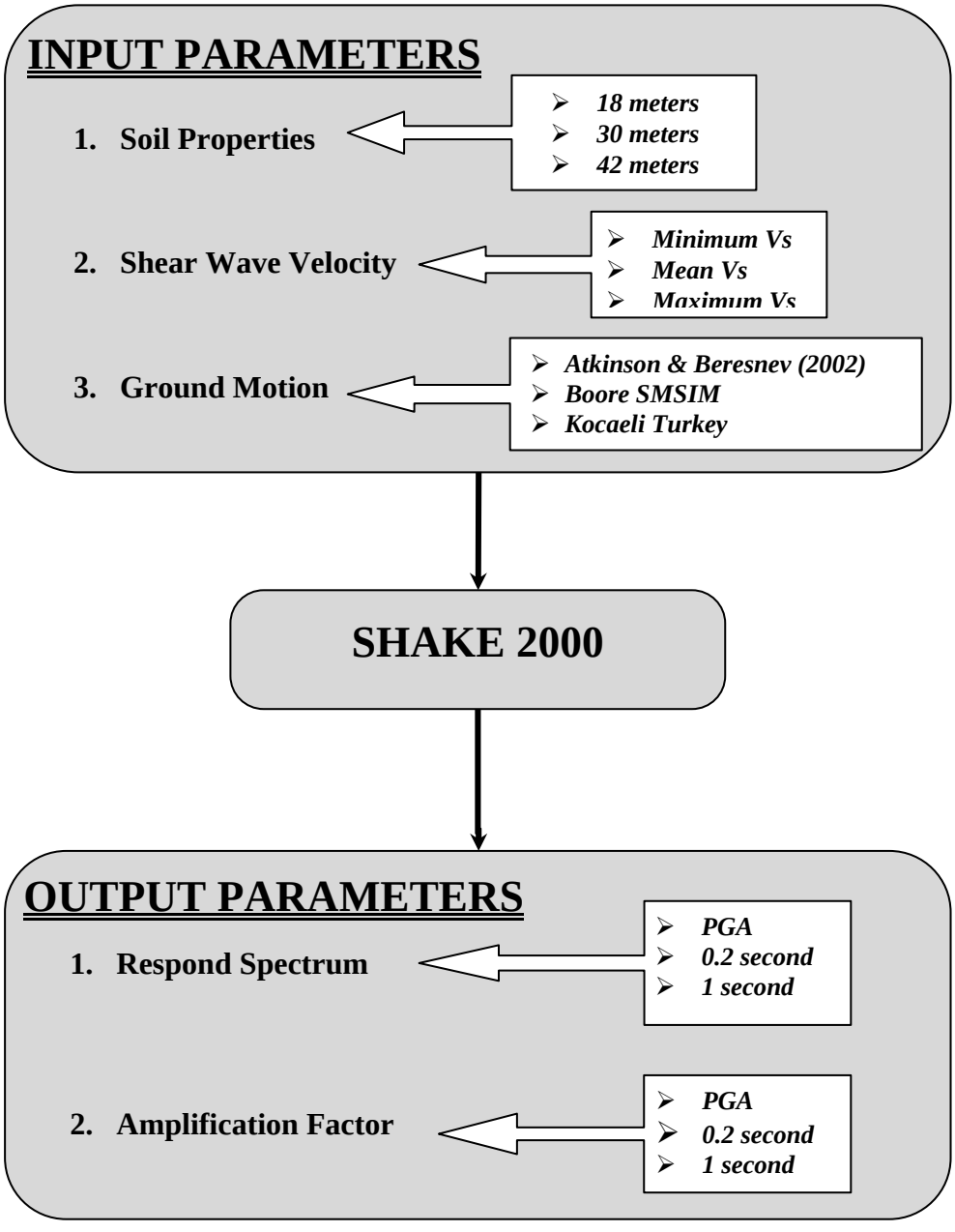

Figure 3.1. Flow Chart of sensitivity analyses

3.2.2. Input Ground Motion. In order to perform site response analysis, appropriate earthquake accelerations should be determined first. Characteristics and the form of the accelerations should be representative of the adjacent rock formations (Seed and Idriss, 1969). New Madrid seismic zone has been surrounded by seismograph stations and majority of these stations has been operated by St. Louis University which began recording in 1908 (MoDNR, 2008). Since 1811 and 1812, Central and Eastern United States (CEUS) has not experienced a large magnitude earthquake (Moment Magnitude >7), because of that reason, recorded time histories for earthquakes larger than 7.0 magnitude are not available for St. Louis area. As explained in previous section, for both New Madrid and Wabash Valley seismic zones maximum expected magnitude is 7.5 according to Peterson et al (2008). Therefore, simulated (synthetic) ground motions have been developed to close this gap. In this study two artificial time histories has been employed in site screening analysis; Atkinson and Beresnev's (2002) model and Boore's SMSIM v2.2 model.

Atkinson and Beresnev (2002) have created a magnitude 7.5 synthetic earthquake for Memphis, Tennessee (about 60km from NMSZ) and St. Louis, Missouri (about 200km from NMSZ). The simulations were based on finite-fault simulation program (FINSIM) and made for representative soil profiles and bedrock conditions for each city (Atkinson and Beresnev, 2002).

The second artificial time history record is simulated using Boore's SMSIM v2.2 code for a moment magnitude 7.5 earthquake at a distance of 200 km. The SMSIM ground motion simulations are based on stochastic method and can calculate the acceleration time histories for a given earthquake and magnitude (Boore, 2003).

In addition to these simulations, an actual ground motion record from the 1999 Kocaeli Turkey Earthquake, which had a magnitude of 7.4 at a distance of 210 km was obtained from Turkish General Directorate of Disaster Affairs and used for site response analyses (http://www.deprem.gov.tr/).

Although all of the selected input ground motions were in same distance and have same magnitude, they have different characters. These characteristic differences are illustrated in Figure 3.2 and summarized in the subsequent paragraphs.

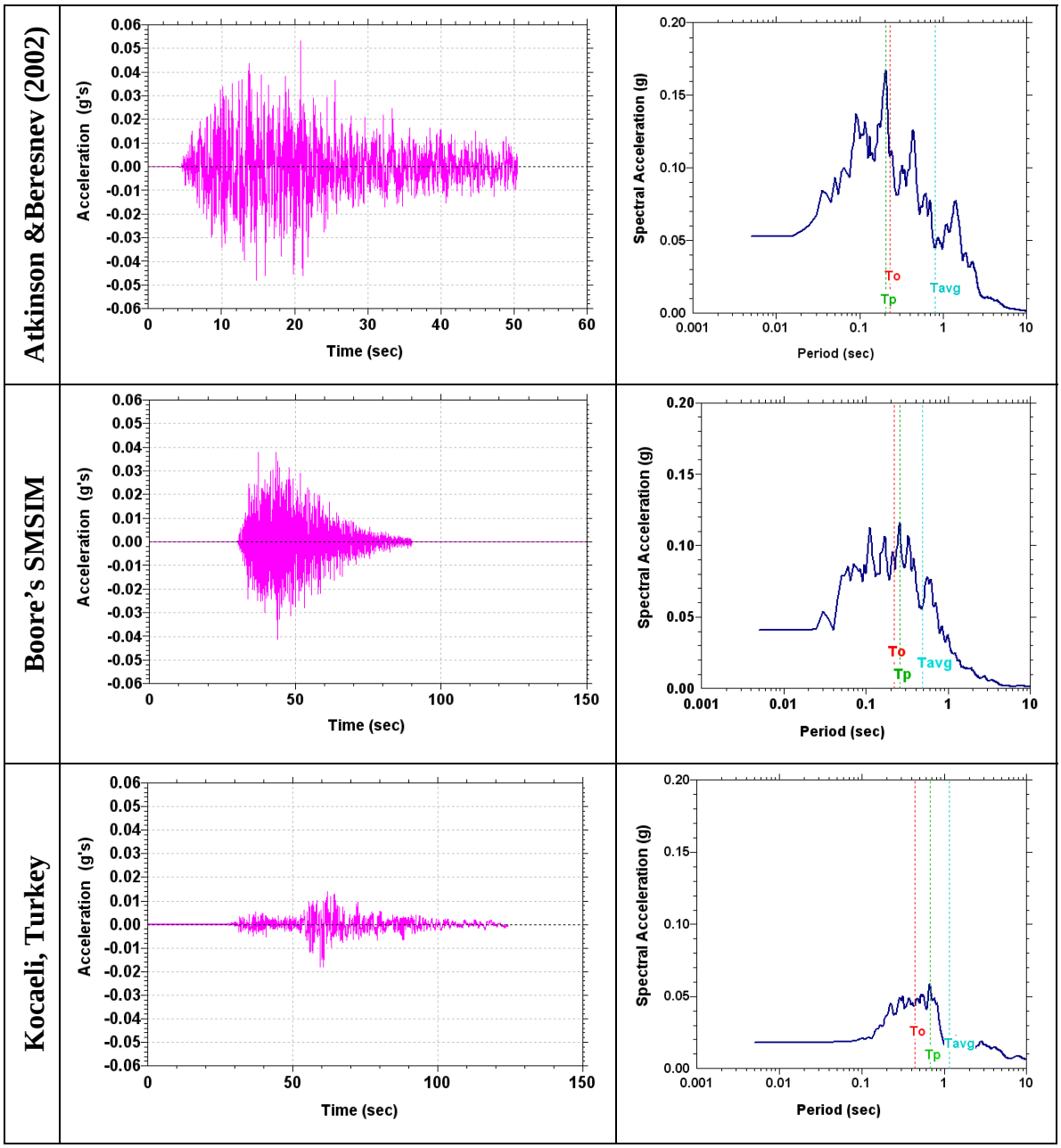

Figure 3.2. Time histories and acceleration response spectra for the three ground motion

The damage of an earthquake can be evaluated by considering the most important characteristics of rock motion such as peak acceleration, duration and frequency content (predominant period). Table 3.1 presents a summary of parameters used to characterize the rock motions.

The peak acceleration value is the maximum absolute horizontal acceleration value of the ground motion and is observed the highest for Atkinson & Beresnev's and the smallest for Kocaeli, Turkey earthquake. The potential destructiveness of an earthquake is represented by the Arias Intensity (Ordonez, 2006). Atkinson & Beresnev's has a high energy compared to Boore's and Kocaeli earthquakes; and Kocaeli earthquake has a low energy compared to the other two earthquakes. The time between the beginning and ending of an earthquake is recorded by an accelerogram; of which only the strong motion portion of the accelerogram is used for engineering purposes. The bracketed duration of strong motion is the interval time between the first and last expedience of threshold acceleration (Kramer, 1996) and is observed highest for the weaker rock acceleration, Kocaeli earthquake.

High peak ground accelerations and high arias intensity values may point the potentially hazardous motion, but duration of ground motion also affects the intensity of motion. If the ground motion is developed for only short period of time it will cause little damage, consequently motion which continuous for a number of seconds with small amplitude can build up more damage (Seed and Idriss 1982).

Table 3.1. Characteristics' of Selected Ground Motions

Characteristics' of Ground Motions	**Atkinson & Beresnev Earthquake**	**Boore's SMSIM Earthquake**	**Kocaeli, Turkey Earthquake**
Peak Acceleration Value (g)	0.053	0.041	0.018
Arias Intensity ft/sec	0.2563	0.1926	0.0374
Duration (sec)	31.6	29.2	52.4
Smoothed Spectral Predominant Period, T_o (sec)	0.229	0.217	0.443
Predominant Spectral Period, T_p (sec)	0.205	0.255	0.67
Average Spectral Period, T_{avg} (sec)	0.805	0.49	1.146

The intensity of ground shaking Predominant period, T_p, is approximate representation of the frequency content of a ground motion and defined as the period of maximum spectral acceleration (Rathje et al., 2004). The smoothed spectral predominant period, T_o, defines the peak in the response spectrum by smoothing the spectral accelerations over the range where spectral accelerations are greater than 1.2*PGA (Rathje et al., 2004). The average spectral period, T_{avg}, is an average period weighted by the spectral accelerations (Rathje et al., 2004; Ordonez 2006). These periods; $T_{p,}$ T_o, and T_{avg}, were greatest for the weakest motion Kocaeli Earthquake compared to other earthquakes in consideration.

3.2.3. Shear Wave Velocity. Shear wave velocity is one of the important parameter effecting ground motion amplifications which explained in Section 2. For an appropriate seismic site response calculations and ascertain proper lateral loads on structures, near surface shear wave velocity is required (Dobry et al, 2000). Experience with earthquake damage due to the amplification of ground motions has brought out the change of building codes. As a result, estimation of seismic demand on structures is now require the shear wave velocity in the upper 30 meters (V_s30) which is believed to determine the appropriate amplification factors (Dobry et al. 2000; Holzer et al., 2005).

Statistical distribution and depth dependence of shear wave velocities of the geologic units were examined in a recent study by Karadeniz (2007) for Granite City, Monks Mound and Colombia Bottom Quadrangles. Karadeniz (2007) collected data from Missouri Department of Natural Recourse, United States Geological Survey, Missouri University Science & Technology, and Illinois State Geological Survey, and analyzed them basing on the local geographic and lithologic characteristics, and then recompiled to develop regional generic profiles. Finally, the mean shear velocity values were determined with the associated uncertainties for upper 30 meters by applying statistical lognormal distribution. The table of regional shear wave velocities with recognized depth thickness and surficial geologic units (alluvium and loess) was provided by Karadeniz (2007). The weathered bedrock shear wave velocity value was predicted to be 1500m/sec by Karadeniz (2007) and the weathered bedrock shear wave velocity was estimated to be 2800m/sec by United States Geological Survey.

Table 3.2. Determined average shear wave velocities with associated uncertainties for alluvium and loess (adapted from Karadeniz, 2007)

Soil thickness from the ground surface	ALLUVIUM		LOESS	
	Mean Vs (m/sec)	Standard Error (m/sec)	Mean Vs (m/sec)	Standard Error (m/sec)
0m-5m	134	33	179	51
5m-10m	180	32	241	86
10m-15m	222	34	325	116
15m-20m	250	50	443	167
20m-25m	256	50	481	211
25m-30m	286	53	539	217

In this study estimation of the seismic site response change due to the uncertainties, the shear wave velocity values and standard errors were used as input parameters, then effect of variations in shear wave velocity discussed in Section 4.

3.2.4. Subsurface Soil Thickness. Soil thickness is one of the most important parameter which symbolizes the local site characteristic and the previous earthquakes proved its role on seismic site response. As explained in Section 1 subsurface soil thickness with associated standard errors were determined using kriging method on ArcGIS by Karadeniz (2007). One location was selected in this study from each units (alluvium and loess) to analyze the influence of soil thickness on site response. These are the locations where the estimated soil thickness was 30 meters. Required shear wave velocities for the upper 30 meters by International Building Code (IBC), led 30 meters to be selected for the analyses. The scope of this study is to observe the impact of uncertainties on site response, therefore the maximum standard error (+ 12 meters) of 30 meters soil thickness which was estimated through the cross-sections was preferred for site response analyses for both alluvium and loess (Figure 3.3)

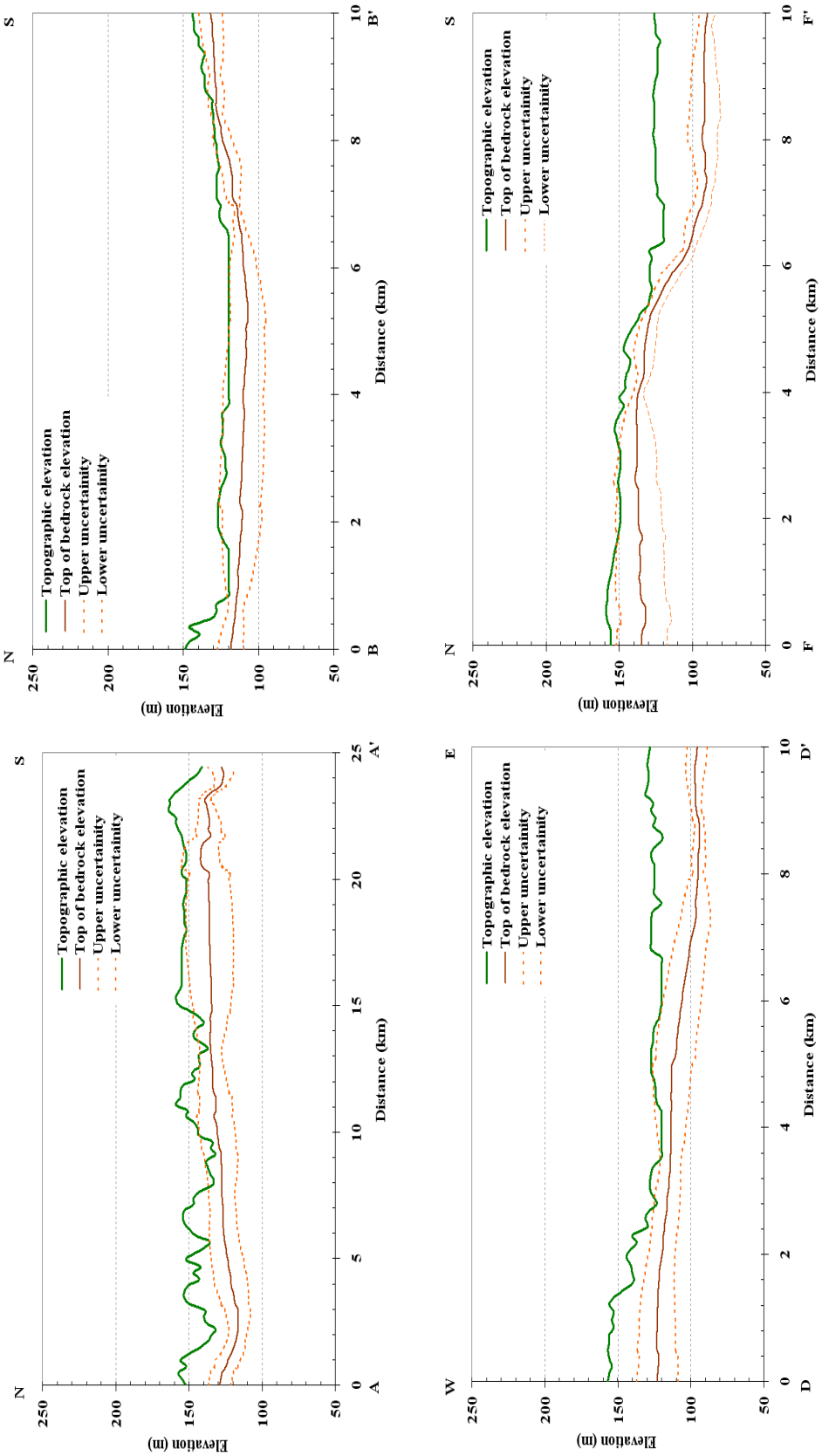

Figure 3.3. Locations of 30 meters soil cap with associated maximum standard error and cross-sections showing the uncertainty of the top of bedrock (see Figure 2.3 for the locations of the profiles).

3.2.5. Density. The ground motion amplification could also effected by density, since it's related to the shear wave velocity and the shear modulus. Density values were collected and statistical calculations were applied by Karadeniz (2007) and lognormal mean of density values with depth summarized in Figure 3.4. The predicted mean density values were 2 g/cm3 for both alluvium and loess.

3.2.6. Dynamic Soil Properties. Measure of the stiffness (shear modulus) and the ability of the soil to dissipate seismic energy (damping ratio) are the key parameters determining the susceptibility of a soil deposit to ground motion amplification (Romero and Rix, 2001). Therefore, dynamic soil properties also play an important role on local site effect and earthquake damage.

In this study, for site response analysis the EPRI (1993) shear modulus and damping ratio relations were obtained due large database of laboratory tests and usage in the recent studies such as Romero and Rix (2001), Cramer (2006b) and Karadeniz (2007). These relations were provided in Figure 3.5.

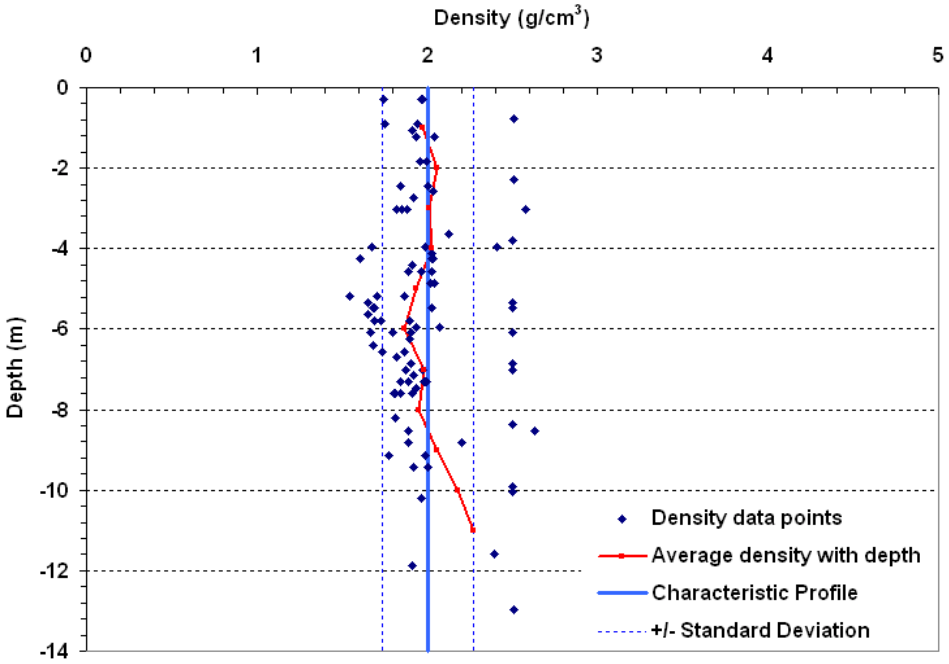

Figure 3.4. The measurements of density with depth and the calculated mean density (adapted from Karadeniz, 2007)

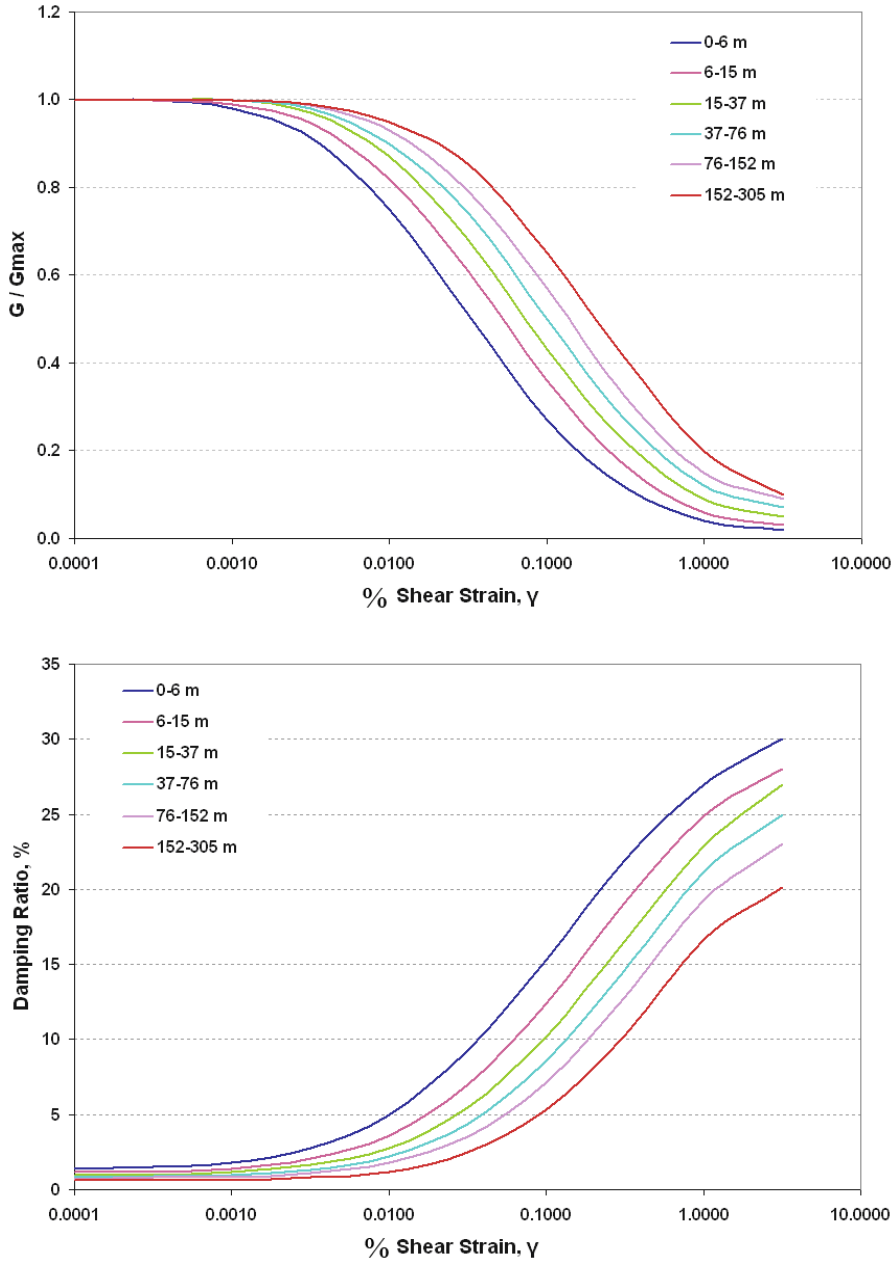

Figure 3.5. Shear modulus reduction curves and damping curves (adapted from EPRI 1993)

4. RESULTS OF SENSITIVITY ANALYSES

4.1. SENSITIVITY TO SPECTRAL ACCELERATIONS

After an earthquake, seismic energy radiates outward from the causative fault rupture as a series of P and S waves, shear waves, and a variety of surface waves (shear waves cannot be transmitted through fluids). As this seismic energy moves outward, its energy is diminished over an expanding area and some portion of the wave energy is absorbed by natural attenuation of the media through which it travels. As a consequence, the wave amplitudes tend to decrease with distance, depending on site conditions, such as rock and soil properties, site topography, and other characteristics of the input motion. Response spectra vary depending on the thickness of the soil cap, the soil age and type, its stiffness, and the engendered state of behavior of the soil (once soil liquefies, it behaves as a fluid, damping incoming wave energy) [Rogers, 2007]. Newton's Second Law of Dynamics states that a force on an object is equal to the mass of the object multiplied by its acceleration:

$$F = M*a \tag{4.1}$$

where F is force, M is mass, and a is acceleration. Since the mass of building is constant during the earthquake, the dynamic forces acting on a building tend to increase with increasing acceleration, depending on the stiffness of the structural frame (which can be degraded with each cycle of loading), system damping, and acceleration. What threshold of ground motion needs to be exceeded to be considered "strong motion" has never been defined quantitatively, so as to enjoy universal application (Anderson, 2003). This is because the underlying site geology exerts such remarkable influence on the severity of shaking and the style of rupture (e.g. strike-slip versus reverse, versus zippering thrust) and mechanism of rupture (uniaxial versus bi-axial rupture) both influence quake duration. The highest recorded peak accelerations of strong earthquakes are between 1g and 3g, but are rarely observed (Anderson, 2003). Ground accelerations are also locally

modified by uncertainties in the geometry and geophysical characteristics of the Earth's crust, especially, in the upper 30 m.

Response spectra results are tabulated in Appendix A. Table 4.1 presents an overview of the resulting output for PGA, 0.2 second, and 1 second periods. Peak accelerations and corresponding periods have also been summarized in Table 4.2. Sensitivity analyses were performed for these results and are explained in following subsections.

The peak spectral accelerations and their associated periods are also identified. The maximum predicted accelerations were 0.84 g for alluvium, using Atkinson & Beresnev input ground motion, and 0.82 g for loess, using Boore's SMSIM input ground motion.

4.1.1. Influence of Input Time Histories on Predicted Spectral Accelerations. The physical properties and geometry of the soil cap govern predicted acceleration and site amplification, but the magnitude and character of the earthquake energy propagating through the soil cap can also exert a marked influence on site response. The free field site response measured at the ground surface (PGA) and the amplification of this seismic energy is largely influenced by the amplitude and frequency content of the input rock motions. In this study, three input rock motions were selected, as explained in Section 3. Of these three, Atkinson & Beresnev (2002) and Boore's SMSIM code are both synthetically generated acceleration-time histories. Synthetic ground motions tend to be more homogeneous in nature, but they are widely accepted as being more representative of CEUS source characteristics with representative levels of attenuation/damping. The 1999 Kocaeli earthquake was also selected in order to capture some of the complexities of actual earthquake-time histories. It is customary practice to employ similar magnitude (~M 7.5) earthquake at similar focal distances (~200 km) when making such comparisons. The salient characteristics (peak acceleration, mean period, etc.) of the selected acceleration time-histories were summarized in Table 3.1 and compared with response spectra results summarized in Figures 4.1 through 4.6.

Table 4.1. Response Spectra for alluvium and loess covered sites for PGA, 0.2 second, and 1 second periods for alluvial and loess covered sites

Soil Type	Time history	Min Vs			Mean Vs			Max Vs			Soil Thickness (m)
		PGA	0.2 sec	1 sec	PGA	0.2 sec	1 sec	PGA	0.2 sec	1 sec	
ALLUVIUM	Atkinson & Beresnev (2002)	*0.12*	*0.32*	*0.09*	*0.15*	*0.35*	*0.07*	*0.15*	*0.27*	*0.06*	18
		0.11	*0.31*	*0.13*	*0.15*	*0.45*	*0.10*	*0.16*	*0.45*	*0.08*	30
		0.12	*0.34*	*0.25*	*0.11*	*0.32*	*0.13*	*0.14*	*0.39*	*0.10*	42
	Boore's SMSIM	*0.11*	*0.21*	*0.08*	*0.11*	*0.17*	*0.05*	*0.13*	*0.21*	*0.05*	18
		0.10	*0.16*	*0.12*	*0.12*	*0.29*	*0.09*	*0.13*	*0.23*	*0.06*	30
		0.11	*0.24*	*0.16*	*0.10*	*0.17*	*0.12*	*0.11*	*0.27*	*0.10*	42
	Kocaeli, Turkey	*0.06*	*0.14*	*0.03*	*0.06*	*0.10*	*0.03*	*0.06*	*0.11*	*0.02*	18
		0.08	*0.12*	*0.07*	*0.07*	*0.17*	*0.04*	*0.06*	*0.10*	*0.03*	30
		0.06	*0.12*	*0.09*	*0.08*	*0.11*	*0.07*	*0.08*	*0.13*	*0.04*	42

Soil Type	Time history	Min Vs			Med Vs			Max Vs			Soil Thickness (m)
		PGA	0.2 sec	1 sec	PGA	0.2 sec	1 sec	PGA	0.2 sec	1 sec	
LOESS	Atkinson & Beresnev (2002)	*0.15*	*0.39*	*0.08*	*0.14*	*0.52*	*0.05*	*0.18*	*0.81*	*0.05*	18
		0.15	*0.42*	*0.10*	*0.16*	*0.38*	*0.06*	*0.17*	*0.81*	*0.05*	30
		0.13	*0.34*	*0.12*	*0.18*	*0.58*	*0.06*	*0.16*	*0.55*	*0.05*	42
	Boore's SMSIM	*0.11*	*0.17*	*0.06*	*0.15*	*0.33*	*0.04*	*0.14*	*0.40*	*0.04*	18
		0.15	*0.24*	*0.09*	*0.15*	*0.27*	*0.05*	*0.14*	*0.53*	*0.04*	30
		0.12	*0.18*	*0.11*	*0.14*	*0.29*	*0.05*	*0.15*	*0.34*	*0.04*	42
	Kocaeli, Turkey	*0.05*	*0.10*	*0.03*	*0.04*	*0.13*	*0.02*	*0.03*	*0.14*	*0.02*	18
		0.07	*0.13*	*0.04*	*0.06*	*0.12*	*0.02*	*0.05*	*0.17*	*0.02*	30
		0.09	*0.14*	*0.06*	*0.07*	*0.12*	*0.03*	*0.05*	*0.13*	*0.02*	42

Table 4.2. Peak Spectral Accelerations (a_{peak}) and associated periods for alluvial and loess covered sites

Soil Type	Time history	Min Vs		Mean Vs		Max Vs		Soil Thickness (m)
		Period	a peak	Period	a peak	Period	a peak	
ALLUVIUM	Atkinson & Beresnev (2002)	*0.45*	*0.45*	*0.42*	***0.84***	*0.35*	*0.58*	18
		0.7	*0.55*	*0.58*	*0.49*	*0.45*	***0.76***	30
		0.35	*0.34*	*0.70*	*0.55*	*0.6*	*0.50*	42
	Boore's SMSIM	*0.55*	*0.44*	*0.38*	*0.59*	*0.32*	*0.69*	18
		0.7	*0.32*	*0.56*	*0.50*	*0.43*	*0.43*	30
		0.34	*0.43*	*0.25*	*0.34*	*0.56*	*0.46*	42
	Kocaeli, Turkey	*0.48*	*0.33*	*0.38*	*0.37*	*0.32*	*0.32*	18
		0.68	*0.45*	*0.55*	*0.35*	*0.41*	*0.33*	30
		0.82	*0.29*	*0.68*	*0.44*	*0.56*	*0.36*	42
LOESS	Atkinson & Beresnev (2002)	*0.45*	***0.72***	*0.25*	*0.66*	*0.2*	***0.81***	18
		0.58	*0.49*	*0.32*	*0.66*	*0.2*	***0.81***	30
		0.7	*0.55*	*0.42*	*0.62*	*0.25*	*0.56*	42
	Boore's SMSIM	*0.38*	*0.44*	*0.26*	***0.82***	*0.18*	*0.57*	18
		0.56	*0.53*	*0.32*	***0.73***	*0.21*	*0.61*	30
		0.32	*0.46*	*0.38*	*0.67*	*0.25*	***0.70***	42
	Kocaeli, Turkey	*0.4*	*0.41*	*0.25*	*0.21*	*0.2*	*0.14*	18
		0.53	*0.35*	*0.32*	*0.30*	*0.23*	*0.19*	30
		0.68	*0.43*	*0.38*	*0.30*	*0.27*	*0.20*	42

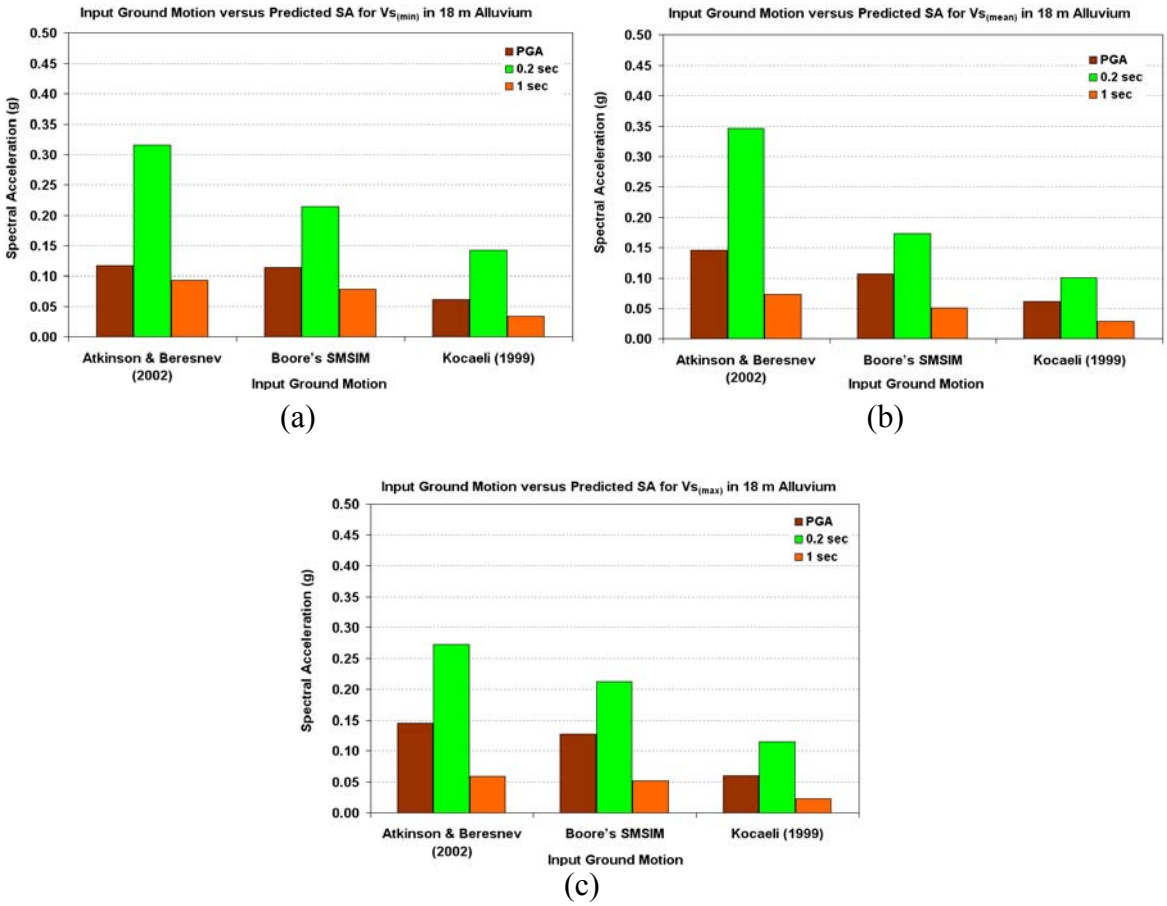

Figure 4.1. The effect of ground motion on spectral acceleration for sites underlain by 18 m of alluvium, assuming a) $Vs_{(min)}$ b) $Vs_{(mean)}$, and c) $Vs_{(max)}$ at ground surface, 0.2 sec and 1 sec periods

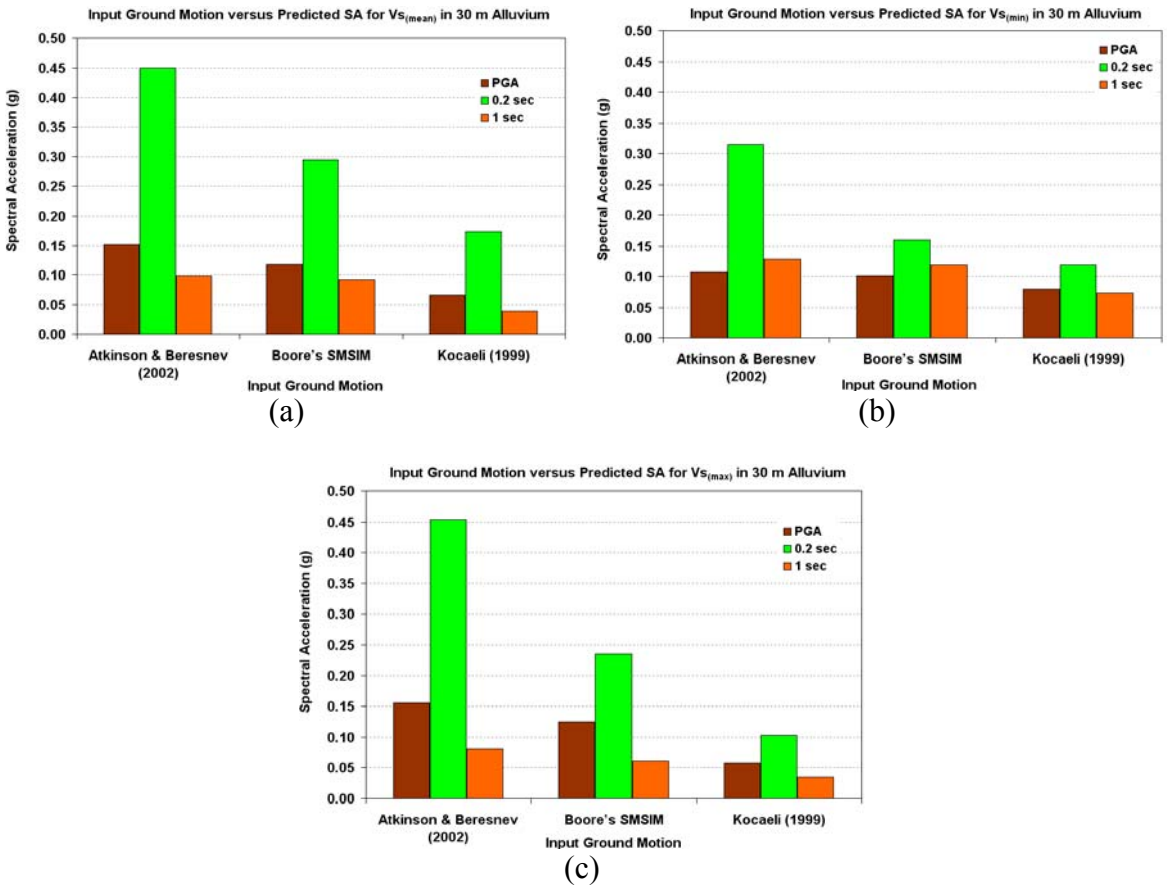

Figure 4.2. The effect of ground motion on spectral acceleration for sites underlain by 30 m of alluvium, assuming a) $Vs_{(min)}$ b) $Vs_{(mean)}$,and c) $Vs_{(max)}$ at ground surface, 0.2 sec and 1 sec periods

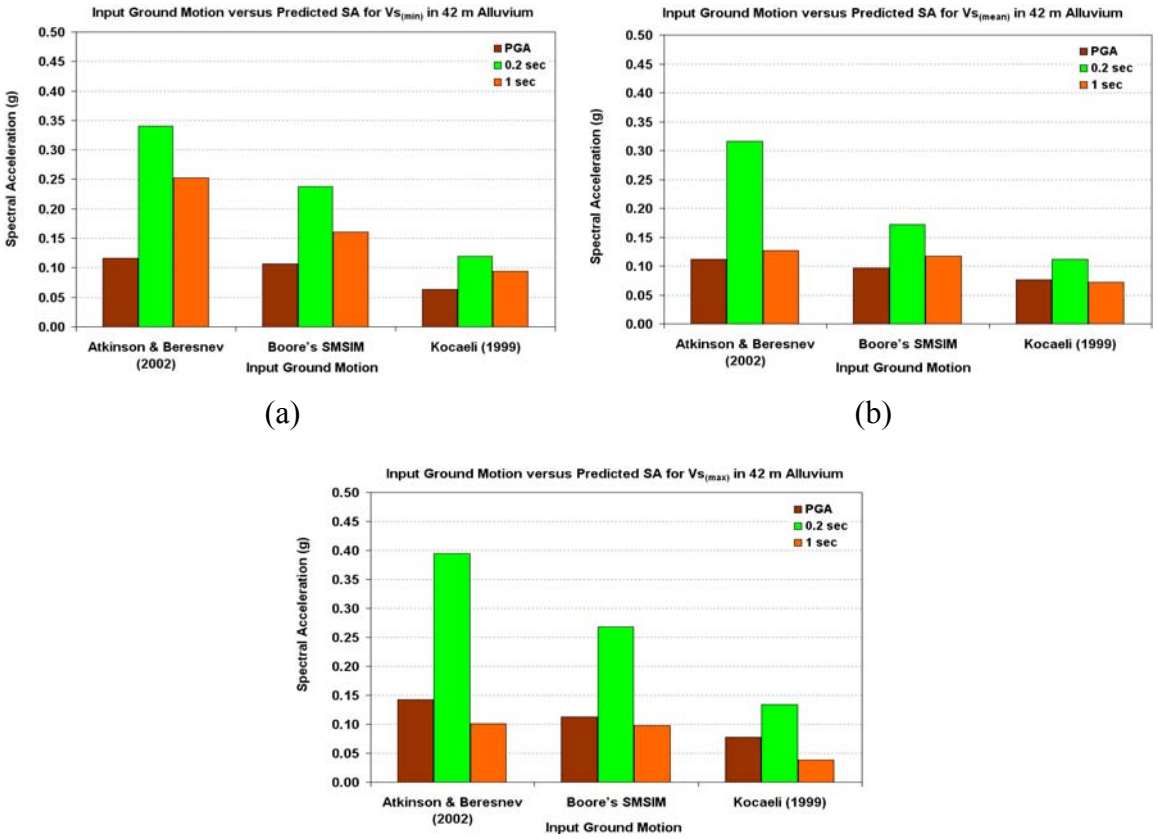

Figure 4.3. The effect of ground motion on spectral acceleration for sites underlain by 42 m of alluvium and a) $Vs_{(min)}$ b) $Vs_{(mean)}$ and c) $Vs_{(max)}$ at ground surface, 0.2 sec and 1 sec periods

The effects of different input rock motions are summarized in Figures 4.1 through 4.3, where ground motion parameters were compared separately for 18, 30 and 42 meter thick alluvial deposits. These histograms were prepared for PGA, 0.2 sec, and 1 sec periods, based on provisions contained in the International Building Code (IBC, 2003) and the USGS National Seismic Hazard Maps. These figures suggest that 0.2 sec period is more sensitive to the selected input time histories, where the differences in response range between 0.45 g and 0.10 g. On the other hand, 1 sec period and PGA values do not exhibit large differences, even though the input time histories vary considerably, with a

maximum difference in response of up to 0.15 g. These same comparisons were also carried out for sites underlain by 18, 30, and 42 meters of loess, as shown in Figures 4.4 through 4.6. In this case, 0.2 sec periods appear to be more sensitive to selected input motions than those predicted for 1 sec period and PGA. The range in acceleration for loess sites at 0.2 sec period range from 0.81 g to 0.10 g, and for PGA and 1 sec period, with a maximum difference in response of up to 0.14 g, close to that predicted for alluvial sites.

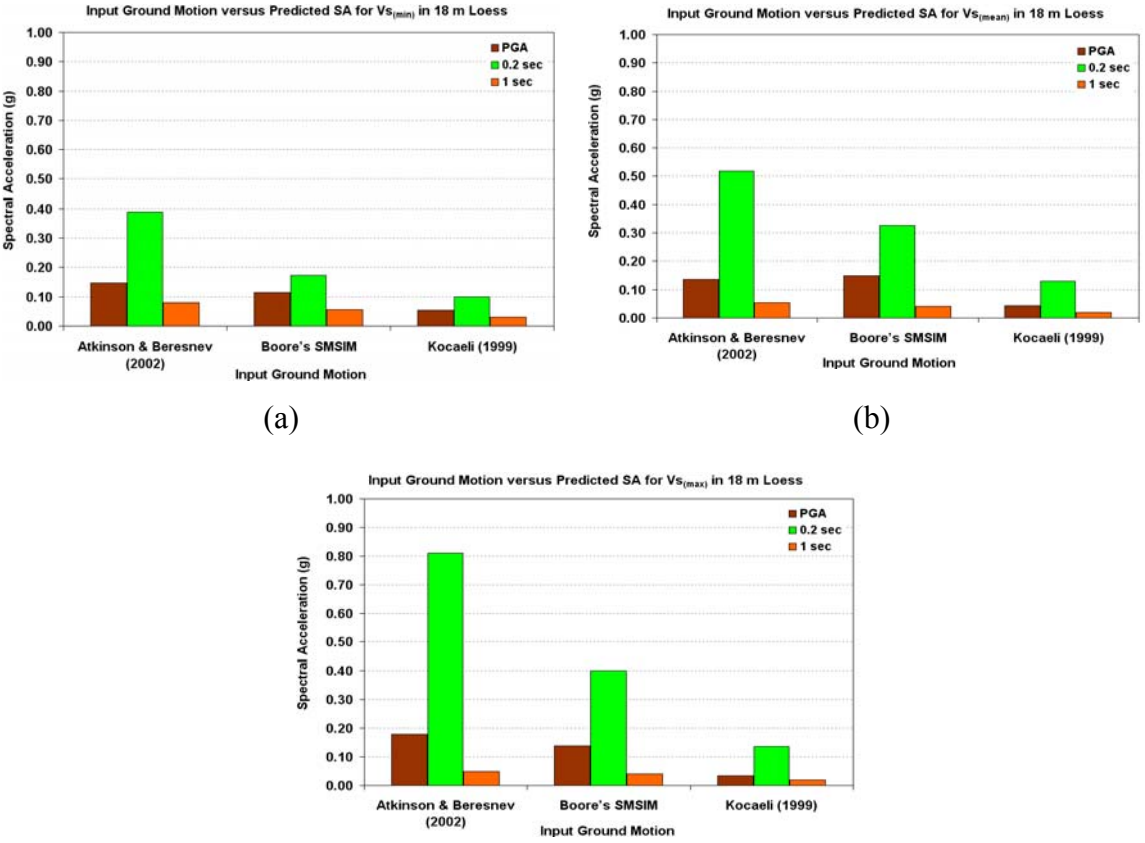

Figure 4.4. The effect of ground motion on spectral acceleration for sites underlain by 18 m of loess, with a) $Vs_{(min)}$ b) $Vs_{(mean)}$, and c) $Vs_{(max)}$ at ground surface, 0.2 sec and 1 sec periods

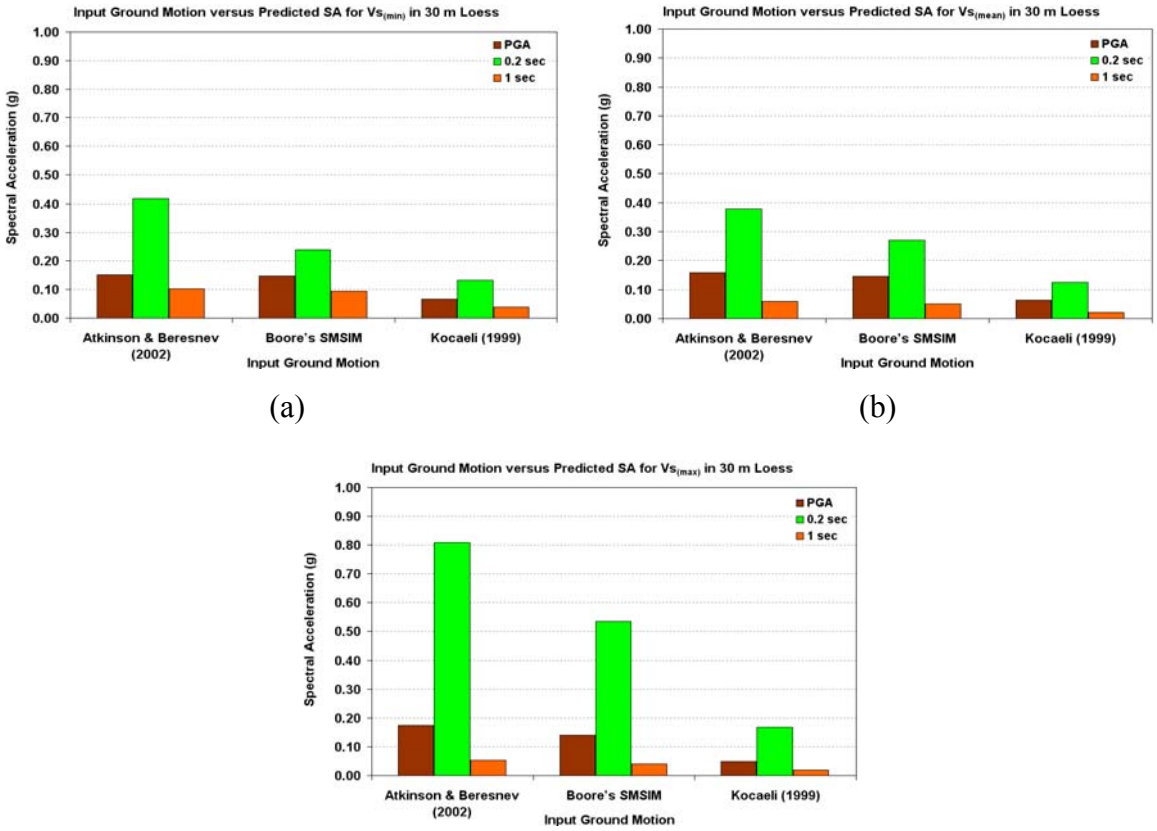

Figure 4.5. The effect of ground motion on spectral acceleration for sites underlain by 30 m of loess with a) $Vs_{(min)}$ b) $Vs_{(mean)}$,and c) $Vs_{(max)}$ at ground surface, 0.2 sec and 1 sec periods

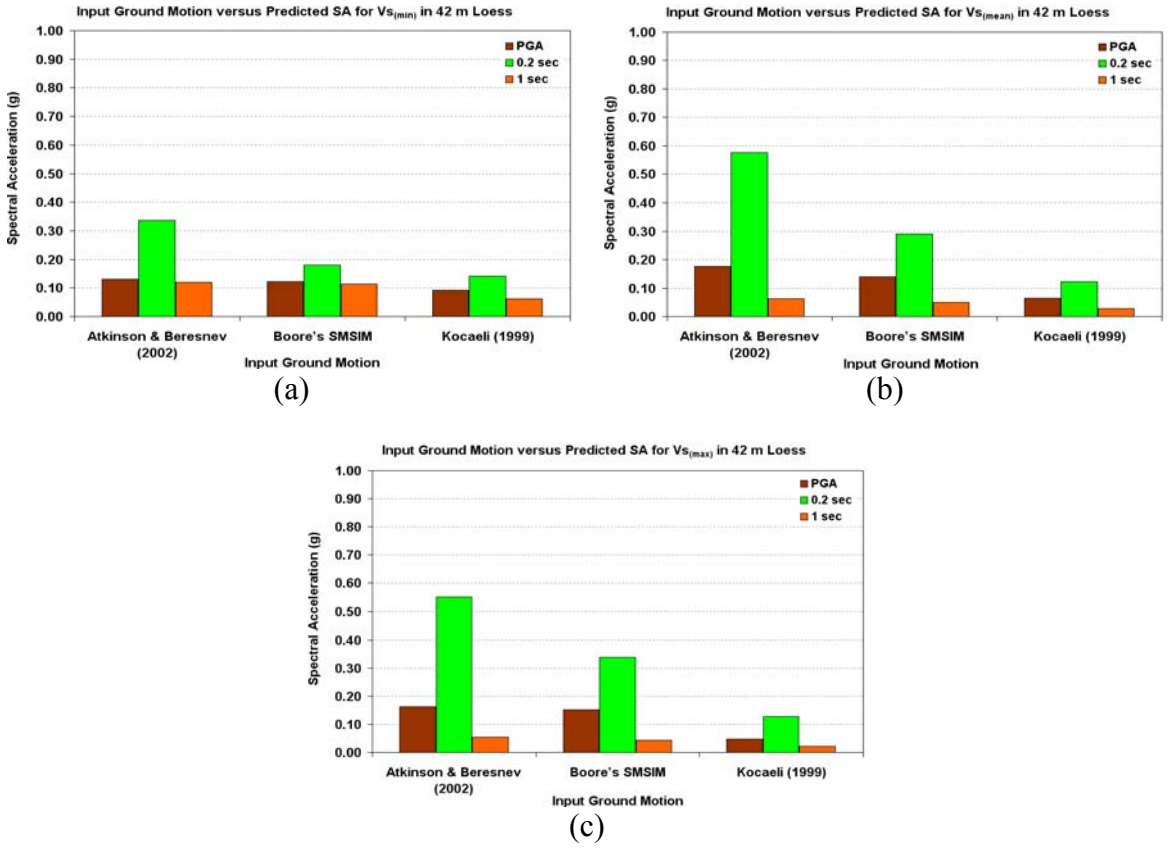

Figure 4.6. The effect of ground motion on spectral acceleration for sites underlain by 42 m of loess, with a) $Vs_{(min)}$ b) $Vs_{(mean)}$ and c) $Vs_{(max)}$ at ground surface, 0.2 sec and 1 sec periods

The input ground motions (either synthetic or actually recorded) on rock could have high acceleration values in their time domain records which also characterize the severity of the input motion. The maximum value of the record is commonly referred to as the peak acceleration. In Section 3, the peak accelerations of the selected earthquake were summarized in Table 3.1. The highest peak accelerations were calculated using input time histories from the Atkinson & Beresnev (2002) model, while the Kocaeli, Turkey Earthquake exhibited the lowest values. The Atkinson & Beresnev model also yielded higher spectral accelerations than the Boore SMSIM model. The lowest spectral accelerations were generated using the Kocaeli time history for PGA, 0.2 sec, and 1 sec

periods for the alluvium and the loess. The values listed in Figures 4.1 through 4.6 show different response characteristics for the three input time-histories. The difference between these earthquakes can vary as much as 83%, even when using the similar soil cap thickness and Vs values. The two synthetic earthquake time-histories are intended to better reflect the unusual paucity of wave energy damping in the CEUS, which contrasts markedly with earthquake-prone regions situated along recognized tectonic boundaries (Bolt, 1993). There remains considerable variation between the Atkinson & Beresnev (2002) and Boore SMSIM models, with the former predicting spectral accelerations as much as double those of the latter.

Predicted peak accelerations and periods contrast significantly for the different scenarios. The fundamental site periods were found to vary between 0.2 and 0.82 seconds. To examine the impact of these physical characteristics on predicted ground motion and the impact of local soil conditions on shape of the response spectra, the amplitude of surface accelerations have been normalized with respect to peak ground accelerations. This method has proven useful to create representative plots that compare the effects the physical variables controlling seismic site response (Seed et al., 1976). The normalized response spectra graphs are presented in Appendix B and the peak periods summarized below, in Table 4.3.

The response spectra is normalized by dividing the spectral accelerations by the maximum ground acceleration. The shape of response spectra can then be compared for different ground motions holding the shear wave velocity constant. For example, by assigning the mean shear wave velocity values to the soil caps, it was found that the peak period is developed at 0.4 seconds for alluvial sites 18 meters thick. The peak period gradually increases, with increasing thickness of the soil cap (see Table 4.3). A similar relationship was predicted for loess deposits (also shown in Table 4.3). For shallow loess deposits (~ 18 m thick), the peak acceleration is developed at 0.25 second period, which also increases with increasing thickness of the loess cap. When the mean shear wave velocities are assumed for alluvial sites, the maximum accelerations can be expected for: ~ 4-story structures on a 18 m thick cap; ~ 6-story structures on a 30 m cap; and ~ 7-story structures on 42 m caps of alluvium. Dual resonance was predicted when the soil thickness approaches 42 m, assuming minimum shear wave velocities ($Vs_{(min)}$). As

shown in Table 4.3, the peak (maximum) spectral accelerations are predicted at similar periods for all three earthquake models. It appears that the character of the input ground motion does not have a significant effect on the predicted period of the peak spectral acceleration. These comparisons also suggest that the peak periods increase with increasing soil thickness and tend to decrease with increasing shear wave velocity.

Table 4.3. Periods at which maximum spectral acceleration (Normalized) is developed within Alluvium and Loess deposits (values are in seconds)

Thickness of Alluvium	**Approximate Periods at which Maximum Spectral Acceleration is developed (from NORMALIZED DATA)**								
	Atkinson & Beresnev			**Boore's SMSIM**			**Kocaeli, Turkey**		
	$Vs_{(min)}$	**$Vs_{(mean)}$**	**$Vs_{(max)}$**	**$Vs_{(min)}$**	**$Vs_{(mean)}$**	**$Vs_{(max)}$**	**$Vs_{(min)}$**	**$Vs_{(mean)}$**	**$Vs_{(max)}$**
18 m	0.5	0.4	0.3	0.5	0.4	0.3	0.5	0.4	0.3
30 m	0.7	0.6	0.5	0.7	0.6	0.5	0.7	0.6	0.5
42 m	0.4/0.9	0.7	0.6	0.4/0.9	0.7	0.6	0.4/0.9	0.7	0.6
Thickness of Loess	**Atkinson & Beresnev**			**Boore's SMSIM**			**Kocaeli, Turkey**		
	$Vs_{(min)}$	**$Vs_{(mean)}$**	**$Vs_{(max)}$**	**$Vs_{(min)}$**	**$Vs_{(mean)}$**	**$Vs_{(max)}$**	**$Vs_{(min)}$**	**$Vs_{(mean)}$**	**$Vs_{(max)}$**
18 m	0.4	0.25	0.18	0.4	0.25	0.18	0.4	0.25	0.18
30 m	0.6	0.32	0.21	0.6	0.32	0.21	0.6	0.32	0.21
42 m	0.7	0.4	0.27	0.7	0.4	0.27	0.7	0.4	0.27

4.1.2. Influence of Surficial Geology and Thickness on Spectral Accelerations. Borehole data were plotted using the program ArcGIS and a top-of-bedrock elevation map was created using the Kriging method (Karadeniz, 2007). A soil cap thickness map was then prepared by subtracting the top-of-bedrock surface from the USGS digital elevation map (DEM) using the "spatial analyst tool" subroutine in ArcGIS9.2, described previously in Section 1. These operations produced a "prediction soil thickness map" of the unconsolidated surficial materials, with associated uncertainties.

In this study, the influence of varying soil thicknesses on the site response was evaluated by assigning 30 meters as a "mean soil thickness," and assuming 12 meters of error for both the alluvium and loess units. These values were selected because: i) 12 meters corresponds to maximum error for both geologic units (alluvium and loess); ii) to provide six subunit layers of equal (5 m) thicknesses. The influence of soil cap thickness on spectral accelerations for alluvium and loess are plotted graphically in Figures 4.7 through 4.12.

According to the analyses carried out as described above and summarized in Figures 4.7 thru 4.12, it appears that variations in soil thickness, of both alluvial and loess deposits, have negligible effects on the predicted PGA. When a given earthquake is evaluated using the three different models, the maximum variance in spectral accelerations is about 0.04 g for both the alluvium and the loess. This suggests that the predicted PGA is not overly sensitive to the thickness of the soil cap. However, variations in thickness of the soil cap are easily discerned at ~0.2 sec periods. This difference in response is most pronounced when alluvium and loess are 30 m thick and shear wave velocity is greater than the mean value. For example, the greatest difference in predicted spectral acceleration due to soil thickness is about 0.18 g for alluvium and 0.26 g for loess deposits. Hence, 0.2 sec periods appear to be more sensitive to variations in soil thickness. A proportional relationship is suggested at 1 sec period for spectral accelerations, where increasing soil thickness appears to cause higher spectral accelerations and; hence, marked differences in response. This relationship is very noticeably, especially, for alluvium. At 1 sec periods the change in soil thickness also triggers corresponding changes in the predicted spectral accelerations, of up to 0.16g. The

difference in spectral accelerations caused by changes in soil thickness is greatest when the minimum shear wave velocities are assumed, but this variance decreases with increasing shear wave velocity. Moreover, variations in soil thickness do not appear to have any significant impact on the predicted spectral accelerations for loess deposits, when assuming maximum shear wave velocities at 1 second periods. It appears that 1 second periods are more sensitive to changes in soil thickness for lower shear wave velocities and much less sensitive as shear wave velocities increase.

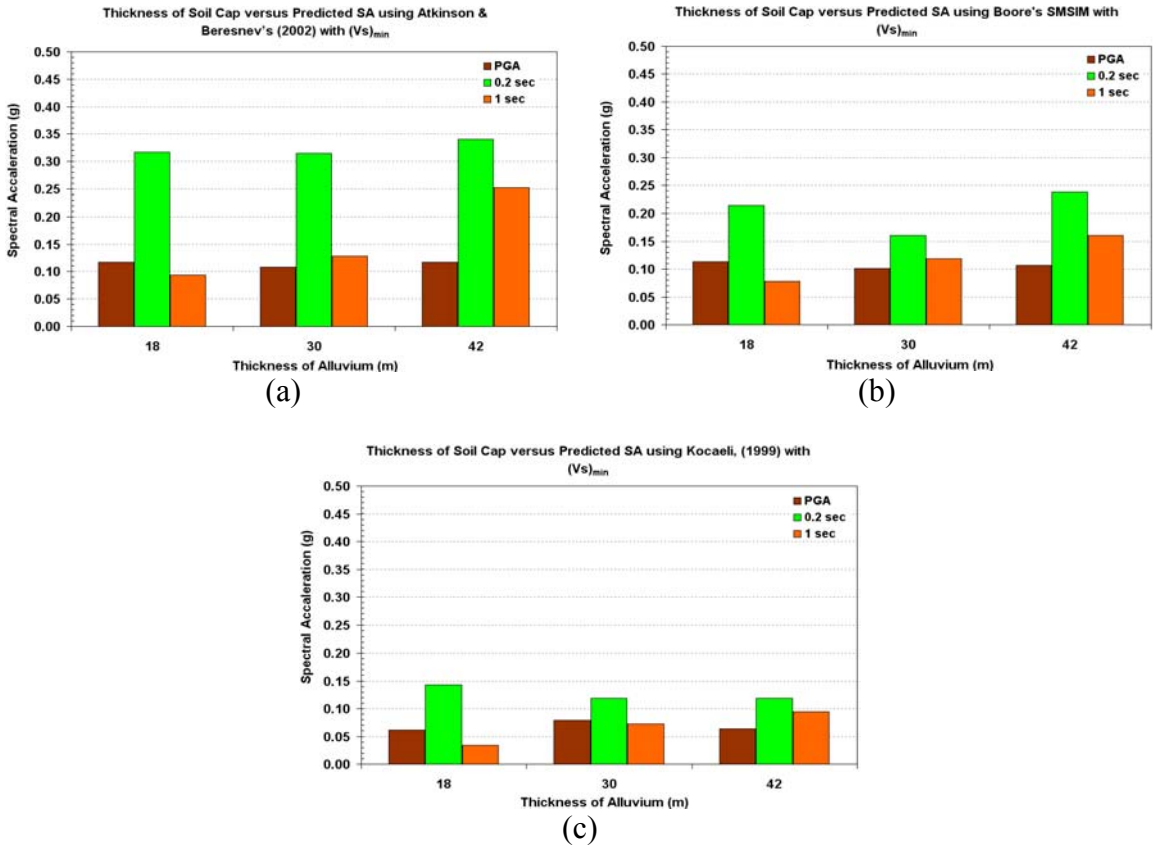

Figure 4.7. The effect of alluvium thickness on spectral acceleration for $Vs_{(min)}$, using: a) Atkinson & Beresnev (2002); b) Boore SMSIM; and, c) Kocaeli earthquake ground motions at the ground surface, 0.2 sec, and 1 sec periods.

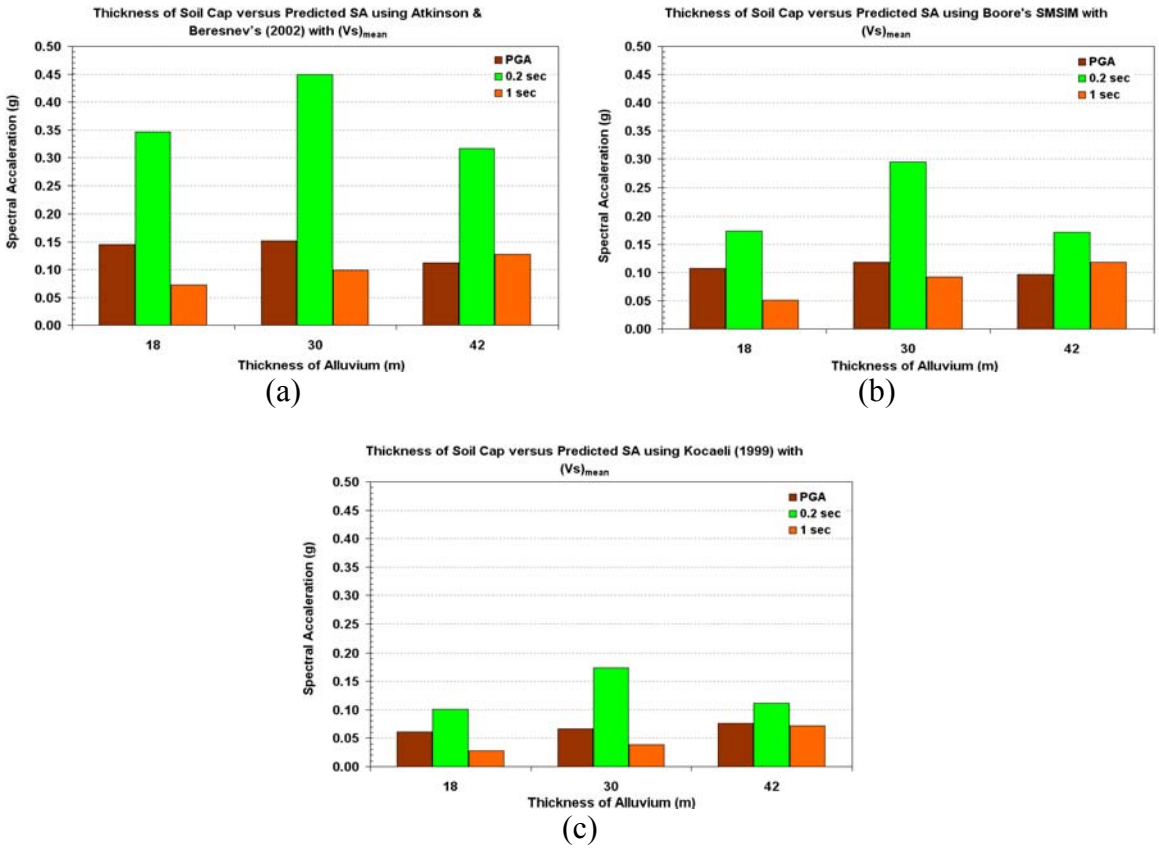

Figure 4.8 The effect of alluvium thickness on spectral acceleration for $Vs_{(mean)}$ using: a) Atkinson & Beresnev (2002) b) Boore SMSIM and c) Kocaeli earthquake at ground surface, 0.2 sec and 1 sec periods

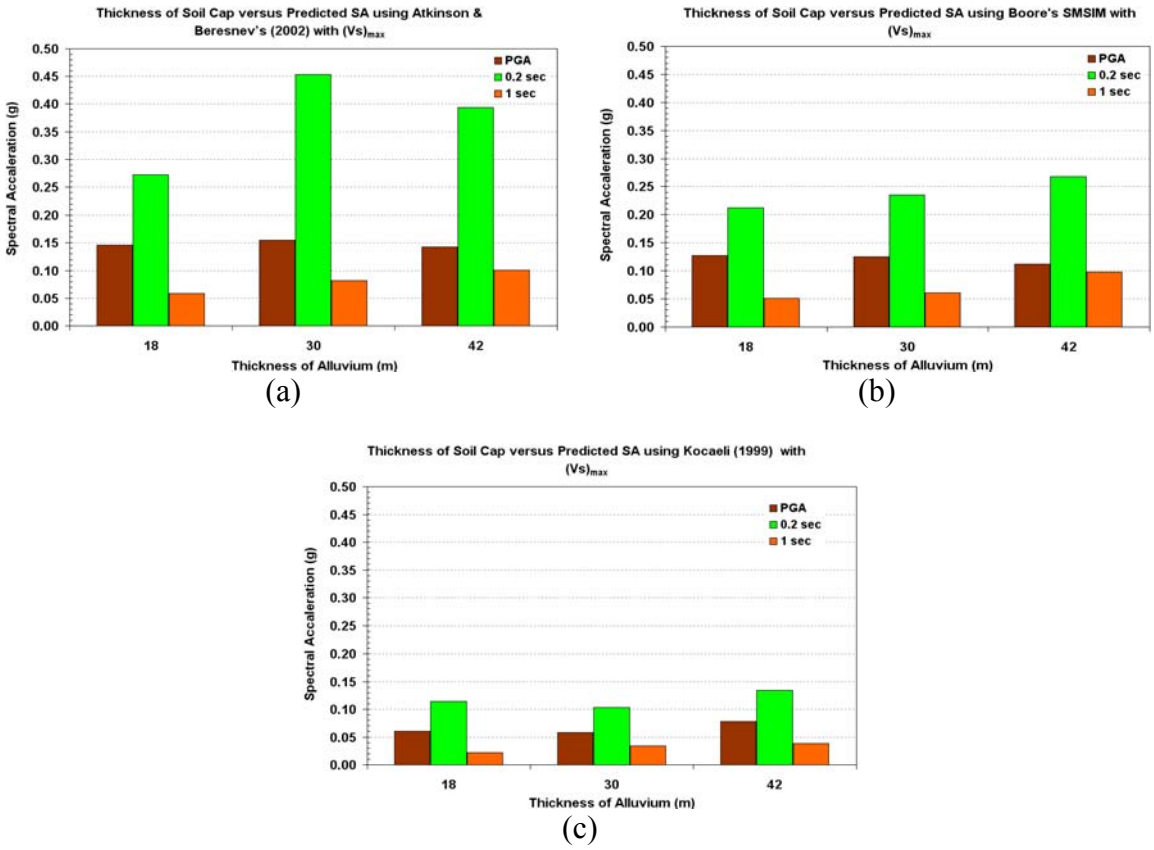

Figure 4.9. The effect of alluvium thickness on spectral acceleration for $Vs_{(max)}$, calculated using: a) Atkinson & Beresnev (2002) b) Boore SMSIM and c) Kocaeli earthquake at ground surface, 0.2 sec and 1 sec periods

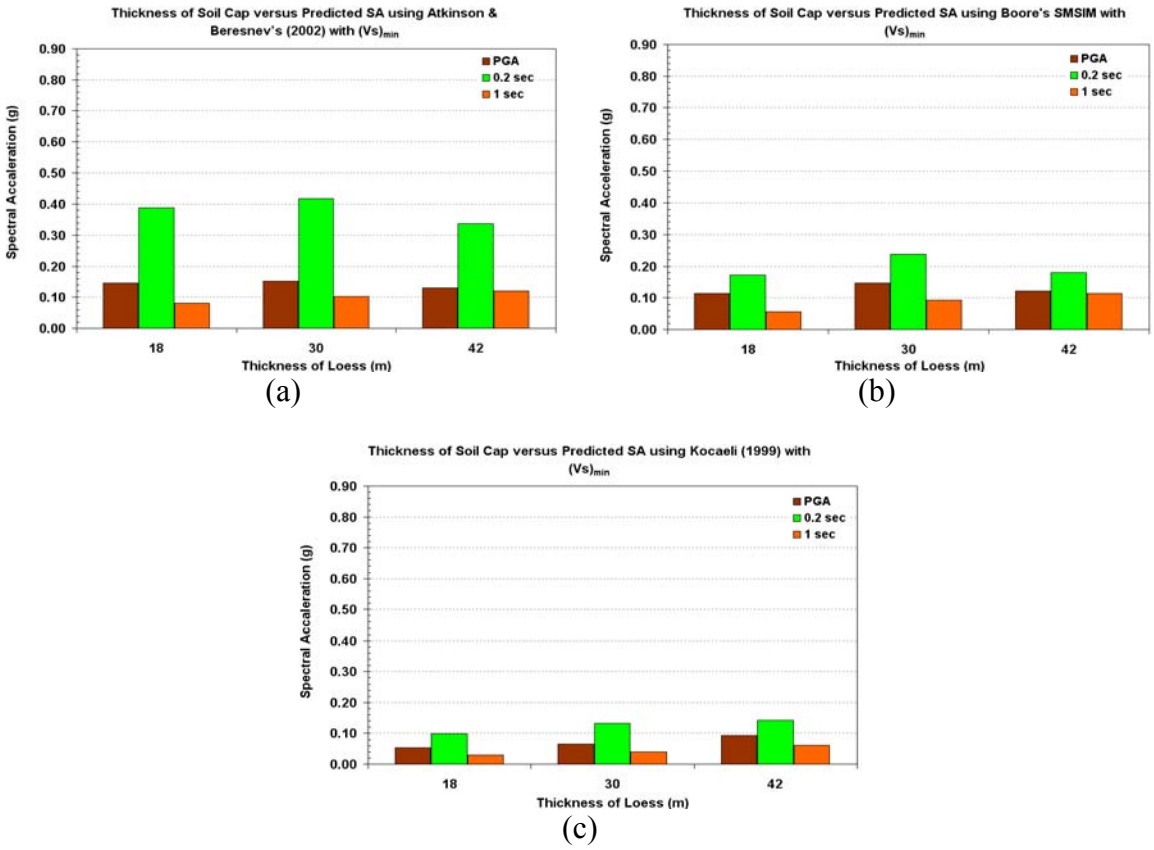

Figure 4.10. The effect of loess thickness on spectral acceleration for $Vs_{(min)}$ using: a) Atkinson & Beresnev (2002) b) Boore SMSIM and c) Kocaeli earthquake at ground surface, 0.2 sec and 1 sec periods

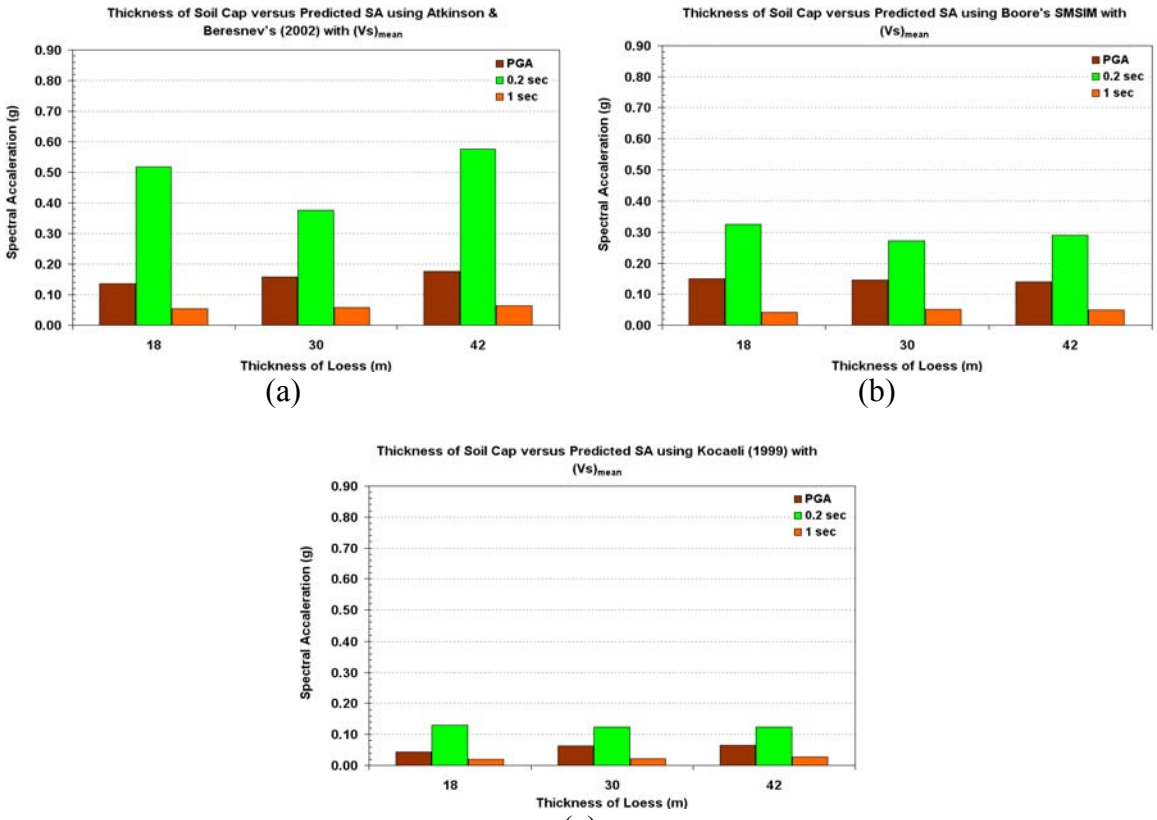

Figure 4.11. The effect of loess thickness on spectral acceleration for $Vs_{(mean)}$ using: a) Atkinson & Beresnev (2002) b) Boore SMSIM and c) Kocaeli earthquake at ground surface, 0.2 sec and 1 sec periods

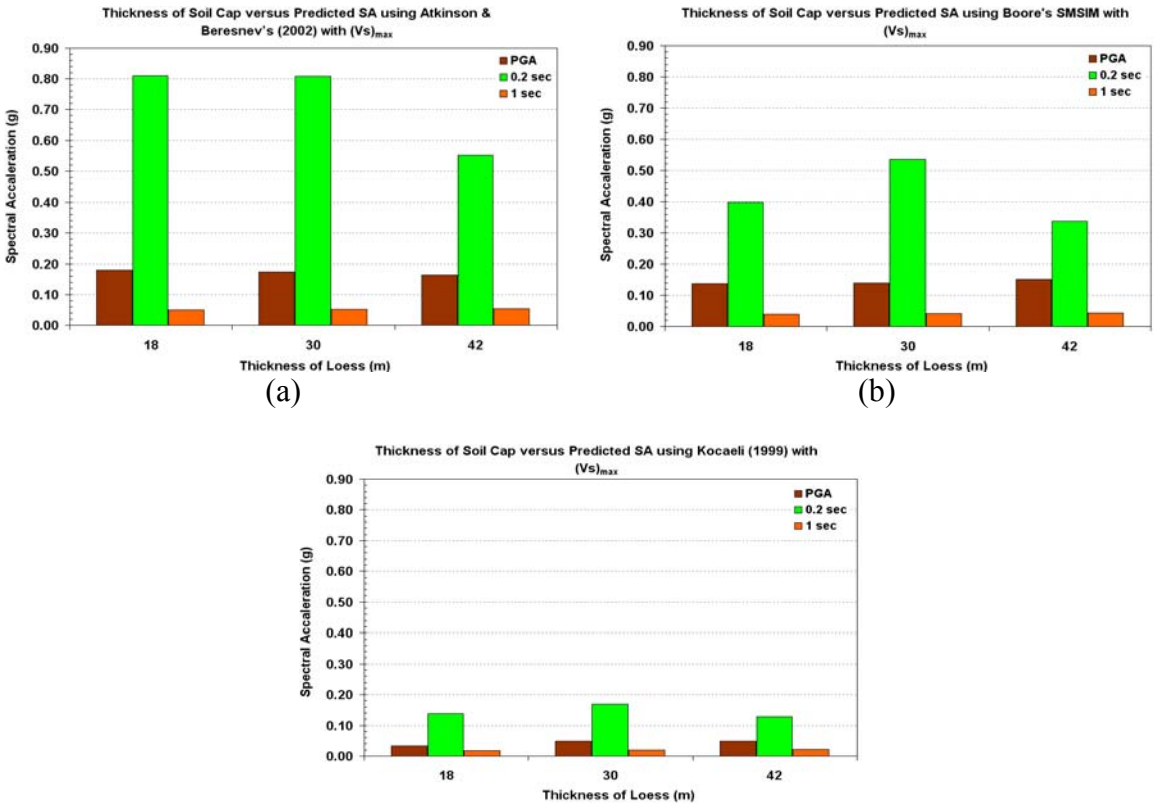

Figure 4.12. The effect of loess thickness on spectral acceleration for $Vs_{(max)}$ using: a) Atkinson & Beresnev (2002) b) Boore SMSIM and c) Kocaeli earthquake at ground surface, 0.2 sec and 1 sec period

Loess and alluvium deposits were also compared for their peak periods. As presented in Table 4.2, lower peak periods were observed for loess deposits, as compared to alluvial sites of equal thickness. Loess deposits, as discussed in Section 2, tend to exhibit greater stiffness than the alluvial deposits due to their Aeolian deposition (much less moisture at time of deposition) and subsequent diagenetic effects, such as wetting-drying cycles, desiccation, and oxidation. This stiffness contrast causes the peak periods to decrease in loess, as compared to alluvium, for the same thickness. The maximum spectral acceleration was predicted to occur at 0.6 seconds for alluvium, and 0.32 seconds for loess, assuming both units were 30 m thick. Those sites underlain by stiffer soils tend

to exhibit peak spectral accelerations at lower periods, while the converse of this holds for sites underlain by softer deposits, which tend to exhibit peak spectral accelerations at much higher periods. The suggested variance in peak periods suggests that soil stiffness exerts a controlling influence on the predicted response spectra.

Seismic energy can be trapped in the soil cap when the period of the arriving energy pulses becomes coincident with the fundamental site period, or with harmonics of the fundamental site period. Resonance realizes its maximum effect when the returning and sending seismic waves become in phase with each other (Reiter, 1990). The characteristic site (natural) period, T_s, is a useful indication of the period where the highest spectral accelerations can be expected, and it is usually a function of the soil unit thickness and its respective shear wave velocity. The characteristic, or natural, site period (T_s) is commonly estimated by;

$$T_S = \frac{4H}{V_s} \tag{2}$$

Where H is soil thickness and Vs is mean shear wave velocity (Kramer, 1996; Dobry et al., 2000). As mentioned previously, in this study the soil profiles were subdivided into layers of equal thickness and assigned their respective shear wave velocity values. The harmonic means of shear wave velocities were calculated for soil caps of 18 m, 30 m, and 42 m, using the methodology suggested by Dobry et al. (2000). The harmonic means method of computing the characteristic site period yields more appropriate results for site response analyses. By applying the harmonic means method to Equation 2, the characteristic site period of alluvial and loess covered sites were calculated using wave length analyses (Cramer, 2008) and the results are presented in Table 4.4. Characteristic site periods are range from 0.33 to 0.93 for alluvium and 0.21 to 0.74 for loess.

The peak periods calculated using Shake2000 (Table 4.3) and the characteristic site periods calculated using Equation 2 (Table 4.4) exhibit very similar results, for both alluvium and loess covered sites. This finding highlights the importance of local site effects on the predicted response spectra, and serves to validate Equation 2. The peak acceleration and periods are markedly different for different soil thicknesses and shear

wave velocities. In addition, it reinforces the efficacy of wave length analyses techniques to estimate the characteristic site periods.

The peak accelerations tend to occur at rather high periods on thicker (~42 m) soil deposits. In addition, as the stiffness of soil increases, the peak period tends to diminish. The thickness and stiffness of the soil column directly affects the characteristic site period. The characteristic site period increases as the thickness of the soil cap increases, probably, due to increasing confinement. In summary, high-rise structures could be expected to suffer more damage on thicker soil deposits than low-rise structures; while, at the same time, low-rise structures could be expected to suffer more damage on shallow soil deposits than taller structures, as illustrated in Figure 4.13.

Overall, the general "sensitivity" of site response to variations in soil cap thickness suggest the following: a) at 0.2 sec periods, the 30 m thick soil cap exhibits either similar or higher response than 18 m and 42 m thick soil caps, for both alluvial and loess deposits; and, b) at 1 sec periods, the response of a 30 m thick soil cap is either between the response of 18 m and 42 m thick soil caps, or the response did not exhibit any marked change.

4.1.3. Influence of Weathered Rock on Spectral Accelerations. As mentioned in Section 2, 2 m of weathered rock residuum is usually observed capping the Paleozoic-age strata underlying loess deposits on the Missouri side of the Granite City Quadrangle. Response spectrum analyses were carried out for loess deposits with and without considering this weathered residuum and the response compared, in Figures 4.14 thru 4.16. The difference between spectral accelerations for PGA, 0.2 second, and 1 second with and without the weathered residuum was very slight, in all cases. The maximum difference in site response for loess due to the presence of 2 m of weathered residuum is only ~0.01 g. Therefore, predictions of seismic site response on the Missouri side of the Mississippi River do not appear to be sensitive to the existence of this residuum layer.

4.1.4. Influence of Shear Wave Velocity on Spectral Accelerations. As mentioned previously, in a recent study Karadeniz (2007) compiled representative shear wave velocity profiles for the St Louis Metro Area from various sources. These data were analyzed statistically, based on local lithologic and stratigraphic characteristics, and then

recompiled into nine generic profiles, felt to be representative of the various geomorphic and physiographic provinces comprising the greater metro area. Table 3.2 summarizes the shear wave velocity profiles with their associated uncertainties. Mean shear wave velocities range between 134 m/sec and 286 m/sec in alluvium, and 179 m/sec to 539 m/sec in loess, to a depth of 30 meters. Using these hybrid shear wave velocity values, 30 m soil profiles were divided into six homogeneous layers (each 5 m thick) and site response analysis were undertaken.

Table 4.4. Wave Length Analysis Results for Alluvium and Loess

Soil Thickness	**Characteristic Site period T_s (sec)**					
	Alluvium			**Loess**		
	Min Vs	**Mean Vs**	**Max Vs**	**Min Vs**	**Mean Vs**	**Max Vs**
18 m	0.5	0.40	0.33	0.42	0.28	0.21
30 m	0.72	0.58	0.48	0.59	0.38	0.28
42 m	0.93	0.75	0.62	0.74	0.47	0.35

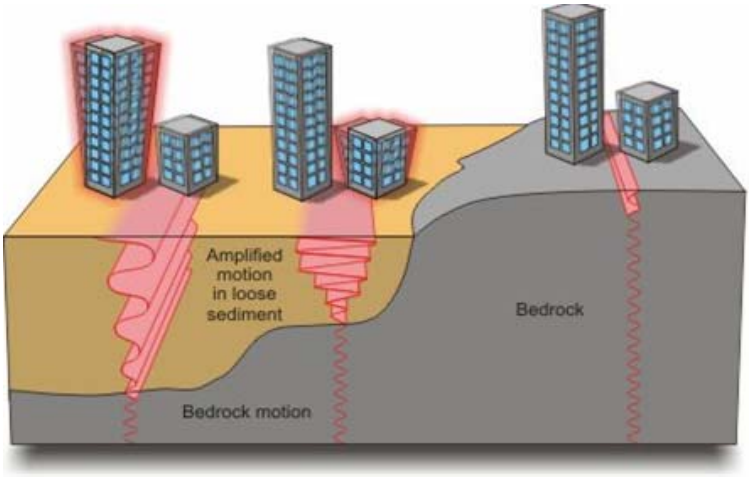

Figure 4.13. Effect of soil thickness on structures of varying height (adapted from Clague and Turner, 2003)

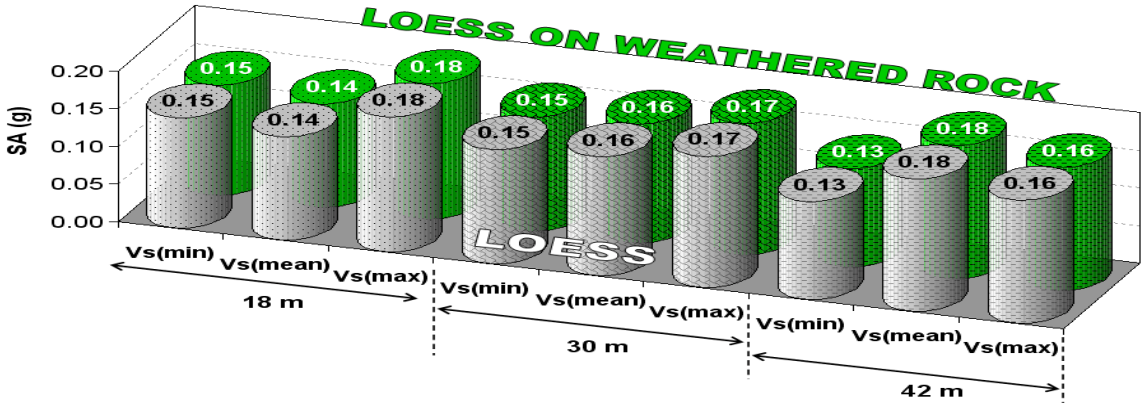

a) PGA

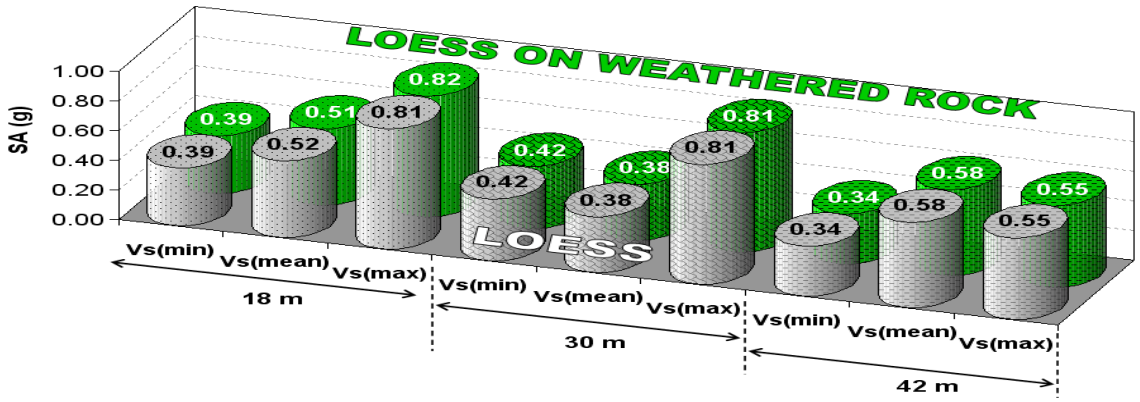

b) 0.2 sec period

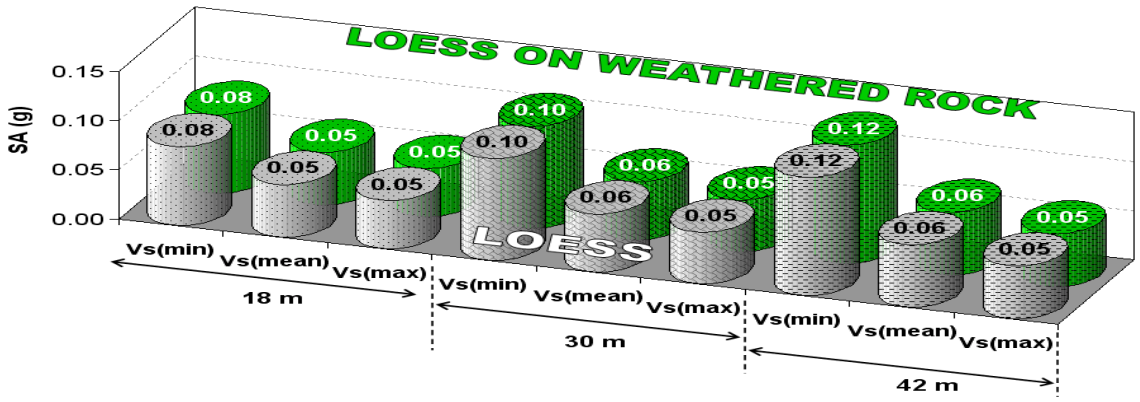

c) 1 sec period

Figure 4.14. The influence of a 2 m thick layer of residuum over Paleozoic age bedrock on spectral acceleration for loess soil cap, using the Atkinson & Beresnev (2002) model.

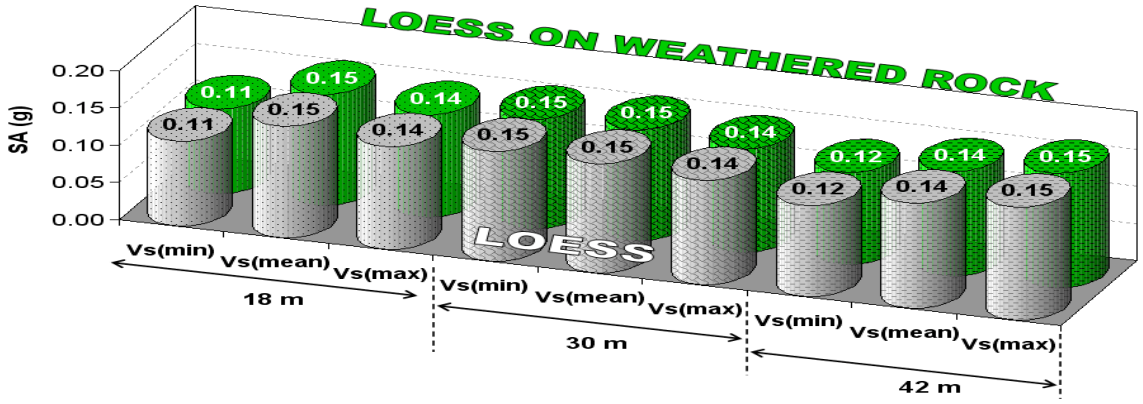

a) PGA

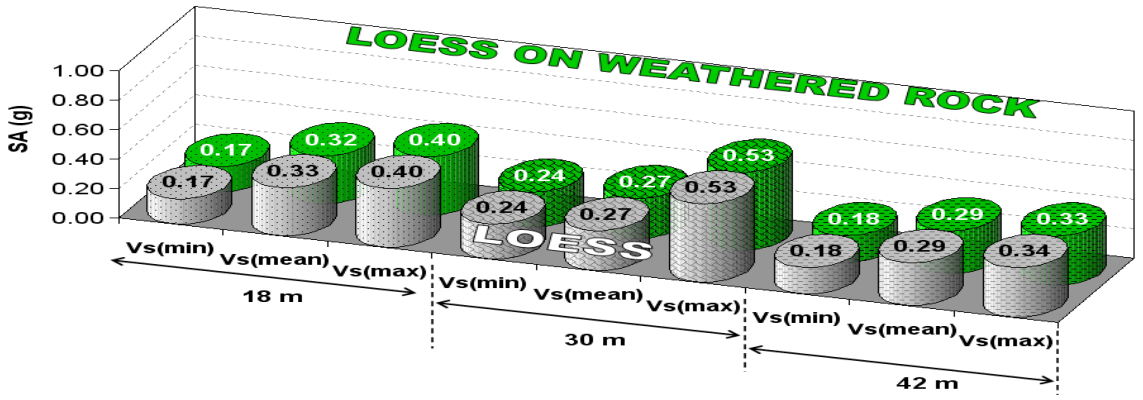

b) 0.2 sec period

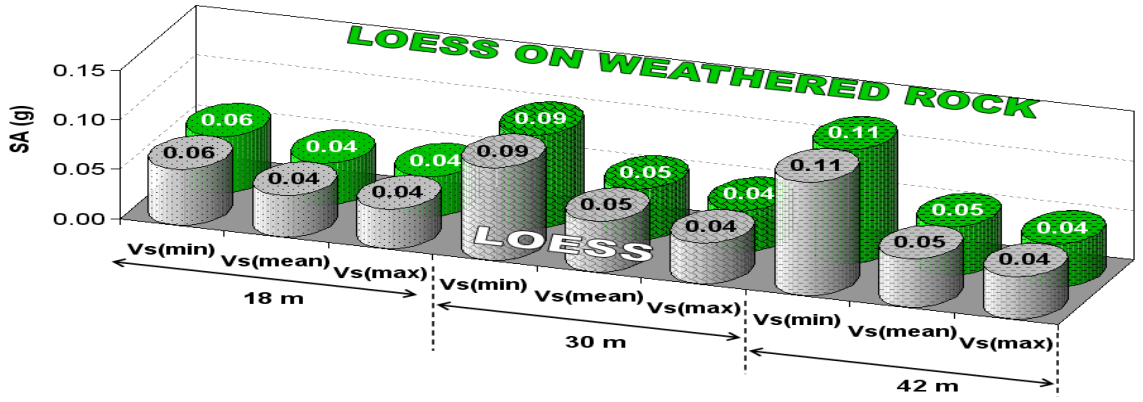

c) 1 sec period

Figure 4.15. The influence of a 2 m thick layer of residuum over Paleozoic age bedrock on spectral acceleration for loess soil cap, using the Boore's SMSIM model.

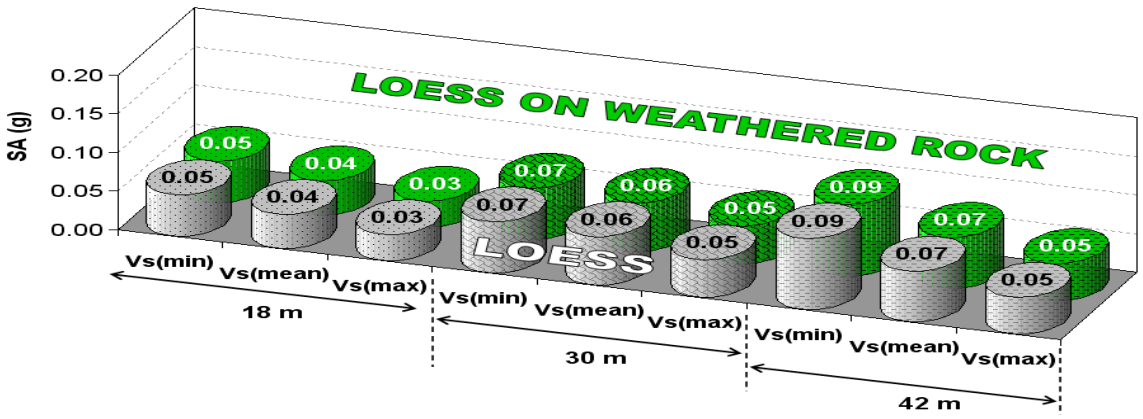

a) PGA

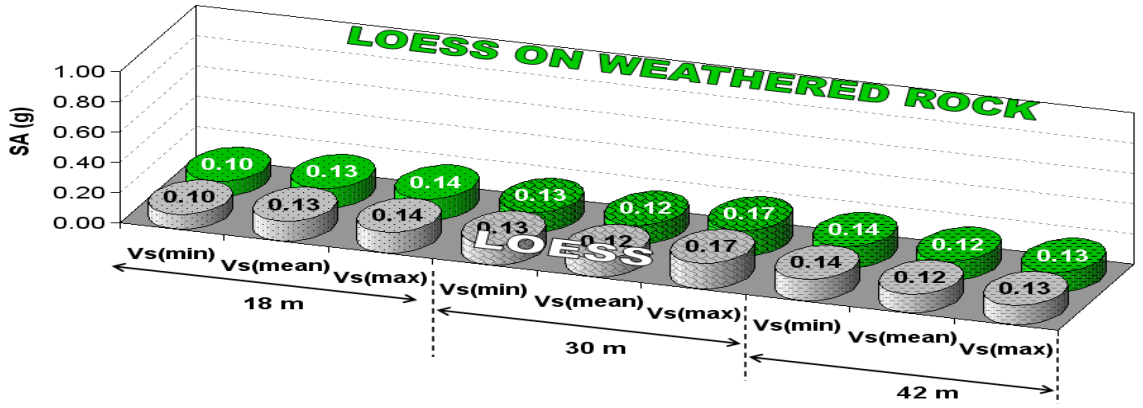

b) 0.2 sec period

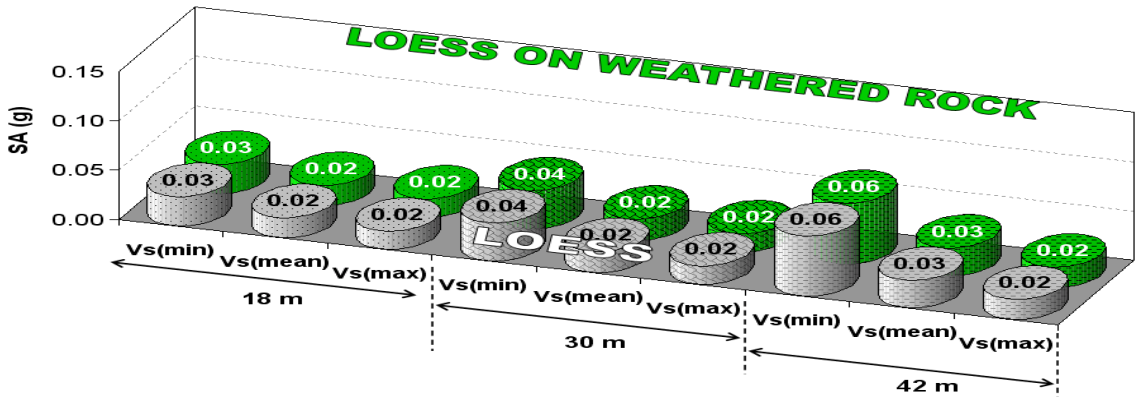

c) 1sec period

Figure 4.16. The influence of a 2 m thick layer of residuum over Paleozoic age bedrock on spectral acceleration for loess soil cap, using the 1999 Kocaeli earthquake.

Figure 4.17 and Figure 4.18 present test results for both alluvium and loess covered sites. These suggest that shear wave velocity has negligible effects on estimating the PGA for both alluvium and loess covered sites. The maximum difference in response was between zero and 0.04 g. When the input motions and soil thickness were held constant, the maximum shift in spectral accelerations for PGA was predicted for 30 m thick cap of alluvium. However, the corresponding variance for loess was lowest for a 30 meter thick sequence. This disparity is likely ascribable to the increased thickness of the loess as compared to alluvium.

The most significant effect of shear wave velocity on spectral acceleration is seen at 0.2 sec periods, for 18 meters and 30 meters of loess, where the maximum difference in predicted response reached 0.43g. Spectral accelerations calculated on alluvial deposits of 30 meters thickness exhibited a noticeable difference at 0.2 sec period, up to 0.14 g. This is likely because the characteristic period of the loess covered sites is close to 0.2 seconds.

At 1 sec periods, an inverse relationship was observed between the shear wave velocity and spectral acceleration values, for both alluvium and loess. In general, the higher the shear wave velocities, the lower the predicted spectral accelerations. The maximum variance in spectral acceleration due to varying the shear wave velocities was no more than 0.15g at 1 sec period.

4.2. AMPLIFICATION

Amplification factors for different scenarios were plotted and compared for alluvium and loess deposits for PGA, 0.2 sec, and 1 sec periods. These results are summarized in Figures 4.19, 4.20, and Table 4.5. Within 54 different scenarios, the amplification varies between about 2 to 4.4 for PGA, 1.7 to 5.3 at 0.2 seconds, and 1.2 to 5.4 at 1 second periods. The minimum observed amplification factor was 1 and deamplification was not predicted in either loess or alluvium. As discussed in Section 2 and Figures 4.14 thru 4.16, a 2 m thick seam of residuum between the underlying bedrock and the unconsolidated loess cap does not exert any noticeable influence on the response spectra. The predicted response spectra and amplification factors for loess-over-bedrock

and loess-over-weathered residuum-over-bedrock were essentially the same. It would appear that the 2 m seam is of insufficient thickness to make any appreciable difference.

4.2.1. Influence of Shear Wave Velocities on Amplification. Changes in shear wave velocity appear to have little effect on amplification for PGA when the alluvial soil cap is ~18 m thick and about 30 m thick for loess. On the other hand, changes in amplification appear more significant for alluvial sites of medium thickness (~30 m) and loess sites of extreme thickness (~42 m), assuming similar changes in shear wave velocity.

It is observed that highest amplifications are caused by the combination of same intensity of ground motion and shear wave velocity when PGA is in consideration for 18 meters of loess. The scenario which involves Atkinson & Beresnev earthquake (the strongest ground motion) and maximum shear wave velocity, highest amplification is observed. Similarly, the highest amplification is observed for another scenario where Boore earthquake (medium intensity ground motion), and mean shear wave velocity are used. Likewise, the combination of Kocaeli earthquake (least strong motion), and minimum shear wave velocity resulted with the highest amplification. Interestingly, the opposite relationship is observed for 18 meters of alluvium for PGA where small intensity of input ground motion and shear wave velocity causes lowest amplifications. Conversely, the strongest ground motion and minimum shear wave velocity combined exhibits the lowest amplifications. The highest amplifications appear to be triggered by maximum shear wave velocities for PGA when the alluvium thickens to its maximum value of ~42 m. No similar relation was predicted in loess covered sites for PGA. The shear wave velocities tend to increase with increasing depth and confinement.

On alluvium, at 0.2 sec period, $Vs_{(mean)}$ were found to trigger the highest amplifications in 30 m thick soil caps, but the lowest amplifications in caps of 42 m thickness. On Loess, at 0.2 sec period, $Vs_{(max)}$ velocities engendered the highest amplifications while $Vs_{(mean)}$ values yielded the lowest amplifications, for both 18 m and 30 m unit thicknesses. The amplification factors of loess deposits were generally higher than the alluvial deposits, to as much as 190% (Figure 4.19 and Figure 4.20).

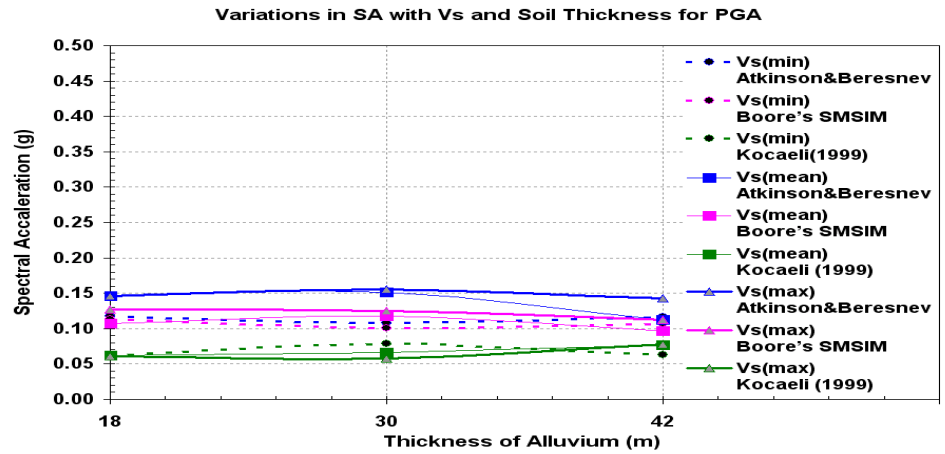

(a)

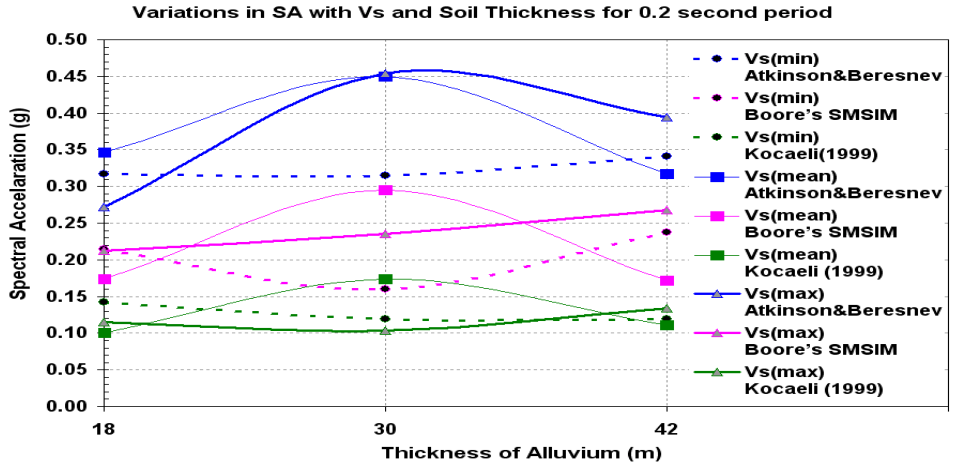

(b)

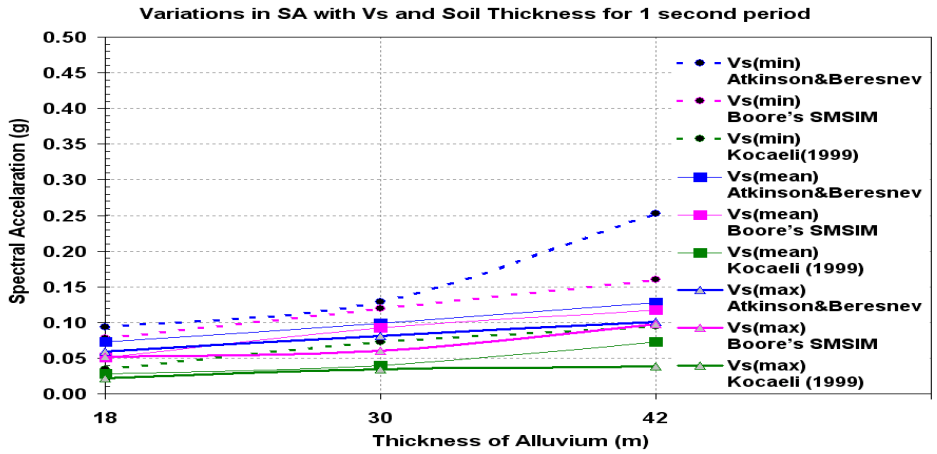

(c)

Figure 4.17. The effect of shear wave velocity and thickness of the soil cap on spectral accelerations for alluvium, at: a) ground surface, b) 0.2 sec and c) 1 sec periods

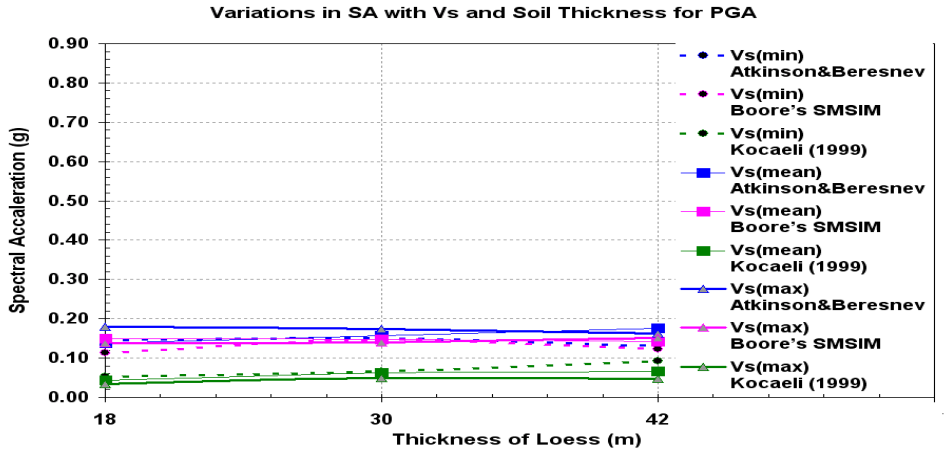

(a)

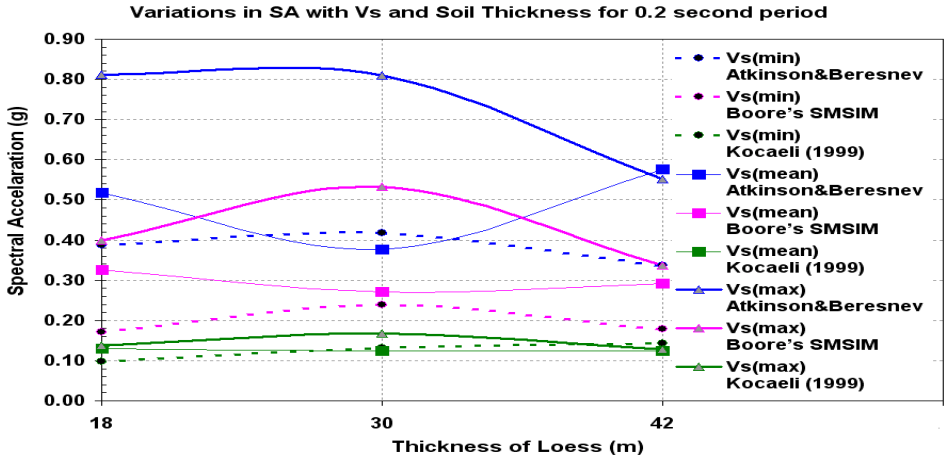

(b)

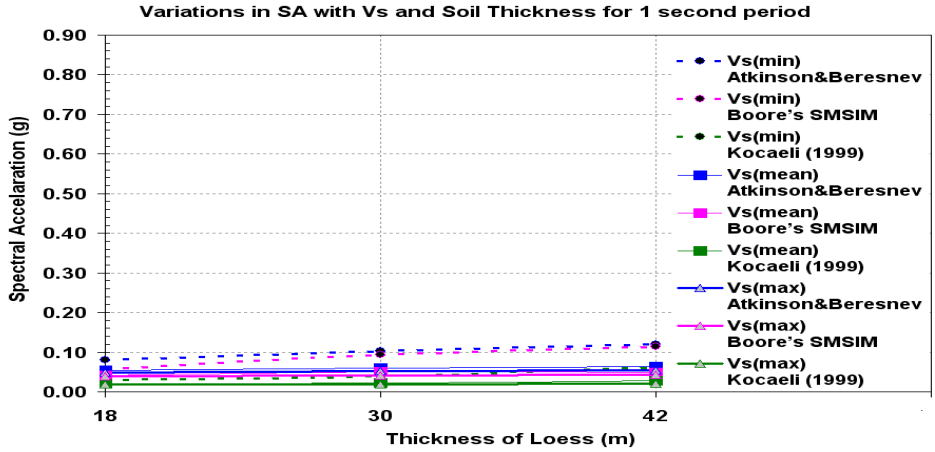

(c)

Figure 4.18. The effect of shear wave velocity and thickness of the soil cap on spectral accelerations for loess, at: a) ground surface, b) 0.2 sec and c) 1 sec periods

Table 4.5. Calculated amplification factor for all scenarios

Soil Type	Time history	Min Vs			Mean Vs			Max Vs			Soil Thickness (m)
		PGA	0.2 sec	1 sec	PGA	0.2 sec	1 sec	PGA	0.2 sec	1 sec	
ALLUVIUM	Atkinson & Beresnev (2002)	2.2	1.9	2.0	2.8	2.1	1.5	2.8	1.7	1.2	18
		2.0	1.9	2.7	2.9	2.7	2.1	2.9	2.8	1.7	30
		2.2	2.1	5.3	2.1	1.9	2.7	2.7	2.4	2.1	42
	Boore's SMSIM	2.8	2.6	2.1	2.6	2.1	1.4	3.1	2.6	1.4	18
		2.5	1.9	3.2	2.9	3.5	2.5	3.0	2.8	1.6	30
		2.6	2.9	4.3	2.3	2.1	3.1	2.7	3.2	2.6	42
	Kocaeli, Turkey	3.4	4.3	2.0	3.4	3.0	1.6	3.3	3.5	1.2	18
		4.4	3.6	4.1	3.6	5.3	2.2	3.2	3.1	1.9	30
		3.5	3.6	5.4	4.2	3.4	4.1	4.3	4.0	2.2	42

Soil Type	Time history	Min Vs			Med Vs			Max Vs			Soil Thickness (m)
		PGA	0.2 sec	1 sec	PGA	0.2 sec	1 sec	PGA	0.2 sec	1 sec	
LOESS	Atkinson & Beresnev (2002)	2.8	2.4	1.7	2.6	3.2	1.1	3.4	4.9	1.0	18
		2.9	2.6	2.2	3.0	2.3	1.2	3.3	4.9	1.1	30
		2.5	2.1	2.5	3.3	3.5	1.3	3.1	3.4	1.1	42
	Boore's SMSIM	2.8	2.1	1.5	3.6	3.9	1.1	3.3	4.8	1.1	18
		3.6	2.9	2.5	3.6	3.3	1.4	3.4	6.4	1.1	30
		3.0	2.2	3.1	3.4	3.5	1.3	3.7	4.1	1.1	42
	Kocaeli, Turkey	3.0	3.0	1.7	2.4	3.9	1.2	1.9	4.1	1.0	18
		3.6	4.0	2.2	3.5	3.7	1.2	2.7	5.1	1.1	30
		5.1	4.3	3.5	3.6	3.7	1.6	2.6	3.9	1.2	42

At 1 sec periods for both alluvium and loess, the input of $Vs_{(min)}$ values resulted in highest predicted amplifications, while $Vs_{(max)}$ values resulted in the lowest amplifications for the range of soil thicknesses evaluated (18 to 42 m). In addition, as the thickness of the soil cap increases the predicted differences between amplification factors for different shear wave velocities becomes increasingly significant (figures 4.19 and 4.20).

4.2.2. Influence of Soil Cap Thickness on Site Amplification. Loess and alluvium exhibited contrasting amplification characteristics for three different ground motions and ground motion parameters (PGA, 0.2sec and 1 sec). The highest amplifications were usually predicted in 30 m and 42 m thick caps for PGA and 0.2 sec periods. At 1 sec periods for both alluvium and loess, the amplification factor appears to increase with increasing thickness of the soil cap. The less-stiff (softer) alluvial deposits generally exhibit higher amplifications than stiffer loess deposits. For both alluvial and loess covered site, the lowest amplifications were observed when the soil cap was only 18 m thick, while the highest amplifications were predicted for the much thicker soil caps (~42 m) at 1 sec periods.

In summary, higher amplifications are predicted on the thinner (~18 m) soil caps at 0.2 second periods and, conversely, higher amplifications are predicted on deeper (~42 m) soil caps at 1 second periods. An inverse relation between the shear wave velocity and amplification factor is observed at 1 second periods. In general terms the higher the shear wave velocity, the lower the amplification factor.

In Figures 4.21 and 4.22 all 54 scenarios (described in Section 3) are compared by plotting amplification versus spectral acceleration. The plots suggest that the predicted site amplifications and associated uncertainties are very sensitive to the input time histories. The Kocaeli earthquake results in much higher amplifications, but lower spectral accelerations, while the Atkinson & Beresnev (2002) model predicts lower amplifications, but with much higher spectral accelerations. These findings suggest that we can expect higher amplifications to result from weaker rock accelerations, which is a well recognized premise of site response (Hough et al, 1990). The weaker ground motions engender less shear strain and lower damping ratios, which trigger increased site amplification.

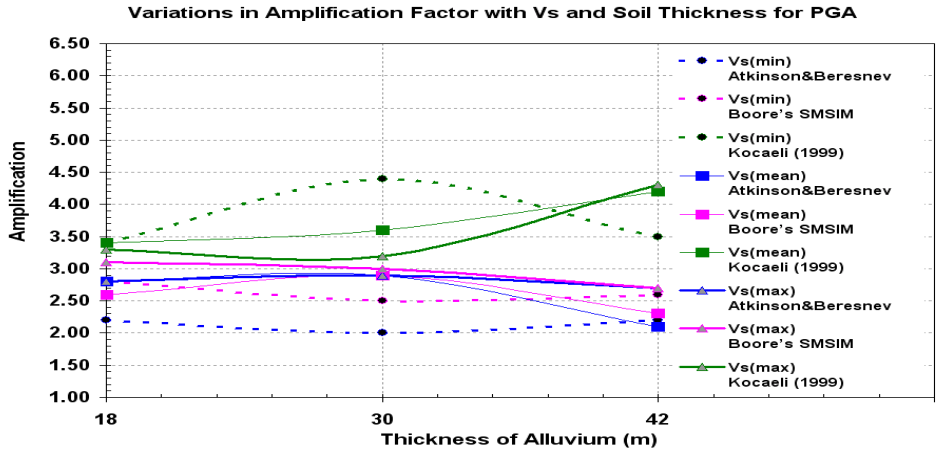

(a)

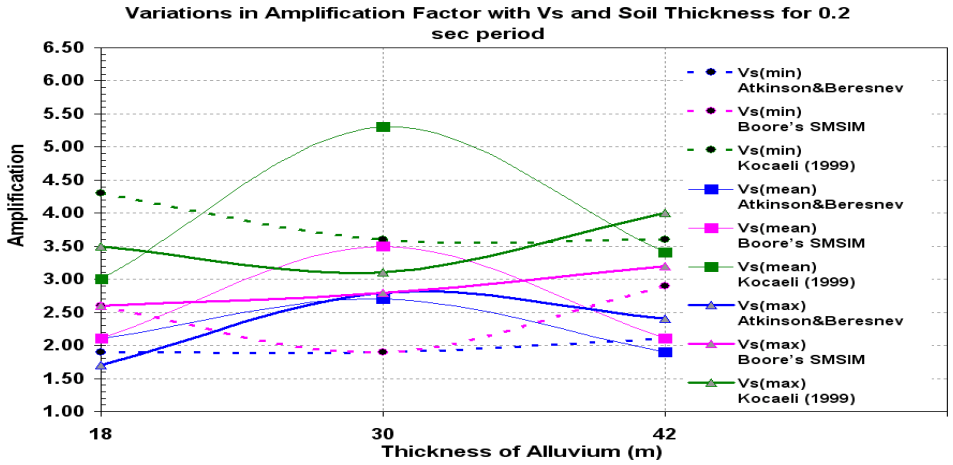

(b)

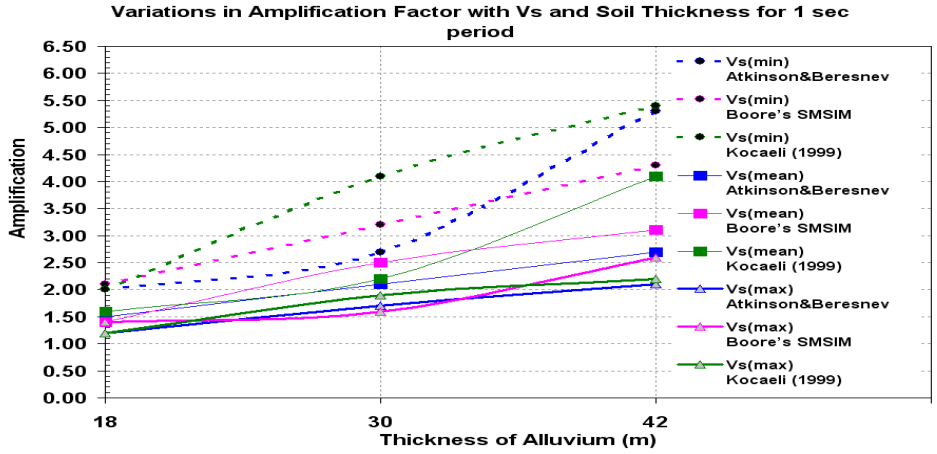

(c)

Figure 4.19. The effect of shear wave velocity and thickness of the soil cap on amplification factors for alluvium, at: a) ground surface, b) 0.2 sec, and c) 1 sec periods

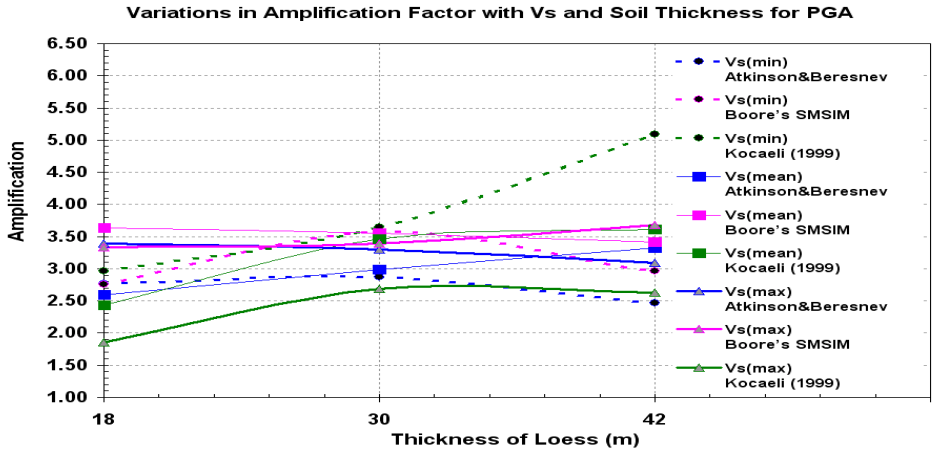

(a)

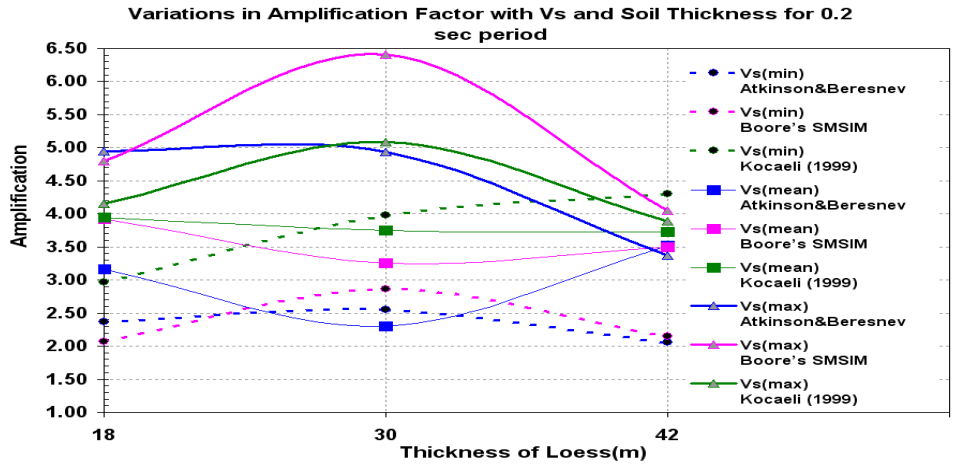

(b)

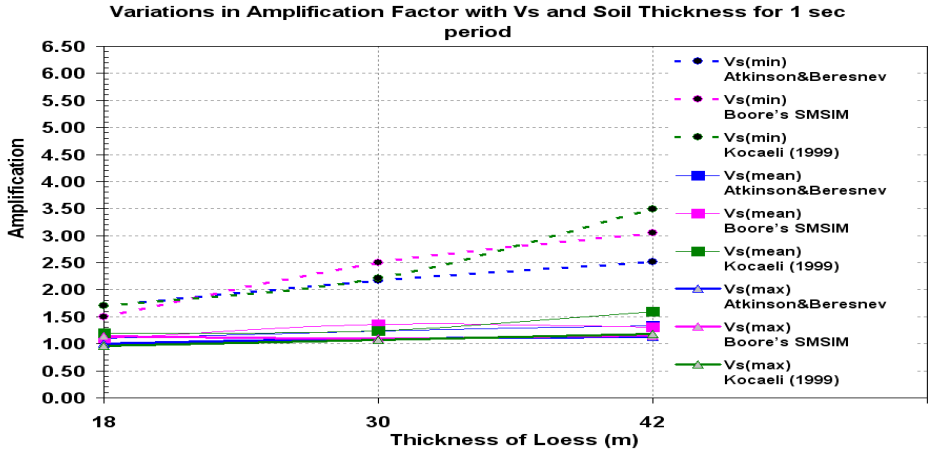

(c)

Figure 4.20. The effect of shear wave velocity and thickness of the soil cap on amplification factors for loess, at: a) ground surface, b) 0.2 sec, and c) 1 sec periods

When Figures 4.21 and Figure 4.22 are compared, it can be seen that the amplification range within loess and alluvial deposits are similar for PGA. The range of amplification values exhibit different characteristics, depending on the site period and the soil type. The predicted amplification is higher for 0.2 sec periods in loess deposits and 1 sec periods for alluvial deposits. On the contrary, amplification the predicted range of amplification at 1 sec periods in loess deposits and 0.2 sec periods in alluvial deposits appears noticeable smaller. These results suggest that even though amplification factors are important in determining accelerations, and hence, the response on the ground surface, they are not the only factors influencing shaking intensity at the ground surface. For instance, the scenario for 1 second periods the amplification factor caused by the strongest motion (Atkinson & Beresnev) and the weakest motion (Kocaeli) are actually quite similar: ~5.4. However, the response acceleration is 0.25 g and 0.09 g for the strongest and weakest motions, respectively.

Although, this study concentrated on PGA, 0.2 sec, and 1 sec periods due their common usage in seismic hazard maps and building codes, the distribution of amplification from 0.01 sec through 2 sec period was also analyzed and these results are provided in Appendix C. It appears that the greatest amplifications can be expected at periods between 0.2 sec and 1 sec. The character of the input ground motions (Figure 3.2) does not appear to have any appreciable effect on the predicted peak periods, as summarized in Table 4.6.

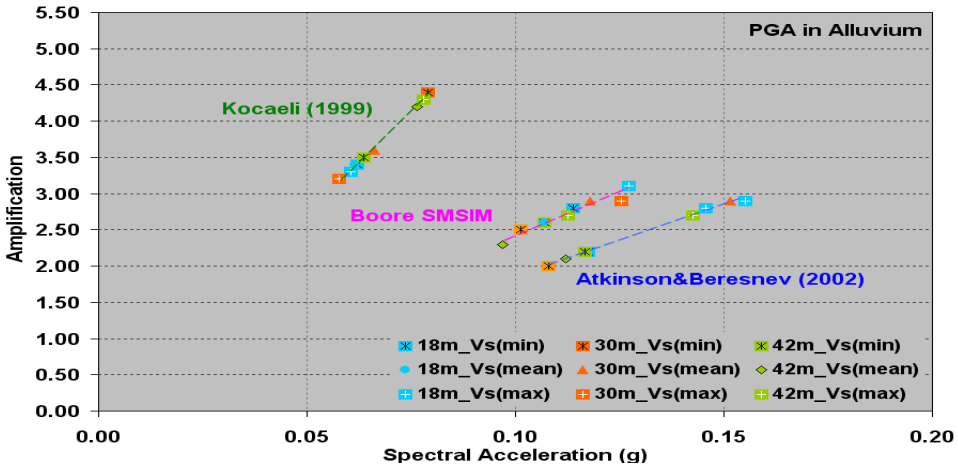

(a)

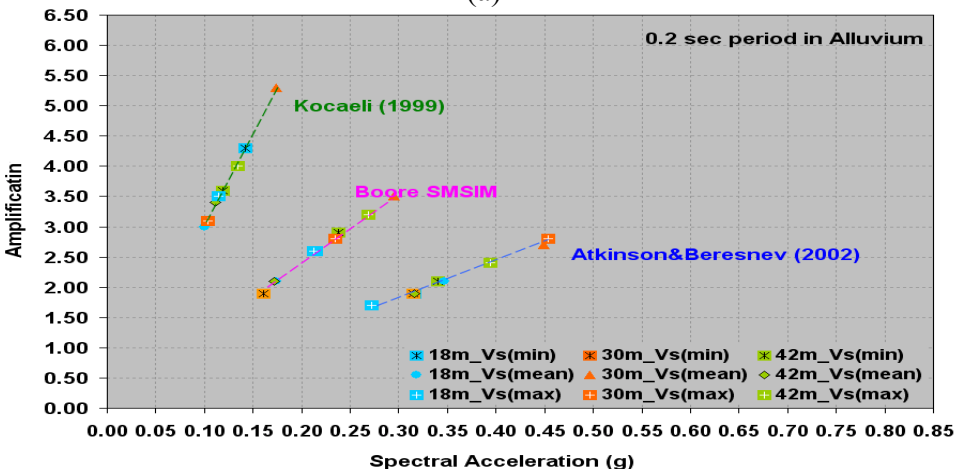

(b)

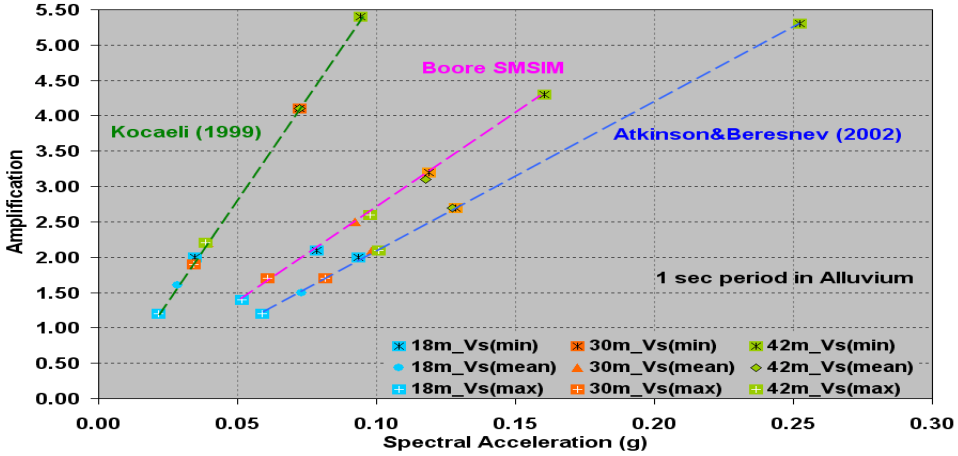

(c)

Figure 4.21. Distribution of amplification with spectral acceleration for alluvium

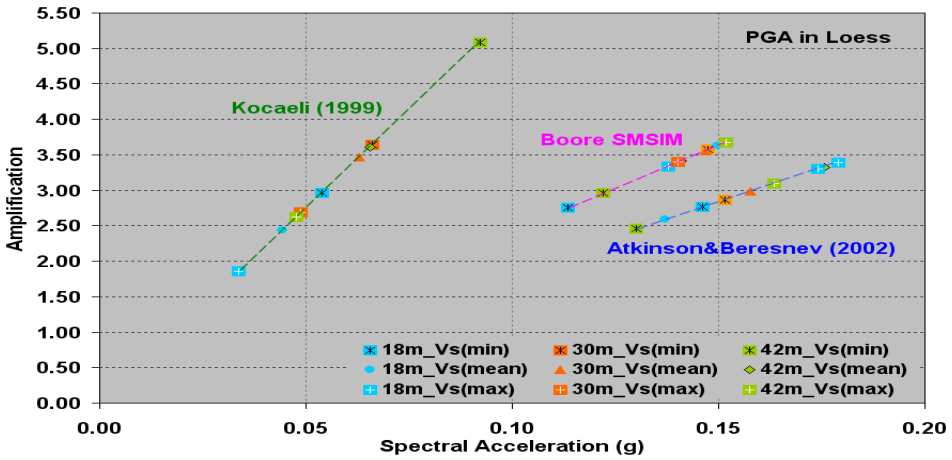

(a)

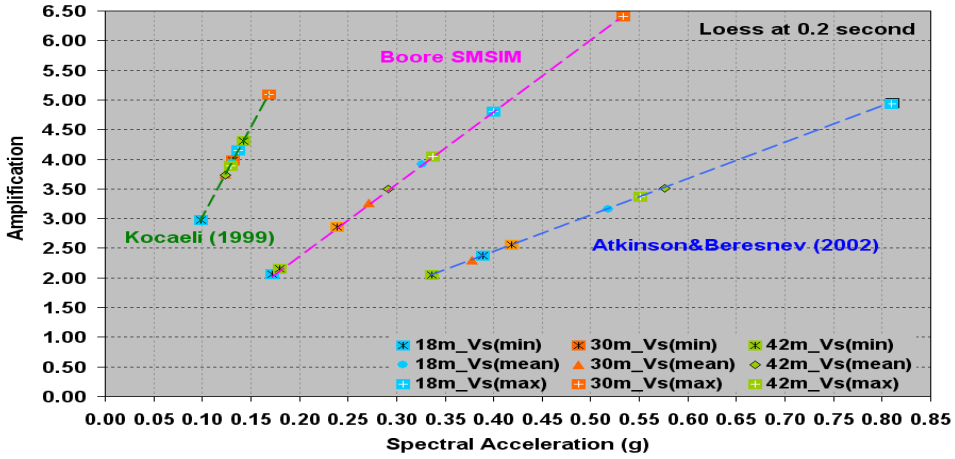

(b)

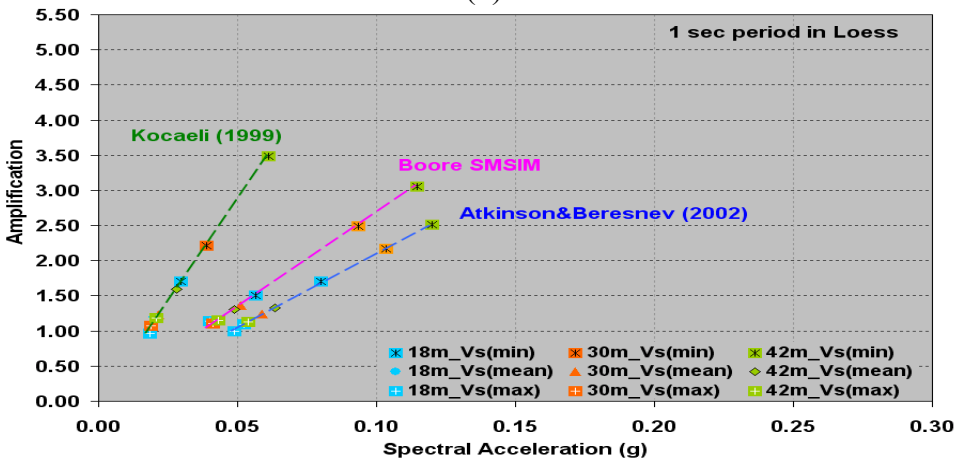

(c)

Figure 4.22. Distribution of amplification with spectral acceleration for loess

Table 4.6. Maximum amplifications ($Amp_{(max)}$) with corresponding periods

Soil Type	Time history	Min Vs		Mean Vs		Max Vs		Soil Thickness (m)
		Period	Amp (max)	Period	Amp (max)	Period	Amp (max)	
ALLUVIUM	Atkinson & Beresnev (2002)	*0.5*	*4.9*	*0.4*	*7.1*	*0.3*	*5.2*	18
		0.7	*7.2*	*0.6*	*5.7*	*0.5*	*5.6*	30
		0.9	*5.8*	*0.7*	*7.1*	*0.6*	*6.1*	42
	Boore's SMSIM	*0.5*	*6*	*0.4*	*6.4*	*0.3*	*6.2*	18
		0.7	*5.6*	*0.5*	*6.7*	*0.4*	*4.8*	30
		0.8	*5.4*	*0.7*	*5.5*	*0.5*	*5.9*	42
	Kocaeli, Turkey	*0.5*	*6.6*	*0.4*	*6.5*	*0.3*	*5.7*	18
		0.7	*7.6*	*0.5*	*6.3*	*0.4*	*7.4*	30
		0.9	*7.1*	*0.7*	*7.4*	*0.6*	*5.6*	42
LOESS	Atkinson & Beresnev (2002)	*0.4*	*5.2*	*0.3*	*4*	*0.2*	*4.9*	18
		0.6	*5.8*	*0.3*	*6*	*0.2*	*4.9*	30
		0.7	*7.1*	*0.4*	*5.7*	*0.3*	*3.8*	42
	Boore's SMSIM	*0.4*	*5.2*	*0.3*	*5*	*0.2*	*4.8*	18
		0.5	*7.2*	*0.3*	*7*	*0.2*	*6.4*	30
		0.6	*5.6*	*0.4*	*6.7*	*0.3*	*4.8*	42
	Kocaeli, Turkey	*0.4*	*9.3*	*0.2*	*3.9*	*0.2*	*4.1*	18
		0.5	*6.8*	*0.3*	*5.8*	*0.2*	*5.1*	30
		0.7	*7.2*	*0.4*	*5.5*	*0.2*	*5.1*	42

5. DISCUSSIONS AND CONCLUSIONS

5.1. COMPARISON OF TEST RESULTS WITH PREVIOUS STUDIES

Karadeniz (2007) used a probabilistic approach applying a numerical statistical simulation method, Monte Carlo randomization, to generate site-amplification distributions for the Granite City, Monks Mound and Columbia Bottom Quadrangles. The statistical simulation was performed by randomly selecting ground motion records, shears wave velocities, and associated soil depths, and then calculating the site response of each "virtual boring" 100 times (these virtual borings were spaced 500 m apart, on a regular grid pattern). After these initial calculations were performed, a mean and standard deviation of the 100 separate estimates of site amplification were determined (Karadeniz, 2007). This process resulted in Karadeniz (2007) performing about 5,400,000 calculations on the three study quadrangles in order to generate the amplification distributions for alluvium and loess deposits.

Figures 5.1 and 5.2 present comparisons between the probabilistic amplification results performed by Karadeniz (2007) and the author's deterministic amplification results performed as part of this study. The blue colored symbols show the amplification for 18, 30 and 42 meters for 0.01g and 0.05g rock accelerations as determined by Karadeniz (2007). The amplification values determined in this study were plotted for peak rock accelerations from Kocaeli earthquake (0.018g), Boore SMSIM (0.041g), and Atkinson & Beresnev (2002) (0.053g) and are shown in orange, pink and green colored symbols which represents different soil thickness. Occurrence of the same color three times for the same input ground motion is due to the different shear wave velocities.

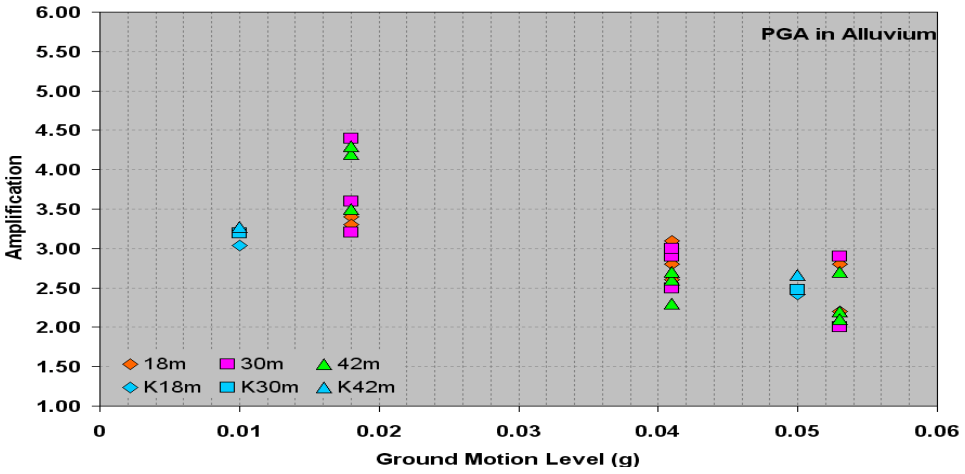

(a)

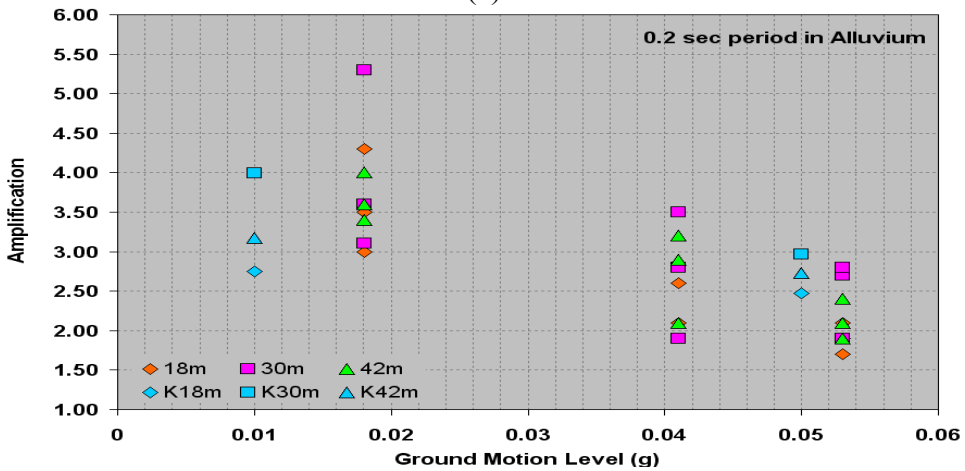

(b)

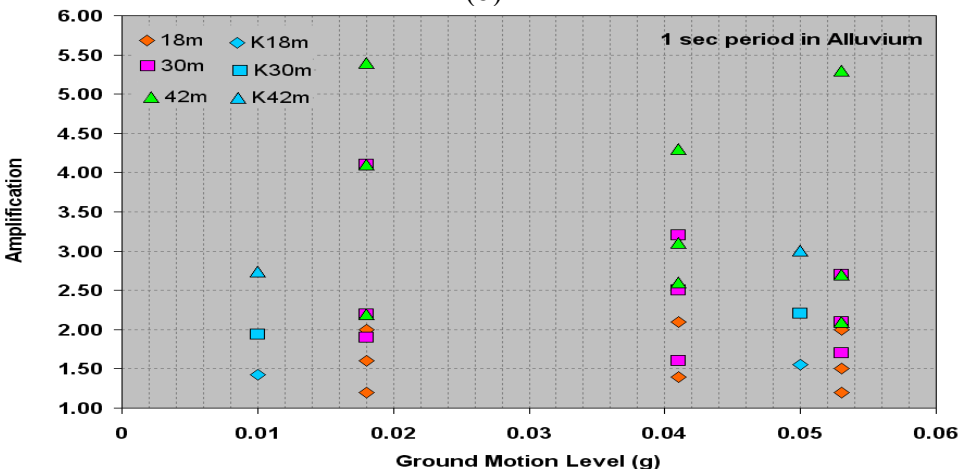

(c)

Figure 5.1. Comparison of the amplification values estimated in this study with the amplification values estimated by Karadeniz (2007) for alluvium.

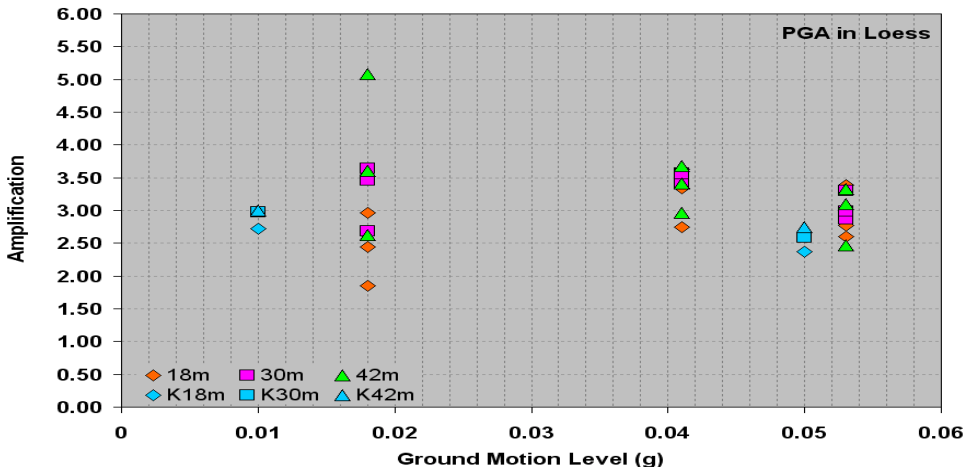

(a)

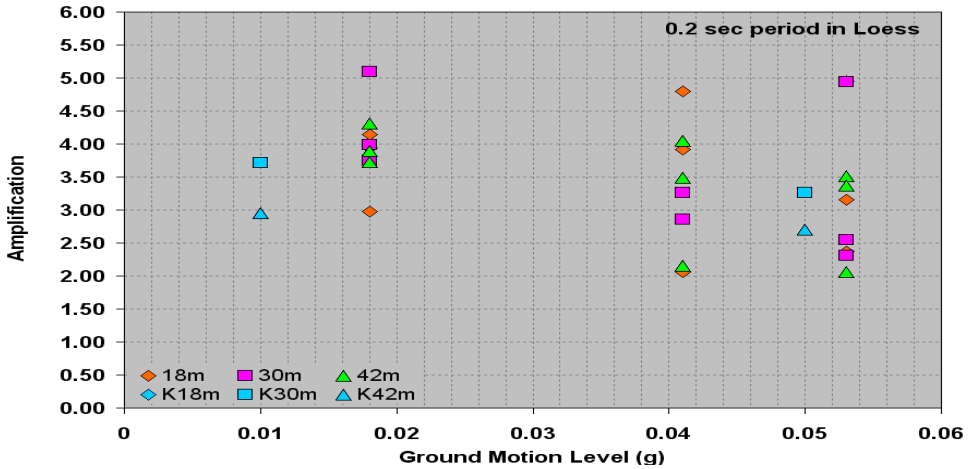

(b)

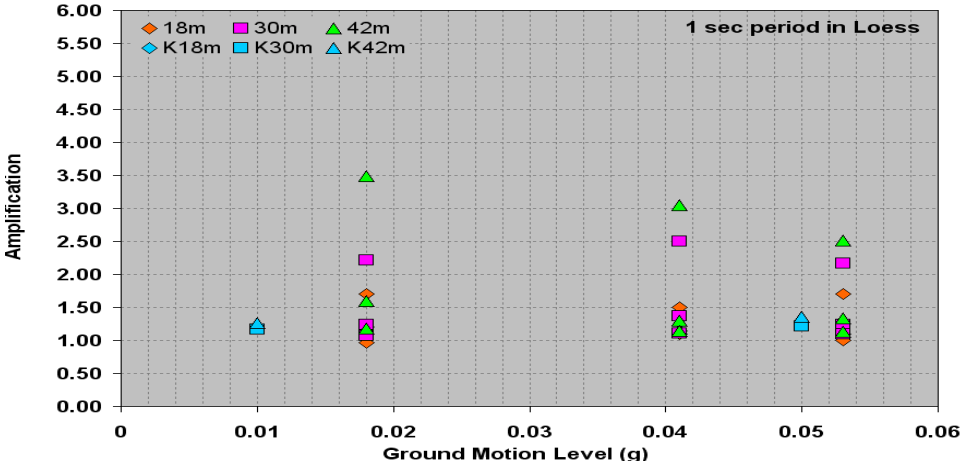

(c)

Figure 5.2. Comparison of the amplification values estimated in this study with the amplification values estimated by Karadeniz (2007) for loess.

This study estimated similar levels of site amplification as Karadeniz (2007) when the input rock accelerations were about 0.05g. At 0.05g the predicted site amplification for peak ground acceleration (PGA) and 0.2 sec spectral acceleration for alluvial deposits, and the PGA and 1.0 sec spectral acceleration for loess deposits appeared very similar to those estimated by Karadeniz (2007). The slight variances can be attributed to differences in the input shear wave velocity values. These differences were much more noticeable in the author's estimates of site amplification for smaller rock accelerations, less than 0.02g. As the input ground motion diminished, the predicted site amplification appeared to increase markedly, as shown in the upper diagram of Figure 5.1. These differences are likely attributed to variations in the assumed shear wave velocities of the soil cap.

Karadeniz (2007) spectral acceleration results were also compared by plotting 2%, 5% and 10% probability of exceedance (POE) in 50 years estimates with the acceleration values estimated in this study and are shown in Figures 5.3 and 5.4. The blue colored symbols show Atkinson & Beresnev (2002), the pink colored symbols show Boore's SMSIM, and the green colored symbols show Kocaeli (1999). Black, orange & white colored stars show 2%, 5%, 10% probability of exceedance in 50 years as determined by Karadeniz (2007). Occurrence of the same color three times for the same input ground motion is due to the different shear wave velocities.

These plots suggest that the estimated accelerations in this study can be as high as accelerations predicted for 2% probability of exceedance by Karadeniz (2007). As shown in the Figures the estimated accelerations are well within 2% POE and 10% POE or smaller. The larger deviations are seen mostly for 0.2 sec period and from these comparisons it can be argued that Karadeniz (2007) may have underestimated the accelerations predicted by the probabilistic methods. This might also imply the importance of accurately estimating the shear wave velocity since the response deviates largely even for the same soil cap thickness.

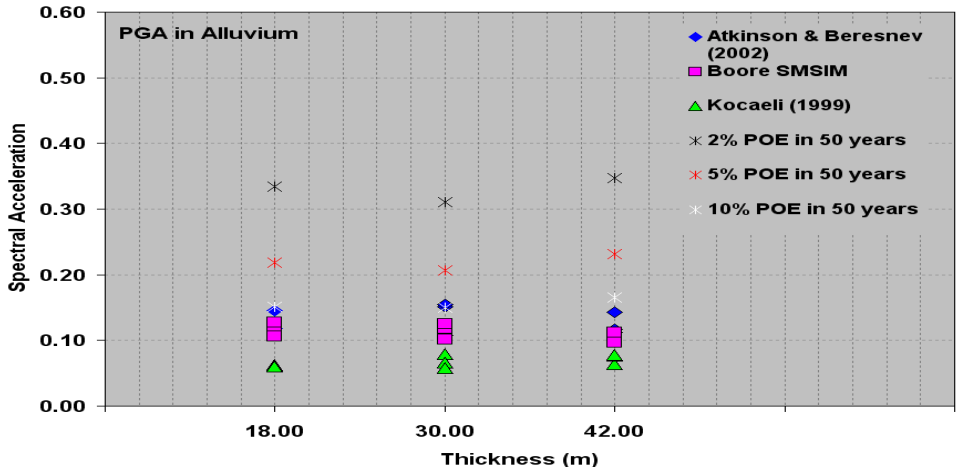

(a)

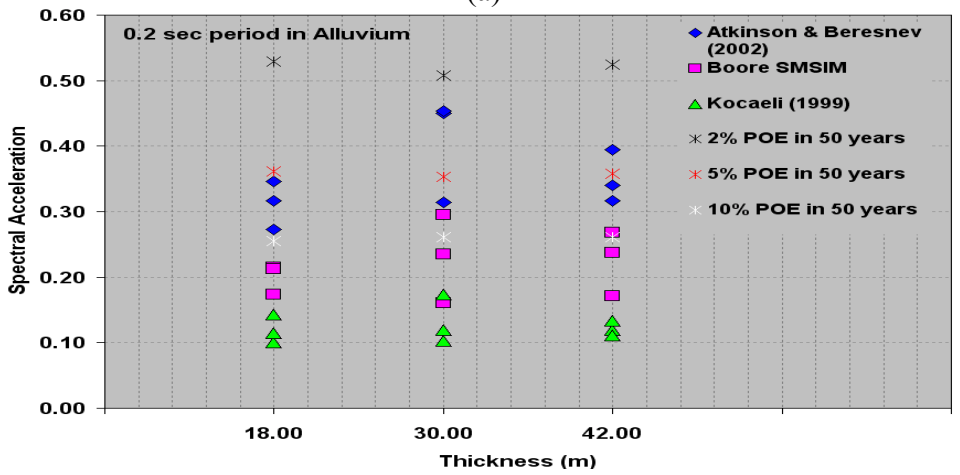

(b)

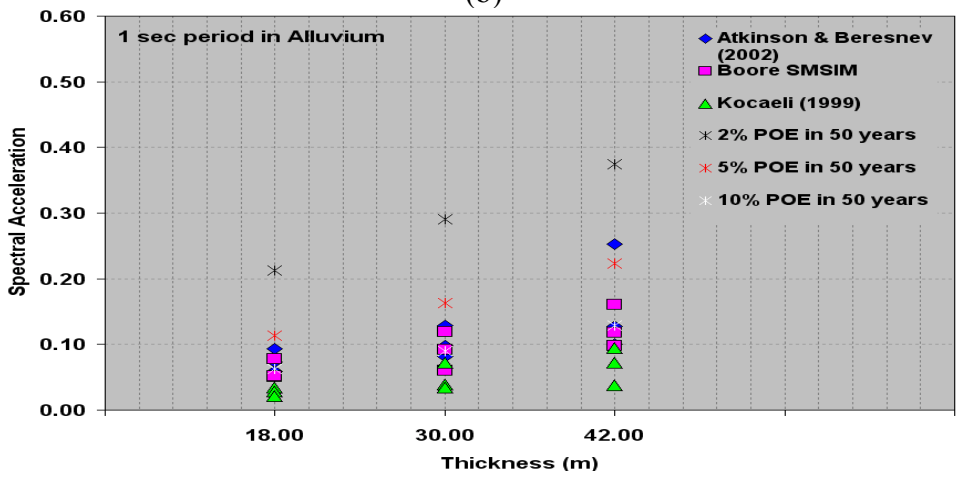

(c)

Figure 5.3. Comparison of the spectral acceleration values estimated in this study with %2, %5, and %10 probability of exceedance in 50 years spectral acceleration estimates by Karadeniz (2007) for alluvium.

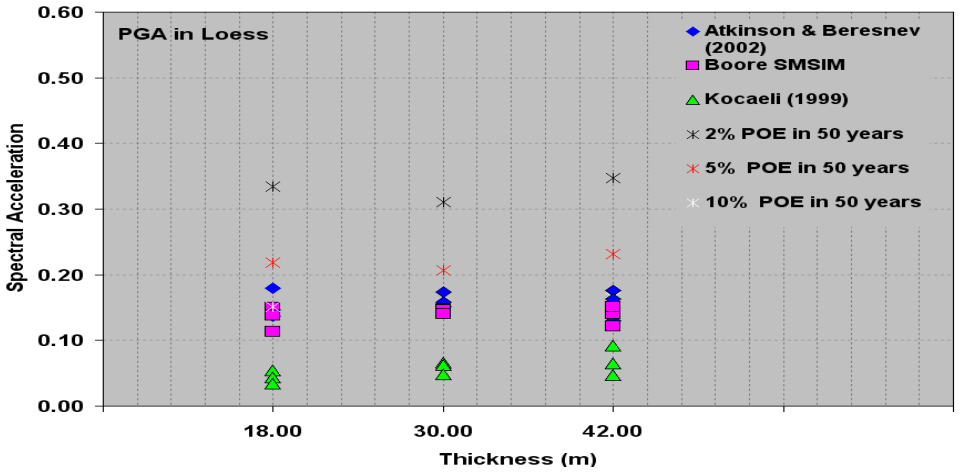

(a)

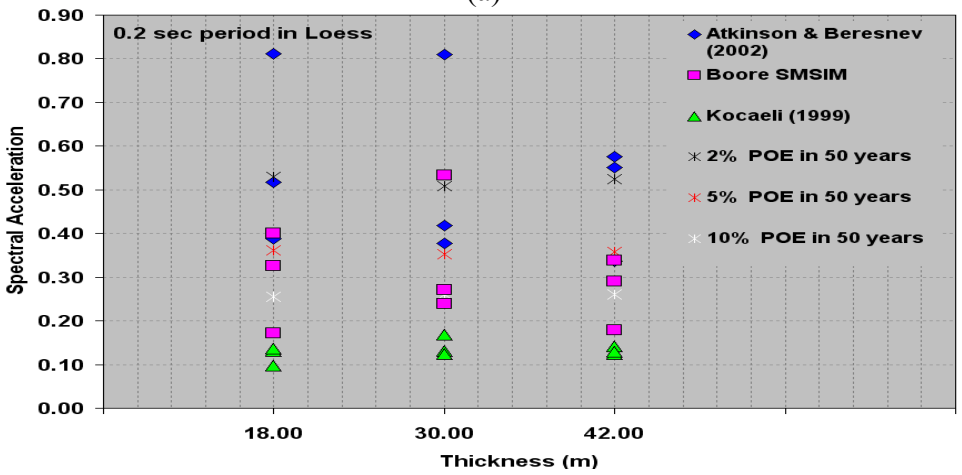

(b)

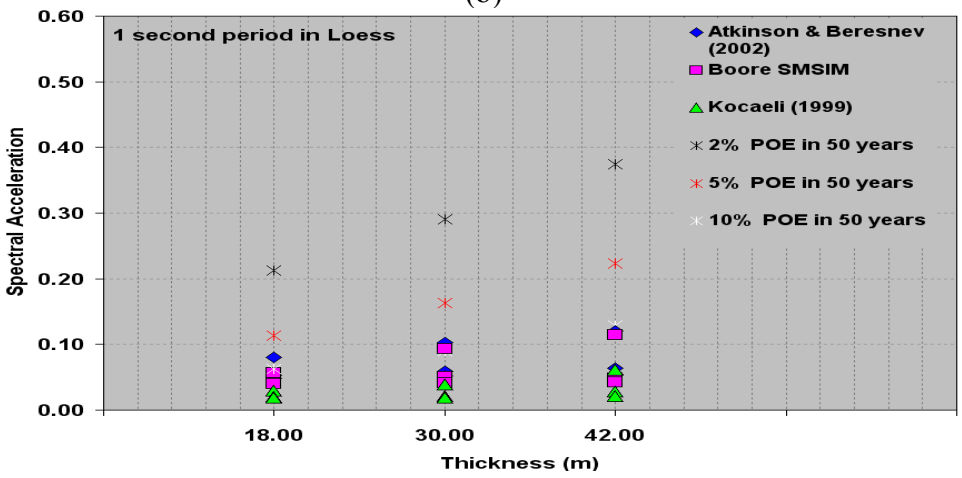

(c)

Figure 5.4. Comparison of the spectral acceleration values estimated in this study with %2, %5, and %10 probability of exceedance in 50 years spectral acceleration estimates by Karadeniz (2007) for loess.

5.2. DISCUSSIONS

Statistical uncertainties are unavoidable in site response predictions because of the natural variations in the stratigraphy, spatial variance (such as natural truncations), hydraulic sorting, and geologic structure of any depositional system. Considerable differences in spectral accelerations and amplifications can be expected, and these are easily discerned when all the uncertainties associated with shear wave velocity, soil cap thickness, and input ground motion were combined in each calculation set. When combined these uncertainties will either engender lower or higher values than those predicted using mean values. The sensitivity analyses performed as part of this study were intended to ascertain the range of possible values when a set of known parameters with their associated range of statistical error were applied. The sensitivity analyses performed for this study showed that seismic site response can be noticeably affected by various combinations of the physical input parameters. Attempts were made to differentiate the complex relations between the input parameters and the results, using graphical interpolations. These interpolations proved most useful, although it was often difficult to excise simple patterns of behavior. Nevertheless, the following generalizations can be drawn from these results:

The scenarios which resulted in the highest accelerations and amplifications for all levels of input rock acceleration are identified and summarized in Table 5.1. At 1 sec period the highest spectral accelerations and amplifications were consistently obtained for values of minimum shear wave velocity, in both alluvium and loess deposits; even when varying the soil cap thicknesses. In loess, the highest spectral accelerations and site amplification at 0.2 sec period were predicted when applying $Vs_{(max)}$ values to layers 18 and 30 m thick. In alluvium, the highest spectral accelerations and site amplification at 0.2 sec period were predicted when applying $Vs_{(mean)}$ with 30 m layers and $Vs_{(max)}$ with 42 m thick layers.

The input parameters engendering the highest accelerations, regardless of the input ground motion, are summarized in Table 5.2. Once again, these results suggest that the ~30 m thick soil deposits (regardless of soil type) will most affect short-period buildings, especially when shear wave velocity is equal to, or higher than, the mean Vs values estimated by Karadeniz (2007). Likewise, the sites underlain by the thickest soil

caps (more than ~30 m), will affect taller, long-period structures, especially, when the shear wave velocity (Vs) is less than the mean value.

Table 5.1. Physical parameters engendering the highest spectral accelerations and highest amplifications, exclusive of input ground motion

Soil Type	Highest Spectral accelerations		Highest amplifications	
	0.2 sec period	1 sec period	0.2 sec period	1 sec period
Alluvium	30 m + $Vs_{(mean)}$ 42 m + $Vs_{(max)}$	18m + $Vs_{(min)}$ 30m + $Vs_{(min)}$ 42m + $Vs_{(min)}$	30 m + $Vs_{(mean)}$ 42 m + $Vs_{(max)}$	18m + $Vs_{(min)}$ 30m + $Vs_{(min)}$ 42m + $Vs_{(min)}$
Loess	18m + $Vs_{(max)}$ 30m + $Vs_{(max)}$	18m + $Vs_{(min)}$ 30m + $Vs_{(min)}$ 42m + $Vs_{(min)}$	18m + $Vs_{(max)}$ 30m + $Vs_{(max)}$	18m + $Vs_{(min)}$ 30m + $Vs_{(min)}$ 42m + $Vs_{(min)}$

Table 5.2. Physical parameters engendering the greatest site amplification and peak spectral acceleration, exclusive of input ground motion

Alluvium	Loess	Impacted structures
30 meters thickness with Vs (mean)	30 meters thickness with Vs (max)	Short buildings (0.2 sec period; less than 7 stories)
42 meters thickness with Vs (min)	42 meters thickness with Vs (min)	High rise buildings (1 second period; 7 stories or higher)

5.3. CONCLUSIONS

The following conclusions can be drawn from the results and interpolations of these site screening and sensitivity analyses:

1. The character of the input ground motion appears to exert a dominant affect on the predicted site response. In the majority of cases, the lowest spectral accelerations and highest site amplification were produced by weaker rock motions.
2. The character of the input motion did not appear to exert any significant impact on the peak spectral periods.
3. The peak spectral accelerations and site amplifications appear to be most influenced by resonance, where the period of the incoming seismic wave energy is similar to the natural site period.
4. The predicted PGA does not appear to be particularly sensitive to the choice of shear wave velocity or thickness of the soil cap.
5. Changes in shear wave velocity (Vs) and soil cap thickness cause noticeable variations in site response at periods of 0.2 sec. This difference in response is most pronounced when soil cap is 30 meters thick and shear wave velocity exceeds the mean value for the soil cap.
6. At 1 sec period, spectral accelerations increase with increasing soil thickness and decrease with increasing shear wave velocity.
7. When ground motion periods (PGA, 0.2 sec and 1 sec) are compared; the highest spectral accelerations were observed at 0.2 second period for both alluvium and loess soil caps.
8. The existence of a 2 m weathered rock horizon beneath the loess soil cap (on the Missouri side of the Mississippi River) does not appear to exert any noticeable impact on site response.
9. In alluvial deposits, the highest spectral acceleration (0.84g) was predicted for sites with an 18 m thick soil cap, mean shear wave velocity, and the strongest ground motion (using Atkinson and Beresnev, 2002) as the input parameters.

10. In loess the highest spectral acceleration (0.82g) was predicted for sites underlain 18 m soil cap, using mean shear wave velocities and the medium ground motion (Boore SMSIM) as the input parameters.
11. The greatest differences in predicted site response appear to be ascribable to combined uncertainties of soil thickness and shear wave velocities. These differences were considerable at 0.2 sec period for both the loess and the alluvium soil caps. This implies that 0.2 sec spectral period is more sensitive to the choice of these input parameters.
12. It appears that variations in shear wave velocity engender more significant impacts on site amplification in 30 m thick of soil cap at 0.2 second period and in 42 m thick soil cap at 1 second periods.
13. Maximum spectral accelerations occurred when the spectral period more-or-less equals the characteristic site period of the soil cap. Since the characteristic site period depends on the shear wave velocity and soil thickness, it was difficult to distinguish which parameter (shear wave velocity and soil thickness) most affects site response.
14. When all three input parameters are compared, the most important parameters affecting predicted spectral accelerations and site amplification appear to be, in descending order of importance: 1) the input motion (acceleration-time history); and 2) the shear wave velocity and the soil thickness.
15. Even though two synthetically generated earthquake models created specially for CEUS rock properties were used in this study; some of the response estimates varied considerably. This suggests that more dependable and accurate synthetic earthquake models need to be created specifically for the CEUS, which have much higher impedance contrasts than most other sites, world-wide.
16. This study concentrated on PGA, 0.2 sec, and 1 sec periods due their predominance in seismic hazard products and building codes. However, the distribution of site amplification between 0.01 and 2 sec periods were also analyzed. It appears that the maximum site amplifications generally occur at periods somewhere between 0.2 and 1 sec, depending on the depth of the soil cap.

APPENDIX A.
RESPONSE SPECTRA

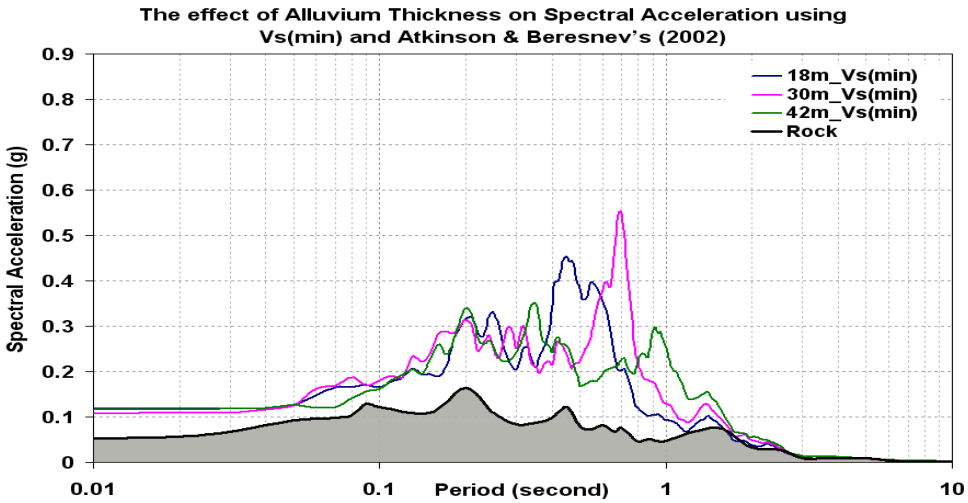
The effect of Alluvium Thickness on Spectral Acceleration using Vs(min) and Atkinson & Beresnev's (2002)
Spectral Acceleration (g)
0.9
0.8
0.7
0.6
0.5
0.4
0.3
0.2
0.1
0
0.01
0.1
Period (second)
1
10
18m_Vs(min)
30m_Vs(min)
42m_Vs(min)
Rock

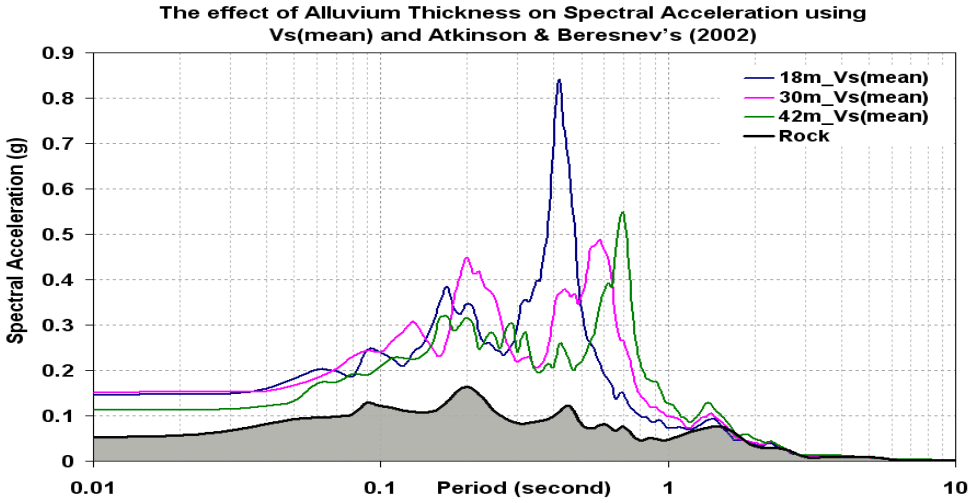
The effect of Alluvium Thickness on Spectral Acceleration using Vs(mean) and Atkinson & Beresnev's (2002)
Spectral Acceleration (g)
0.9
0.8
0.7
0.6
0.5
0.4
0.3
0.2
0.1
0
0.01
0.1
Period (second)
1
10
18m_Vs(mean)
30m_Vs(mean)
42m_Vs(mean)
Rock

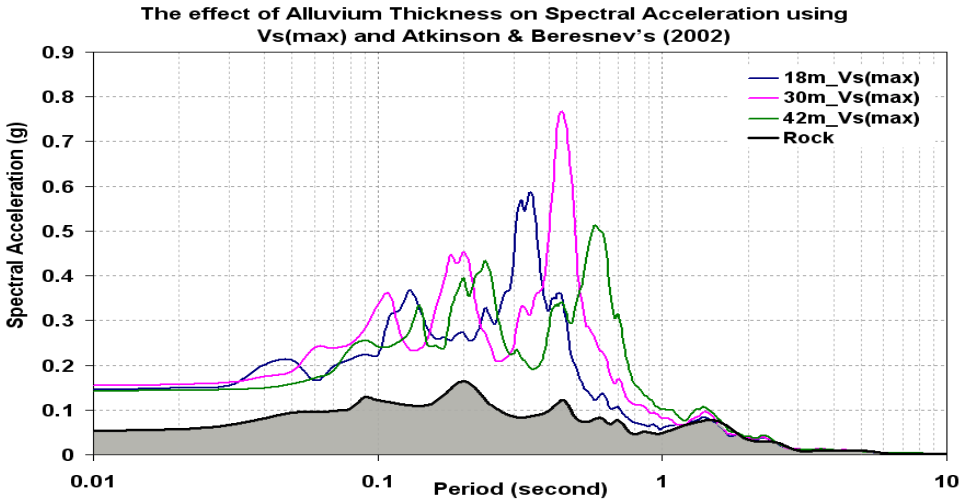
The effect of Alluvium Thickness on Spectral Acceleration using Vs(max) and Atkinson & Beresnev's (2002)
Spectral Acceleration (g)
0.9
0.8
0.7
0.6
0.5
0.4
0.3
0.2
0.1
0
0.01
0.1
Period (second)
1
10
18m_Vs(max)
30m_Vs(max)
42m_Vs(max)
Rock

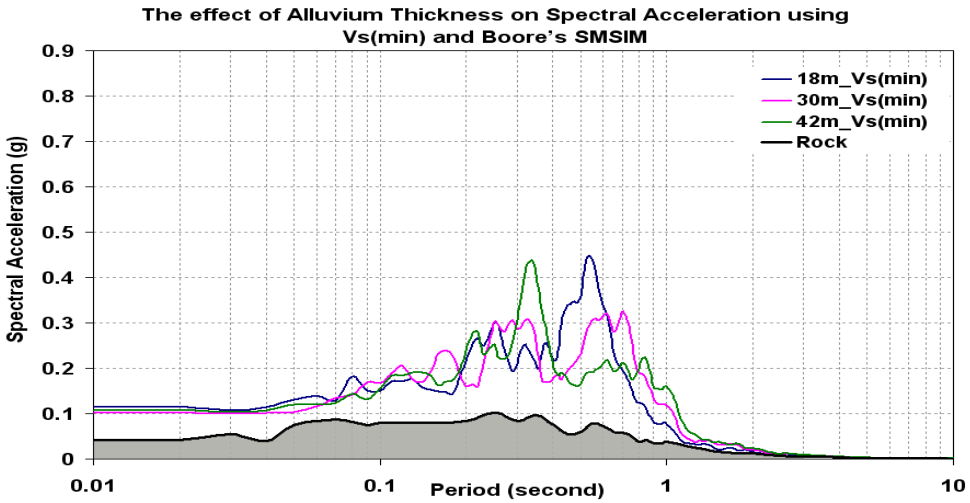
The effect of Alluvium Thickness on Spectral Acceleration using Vs(min) and Boore's SMSIM
Spectral Acceleration (g)
0.9
0.8
0.7
0.6
0.5
0.4
0.3
0.2
0.1
0
0.01
0.1
Period (second)
1
10
18m_Vs(min)
30m_Vs(min)
42m_Vs(min)
Rock

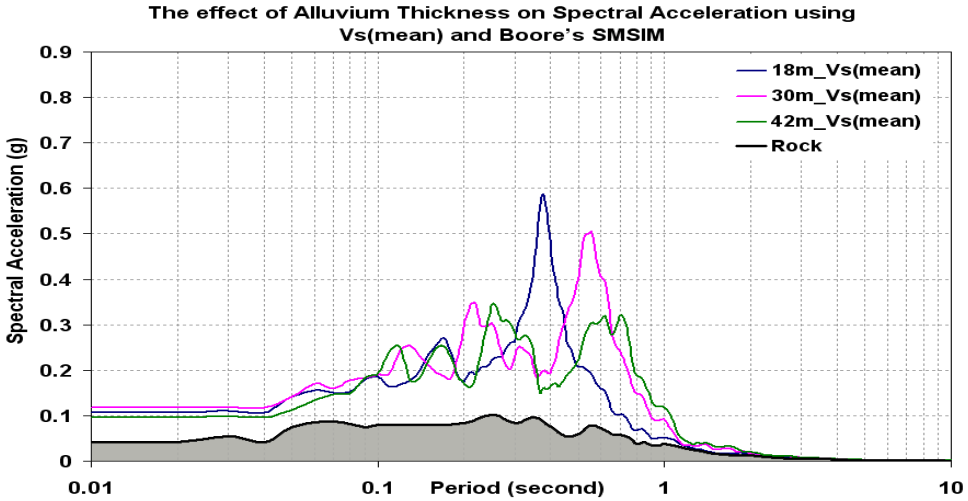
The effect of Alluvium Thickness on Spectral Acceleration using Vs(mean) and Boore's SMSIM
Spectral Acceleration (g)
0.9
0.8
0.7
0.6
0.5
0.4
0.3
0.2
0.1
0
0.01
0.1
Period (second)
1
10
18m_Vs(mean)
30m_Vs(mean)
42m_Vs(mean)
Rock

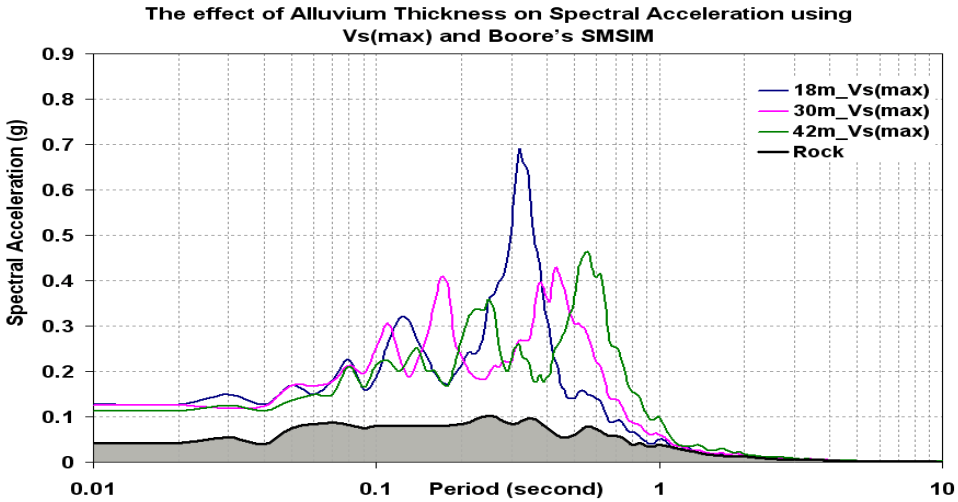
The effect of Alluvium Thickness on Spectral Acceleration using Vs(max) and Boore's SMSIM
Spectral Acceleration (g)
0.9
0.8
0.7
0.6
0.5
0.4
0.3
0.2
0.1
0
0.01
0.1
Period (second)
1
10
18m_Vs(max)
30m_Vs(max)
42m_Vs(max)
Rock

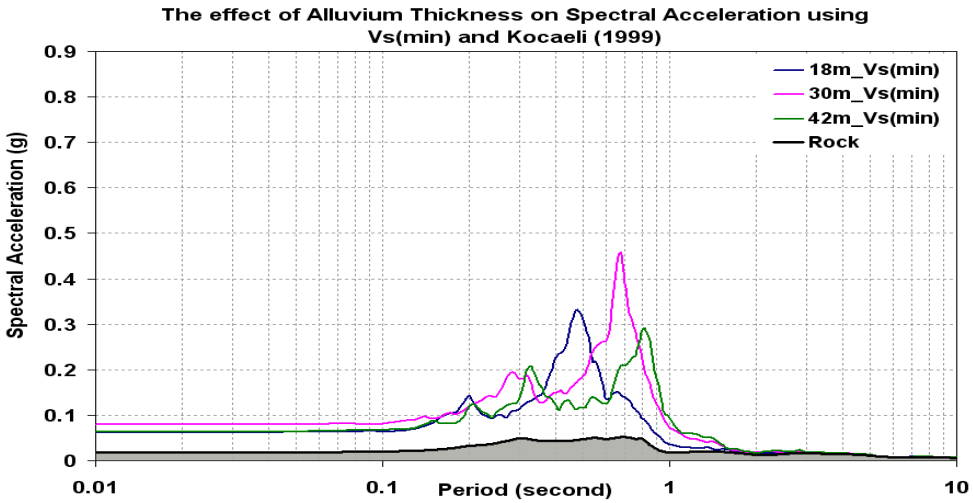
The effect of Alluvium Thickness on Spectral Acceleration using Vs(min) and Kocaeli (1999)
Spectral Acceleration (g)
0.9
0.8
0.7
0.6
0.5
0.4
0.3
0.2
0.1
0
0.01
0.1
Period (second)
1
10
18m_Vs(min)
30m_Vs(min)
42m_Vs(min)
Rock

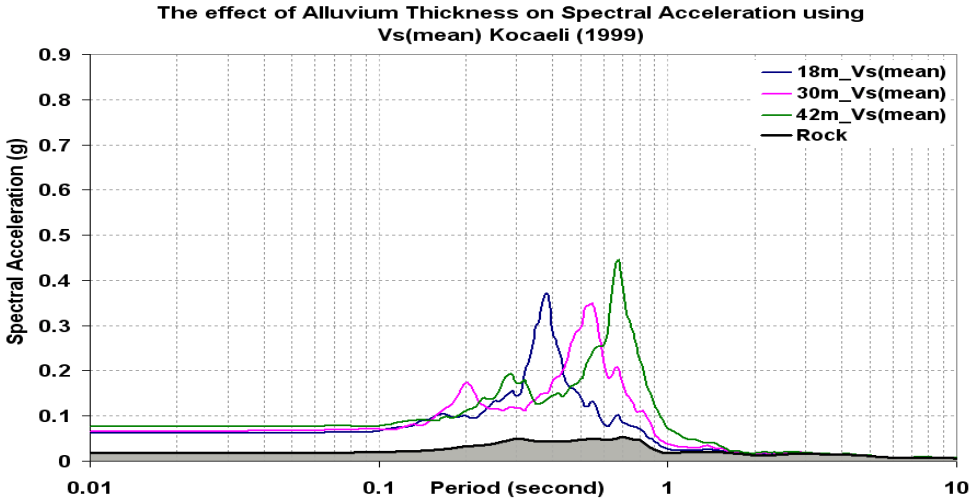
The effect of Alluvium Thickness on Spectral Acceleration using Vs(mean) Kocaeli (1999)
Spectral Acceleration (g)
0.9
0.8
0.7
0.6
0.5
0.4
0.3
0.2
0.1
0
0.01
0.1
Period (second)
1
10
18m_Vs(mean)
30m_Vs(mean)
42m_Vs(mean)
Rock

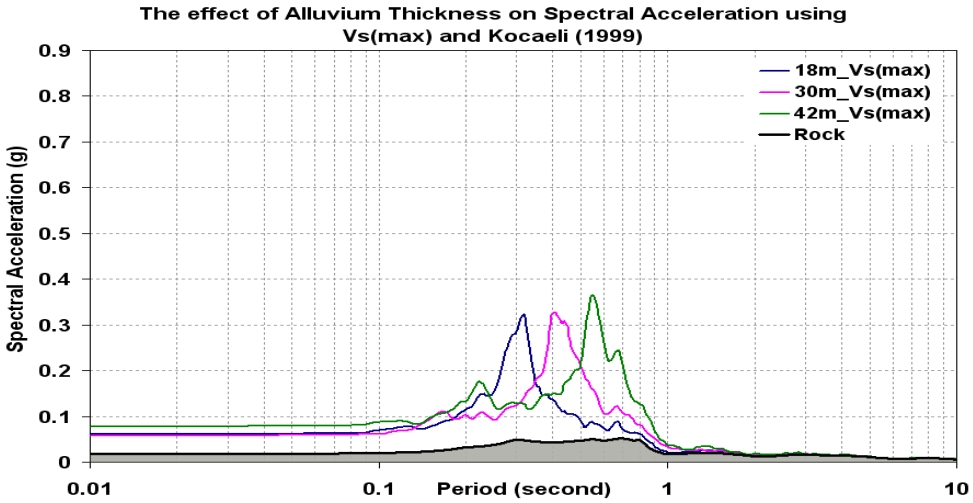
The effect of Alluvium Thickness on Spectral Acceleration using Vs(max) and Kocaeli (1999)
Spectral Acceleration (g)
0.9
0.8
0.7
0.6
0.5
0.4
0.3
0.2
0.1
0
0.01
0.1
Period (second)
1
10
18m_Vs(max)
30m_Vs(max)
42m_Vs(max)
Rock

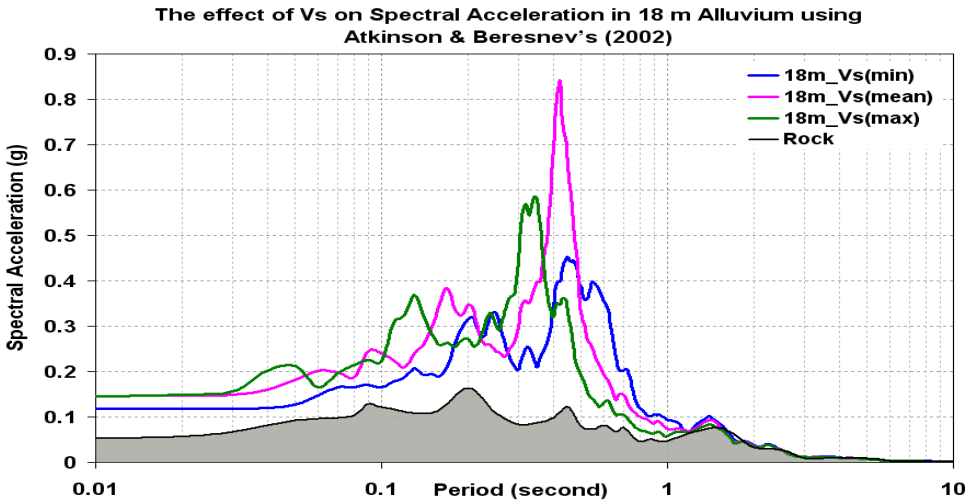
The effect of Vs on Spectral Acceleration in 18 m Alluvium using Atkinson & Beresnev's (2002)
Spectral Acceleration (g)
0.9
0.8
0.7
0.6
0.5
0.4
0.3
0.2
0.1
0
0.01
0.1
Period (second)
1
10
18m_Vs(min)
18m_Vs(mean)
18m_Vs(max)
Rock

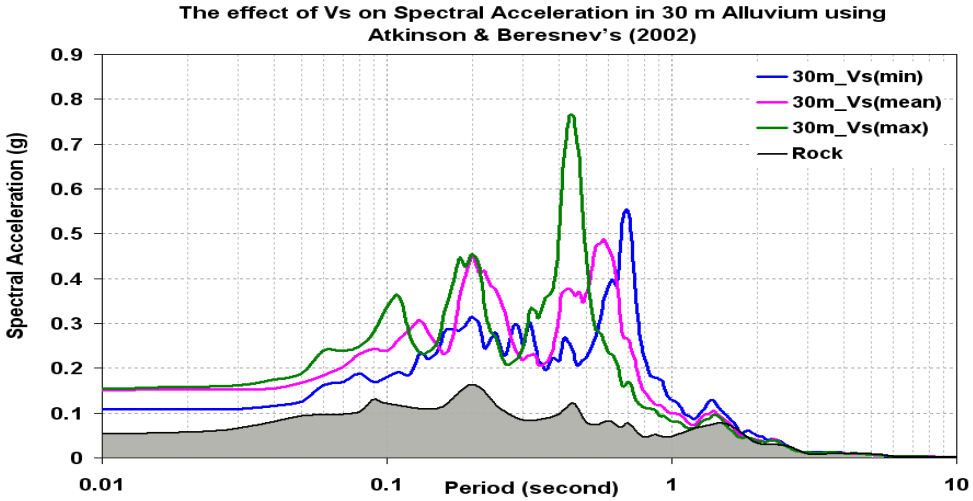
The effect of Vs on Spectral Acceleration in 30 m Alluvium using Atkinson & Beresnev's (2002)
Spectral Acceleration (g)
0.9
0.8
0.7
0.6
0.5
0.4
0.3
0.2
0.1
0
0.01
0.1
Period (second)
1
10
30m_Vs(min)
30m_Vs(mean)
30m_Vs(max)
Rock

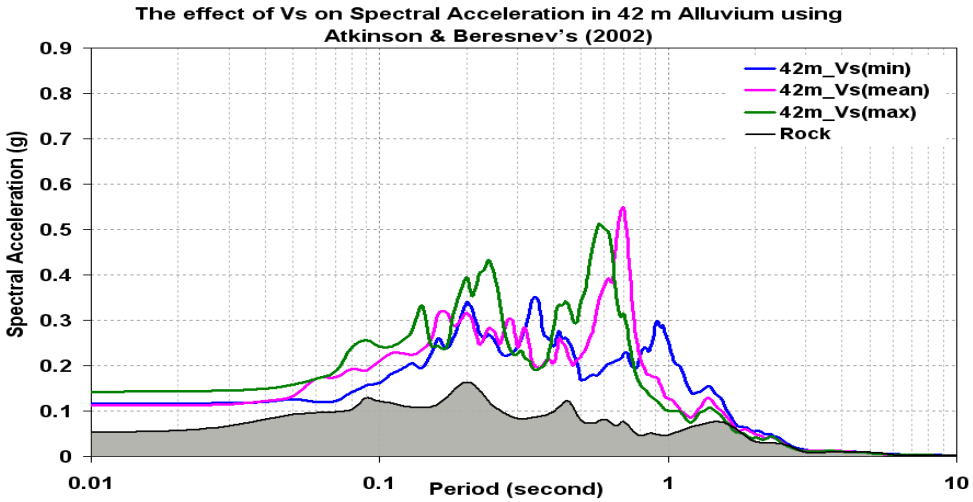
The effect of Vs on Spectral Acceleration in 42 m Alluvium using Atkinson & Beresnev's (2002)
Spectral Acceleration (g)
0.9
0.8
0.7
0.6
0.5
0.4
0.3
0.2
0.1
0
0.01
0.1
Period (second)
1
10
42m_Vs(min)
42m_Vs(mean)
42m_Vs(max)
Rock

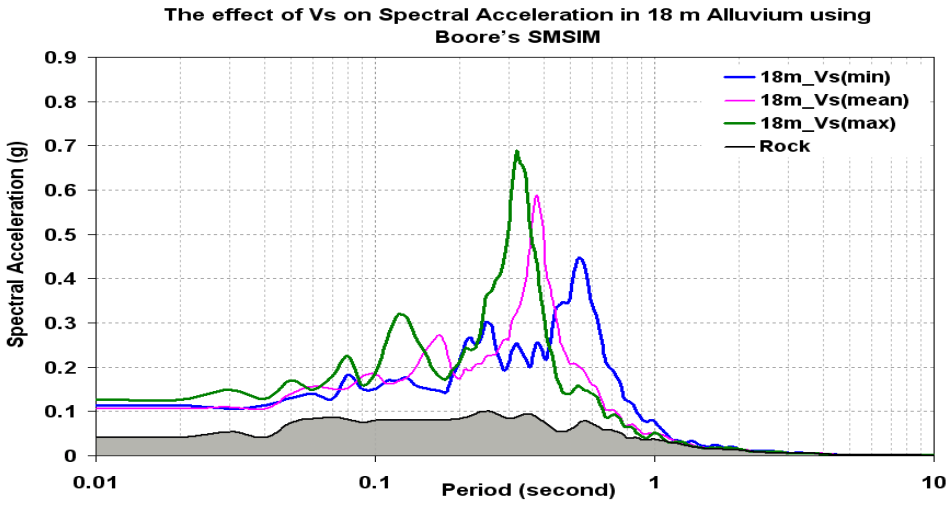
The effect of Vs on Spectral Acceleration in 18 m Alluvium using Boore's SMSIM
Spectral Acceleration (g)
Period (second)
18m_Vs(min)
18m_Vs(mean)
18m_Vs(max)
Rock
0.9
0.8
0.7
0.6
0.5
0.4
0.3
0.2
0.1
0
0.01
0.1
1
10

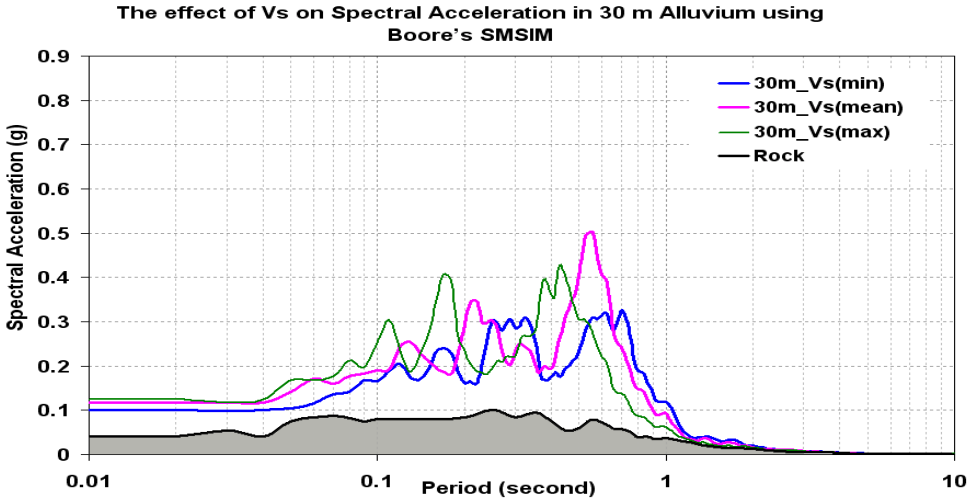
The effect of Vs on Spectral Acceleration in 30 m Alluvium using Boore's SMSIM
Spectral Acceleration (g)
Period (second)
30m_Vs(min)
30m_Vs(mean)
30m_Vs(max)
Rock
0.9
0.8
0.7
0.6
0.5
0.4
0.3
0.2
0.1
0
0.01
0.1
1
10

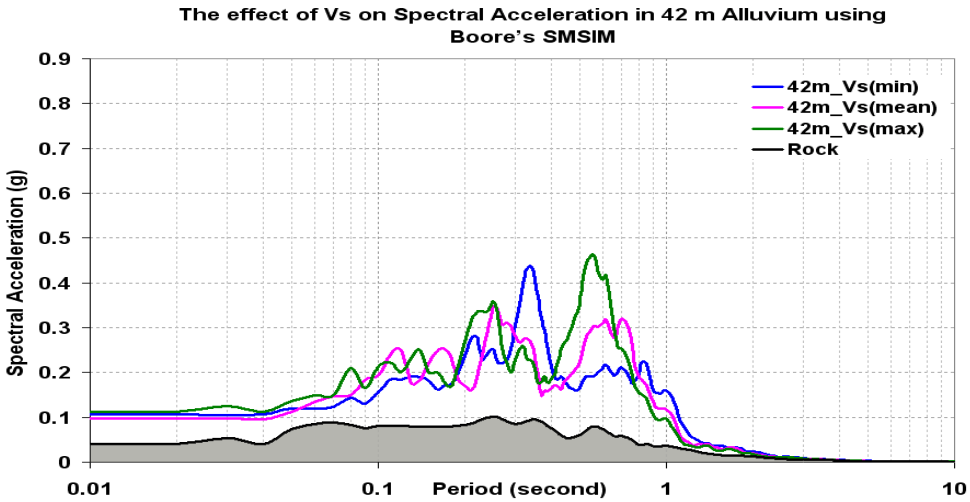
The effect of Vs on Spectral Acceleration in 42 m Alluvium using Boore's SMSIM
Spectral Acceleration (g)
Period (second)
42m_Vs(min)
42m_Vs(mean)
42m_Vs(max)
Rock
0.9
0.8
0.7
0.6
0.5
0.4
0.3
0.2
0.1
0
0.01
0.1
1
10

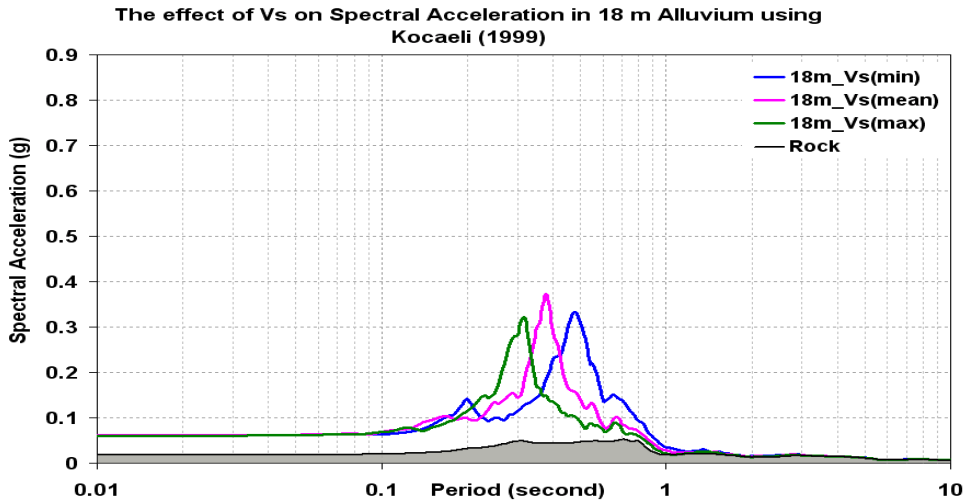
The effect of Vs on Spectral Acceleration in 18 m Alluvium using Kocaeli (1999)
Spectral Acceleration (g)
0.9
0.8
0.7
0.6
0.5
0.4
0.3
0.2
0.1
0
0.01
0.1
Period (second)
1
10
18m_Vs(min)
18m_Vs(mean)
18m_Vs(max)
Rock

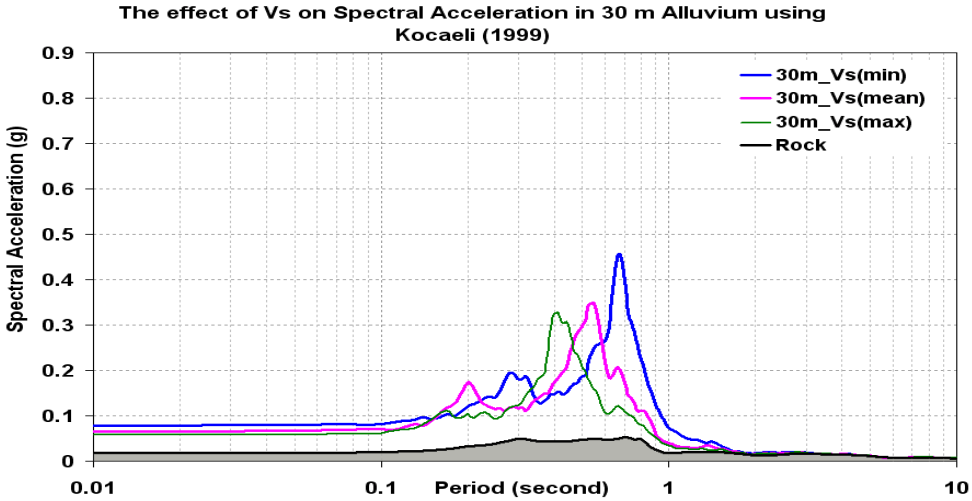
The effect of Vs on Spectral Acceleration in 30 m Alluvium using Kocaeli (1999)
Spectral Acceleration (g)
0.9
0.8
0.7
0.6
0.5
0.4
0.3
0.2
0.1
0
0.01
0.1
Period (second)
1
10
30m_Vs(min)
30m_Vs(mean)
30m_Vs(max)
Rock

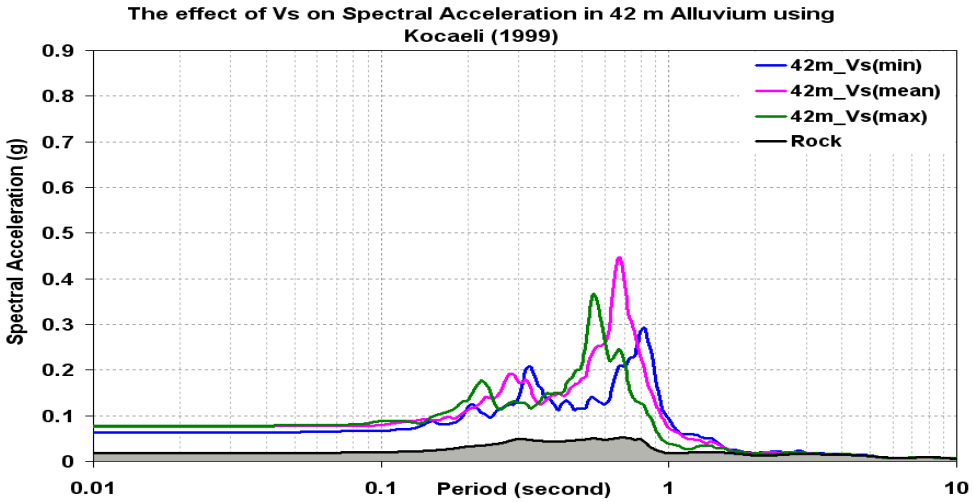
The effect of Vs on Spectral Acceleration in 42 m Alluvium using Kocaeli (1999)
Spectral Acceleration (g)
0.9
0.8
0.7
0.6
0.5
0.4
0.3
0.2
0.1
0
0.01
0.1
Period (second)
1
10
42m_Vs(min)
42m_Vs(mean)
42m_Vs(max)
Rock

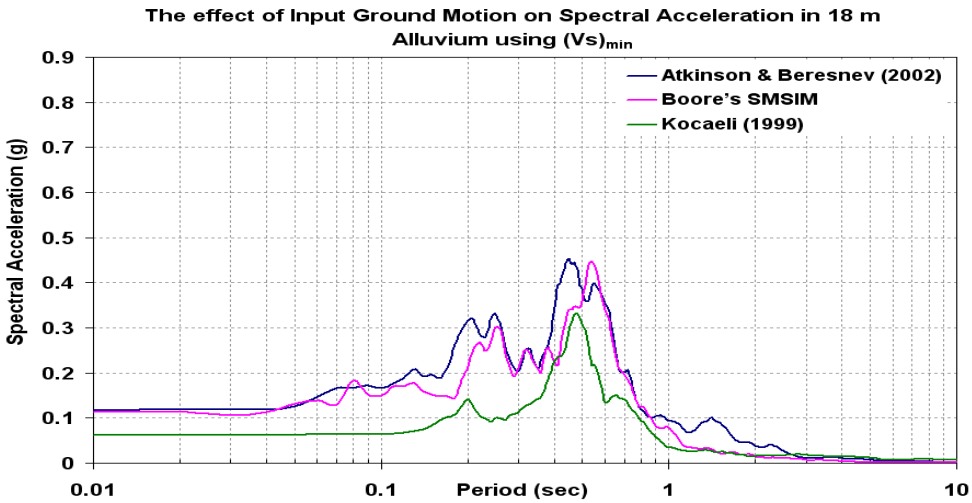
The effect of Input Ground Motion on Spectral Acceleration in 18 m Alluvium using (Vs)min
Atkinson & Beresnev (2002)
Boore's SMSIM
Kocaeli (1999)
Spectral Acceleration (g)
0.9
0.8
0.7
0.6
0.5
0.4
0.3
0.2
0.1
0
0.01
0.1
Period (sec)
1
10

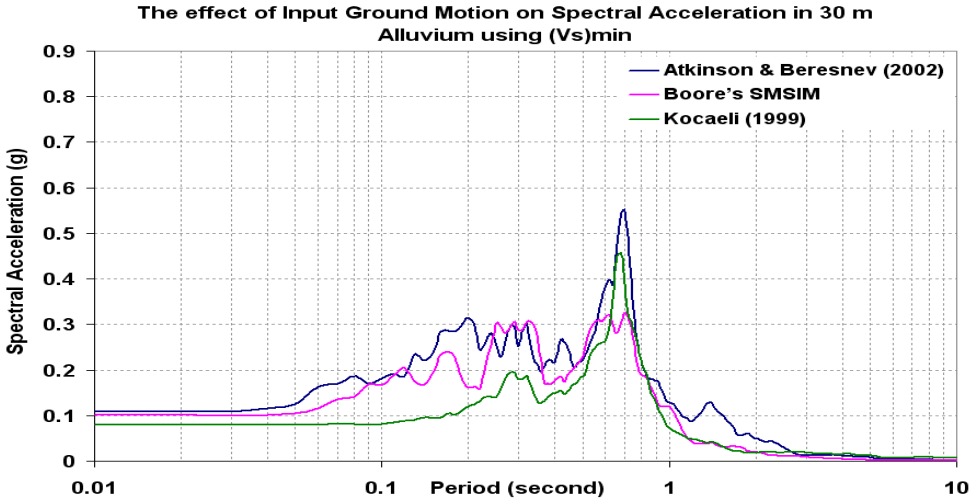
The effect of Input Ground Motion on Spectral Acceleration in 30 m Alluvium using (Vs)min
Atkinson & Beresnev (2002)
Boore's SMSIM
Kocaeli (1999)
Spectral Acceleration (g)
0.9
0.8
0.7
0.6
0.5
0.4
0.3
0.2
0.1
0
0.01
0.1
Period (second)
1
10

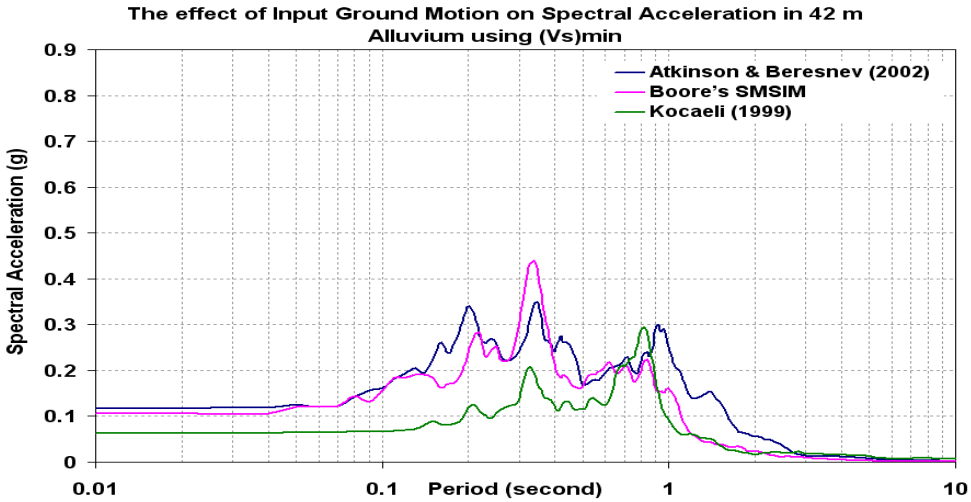
The effect of Input Ground Motion on Spectral Acceleration in 42 m Alluvium using (Vs)min
Atkinson & Beresnev (2002)
Boore's SMSIM
Kocaeli (1999)
Spectral Acceleration (g)
0.9
0.8
0.7
0.6
0.5
0.4
0.3
0.2
0.1
0
0.01
0.1
Period (second)
1
10

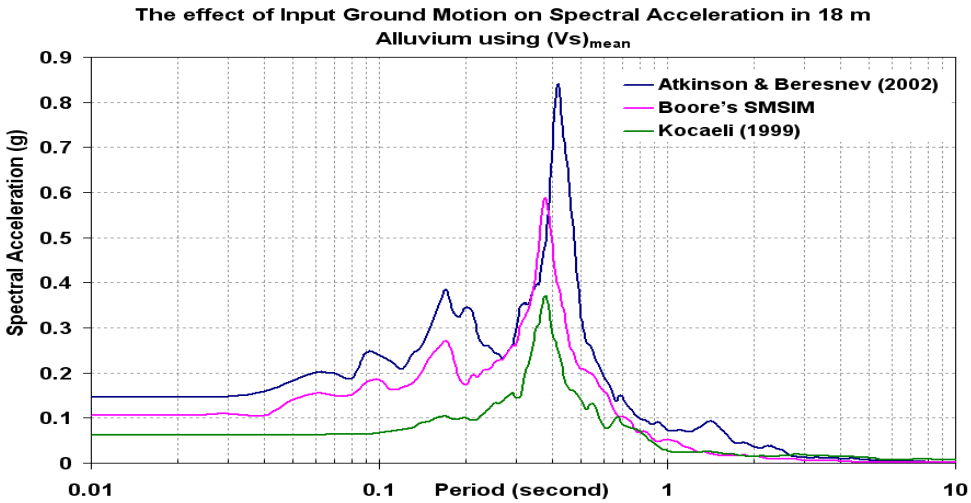
The effect of Input Ground Motion on Spectral Acceleration in 18 m Alluvium using (Vs)mean
Atkinson & Beresnev (2002)
Boore's SMSIM
Kocaeli (1999)
Spectral Acceleration (g)
0.9
0.8
0.7
0.6
0.5
0.4
0.3
0.2
0.1
0
0.01
0.1
Period (second)
1
10

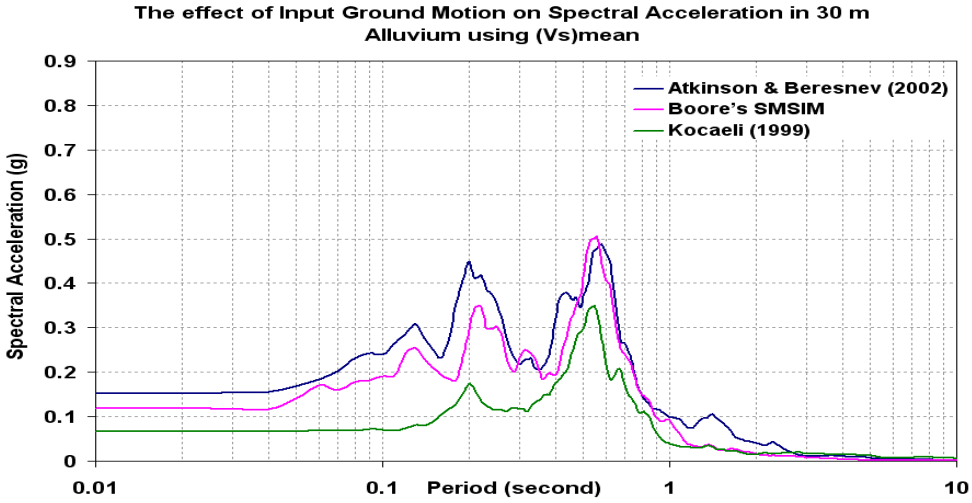
The effect of Input Ground Motion on Spectral Acceleration in 30 m Alluvium using (Vs)mean
Atkinson & Beresnev (2002)
Boore's SMSIM
Kocaeli (1999)
Spectral Acceleration (g)
0.9
0.8
0.7
0.6
0.5
0.4
0.3
0.2
0.1
0
0.01
0.1
Period (second)
1
10

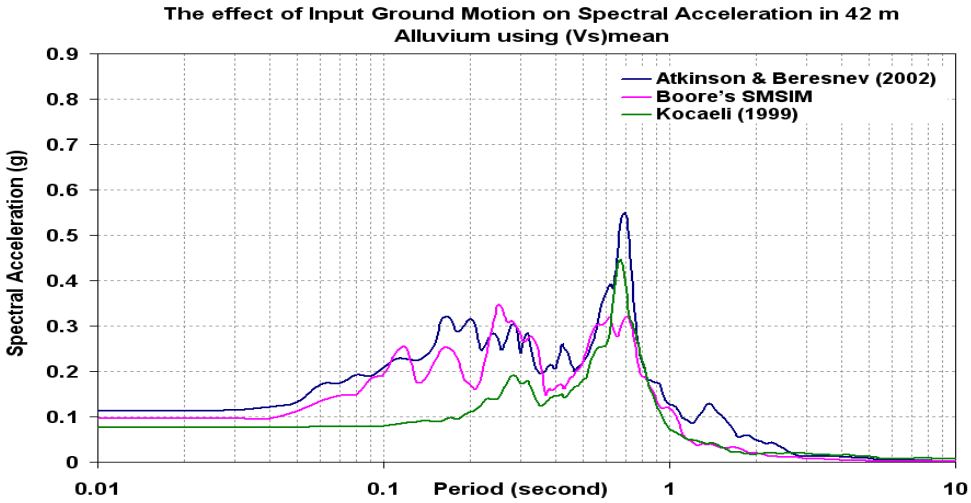
The effect of Input Ground Motion on Spectral Acceleration in 42 m Alluvium using (Vs)mean
Atkinson & Beresnev (2002)
Boore's SMSIM
Kocaeli (1999)
Spectral Acceleration (g)
0.9
0.8
0.7
0.6
0.5
0.4
0.3
0.2
0.1
0
0.01
0.1
Period (second)
1
10

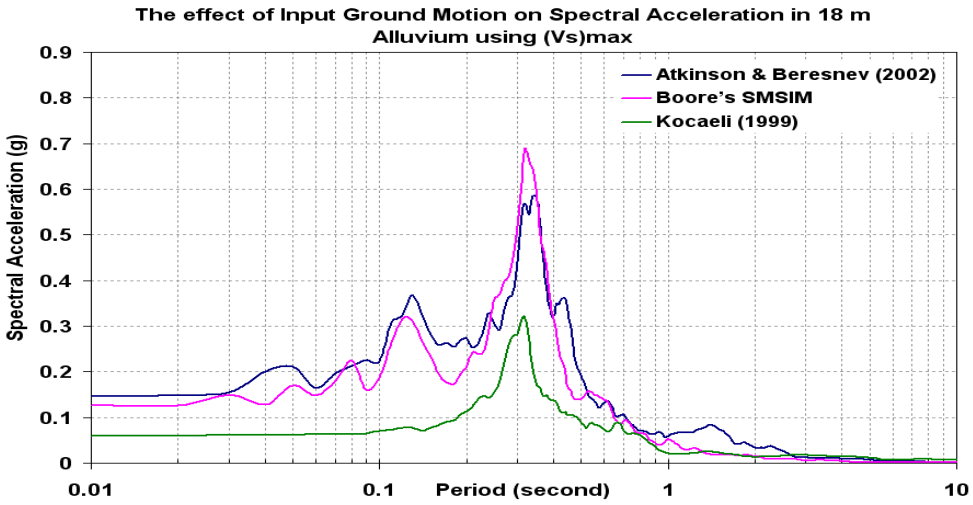
The effect of Input Ground Motion on Spectral Acceleration in 18 m Alluvium using (Vs)max
Atkinson & Beresnev (2002)
Boore's SMSIM
Kocaeli (1999)
Spectral Acceleration (g)
0.9
0.8
0.7
0.6
0.5
0.4
0.3
0.2
0.1
0
0.01
0.1
Period (second)
1
10

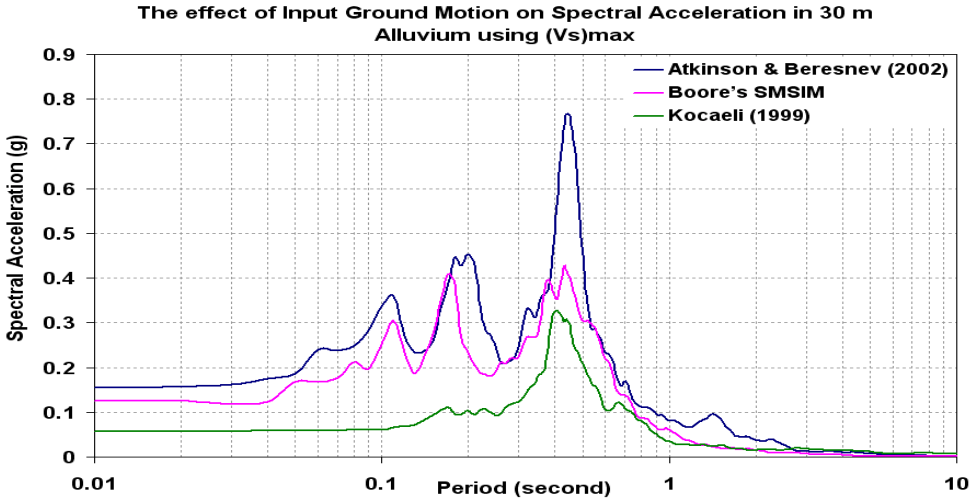
The effect of Input Ground Motion on Spectral Acceleration in 30 m Alluvium using (Vs)max
Atkinson & Beresnev (2002)
Boore's SMSIM
Kocaeli (1999)
Spectral Acceleration (g)
0.9
0.8
0.7
0.6
0.5
0.4
0.3
0.2
0.1
0
0.01
0.1
Period (second)
1
10

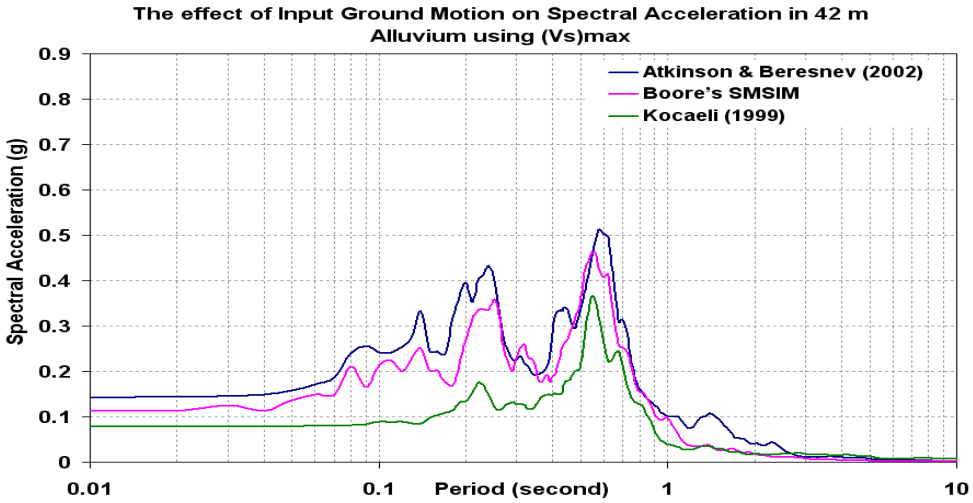
The effect of Input Ground Motion on Spectral Acceleration in 42 m Alluvium using (Vs)max
Atkinson & Beresnev (2002)
Boore's SMSIM
Kocaeli (1999)
Spectral Acceleration (g)
0.9
0.8
0.7
0.6
0.5
0.4
0.3
0.2
0.1
0
0.01
0.1
Period (second)
1
10

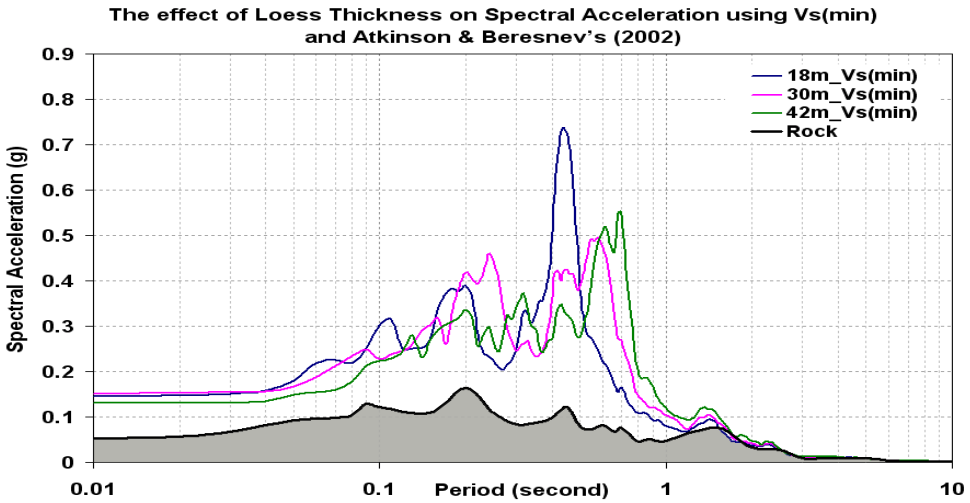
The effect of Loess Thickness on Spectral Acceleration using Vs(min) and Atkinson & Beresnev's (2002)
Spectral Acceleration (g)
0.9
0.8
0.7
0.6
0.5
0.4
0.3
0.2
0.1
0
0.01
0.1
Period (second)
1
10
18m_Vs(min)
30m_Vs(min)
42m_Vs(min)
Rock

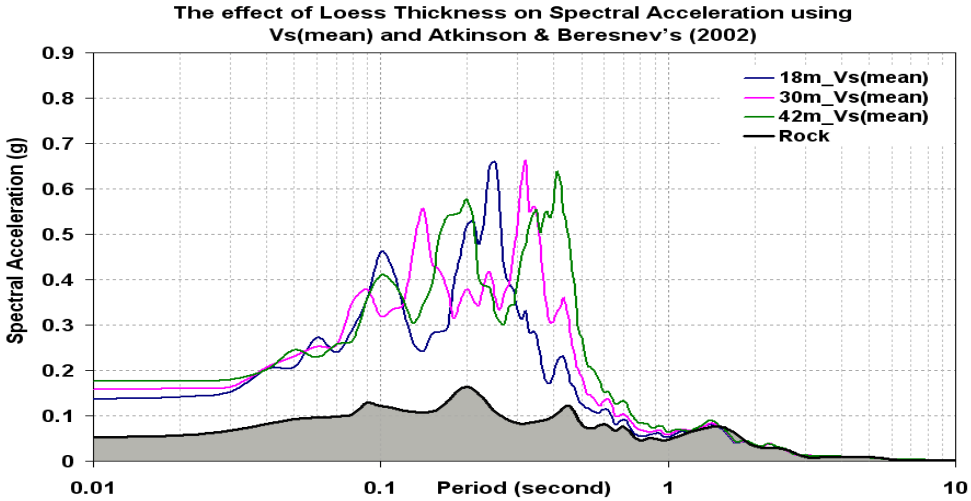
The effect of Loess Thickness on Spectral Acceleration using Vs(mean) and Atkinson & Beresnev's (2002)
Spectral Acceleration (g)
0.9
0.8
0.7
0.6
0.5
0.4
0.3
0.2
0.1
0
0.01
0.1
Period (second)
1
10
18m_Vs(mean)
30m_Vs(mean)
42m_Vs(mean)
Rock

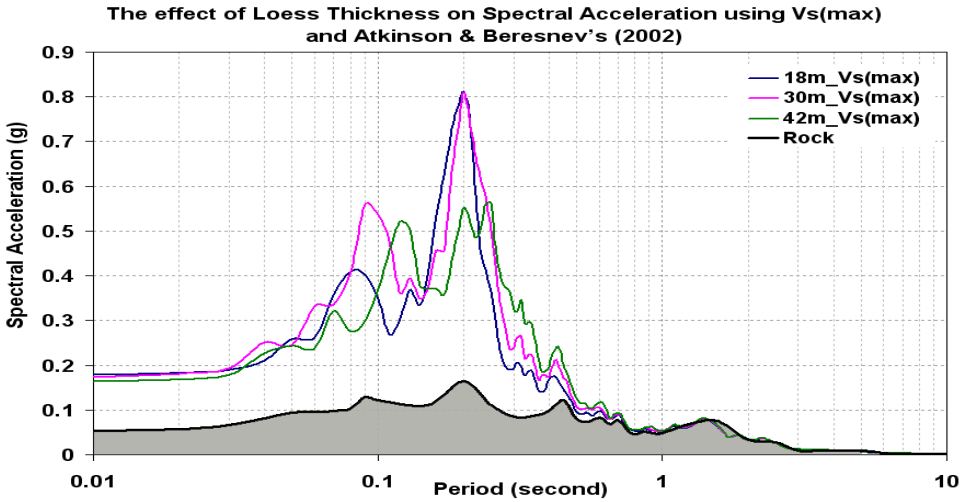
The effect of Loess Thickness on Spectral Acceleration using Vs(max) and Atkinson & Beresnev's (2002)
Spectral Acceleration (g)
0.9
0.8
0.7
0.6
0.5
0.4
0.3
0.2
0.1
0
0.01
0.1
Period (second)
1
10
18m_Vs(max)
30m_Vs(max)
42m_Vs(max)
Rock

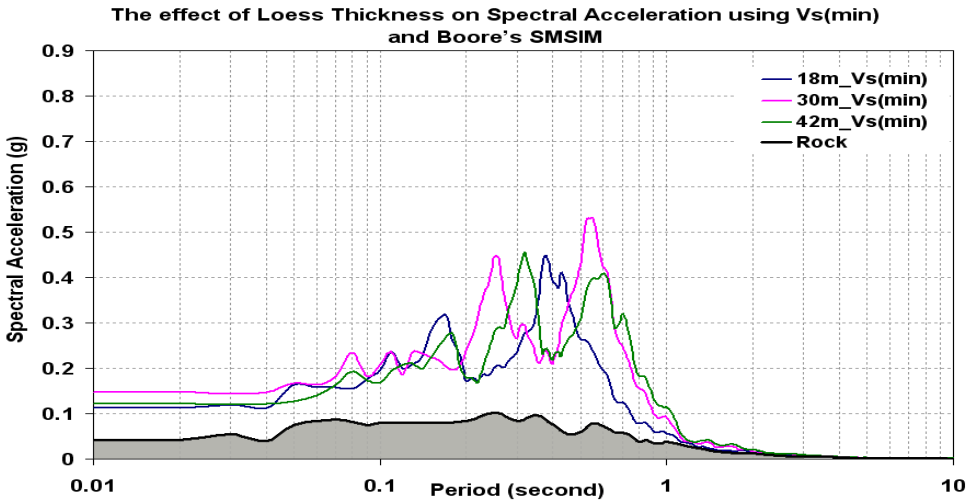
The effect of Loess Thickness on Spectral Acceleration using Vs(min) and Boore's SMSIM
Spectral Acceleration (g)
0.9
0.8
0.7
0.6
0.5
0.4
0.3
0.2
0.1
0
0.01
0.1
Period (second)
1
10
18m_Vs(min)
30m_Vs(min)
42m_Vs(min)
Rock

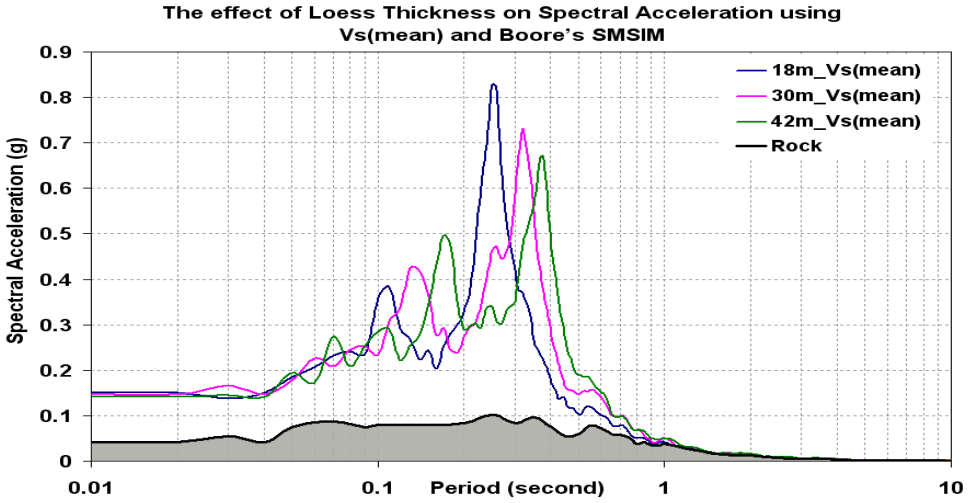
The effect of Loess Thickness on Spectral Acceleration using Vs(mean) and Boore's SMSIM
Spectral Acceleration (g)
0.9
0.8
0.7
0.6
0.5
0.4
0.3
0.2
0.1
0
0.01
0.1
Period (second)
1
10
18m_Vs(mean)
30m_Vs(mean)
42m_Vs(mean)
Rock

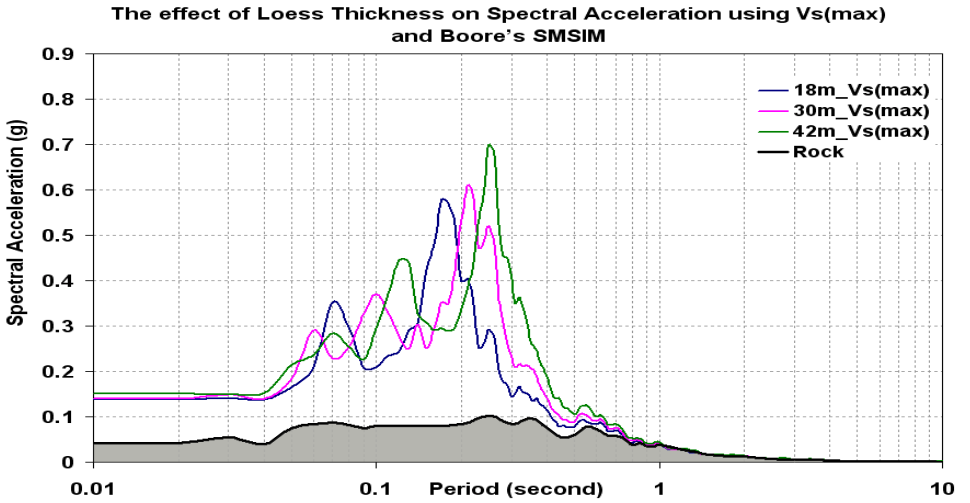
The effect of Loess Thickness on Spectral Acceleration using Vs(max) and Boore's SMSIM
Spectral Acceleration (g)
0.9
0.8
0.7
0.6
0.5
0.4
0.3
0.2
0.1
0
0.01
0.1
Period (second)
1
10
18m_Vs(max)
30m_Vs(max)
42m_Vs(max)
Rock

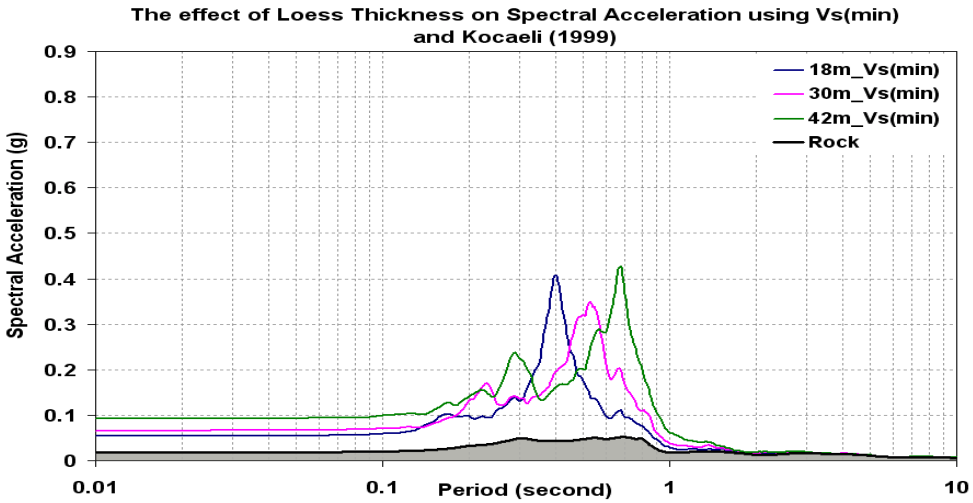
The effect of Loess Thickness on Spectral Acceleration using Vs(min) and Kocaeli (1999)
Spectral Acceleration (g)
0.9
0.8
0.7
0.6
0.5
0.4
0.3
0.2
0.1
0
0.01
0.1
Period (second)
1
10
18m_Vs(min)
30m_Vs(min)
42m_Vs(min)
Rock

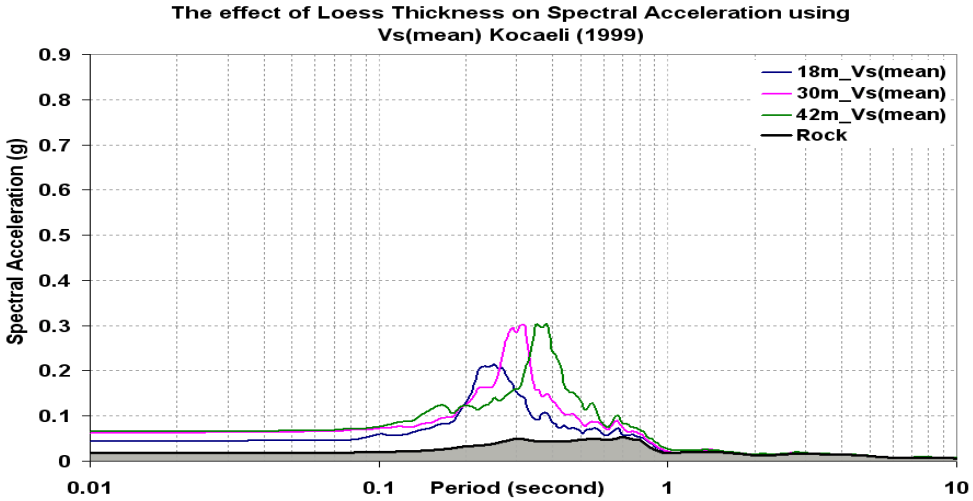
The effect of Loess Thickness on Spectral Acceleration using Vs(mean) Kocaeli (1999)
Spectral Acceleration (g)
0.9
0.8
0.7
0.6
0.5
0.4
0.3
0.2
0.1
0
0.01
0.1
Period (second)
1
10
18m_Vs(mean)
30m_Vs(mean)
42m_Vs(mean)
Rock

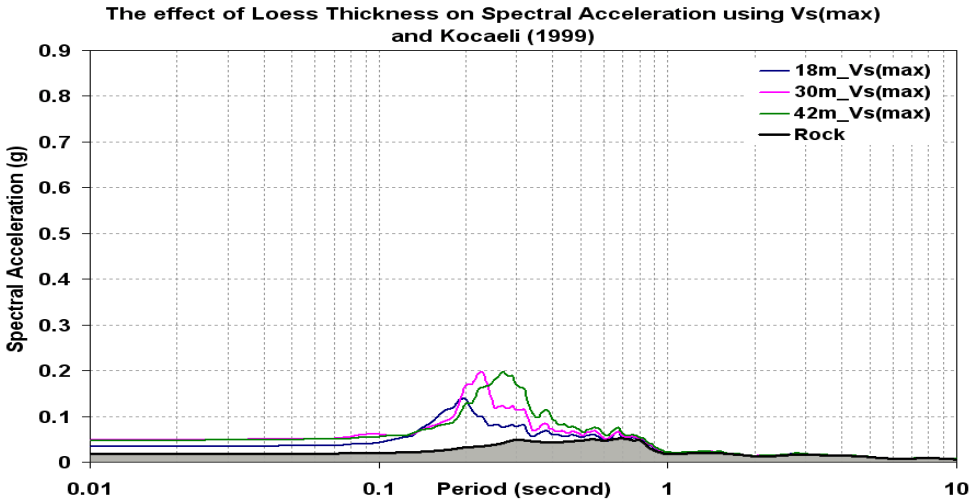
The effect of Loess Thickness on Spectral Acceleration using Vs(max) and Kocaeli (1999)
Spectral Acceleration (g)
0.9
0.8
0.7
0.6
0.5
0.4
0.3
0.2
0.1
0
0.01
0.1
Period (second)
1
10
18m_Vs(max)
30m_Vs(max)
42m_Vs(max)
Rock

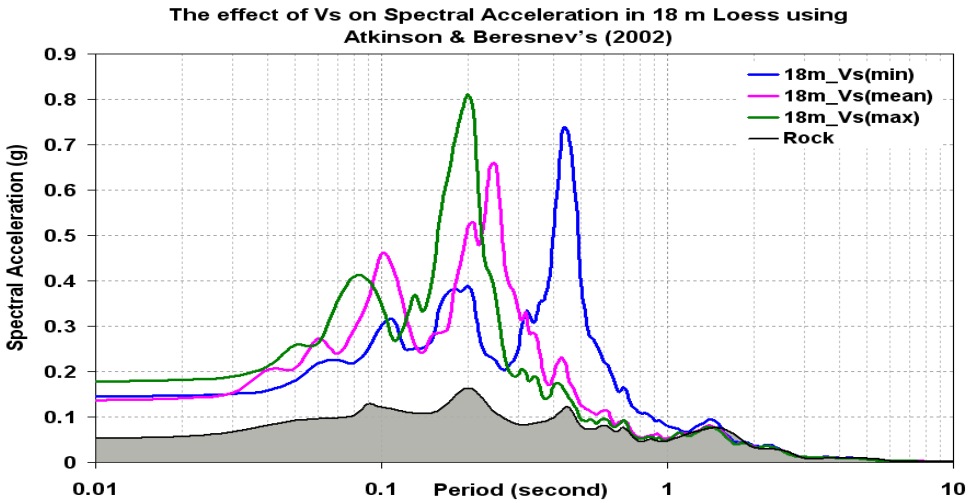
The effect of Vs on Spectral Acceleration in 18 m Loess using Atkinson & Beresnev's (2002)
Spectral Acceleration (g)
0.9
0.8
0.7
0.6
0.5
0.4
0.3
0.2
0.1
0
0.01
0.1
Period (second)
1
10
18m_Vs(min)
18m_Vs(mean)
18m_Vs(max)
Rock

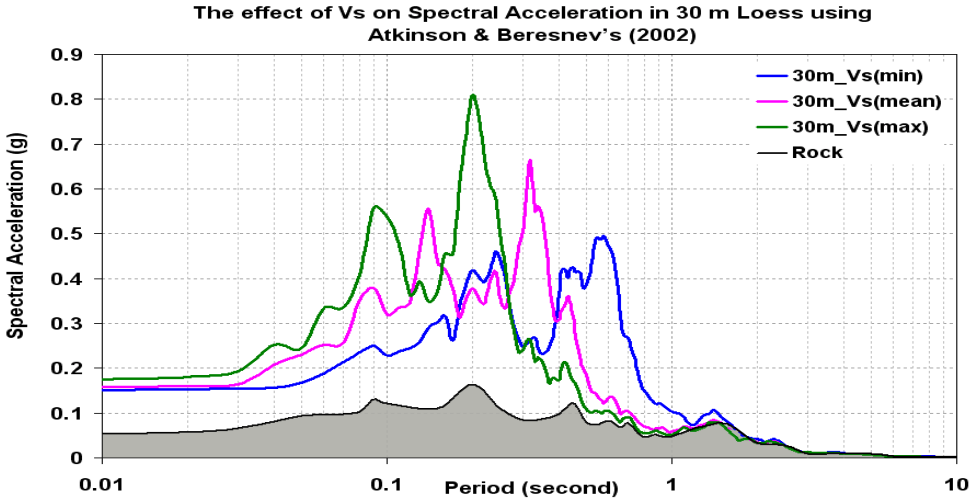
The effect of Vs on Spectral Acceleration in 30 m Loess using Atkinson & Beresnev's (2002)
Spectral Acceleration (g)
0.9
0.8
0.7
0.6
0.5
0.4
0.3
0.2
0.1
0
0.01
0.1
Period (second)
1
10
30m_Vs(min)
30m_Vs(mean)
30m_Vs(max)
Rock

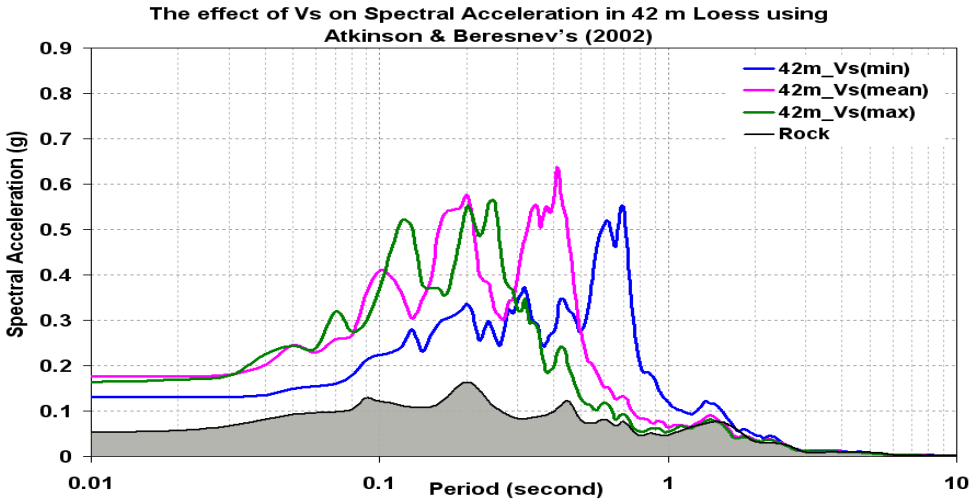
The effect of Vs on Spectral Acceleration in 42 m Loess using Atkinson & Beresnev's (2002)
Spectral Acceleration (g)
0.9
0.8
0.7
0.6
0.5
0.4
0.3
0.2
0.1
0
0.01
0.1
Period (second)
1
10
42m_Vs(min)
42m_Vs(mean)
42m_Vs(max)
Rock

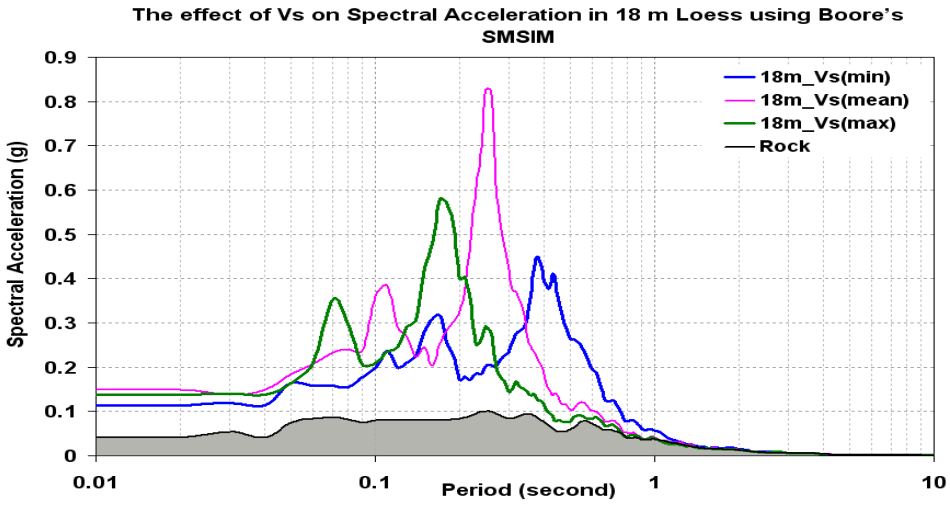
The effect of Vs on Spectral Acceleration in 18 m Loess using Boore's SMSIM
Spectral Acceleration (g)
Period (second)
18m_Vs(min)
18m_Vs(mean)
18m_Vs(max)
Rock
0.9
0.8
0.7
0.6
0.5
0.4
0.3
0.2
0.1
0
0.01
0.1
1
10

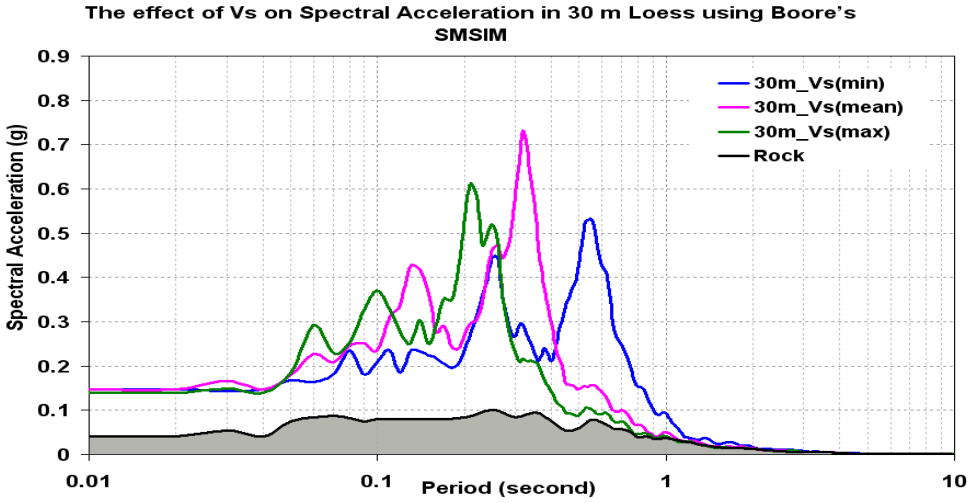
The effect of Vs on Spectral Acceleration in 30 m Loess using Boore's SMSIM
Spectral Acceleration (g)
Period (second)
30m_Vs(min)
30m_Vs(mean)
30m_Vs(max)
Rock
0.9
0.8
0.7
0.6
0.5
0.4
0.3
0.2
0.1
0
0.01
0.1
1
10

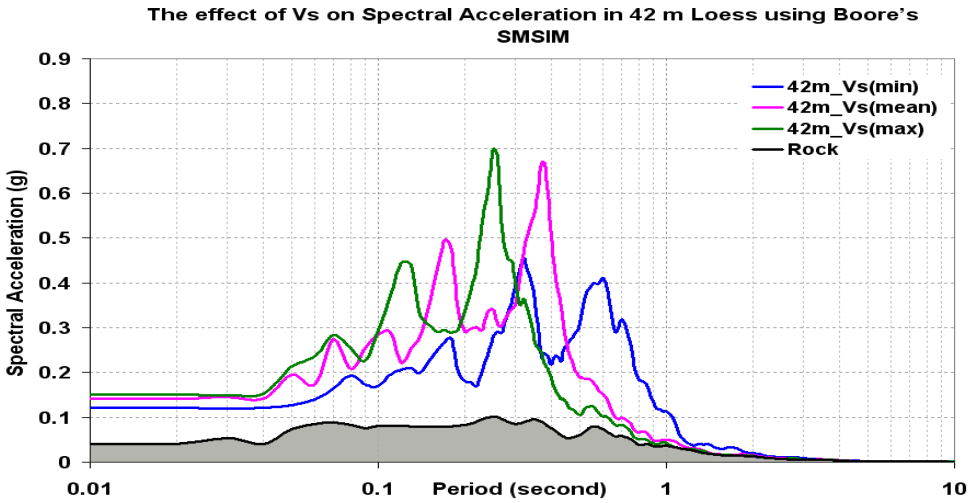
The effect of Vs on Spectral Acceleration in 42 m Loess using Boore's SMSIM
Spectral Acceleration (g)
Period (second)
42m_Vs(min)
42m_Vs(mean)
42m_Vs(max)
Rock
0.9
0.8
0.7
0.6
0.5
0.4
0.3
0.2
0.1
0
0.01
0.1
1
10

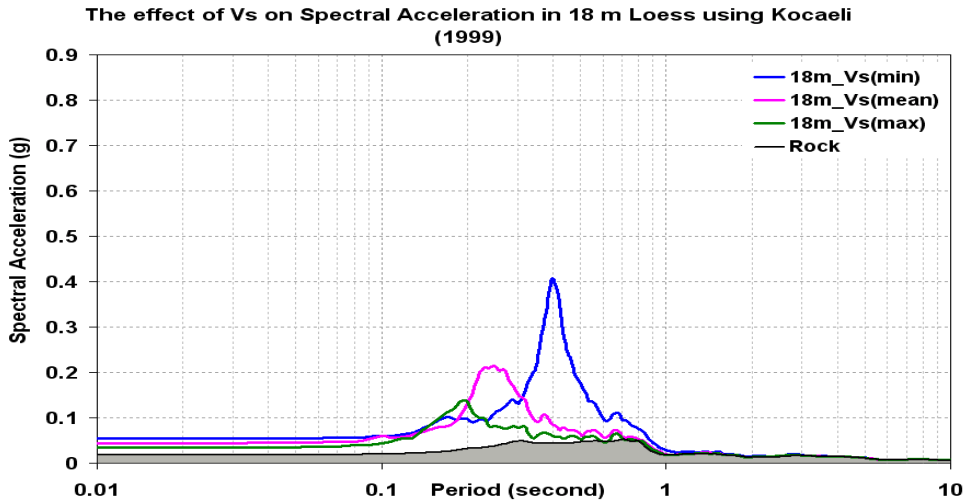
The effect of Vs on Spectral Acceleration in 18 m Loess using Kocaeli (1999)
Spectral Acceleration (g)
0.9
0.8
0.7
0.6
0.5
0.4
0.3
0.2
0.1
0
0.01
0.1
Period (second)
1
10
18m_Vs(min)
18m_Vs(mean)
18m_Vs(max)
Rock

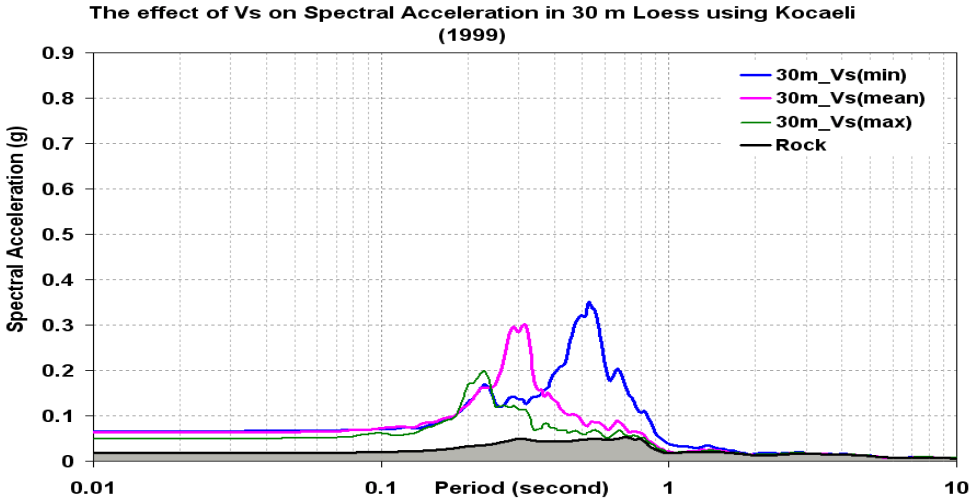
The effect of Vs on Spectral Acceleration in 30 m Loess using Kocaeli (1999)
Spectral Acceleration (g)
0.9
0.8
0.7
0.6
0.5
0.4
0.3
0.2
0.1
0
0.01
0.1
Period (second)
1
10
30m_Vs(min)
30m_Vs(mean)
30m_Vs(max)
Rock

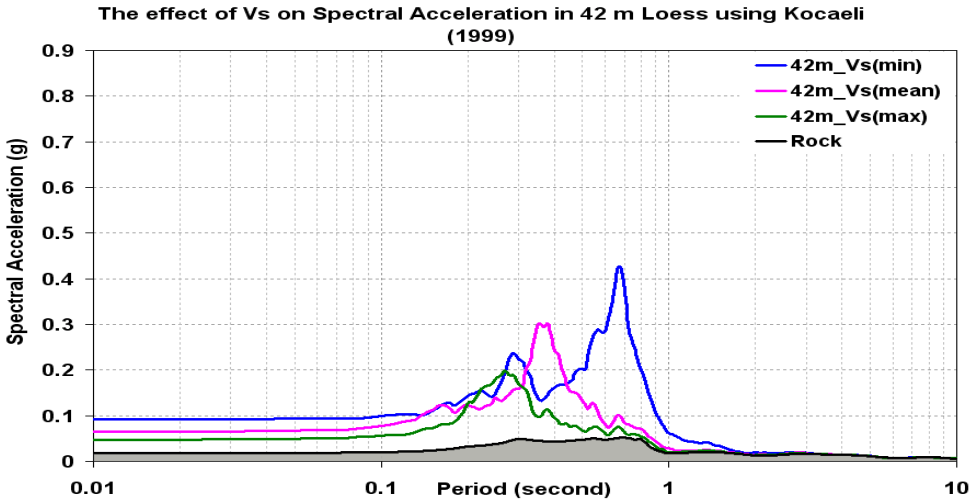
The effect of Vs on Spectral Acceleration in 42 m Loess using Kocaeli (1999)
Spectral Acceleration (g)
0.9
0.8
0.7
0.6
0.5
0.4
0.3
0.2
0.1
0
0.01
0.1
Period (second)
1
10
42m_Vs(min)
42m_Vs(mean)
42m_Vs(max)
Rock

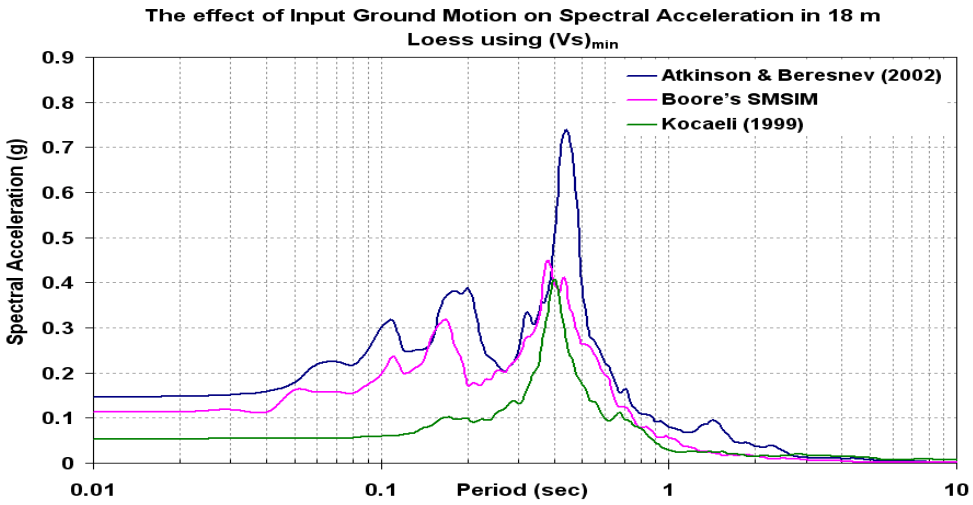
The effect of Input Ground Motion on Spectral Acceleration in 18 m
Loess using (Vs)min
Atkinson & Beresnev (2002)
Boore's SMSIM
Kocaeli (1999)
Spectral Acceleration (g)
0.9
0.8
0.7
0.6
0.5
0.4
0.3
0.2
0.1
0
0.01
0.1
Period (sec)
1
10

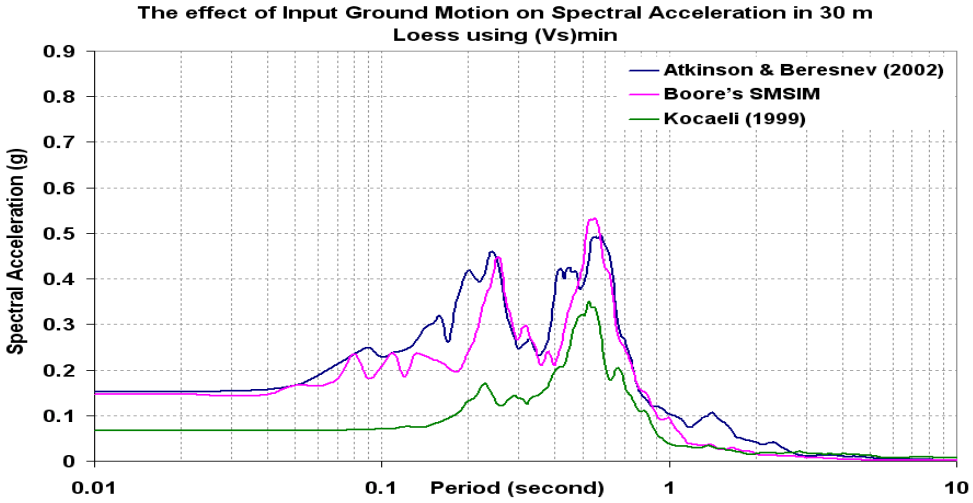
The effect of Input Ground Motion on Spectral Acceleration in 30 m
Loess using (Vs)min
Atkinson & Beresnev (2002)
Boore's SMSIM
Kocaeli (1999)
Spectral Acceleration (g)
0.9
0.8
0.7
0.6
0.5
0.4
0.3
0.2
0.1
0
0.01
0.1
Period (second)
1
10

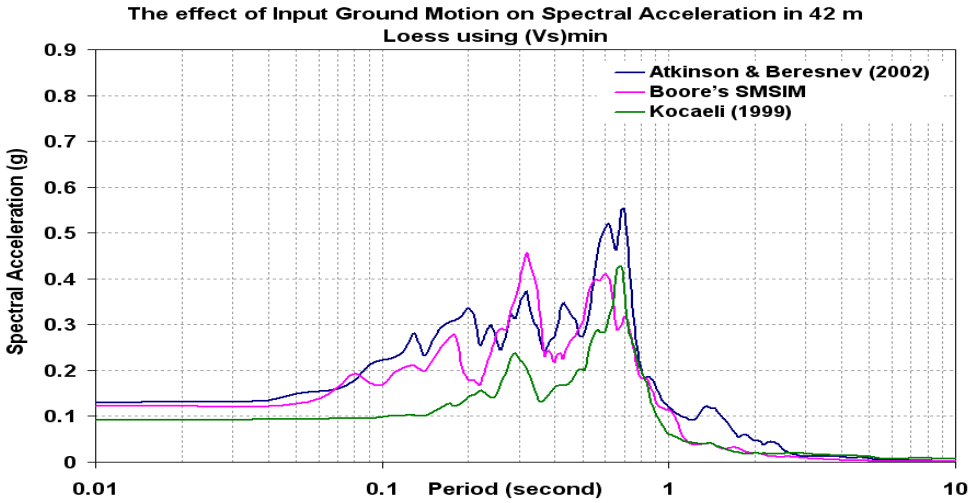
The effect of Input Ground Motion on Spectral Acceleration in 42 m
Loess using (Vs)min
Atkinson & Beresnev (2002)
Boore's SMSIM
Kocaeli (1999)
Spectral Acceleration (g)
0.9
0.8
0.7
0.6
0.5
0.4
0.3
0.2
0.1
0
0.01
0.1
Period (second)
1
10

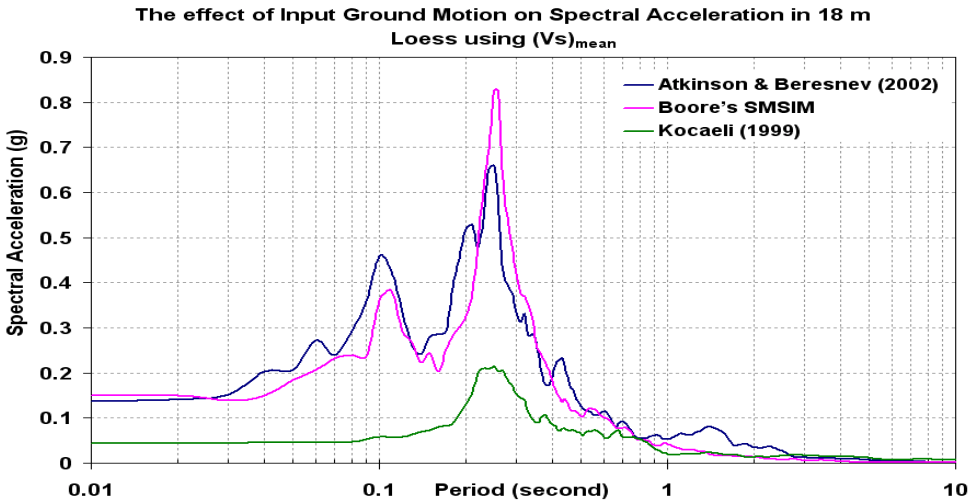
The effect of Input Ground Motion on Spectral Acceleration in 18 m
Loess using (Vs)mean
Atkinson & Beresnev (2002)
Boore's SMSIM
Kocaeli (1999)
Spectral Acceleration (g)
Period (second)
0.9
0.8
0.7
0.6
0.5
0.4
0.3
0.2
0.1
0
0.01
0.1
1
10

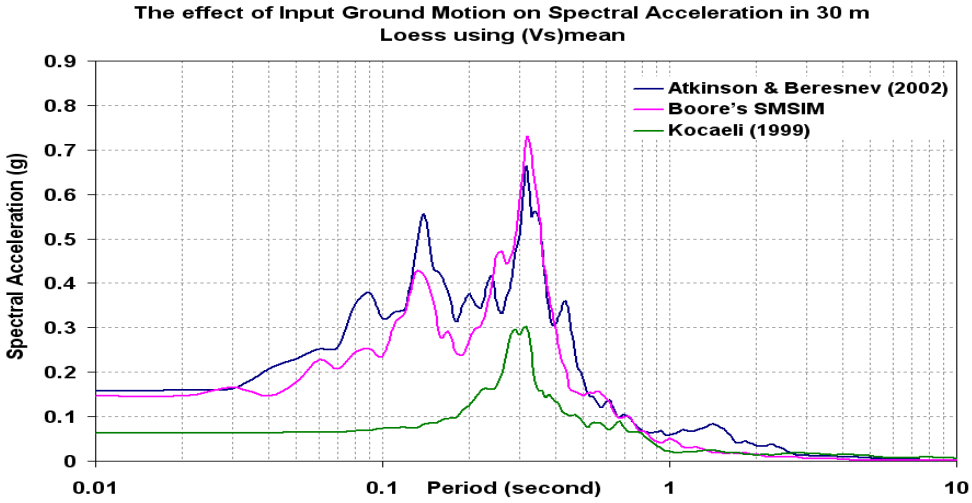
The effect of Input Ground Motion on Spectral Acceleration in 30 m
Loess using (Vs)mean
Atkinson & Beresnev (2002)
Boore's SMSIM
Kocaeli (1999)
Spectral Acceleration (g)
Period (second)
0.9
0.8
0.7
0.6
0.5
0.4
0.3
0.2
0.1
0
0.01
0.1
1
10

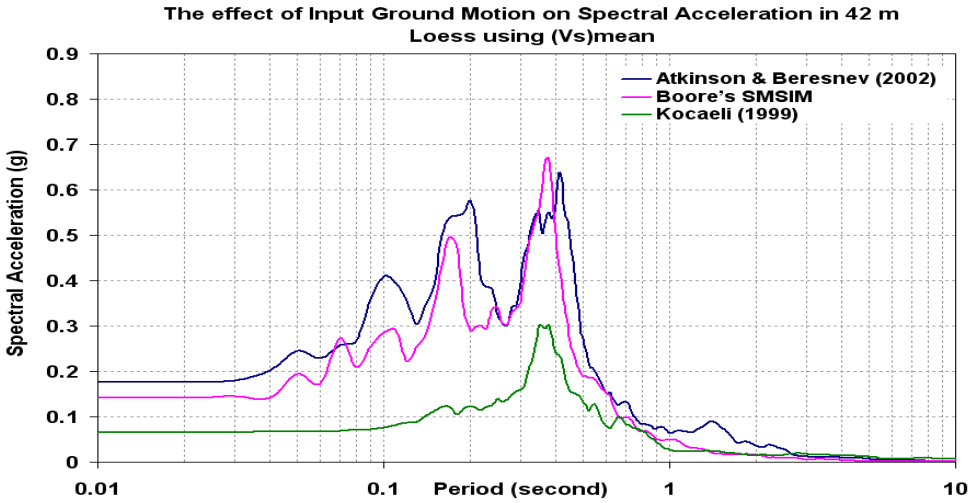
The effect of Input Ground Motion on Spectral Acceleration in 42 m
Loess using (Vs)mean
Atkinson & Beresnev (2002)
Boore's SMSIM
Kocaeli (1999)
Spectral Acceleration (g)
Period (second)
0.9
0.8
0.7
0.6
0.5
0.4
0.3
0.2
0.1
0
0.01
0.1
1
10

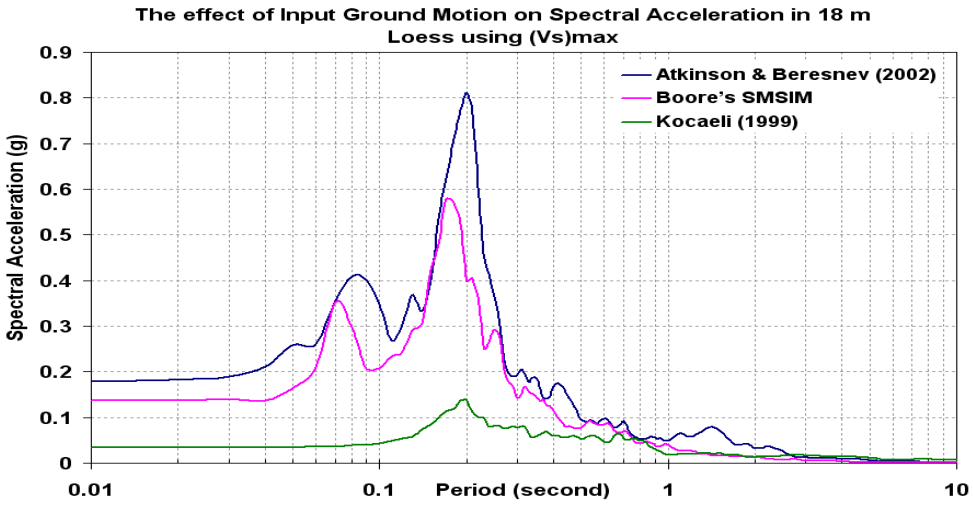
The effect of Input Ground Motion on Spectral Acceleration in 18 m
Loess using (Vs)max
Atkinson & Beresnev (2002)
Boore's SMSIM
Kocaeli (1999)
Spectral Acceleration (g)
0.9
0.8
0.7
0.6
0.5
0.4
0.3
0.2
0.1
0
0.01
0.1
Period (second)
1
10

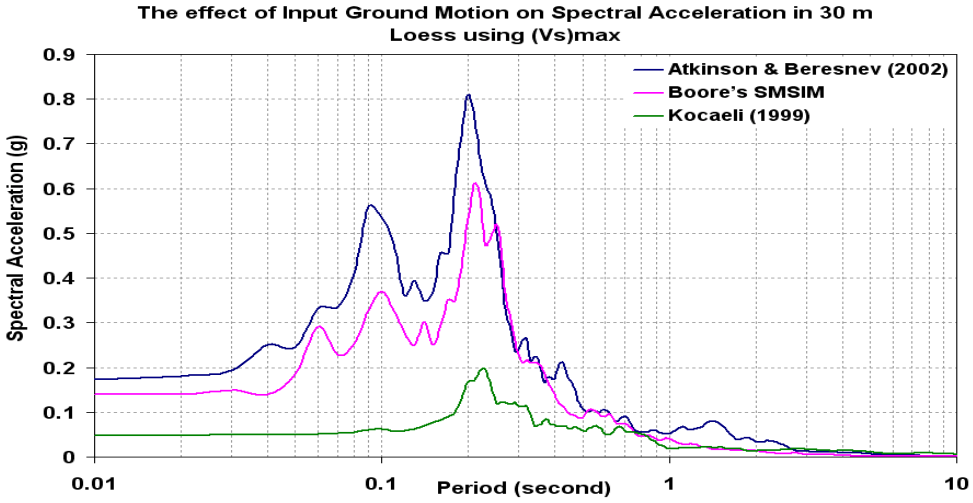
The effect of Input Ground Motion on Spectral Acceleration in 30 m
Loess using (Vs)max
Atkinson & Beresnev (2002)
Boore's SMSIM
Kocaeli (1999)
Spectral Acceleration (g)
0.9
0.8
0.7
0.6
0.5
0.4
0.3
0.2
0.1
0
0.01
0.1
Period (second)
1
10

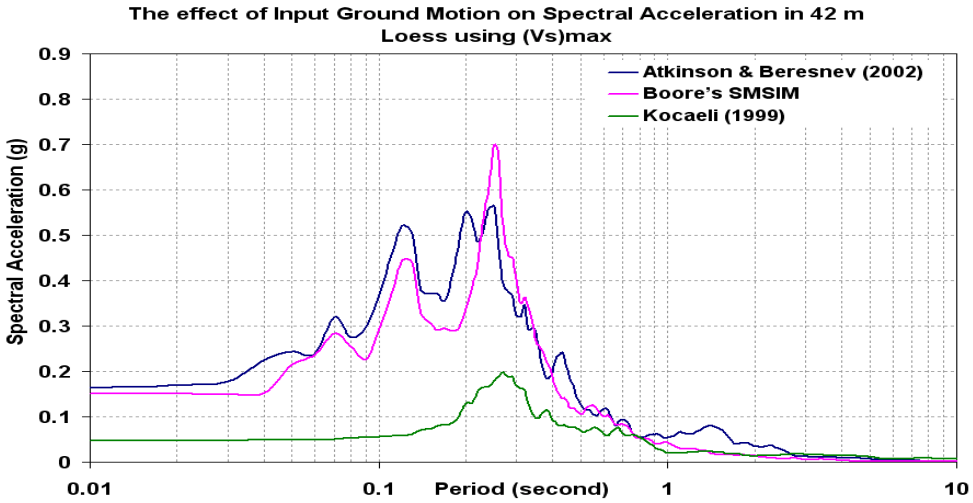
The effect of Input Ground Motion on Spectral Acceleration in 42 m
Loess using (Vs)max
Atkinson & Beresnev (2002)
Boore's SMSIM
Kocaeli (1999)
Spectral Acceleration (g)
0.9
0.8
0.7
0.6
0.5
0.4
0.3
0.2
0.1
0
0.01
0.1
Period (second)
1
10

APPENDIX B.
NORMALIZED RESPONSE SPECTRA

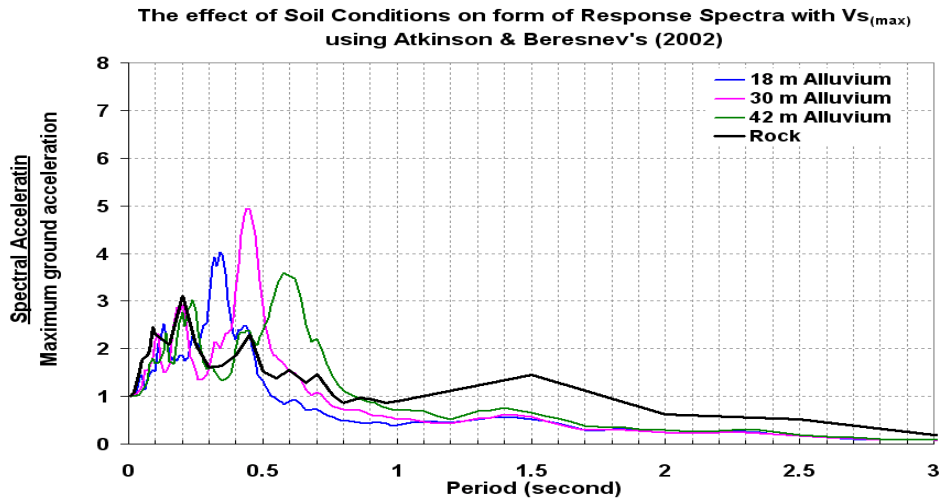
The effect of Soil Conditions on form of Response Spectra with Vs(max)
using Atkinson & Beresnev's (2002)
Spectral Acceleratin
Maximum ground acceleration
18 m Alluvium
30 m Alluvium
42 m Alluvium
Rock
Period (second)

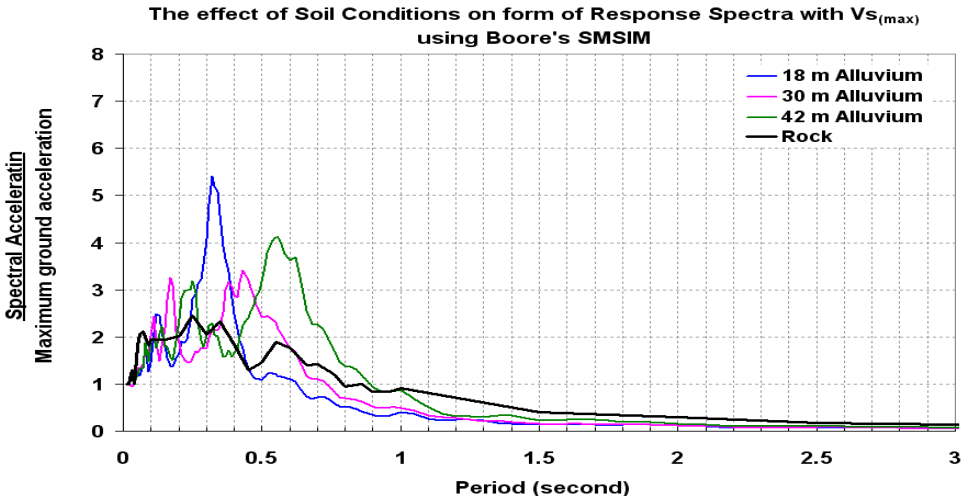
The effect of Soil Conditions on form of Response Spectra with Vs(max)
using Boore's SMSIM
Spectral Acceleratin
Maximum ground acceleration
18 m Alluvium
30 m Alluvium
42 m Alluvium
Rock
Period (second)

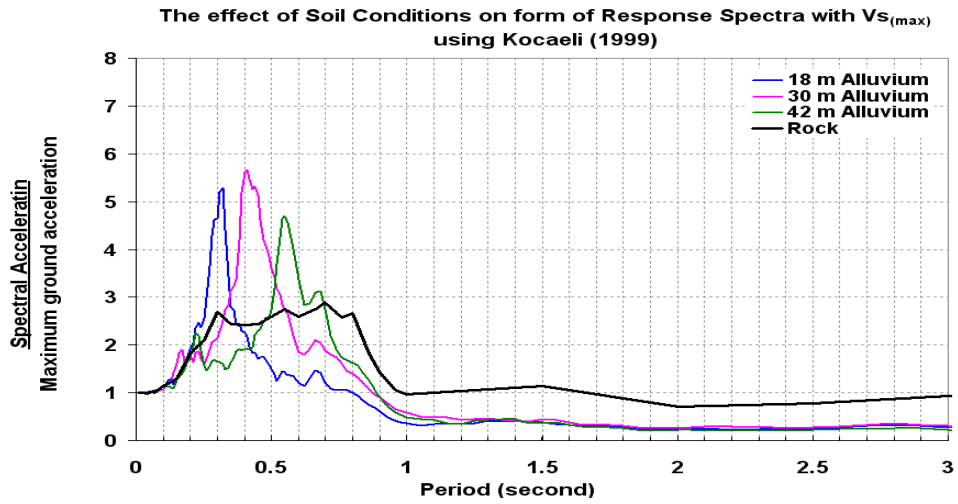
The effect of Soil Conditions on form of Response Spectra with Vs(max)
using Kocaeli (1999)
Spectral Acceleratin
Maximum ground acceleration
18 m Alluvium
30 m Alluvium
42 m Alluvium
Rock
Period (second)

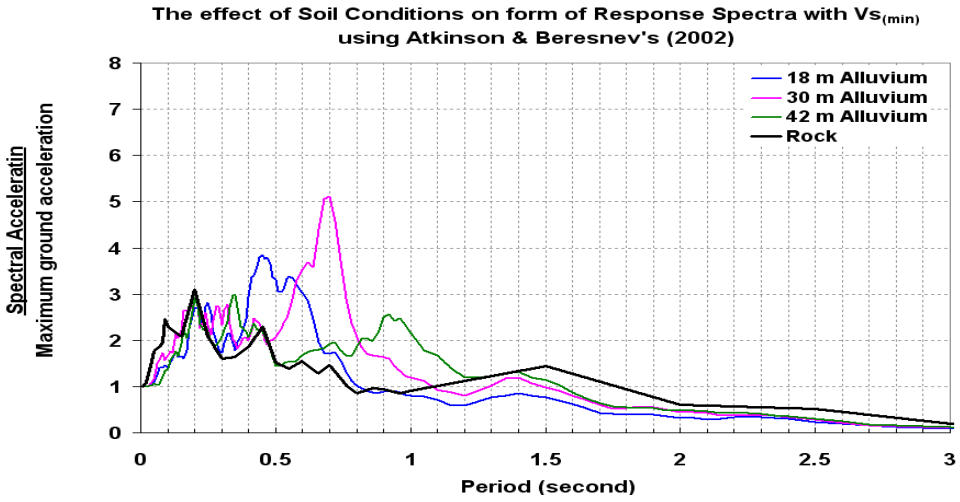
The effect of Soil Conditions on form of Response Spectra with Vs(min) using Atkinson & Beresnev's (2002)
Spectral Acceleratin
Maximum ground acceleration
18 m Alluvium
30 m Alluvium
42 m Alluvium
Rock
Period (second)

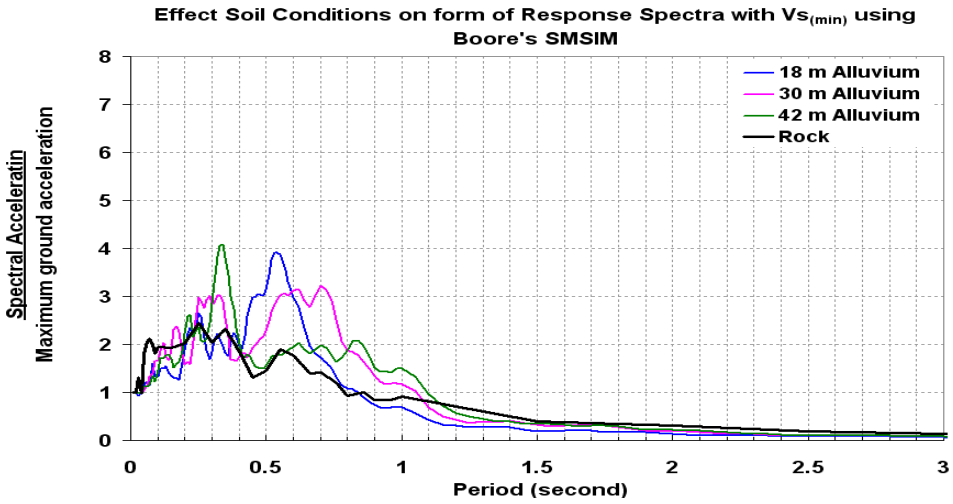
Effect Soil Conditions on form of Response Spectra with Vs(min) using Boore's SMSIM
Spectral Acceleratin
Maximum ground acceleration
18 m Alluvium
30 m Alluvium
42 m Alluvium
Rock
Period (second)

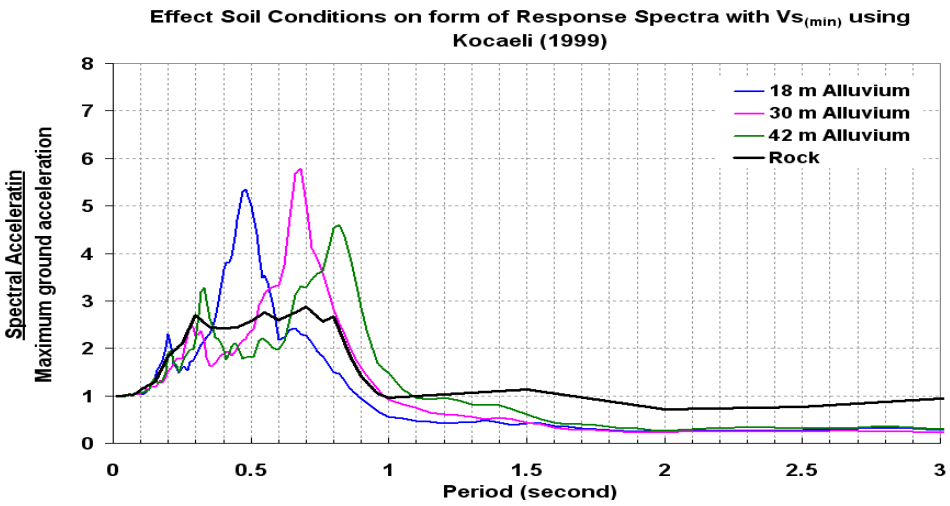
Effect Soil Conditions on form of Response Spectra with Vs(min) using Kocaeli (1999)
Spectral Acceleratin
Maximum ground acceleration
18 m Alluvium
30 m Alluvium
42 m Alluvium
Rock
Period (second)

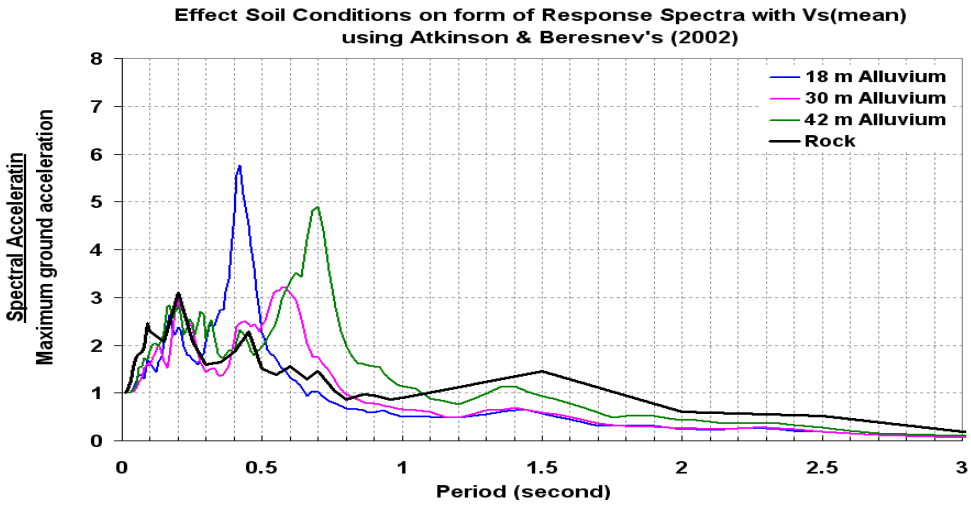
Effect Soil Conditions on form of Response Spectra with Vs(mean)
using Atkinson & Beresnev's (2002)
Spectral Acceleratin
Maximum ground acceleration
18 m Alluvium
30 m Alluvium
42 m Alluvium
Rock
Period (second)

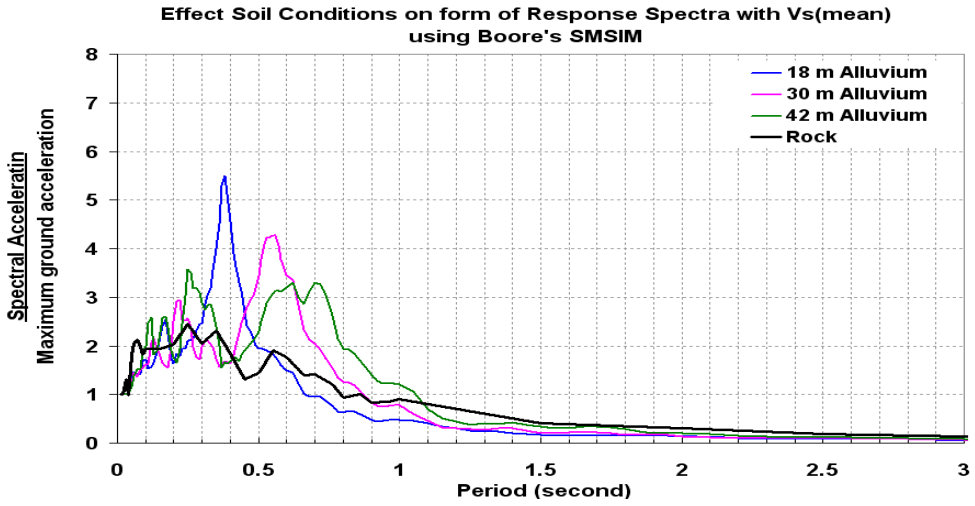
Effect Soil Conditions on form of Response Spectra with Vs(mean)
using Boore's SMSIM
Spectral Acceleratin
Maximum ground acceleration
18 m Alluvium
30 m Alluvium
42 m Alluvium
Rock
Period (second)

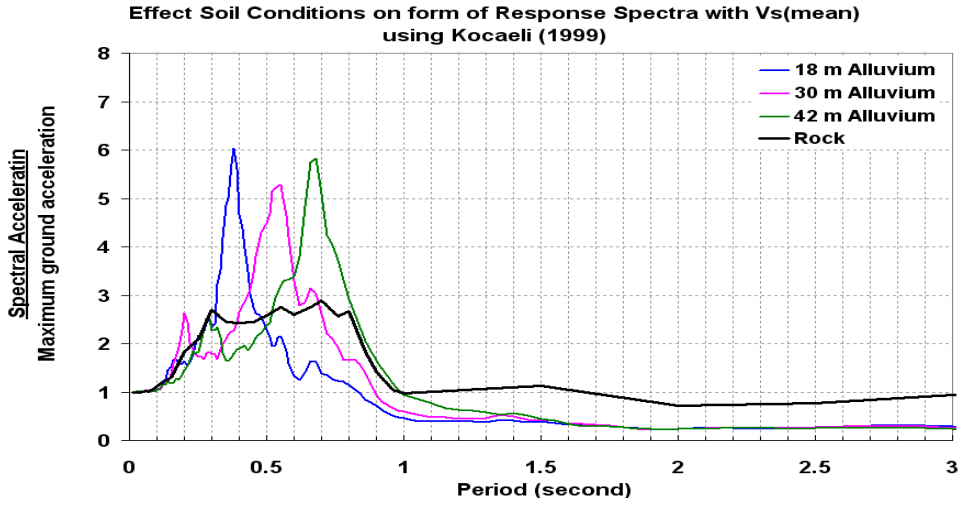
Effect Soil Conditions on form of Response Spectra with Vs(mean)
using Kocaeli (1999)
Spectral Acceleratin
Maximum ground acceleration
18 m Alluvium
30 m Alluvium
42 m Alluvium
Rock
Period (second)

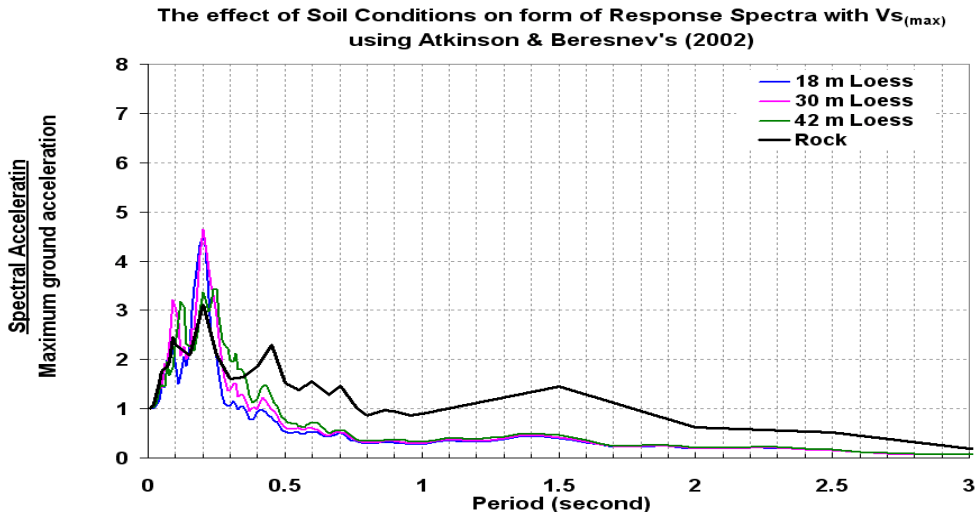
The effect of Soil Conditions on form of Response Spectra with Vs(max)
using Atkinson & Beresnev's (2002)
Spectral Acceleratin
Maximum ground acceleration
18 m Loess
30 m Loess
42 m Loess
Rock
Period (second)

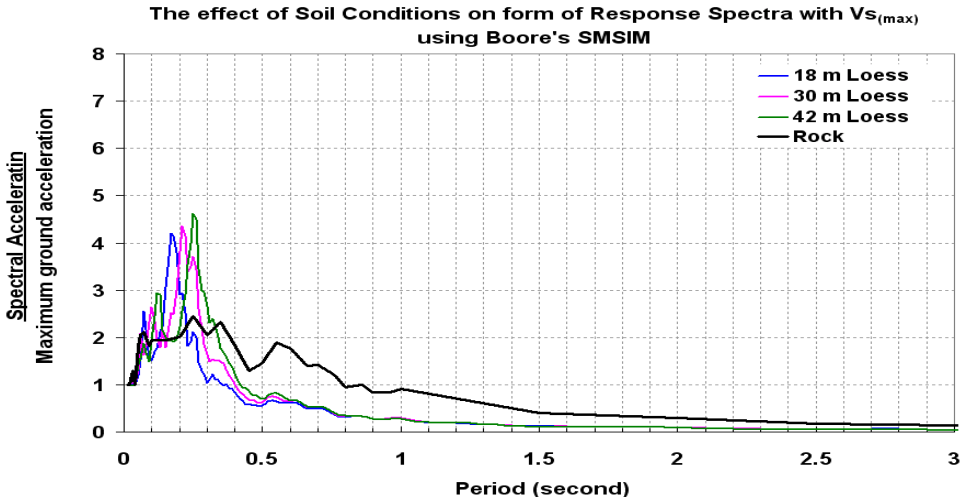
The effect of Soil Conditions on form of Response Spectra with Vs(max)
using Boore's SMSIM
Spectral Acceleratin
Maximum ground acceleration
18 m Loess
30 m Loess
42 m Loess
Rock
Period (second)

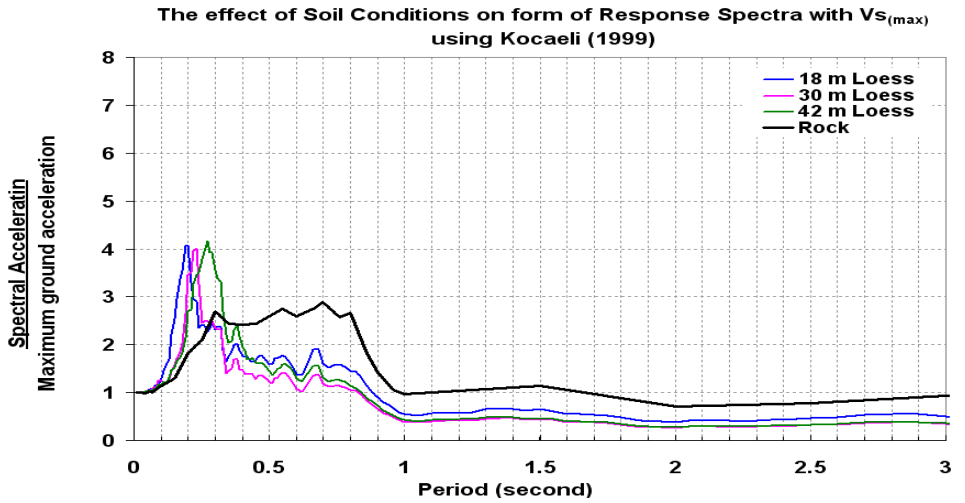
The effect of Soil Conditions on form of Response Spectra with Vs(max)
using Kocaeli (1999)
Spectral Acceleratin
Maximum ground acceleration
18 m Loess
30 m Loess
42 m Loess
Rock
Period (second)

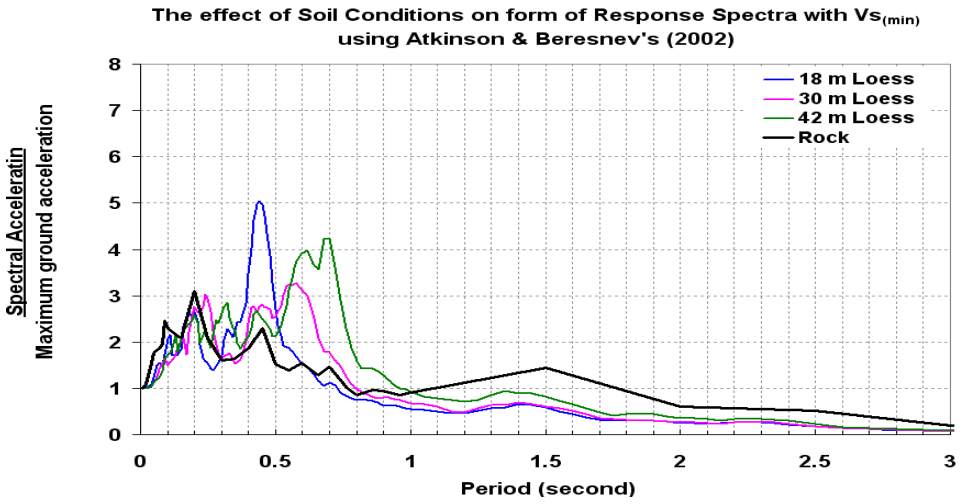
The effect of Soil Conditions on form of Response Spectra with Vs(min) using Atkinson & Beresnev's (2002)
Spectral Acceleratin
Maximum ground acceleration
18 m Loess
30 m Loess
42 m Loess
Rock
Period (second)

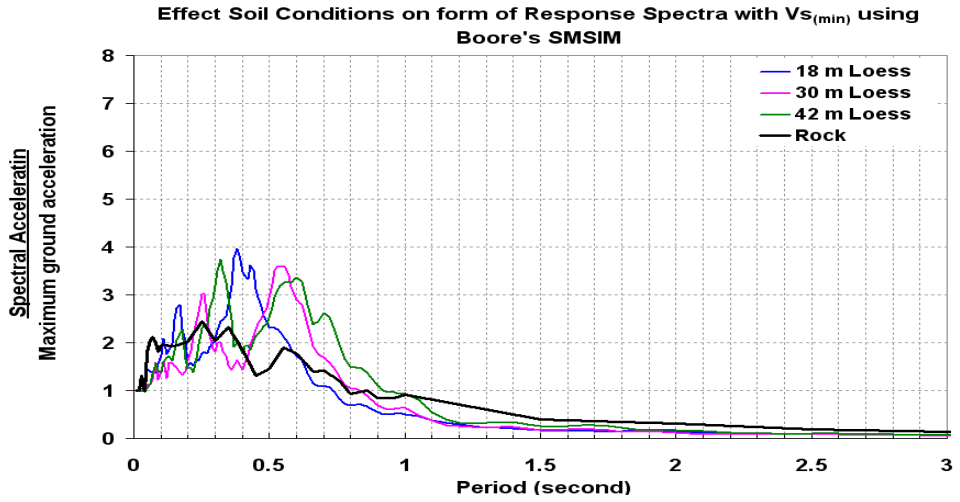
Effect Soil Conditions on form of Response Spectra with Vs(min) using Boore's SMSIM
Spectral Acceleratin
Maximum ground acceleration
18 m Loess
30 m Loess
42 m Loess
Rock
Period (second)

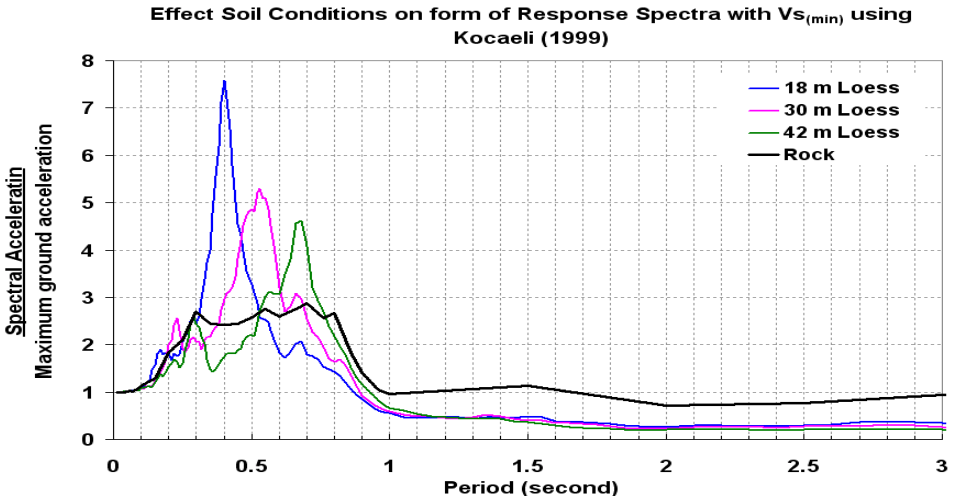
Effect Soil Conditions on form of Response Spectra with Vs(min) using Kocaeli (1999)
Spectral Acceleratin
Maximum ground acceleration
18 m Loess
30 m Loess
42 m Loess
Rock
Period (second)

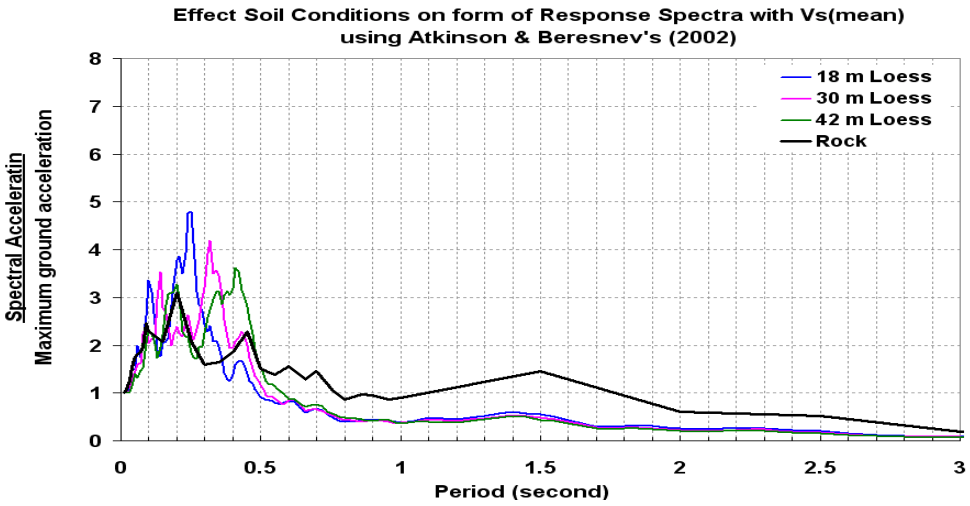
Effect Soil Conditions on form of Response Spectra with Vs(mean)
using Atkinson & Beresnev's (2002)
Spectral Acceleratin
Maximum ground acceleration
18 m Loess
30 m Loess
42 m Loess
Rock
0
1
2
3
4
5
6
7
8
0
0.5
1
1.5
2
2.5
3
Period (second)

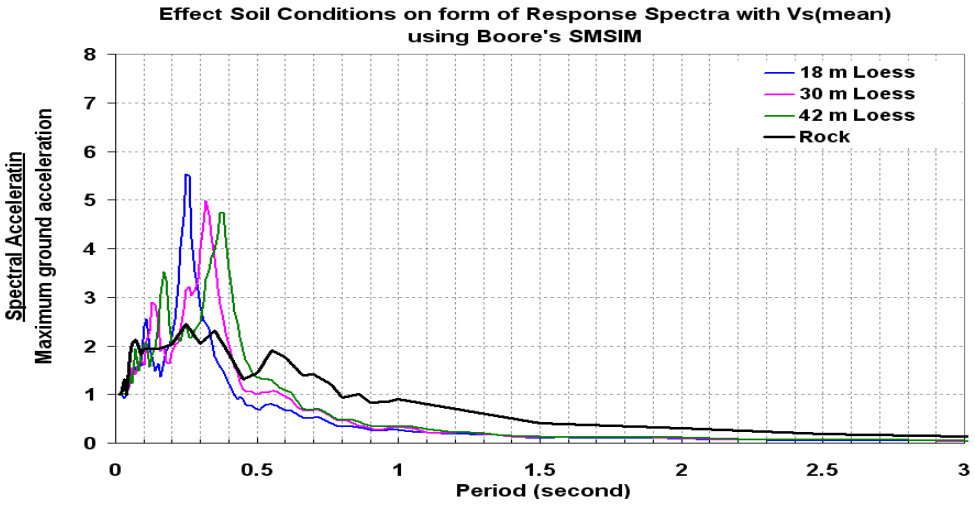
Effect Soil Conditions on form of Response Spectra with Vs(mean)
using Boore's SMSIM
Spectral Acceleratin
Maximum ground acceleration
18 m Loess
30 m Loess
42 m Loess
Rock
0
1
2
3
4
5
6
7
8
0
0.5
1
1.5
2
2.5
3
Period (second)

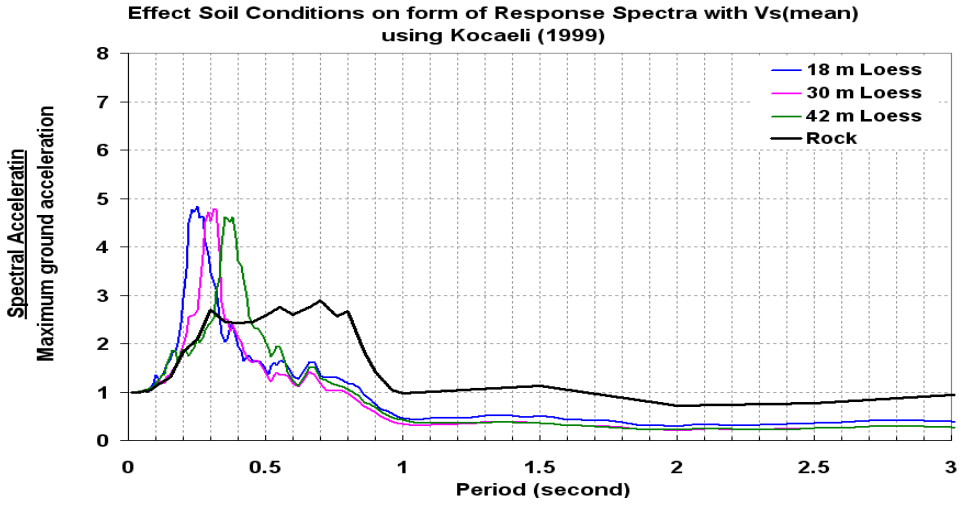
Effect Soil Conditions on form of Response Spectra with Vs(mean)
using Kocaeli (1999)
Spectral Acceleratin
Maximum ground acceleration
18 m Loess
30 m Loess
42 m Loess
Rock
0
1
2
3
4
5
6
7
8
0
0.5
1
1.5
2
2.5
3
Period (second)

APPENDIX C.
THE DISTRIBUTION OF AMPLIFICATION
FROM 0.01 SECOND TO 2 SECOND PERIOD

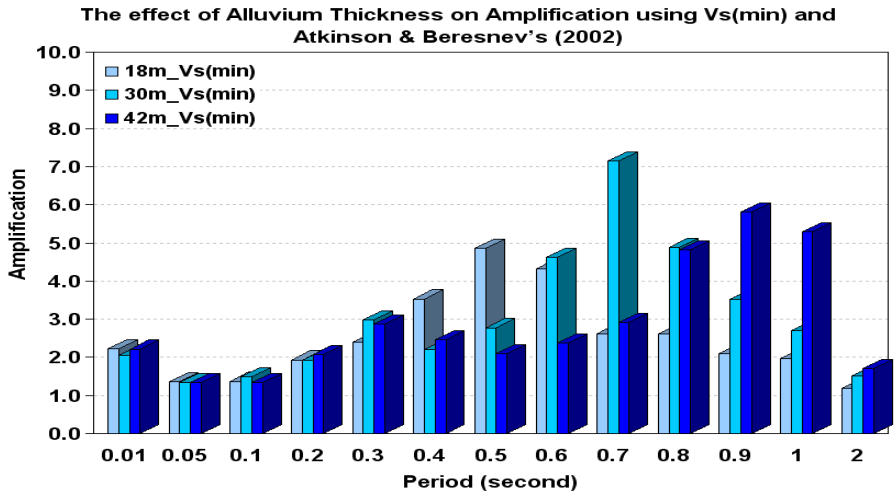
The effect of Alluvium Thickness on Amplification using Vs(min) and Atkinson & Beresnev's (2002)
18m_Vs(min)
30m_Vs(min)
42m_Vs(min)
Amplification
10.0
9.0
8.0
7.0
6.0
5.0
4.0
3.0
2.0
1.0
0.0
0.01 0.05 0.1 0.2 0.3 0.4 0.5 0.6 0.7 0.8 0.9 1 2
Period (second)

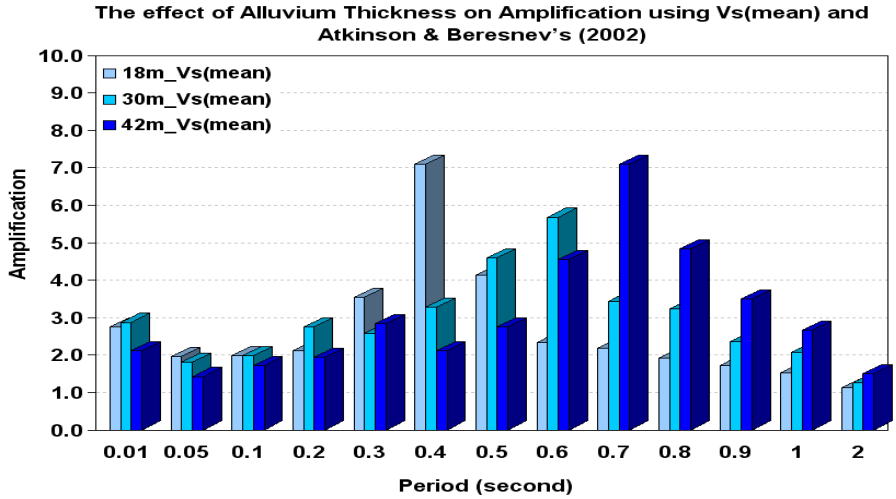
The effect of Alluvium Thickness on Amplification using Vs(mean) and Atkinson & Beresnev's (2002)
18m_Vs(mean)
30m_Vs(mean)
42m_Vs(mean)
Amplification
10.0
9.0
8.0
7.0
6.0
5.0
4.0
3.0
2.0
1.0
0.0
0.01 0.05 0.1 0.2 0.3 0.4 0.5 0.6 0.7 0.8 0.9 1 2
Period (second)

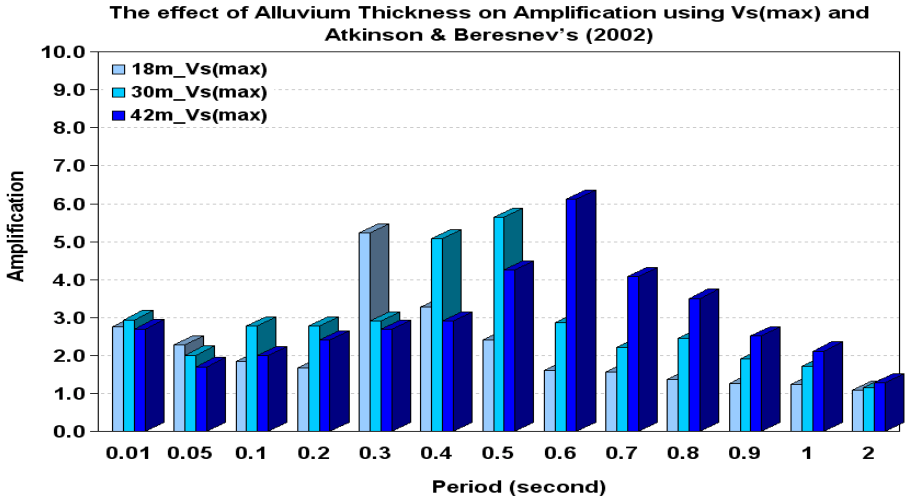
The effect of Alluvium Thickness on Amplification using Vs(max) and Atkinson & Beresnev's (2002)
18m_Vs(max)
30m_Vs(max)
42m_Vs(max)
Amplification
10.0
9.0
8.0
7.0
6.0
5.0
4.0
3.0
2.0
1.0
0.0
0.01 0.05 0.1 0.2 0.3 0.4 0.5 0.6 0.7 0.8 0.9 1 2
Period (second)

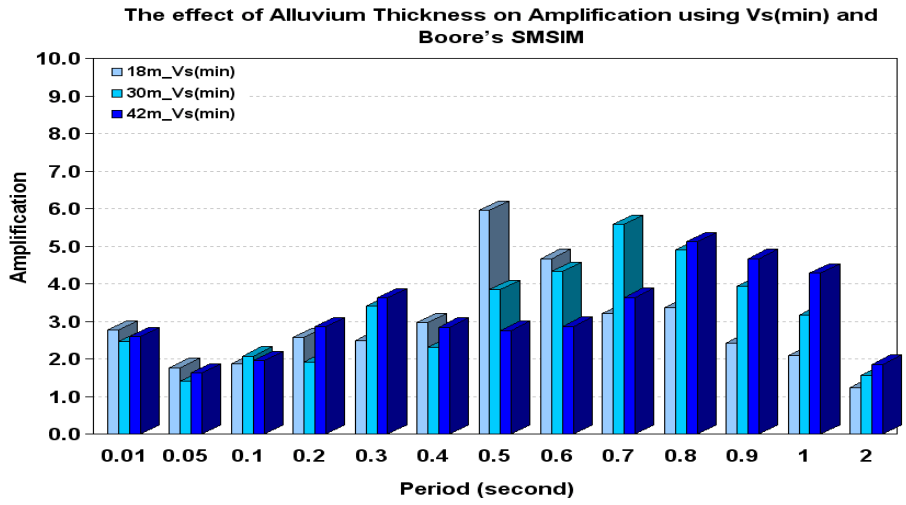
The effect of Alluvium Thickness on Amplification using Vs(min) and Boore's SMSIM
18m_Vs(min)
30m_Vs(min)
42m_Vs(min)
Amplification
10.0
9.0
8.0
7.0
6.0
5.0
4.0
3.0
2.0
1.0
0.0
0.01 0.05 0.1 0.2 0.3 0.4 0.5 0.6 0.7 0.8 0.9 1 2
Period (second)

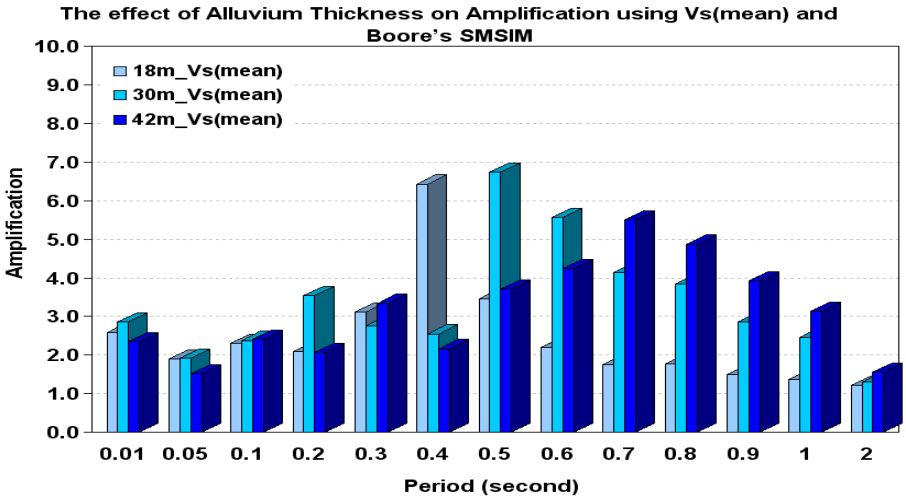
The effect of Alluvium Thickness on Amplification using Vs(mean) and Boore's SMSIM
18m_Vs(mean)
30m_Vs(mean)
42m_Vs(mean)
Amplification
10.0
9.0
8.0
7.0
6.0
5.0
4.0
3.0
2.0
1.0
0.0
0.01 0.05 0.1 0.2 0.3 0.4 0.5 0.6 0.7 0.8 0.9 1 2
Period (second)

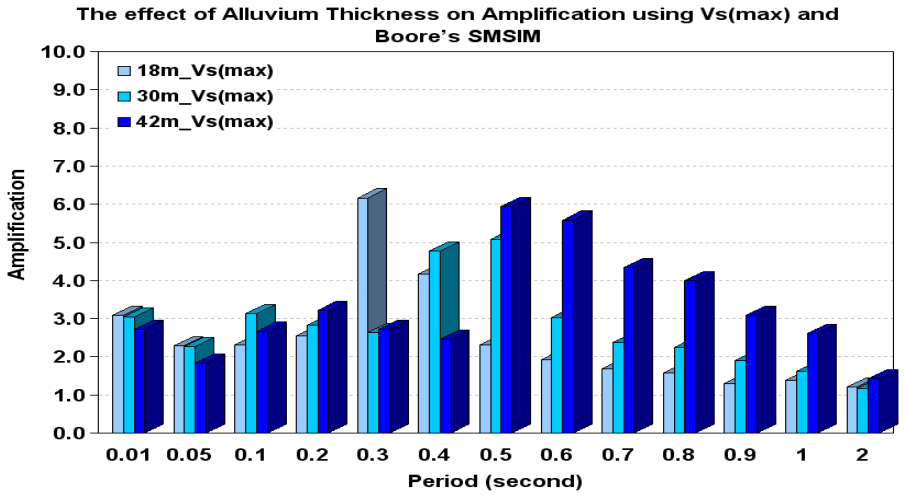
The effect of Alluvium Thickness on Amplification using Vs(max) and Boore's SMSIM
18m_Vs(max)
30m_Vs(max)
42m_Vs(max)
Amplification
10.0
9.0
8.0
7.0
6.0
5.0
4.0
3.0
2.0
1.0
0.0
0.01 0.05 0.1 0.2 0.3 0.4 0.5 0.6 0.7 0.8 0.9 1 2
Period (second)

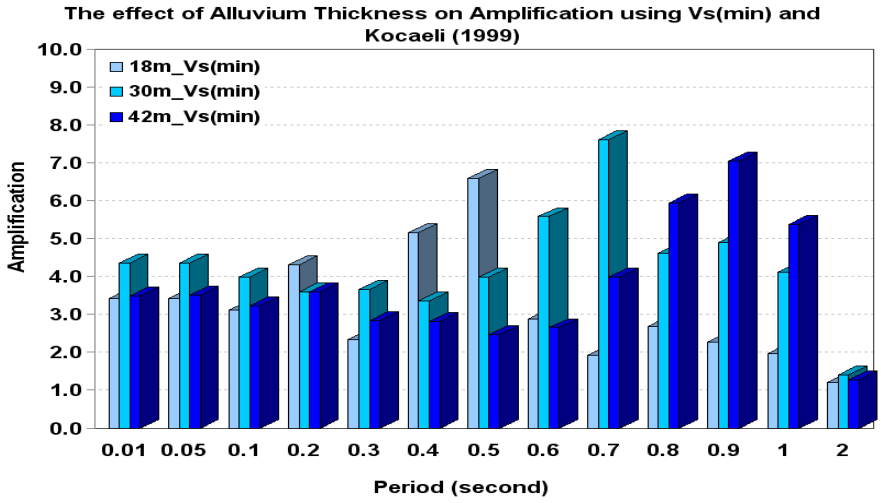
The effect of Alluvium Thickness on Amplification using Vs(min) and Kocaeli (1999)
18m_Vs(min)
30m_Vs(min)
42m_Vs(min)
Amplification
10.0
9.0
8.0
7.0
6.0
5.0
4.0
3.0
2.0
1.0
0.0
0.01 0.05 0.1 0.2 0.3 0.4 0.5 0.6 0.7 0.8 0.9 1 2
Period (second)

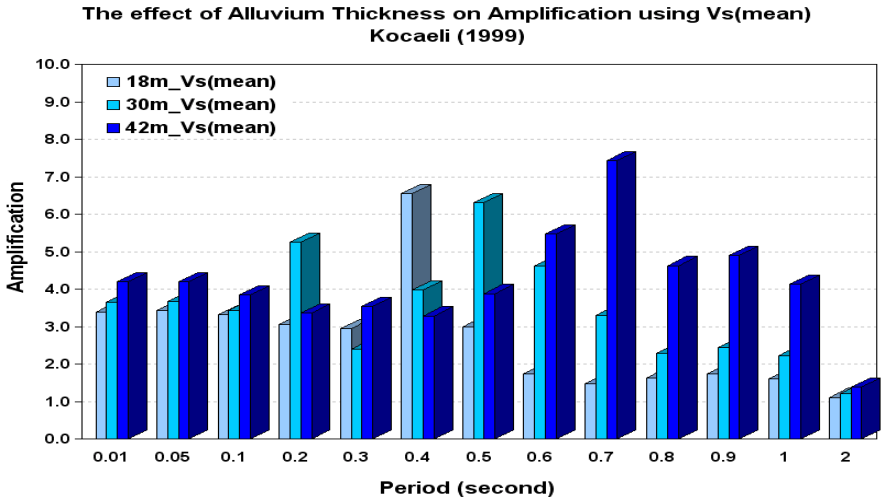
The effect of Alluvium Thickness on Amplification using Vs(mean) Kocaeli (1999)
18m_Vs(mean)
30m_Vs(mean)
42m_Vs(mean)
Amplification
10.0
9.0
8.0
7.0
6.0
5.0
4.0
3.0
2.0
1.0
0.0
0.01 0.05 0.1 0.2 0.3 0.4 0.5 0.6 0.7 0.8 0.9 1 2
Period (second)

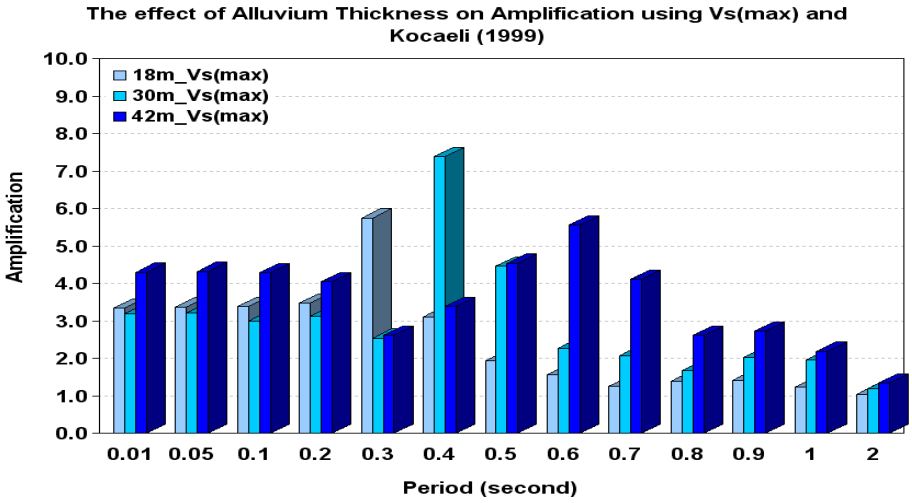
The effect of Alluvium Thickness on Amplification using Vs(max) and Kocaeli (1999)
18m_Vs(max)
30m_Vs(max)
42m_Vs(max)
Amplification
10.0
9.0
8.0
7.0
6.0
5.0
4.0
3.0
2.0
1.0
0.0
0.01 0.05 0.1 0.2 0.3 0.4 0.5 0.6 0.7 0.8 0.9 1 2
Period (second)

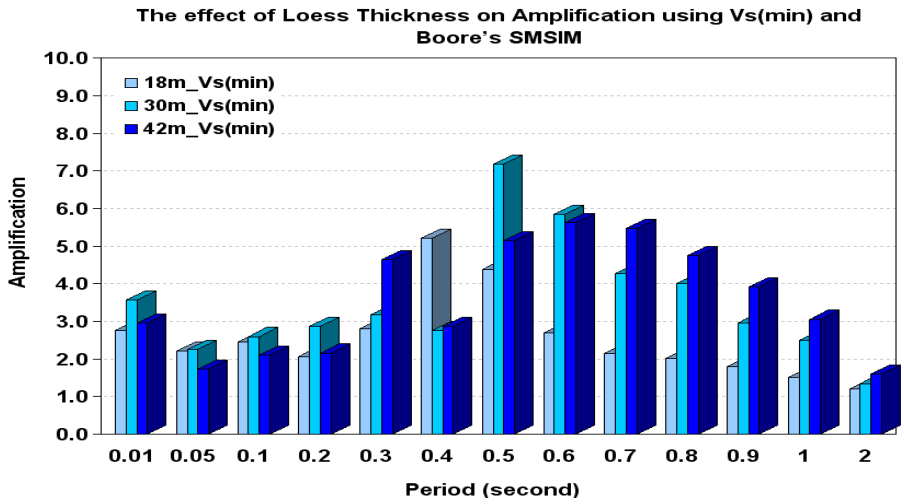
The effect of Loess Thickness on Amplification using Vs(min) and Boore's SMSIM
18m_Vs(min)
30m_Vs(min)
42m_Vs(min)
Amplification
10.0
9.0
8.0
7.0
6.0
5.0
4.0
3.0
2.0
1.0
0.0
0.01 0.05 0.1 0.2 0.3 0.4 0.5 0.6 0.7 0.8 0.9 1 2
Period (second)

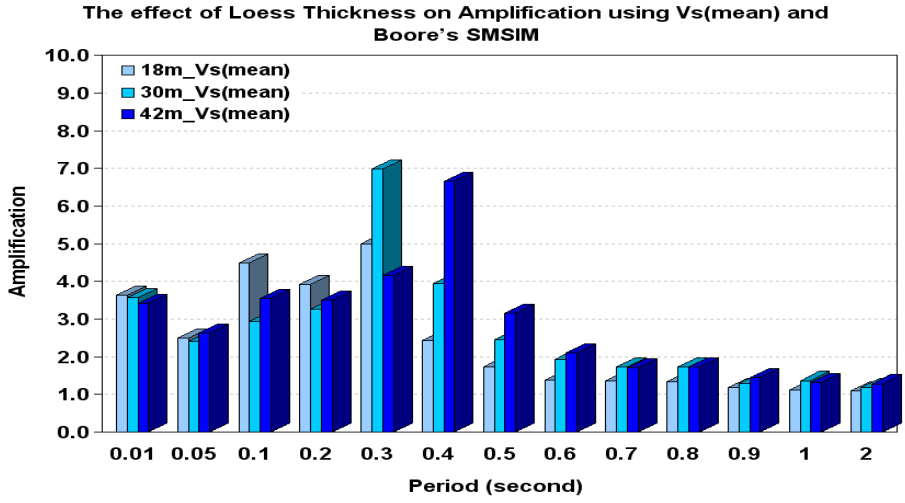
The effect of Loess Thickness on Amplification using Vs(mean) and Boore's SMSIM
18m_Vs(mean)
30m_Vs(mean)
42m_Vs(mean)
Amplification
10.0
9.0
8.0
7.0
6.0
5.0
4.0
3.0
2.0
1.0
0.0
0.01 0.05 0.1 0.2 0.3 0.4 0.5 0.6 0.7 0.8 0.9 1 2
Period (second)

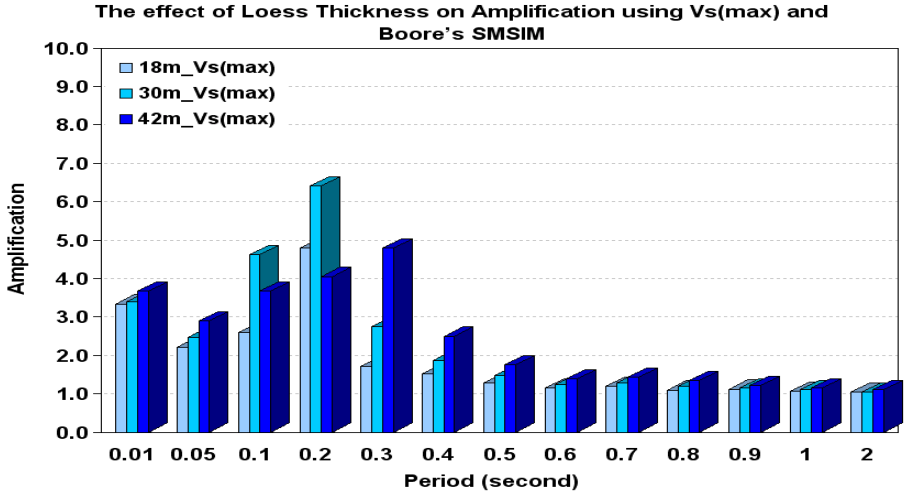
The effect of Loess Thickness on Amplification using Vs(max) and Boore's SMSIM
18m_Vs(max)
30m_Vs(max)
42m_Vs(max)
Amplification
10.0
9.0
8.0
7.0
6.0
5.0
4.0
3.0
2.0
1.0
0.0
0.01 0.05 0.1 0.2 0.3 0.4 0.5 0.6 0.7 0.8 0.9 1 2
Period (second)

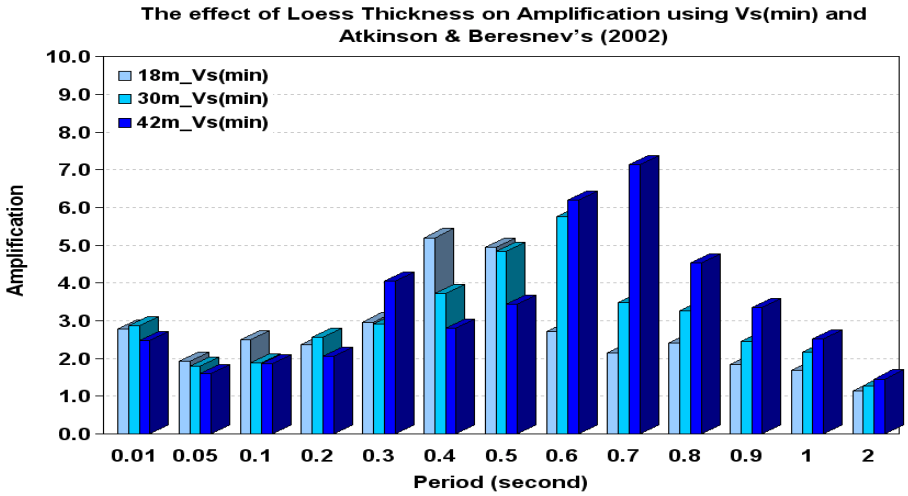
The effect of Loess Thickness on Amplification using Vs(min) and Atkinson & Beresnev's (2002)
18m_Vs(min)
30m_Vs(min)
42m_Vs(min)
Amplification
10.0
9.0
8.0
7.0
6.0
5.0
4.0
3.0
2.0
1.0
0.0
0.01 0.05 0.1 0.2 0.3 0.4 0.5 0.6 0.7 0.8 0.9 1 2
Period (second)

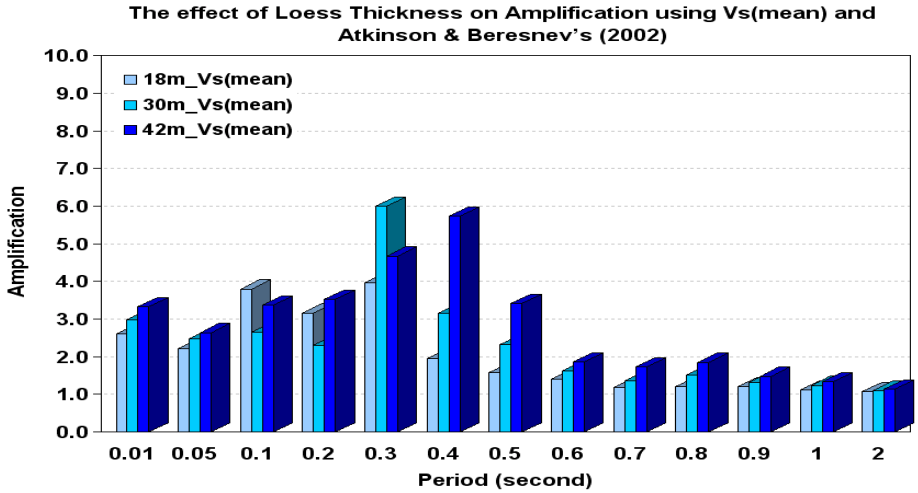
The effect of Loess Thickness on Amplification using Vs(mean) and Atkinson & Beresnev's (2002)
18m_Vs(mean)
30m_Vs(mean)
42m_Vs(mean)
Amplification
10.0
9.0
8.0
7.0
6.0
5.0
4.0
3.0
2.0
1.0
0.0
0.01 0.05 0.1 0.2 0.3 0.4 0.5 0.6 0.7 0.8 0.9 1 2
Period (second)

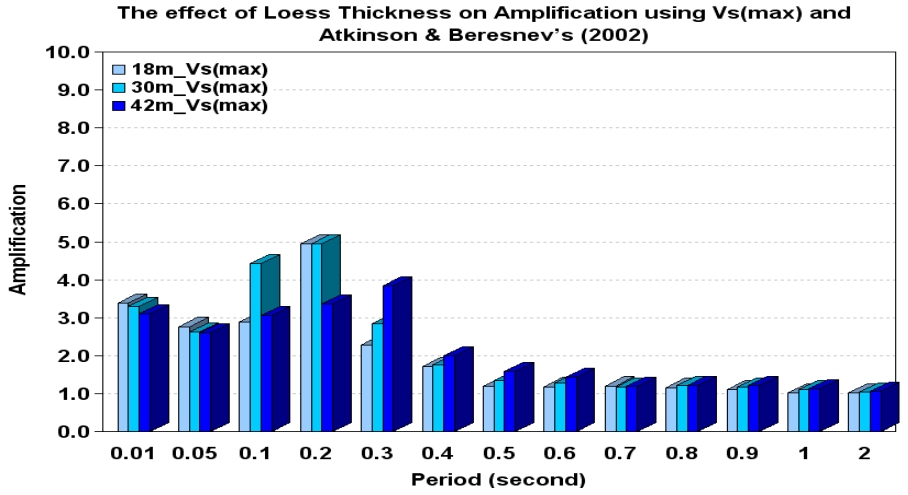
The effect of Loess Thickness on Amplification using Vs(max) and Atkinson & Beresnev's (2002)
18m_Vs(max)
30m_Vs(max)
42m_Vs(max)
Amplification
10.0
9.0
8.0
7.0
6.0
5.0
4.0
3.0
2.0
1.0
0.0
0.01 0.05 0.1 0.2 0.3 0.4 0.5 0.6 0.7 0.8 0.9 1 2
Period (second)

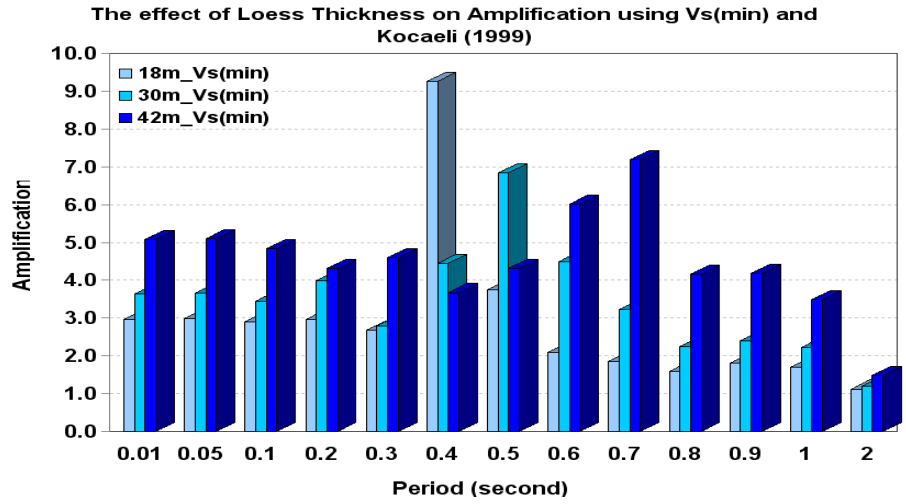
The effect of Loess Thickness on Amplification using Vs(min) and Kocaeli (1999)
18m_Vs(min)
30m_Vs(min)
42m_Vs(min)
Amplification
10.0
9.0
8.0
7.0
6.0
5.0
4.0
3.0
2.0
1.0
0.0
0.01 0.05 0.1 0.2 0.3 0.4 0.5 0.6 0.7 0.8 0.9 1 2
Period (second)

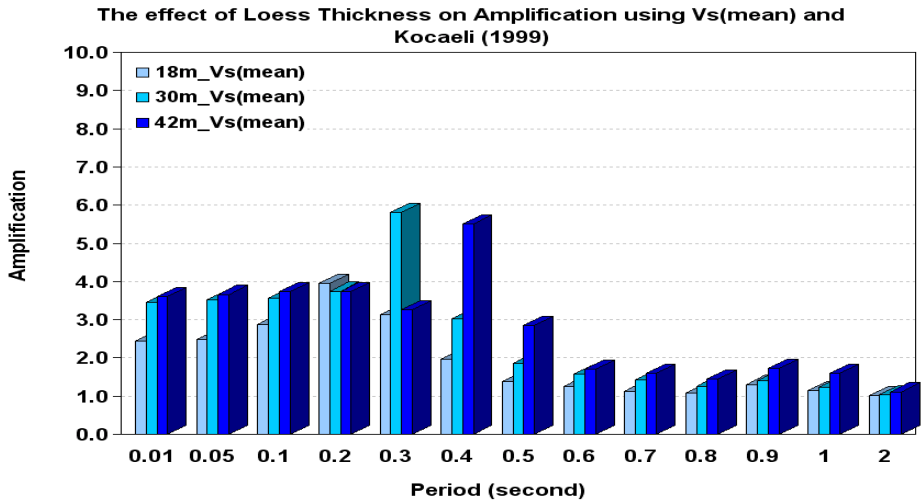
The effect of Loess Thickness on Amplification using Vs(mean) and Kocaeli (1999)
18m_Vs(mean)
30m_Vs(mean)
42m_Vs(mean)
Amplification
10.0
9.0
8.0
7.0
6.0
5.0
4.0
3.0
2.0
1.0
0.0
0.01 0.05 0.1 0.2 0.3 0.4 0.5 0.6 0.7 0.8 0.9 1 2
Period (second)

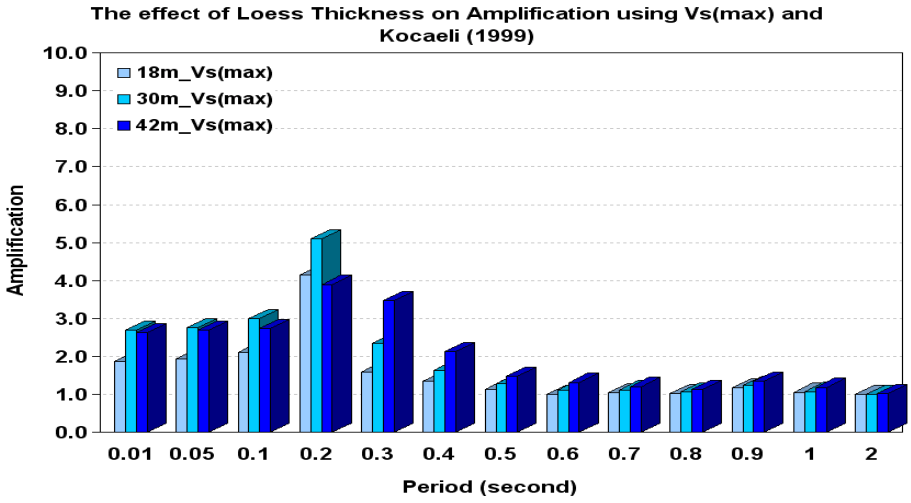
The effect of Loess Thickness on Amplification using Vs(max) and Kocaeli (1999)
18m_Vs(max)
30m_Vs(max)
42m_Vs(max)
Amplification
10.0
9.0
8.0
7.0
6.0
5.0
4.0
3.0
2.0
1.0
0.0
0.01 0.05 0.1 0.2 0.3 0.4 0.5 0.6 0.7 0.8 0.9 1 2
Period (second)

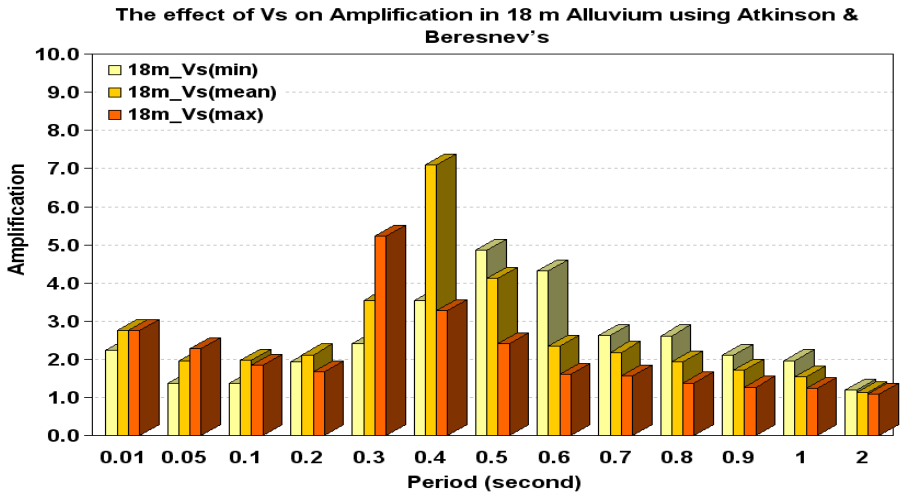
The effect of Vs on Amplification in 18 m Alluvium using Atkinson & Beresnev's
18m_Vs(min)
18m_Vs(mean)
18m_Vs(max)
Amplification
10.0
9.0
8.0
7.0
6.0
5.0
4.0
3.0
2.0
1.0
0.0
0.01 0.05 0.1 0.2 0.3 0.4 0.5 0.6 0.7 0.8 0.9 1 2
Period (second)

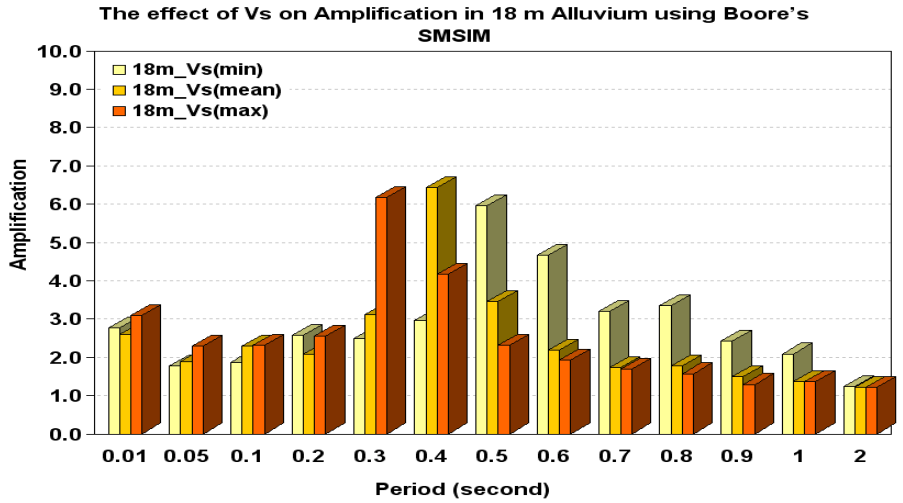
The effect of Vs on Amplification in 18 m Alluvium using Boore's SMSIM
18m_Vs(min)
18m_Vs(mean)
18m_Vs(max)
Amplification
10.0
9.0
8.0
7.0
6.0
5.0
4.0
3.0
2.0
1.0
0.0
0.01 0.05 0.1 0.2 0.3 0.4 0.5 0.6 0.7 0.8 0.9 1 2
Period (second)

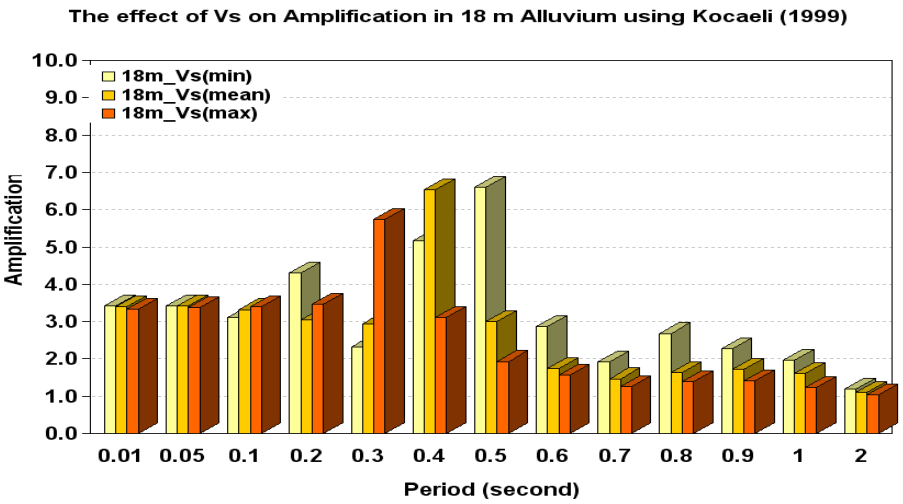
The effect of Vs on Amplification in 18 m Alluvium using Kocaeli (1999)
18m_Vs(min)
18m_Vs(mean)
18m_Vs(max)
Amplification
10.0
9.0
8.0
7.0
6.0
5.0
4.0
3.0
2.0
1.0
0.0
0.01 0.05 0.1 0.2 0.3 0.4 0.5 0.6 0.7 0.8 0.9 1 2
Period (second)

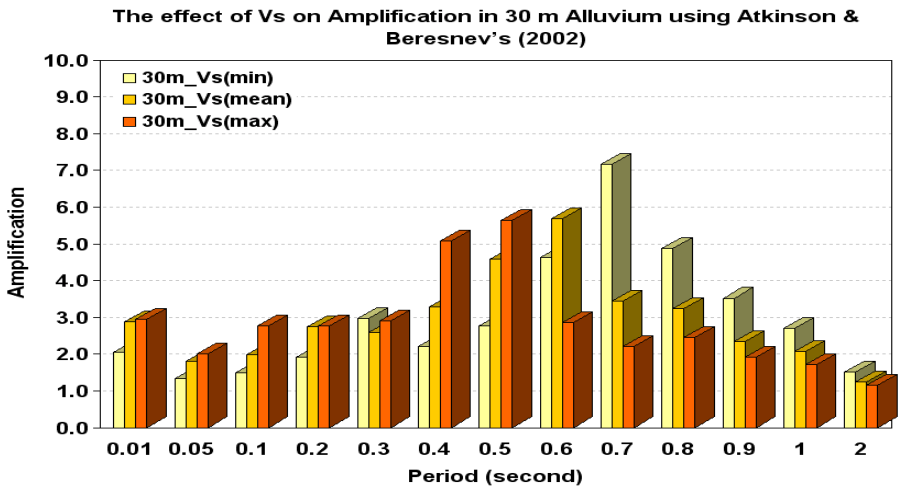
The effect of Vs on Amplification in 30 m Alluvium using Atkinson & Beresnev's (2002)
30m_Vs(min)
30m_Vs(mean)
30m_Vs(max)
Amplification
10.0
9.0
8.0
7.0
6.0
5.0
4.0
3.0
2.0
1.0
0.0
0.01 0.05 0.1 0.2 0.3 0.4 0.5 0.6 0.7 0.8 0.9 1 2
Period (second)

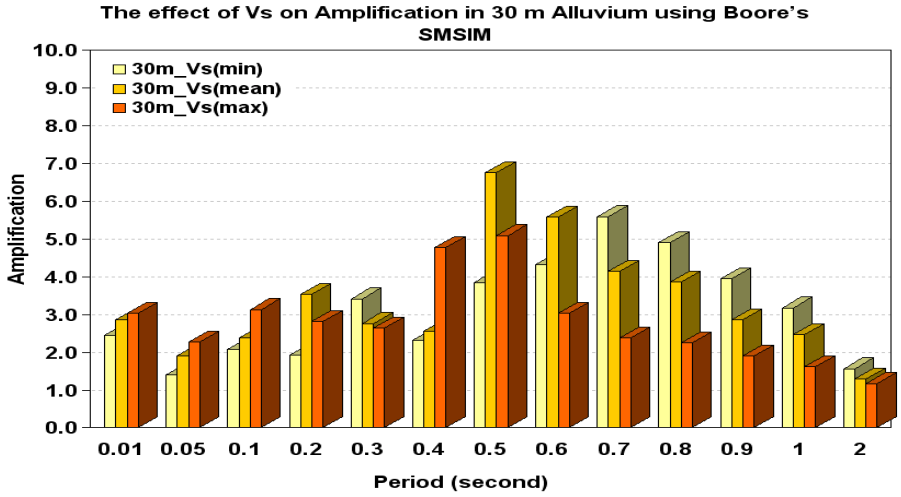
The effect of Vs on Amplification in 30 m Alluvium using Boore's SMSIM
30m_Vs(min)
30m_Vs(mean)
30m_Vs(max)
Amplification
10.0
9.0
8.0
7.0
6.0
5.0
4.0
3.0
2.0
1.0
0.0
0.01 0.05 0.1 0.2 0.3 0.4 0.5 0.6 0.7 0.8 0.9 1 2
Period (second)

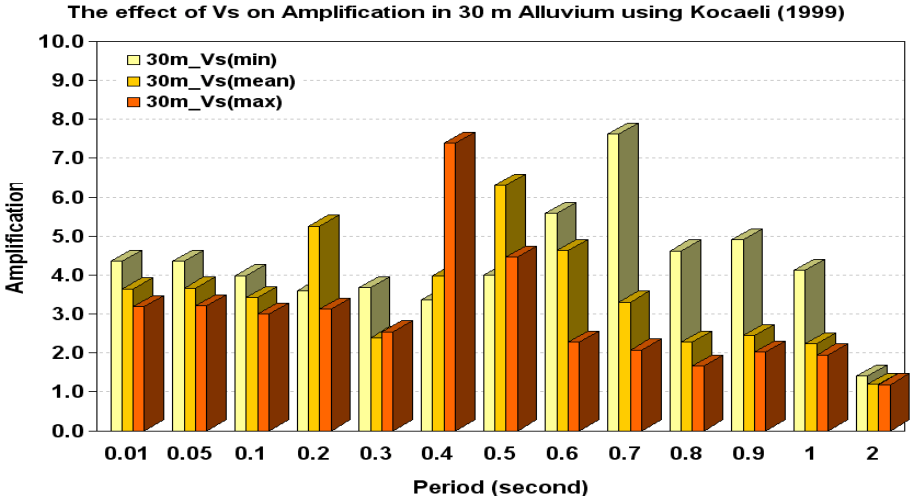
The effect of Vs on Amplification in 30 m Alluvium using Kocaeli (1999)
30m_Vs(min)
30m_Vs(mean)
30m_Vs(max)
Amplification
10.0
9.0
8.0
7.0
6.0
5.0
4.0
3.0
2.0
1.0
0.0
0.01 0.05 0.1 0.2 0.3 0.4 0.5 0.6 0.7 0.8 0.9 1 2
Period (second)

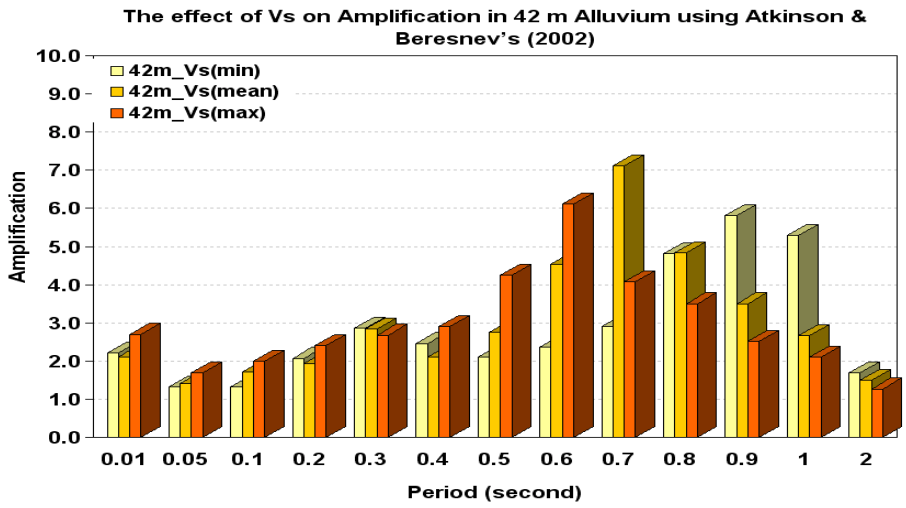
The effect of Vs on Amplification in 42 m Alluvium using Atkinson & Beresnev's (2002)
42m_Vs(min)
42m_Vs(mean)
42m_Vs(max)
Amplification
10.0
9.0
8.0
7.0
6.0
5.0
4.0
3.0
2.0
1.0
0.0
0.01 0.05 0.1 0.2 0.3 0.4 0.5 0.6 0.7 0.8 0.9 1 2
Period (second)

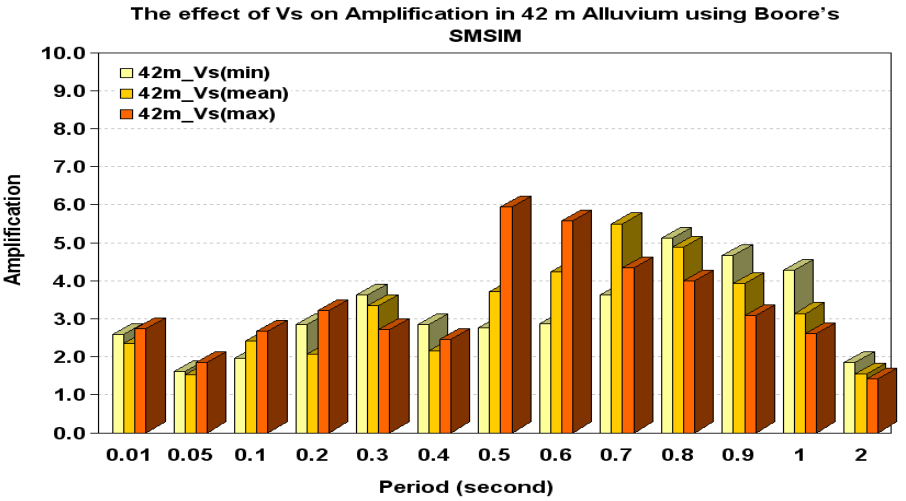
The effect of Vs on Amplification in 42 m Alluvium using Boore's SMSIM
42m_Vs(min)
42m_Vs(mean)
42m_Vs(max)
Amplification
10.0
9.0
8.0
7.0
6.0
5.0
4.0
3.0
2.0
1.0
0.0
0.01 0.05 0.1 0.2 0.3 0.4 0.5 0.6 0.7 0.8 0.9 1 2
Period (second)

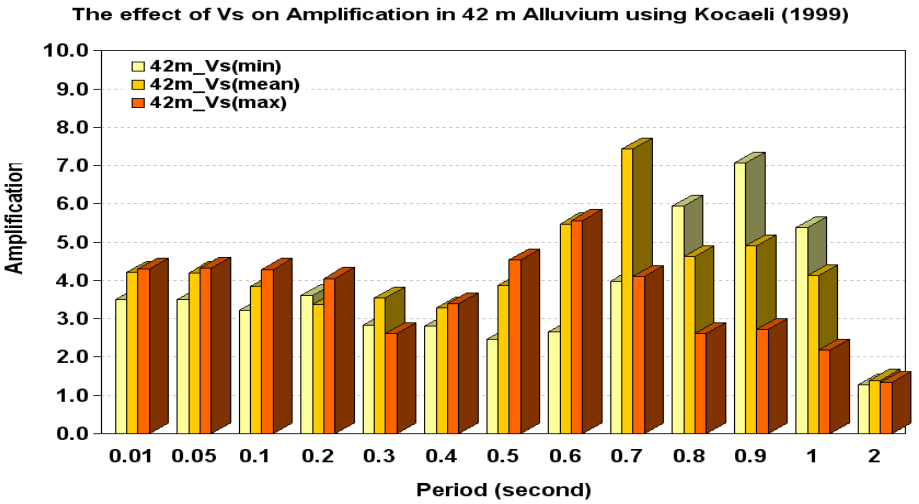
The effect of Vs on Amplification in 42 m Alluvium using Kocaeli (1999)
42m_Vs(min)
42m_Vs(mean)
42m_Vs(max)
Amplification
10.0
9.0
8.0
7.0
6.0
5.0
4.0
3.0
2.0
1.0
0.0
0.01 0.05 0.1 0.2 0.3 0.4 0.5 0.6 0.7 0.8 0.9 1 2
Period (second)

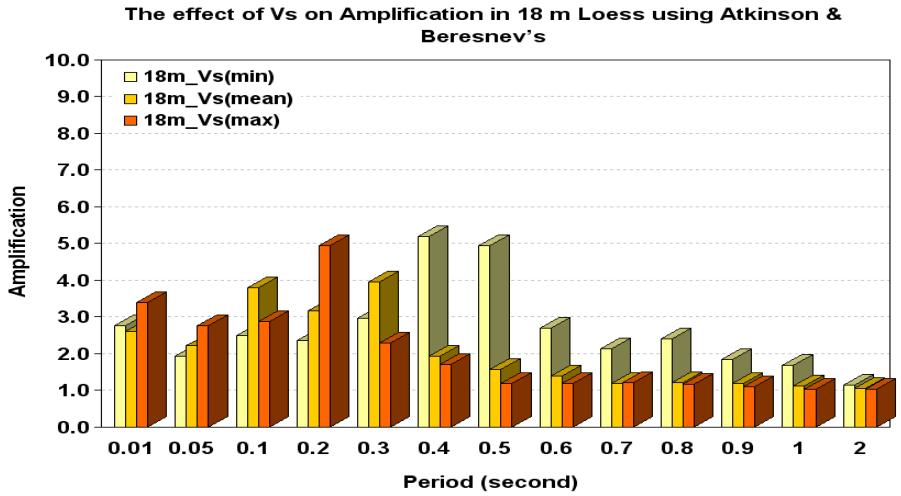
The effect of Vs on Amplification in 18 m Loess using Atkinson & Beresnev's
18m_Vs(min)
18m_Vs(mean)
18m_Vs(max)
Amplification
10.0
9.0
8.0
7.0
6.0
5.0
4.0
3.0
2.0
1.0
0.0
0.01 0.05 0.1 0.2 0.3 0.4 0.5 0.6 0.7 0.8 0.9 1 2
Period (second)

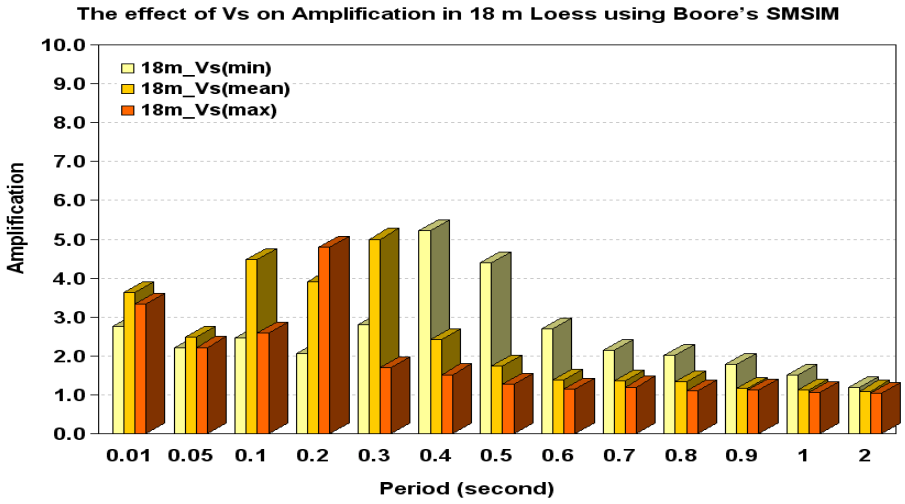
The effect of Vs on Amplification in 18 m Loess using Boore's SMSIM
18m_Vs(min)
18m_Vs(mean)
18m_Vs(max)
Amplification
10.0
9.0
8.0
7.0
6.0
5.0
4.0
3.0
2.0
1.0
0.0
0.01 0.05 0.1 0.2 0.3 0.4 0.5 0.6 0.7 0.8 0.9 1 2
Period (second)

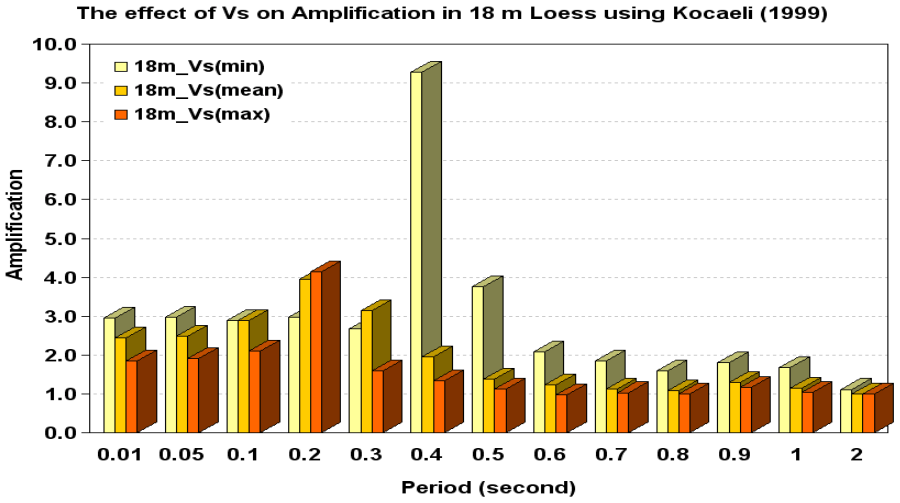
The effect of Vs on Amplification in 18 m Loess using Kocaeli (1999)
18m_Vs(min)
18m_Vs(mean)
18m_Vs(max)
Amplification
10.0
9.0
8.0
7.0
6.0
5.0
4.0
3.0
2.0
1.0
0.0
0.01 0.05 0.1 0.2 0.3 0.4 0.5 0.6 0.7 0.8 0.9 1 2
Period (second)

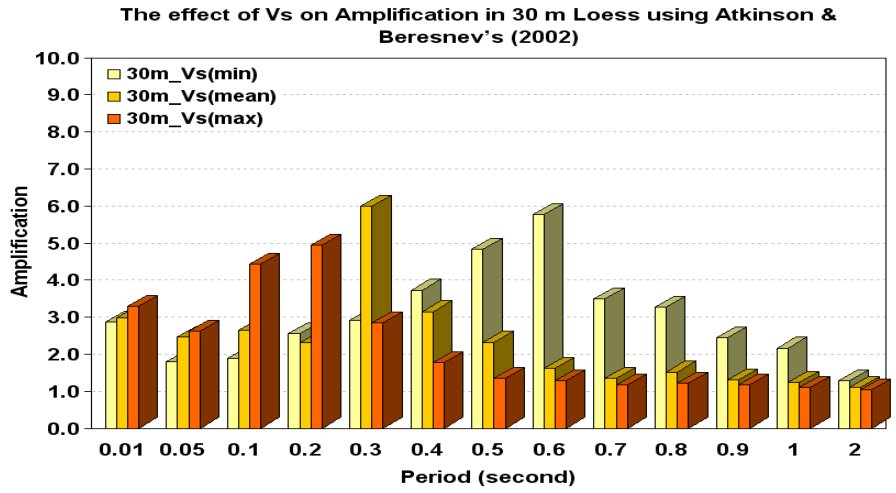
The effect of Vs on Amplification in 30 m Loess using Atkinson & Beresnev's (2002)
30m_Vs(min)
30m_Vs(mean)
30m_Vs(max)
Amplification
10.0
9.0
8.0
7.0
6.0
5.0
4.0
3.0
2.0
1.0
0.0
0.01 0.05 0.1 0.2 0.3 0.4 0.5 0.6 0.7 0.8 0.9 1 2
Period (second)

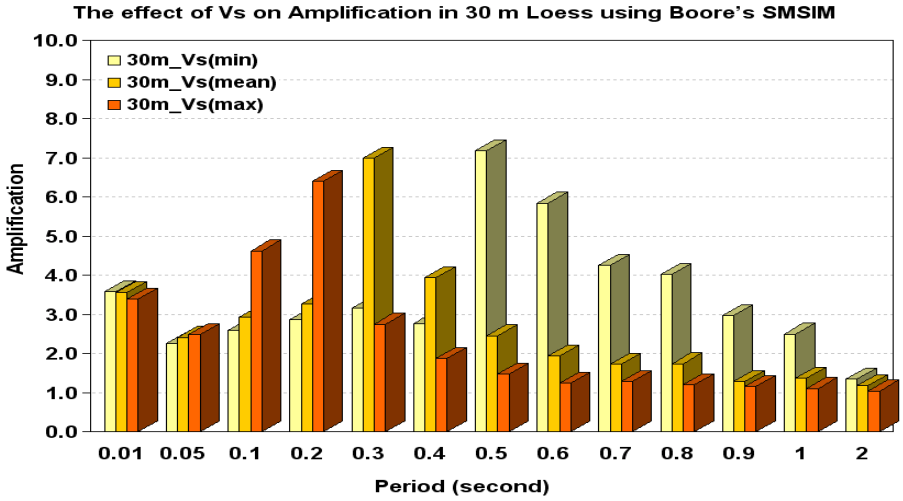
The effect of Vs on Amplification in 30 m Loess using Boore's SMSIM
30m_Vs(min)
30m_Vs(mean)
30m_Vs(max)
Amplification
10.0
9.0
8.0
7.0
6.0
5.0
4.0
3.0
2.0
1.0
0.0
0.01 0.05 0.1 0.2 0.3 0.4 0.5 0.6 0.7 0.8 0.9 1 2
Period (second)

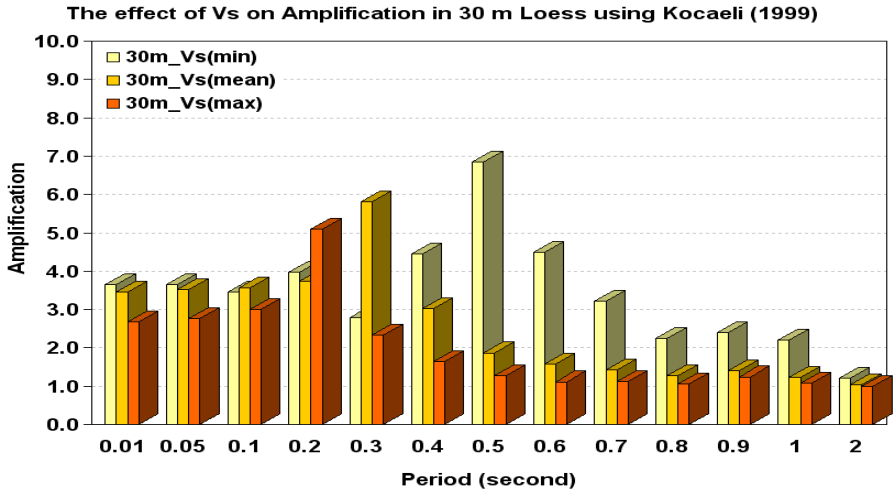
The effect of Vs on Amplification in 30 m Loess using Kocaeli (1999)
30m_Vs(min)
30m_Vs(mean)
30m_Vs(max)
Amplification
10.0
9.0
8.0
7.0
6.0
5.0
4.0
3.0
2.0
1.0
0.0
0.01 0.05 0.1 0.2 0.3 0.4 0.5 0.6 0.7 0.8 0.9 1 2
Period (second)

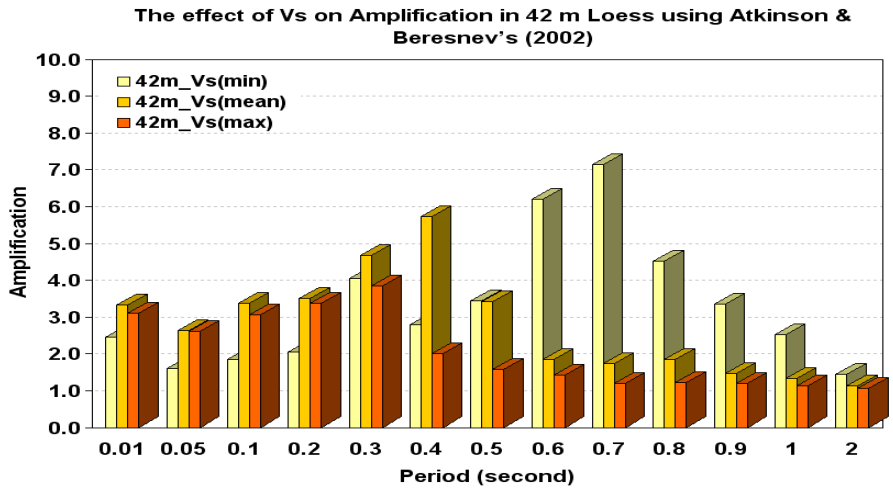
The effect of Vs on Amplification in 42 m Loess using Atkinson & Beresnev's (2002)
42m_Vs(min)
42m_Vs(mean)
42m_Vs(max)
Amplification
10.0
9.0
8.0
7.0
6.0
5.0
4.0
3.0
2.0
1.0
0.0
0.01 0.05 0.1 0.2 0.3 0.4 0.5 0.6 0.7 0.8 0.9 1 2
Period (second)

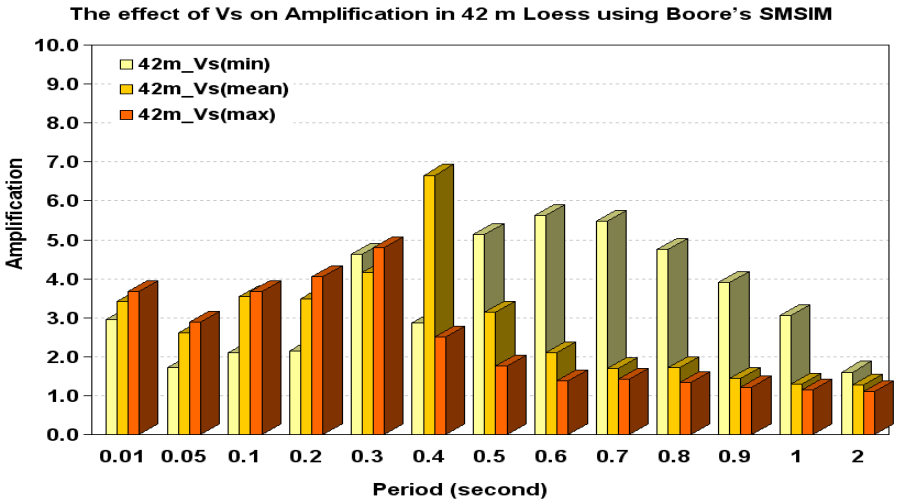
The effect of Vs on Amplification in 42 m Loess using Boore's SMSIM
42m_Vs(min)
42m_Vs(mean)
42m_Vs(max)
Amplification
10.0
9.0
8.0
7.0
6.0
5.0
4.0
3.0
2.0
1.0
0.0
0.01 0.05 0.1 0.2 0.3 0.4 0.5 0.6 0.7 0.8 0.9 1 2
Period (second)

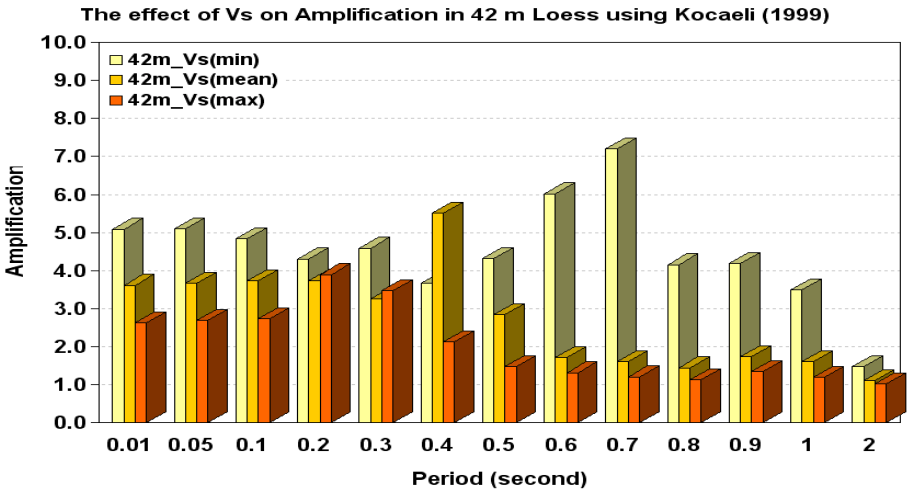
The effect of Vs on Amplification in 42 m Loess using Kocaeli (1999)
42m_Vs(min)
42m_Vs(mean)
42m_Vs(max)
Amplification
10.0
9.0
8.0
7.0
6.0
5.0
4.0
3.0
2.0
1.0
0.0
0.01 0.05 0.1 0.2 0.3 0.4 0.5 0.6 0.7 0.8 0.9 1 2
Period (second)

BIBLIOGRAPHY

Adalier, K., and Aydinoglu, O., 2001, Structural Engineering Aspects of the June 27, 1998 Adana-Ceyhan (Turkey) Earthquake, Engineering Structure, Vol. 23, p. 343–35.

Aki, K., 1988, Local site effects on ground motion, Proc. Earthquake Engineering and Soil Dynamics II, Vol. 103, p.155.

Aki, K., 1993, Local Site Effects on Weak and Strong Ground Motion, Tectonophysics, Vol. 218, p. 93-111.

Alvarez, D., 2008, Understanding the New Seismic Requirements for Ceilings, http://www.seismicceilings.com

Anderson, J. G., Lee, Y., Zeng, Y., and Day, S., 1996, Control of Strong Motion by the Upper 30 Meters, Bulletin of the Seismological Society of America, Vol. 86, No. 6., pp. 1749-1759.

Anderson, 2003, Strong motion seismology, International Handbook of Earthquake and Engineering Seismology, Part B, pp. 937-966.

Ansal, A. M., Iyisan, R., and Gullu, H., 2001, Microtremor Measurements for the Microzonation of Dinar, Pure and Applied Geophysics, Vol. 158, p. 2525-2540.

Atkinson, G. M., and Beresnev, I. A., 2002, Ground motions at Memphis and St. Louis from M 7.5–8.0 Earthquakes in the New Madrid Seismic Zone, Bulletin of the Seismological Society of America, Vol. 92, pp. 1015-1024.

Atkinson, G. M., and Boore, D. M., 2006, Earthquake ground-motion prediction equations for Eastern north America, Bulletin of the Seismological Society of America, Vol. 96, no. 6, pp. 2181-2205.

Bachman, R. E.,1995, Case studies of Kobe earthquake damage; industrial, transportation and port facilities, Structural engineers Association of California, Proceedings, 64th annual convention, p. 41-53

Boore, 2003, SMSIM –Fortran programs for simulating ground motions from earthquakes: Version 2.0 –a revision of OFR 96-80-A, United States Department of Interior United States Geological Survey, p. 56.

Bolt, B.A., 1993, Earthquakes, W. H. Freeman, New York, 331 p.

Carson, D., 2005, Earthquake measuring 5.2 rattles St. Louis region, St Louis Today (internet)

Clague, JJ, and Turner, B., 2003, Vancouver city on the edge, Tricouni Presss, 191 p

Cramer, C. H., 2006, An assessment of the impact of the 2003 EPRI ground-motion prediction models on the USGS national seismic hazard maps, Bulletin of Seismological Society of America, Vol. 96, No. 3, p. 1159-1169

Cramer, C., 2008, University of Memphis, Personal communication.

Cranswick, E., Ozel, O., Meremonte, M., Erdik, M., Safak, E., Mueller, C., Overturf, D., and Frankel, A., 2000, Earthquake Damage, Site Response, and Building Response in Avcilar, West of Istanbul, Turkey, International Journal for Housing science and Its Applications, ISSN 0146-6518, Special Issue: Kocaeli Earthquake 1999, Oktay Ural, Editor-In-Chief, Vol. 24, No. 1, 2000, pp. 85-96.

Celebi, M., 2000, Revelations from a Single Strong-motion Record Retrieved during the 27 June 1998 Adana (Turkey) Earthquake, Soil Dynamics and Earthquake Engineering, Vol. 20, Issues 5-8, p. 283-288

Denny, F. B., and Devera, J. A., 2001, Bedrock Geologic Map of Monks Mound Quadrangle, Madison and St. Clair Counties, Illinois, Department of Natural Resources, Illinois State Geological Survey, 1:24,000.

Denny, F. B., 2003, Bedrock Geology of Granite City Quadrangle, Madison and St. Clair Counties, Illinois and St. Louis County, Missouri, Department of Natural Resources, Illinois State Geological Survey, 1:24,000.

Destegul, U., 2004, Sensitivity Analysis of Soil Site Response Modeling in Seismic Microzonation for Lalitpur Nepal, Master thesis, Department of Earth Resources and Environmental Geosciences, International Institute for Goe-Information Science and Earth Observation Enschede, The Netherlands, unpublished.

Dewell, H.D., 1929a, Earthquake Resistant Construction 1-Data of Design, Engineering News Record, Vol.100, No.17, p.650-655.

Dewell, H.D., 1929b, Earthquake Resistant Construction 2-Principles of Design, Engineering News Record, Vol.100, No.18, p.699-702.

Dobry, R., Borcherdt, R. D., Crouse, C. B., Idriss, I. M., Joyner,W. B., Martin, G. R., Power, M. S., Rinne, E. E., and Seed, R. B., 2000, New site coefficients and site

classification system used in recent building code provisions, Earthquake Spectra, Vol. 16, No. 1, 41–68.

Durakal, E., Erdik, M., Avci, J., Yuzugullu, O., Alpay, Y., Avar, B., Zulfikat, C., Bito, T., and Mert, 1998, Analysis of the strong motion data of the 1995 Dinar, Turkey earthquake, Soil dynamics and earthquake engineering, vol. 17, issue 7-8, p. 557-578.

EPRI, 1993, Guidelines for determining design basis ground motions, Earthquake Engineering Research Institude, TR-102293.

Ergin, M., Ozalaybey, S., Aktar, M., and Yalcin, M.N., 2004, Site Amplification at Avcilar, Istanbul, Tectonophysics, Vol. 391, p. 335-346

Finn, W.D.L., 2000, State-of-the-art of geotechnical earthquake engineering practice, Soil Dynamics and Earthquake Engineering, Vol. 20, p. 1-15.

Grimley, D. A., Phillips, A. C., Follmer, L. R., Wang, H., and Nelson, R. S., 2001, Quaternary and environmental geology of the St Louis Metro East Area, Guidebook for Field Trips for the 35th Annual Meeting of the North-Central Section of the Geological Society of America, Editor: David Malone, ISGS Guidebook 33, p. 21-73.

Grimley, D. A., and Lepley, S. W., 2005, Surficial Geology of Wood River Quadrangle, Madison County, Illinois, Illinois State Geological Survey, Illinois Preliminary Geologic Map, IPGM Wood River-SG, 1:24,000.

Grimley, D. A., Phillips, A. C., and Lepley, S. W., 2007, Surficial Geology of Monks Mound Quadrangle, Madison and St. Clair Counties, Illinois, Illinois State Geological Survey, Illinois Preliminary Geologic Map, IPGM Monks Mound-SG, 1:24,000.

Grimley, D. A., and Lepley, S. W., 2005, Surficial Geology of Wood River Quadrangle, Madison County, Illinois, Illinois State Geological Survey, Illinois Preliminary Geologic Map, IPGM Wood River-SG, 1:24,000.

Goodfield, A. G., 1965, Pleistocene and surficial geology of the city of St. Louis and the adjacent St. Louis County, Missouri, University of Illinois at Urbana-Champaign, p.207, unpublished.

Govindaraju L., Ramana, G. V., Hanumantharao, C., and Sitharam, T. G., Site-specific ground response analysis, Current Science Special Section: Geotechnics and Earthquake Hazards, Vol. 87, No. 10, pp. 1354-1362.

Hajic, E.R., Wiant, M.D., and Oliver. J.J., 1995, Distribution and Dating of Prehistoric Earthquake Liquefaction in Southeastern Illinois, Central U. S. Final Technical Report Submitted to the U. S. Geological Survey National Earthquake Hazards Reduction Program. Contract No. 1434-93-G-2359. 33 p.

Harrison, R. W., 1997, Bedrock geologic map of the St. Louis, 30'x 60' Quadrangle, Missouri and Illinois, US Department of the Interior, US Geological Survey, p. 7.

Heck, N.H., and Neumann, F., 1933, Destructive Earthquake Motions Measured for the First Time, Engineering News Record, p. 804-807.

Holzer, T. L., Padovani, A. C., Bennett, M. J., Noce, T. E., and Tinsley, III, J. C., 2005, Mapping NEHRP Vs30 site classes, Earthquake Spectra, Vol. 21, No. 2, p. 353-370.

Hough, S. E., Armbruster, J. G., and Seeber, L., 2000, On the Modified Mercalli intensities and magnitudes of the 1811-1812 New Madrid earthquakes," Journal of Geophysical Research 105 (B10), 23,869-23,864.

Idriss, I. M., 1990, Response of soft soil sites during earthquakes, Proceedings of H. Bolton Seed Memorial Symposium, BiTech Publication, p. 273-290.

International Building Codes (IBC), 2003.

Jennings, P. C., 2003, An introduction to the earthquake response of structures, International Handbook of Earthquake and Engineering Seismology, Part B, pp. 1097-1126.

Johnston, A. C., and Nava, S. J., 1990, Seismic-hazard assessment in the central United States," in Neotectonics in Earthquake Evaluation, Geological Society of America Reviews in Engineering Geology, Section 3, Vol. 8, pp. 47-57.

Kanli, I. A., Tildy, P., Pronay, Z., Pinar, A., and Hermann, L., 2006, V_S30 mapping and soil classification for seismic site effect evaluation in Dinar region, SW Turkey, Geophysical Journal International, Vol. 165, p. 223-235

Karadeniz, D., 2007, Pilot Program to Assess Seismic Hazards of the Granite City, Monks Mound, and Columbia Bottom Quadrangles, St. Louis Metropolitan Area, Missouri and Illinois, Phd dissertation, Department of Geological Science and Engineering, Missouri University of Science and Technology, unpublished.

Kramer, S. L., 1996, Geotechnical Earthquake Engineering, Prentice Hall, p.653.

Kramer, S. L., and Paulsen, S. B., 2004, Practical use of Geotechnical Site Response Models, Proc., Int. Workshop on Uncertainties in Nonlinear Soil Properties and Their Impact on Modeling Dynamic Soil Response, PEER Center Headquarters, Richmond, Calif., p. 8.

Kramer, S. L., and Arduino, P., 2008, Geotechnical Earthquake Engineering Site response, GeoMo Missouri University of Science and Technology, conference notes.

Lutten, E. E., and Rockaway, J. D., 1987, Engineering geology of St. Louis County, Missouri, Engineering Geology Series No. 4., Missouri Department of Natural Resources, Division of Geology and Land Survey, p. 23.

MoDNR ,2008, http://www.dnr.mo.gov/geology/geosrv/geores/techbulletin1.htm

Munson, P. J., Obermeier, S. F., Munson, C. A., and Hajic, E. R., 1997, Liquefaction evidence for Holocene and latest Pleistocene seismicity in the southern halves of Indiana and Illinois: A preliminary overview, Seismological Research Letters, Vol. 63, No. 4, p. 521-536.

Olson, S. M. Green, R. A., Obermeier, S. F., 2005, Revised Magnitude-bound Relation for the Wabash Valley Seismic Zone of the Central United States, Seismological Research Letters, Vol. 76, no. 6, p. 756-771.

Ordonez A. G., 2006, A Computer program for the 1-D Analysis of the Geotechnical Earthquake Engineering Problems, SHAKE 2000 User's Manual.

Petersen, M. D., Frankel, A. D., Harmsen S. C., Mueller, C. S., Haller, K. M., Wheeler, R. W., Wesson R., L., Zeng, Y., Boyd, O. S., Perkins D. M., Luco N., Field, E. H., Wills C. J., and Rukstales K. S., 2008, Documentation for the 2008 Update of the United States National Seismic Hazard Maps: U.S. Geological Survey Open-File Report 2008–1128, 61 p.

Phillips, A. C., Grimley, D. A., and Lepley, S. W., 2001, Surficial Geology Map of Granite City Quadrangle, Madison and St. Clair Counties, Illinois and St. Louis County, Missouri, Illinois State Geological Survey, 1:24,000.

Rathje, E.M., Fadi, F., Russell, S., and Jonathan, D.B., 2004, Emirical Relationships for Frequency Content Parameters of Earthquake Ground Motions, Earthquake Spectra, Vol. 124, No. 2, p. 150-159

Reiter, L., 1990, Earthquake Hazard Analysis, Issues and Insights, Columbia University Press, New York, p. 254.

Rodriguez-Marek, A., Bray, J.D., and Abrahamson, N., 2001, An empirical geotechnical site response procedure, Earthquake Spectra, Earthquake Engineering Research Institute, Vol. 17, No. 1, p. 65-87.

Romero, S., and Rix, G. J., 2005, Ground Motions Amplification of Soils in the Upper Mississippi Embayment, National Science Foundation Mid America Earthquake Center, Report No GIT-CEE/GEO-01-1, p. 461.

Rogers, J. D., and Figuers, S. H., 1991, Engineering Geologic Site Characterization of the Greater Oakland- Alameda Area, Alameda and San Francisco Counties, California, Final Report, National Science Foundation, Grant BCS-9003785.

Rogers, J. D., 2007, Engineering Geology and Geotechnics, Lecture notes.

Rogers, J. D., Karadeniz, D., and Kraig, C., 2007a, Seismic Site Response Modeling for three Missouri River Highway Bridges, Journal of Earthquake Engineering, 11:3, p. 400-424.

Rogers, J. D., Karadeniz, D., and Chung, J. W., 2007b, The Effect of Site Conditions in the a amplification of Ground Motion in the St. Louis Area, 4th International Conference on Earthquake Geotechnical Engineering, Paper No. 1768.

Romo, M. P., and Seed, H. B., 1986, Analytical Modeling of Dynamic Soil Response in the Mexico Earthquake of Sept. 19, 1985, Proceedings of the International Conference, The Mexico Earthquakes-1985 Factors Involved and Lessons Learned, Mexico City, p. 148-162.

Schweig, E., Gomberg, J., and Hendley J.W., 1995, U.S. Geological Survey Fact Sheet-168-95

Seed, H. B., and Idriss, I. M., 1969a, Influence of soil conditions on ground motions during earthquakes, Journal of the Soil Mechanics and Foundations Division, Proceedings of the American Society of Civil Engineers, Proceeding paper 6347, Vol. 95, No. SM1, p. 99-137.

Seed, H. B., and Idriss, I. M., 1969b, Influence of local soil conditions on building damage potential during earthquakes, Earthquake Engineering Research Center, University of California Berkeley, Report No. EERC 69-15.

Seed, H.B., Murarka, R., Lysmer, J., and Idriss, I.M., 1976, Relationships of the maximum acceleration, maximum velocity, distance from source and local site conditions for moderately stronge earthquakes, Bulletin of the Seismological Society of America, Vol. 66, No.4, p.1323-1342.

Seed, H. B., and Idriss, I. M., 1982, Ground motions and Soil Liquefaction during earthquakes, Earthquake Engineering Research Institute, p.134

Seed, H.B., Romo, M.P., Sun, J.i., Jaime, A., and Lysmer, J., 1988, The Mexico Earthquake of September 19, 1985—Relationships Between Soil Conditions and Earthquake Ground Motions, Earthquake Spectra, Vol. 4, p. 681-729.

Stover, C. W., and Coffman J. L., 1993, Seismicity of the United States, 1568–1989 (Revised), U. S. Geological Survey Professional Paper 1527, p. 418.

Tezcan, S. S., Kaya, E., Bal, I. E., and Ozdemir, Z., 2002, Seismic amplification at Avcilar, Istanbul, Engineering Structures, Vol. 24, pp. 661-667.

USGS, 2007, St Louis Area Earthquake Hazards Mapping Project, U.S. Geological Survey Fact Sheet, FS-3073-508.

USACE, 1999, Response Spectra and Seismic Analysis for Concrete Hydraulic Structures, Engineer Manual 1110-2-6050, Washington DC, p. 248.

Wenk, T., Lavace, C., and Peter, K., 1998, the Adana-Ceyhan Earthquake of June 27, 1998, Reconnaissance Report of the Swiss Society for Earthquake Engineering and Structural Dynamics, Zurich, Switzerland

Wheeler, R. L., Eleanor, M. O., Dart, R. L., Wilkerson G. D., Bradford R. H., 2003, Earthquakes in the Central United States 1699-2002, USGS Open-File Report 03-232.

Willman, H. B., and Frye, J. C., 1970, Pleistocene stratigraphy of Illinois, Illinois State Geological Survey Bulletin, Vol. 94, p. 204.

Yalcinkaya, E., and Alptekin, O., 2005, Site Effect and its Relationship to the Intensity and Damage Observed in the June 27, 1998 Adana-Ceyhan Earthquake, Pure and Applied Geophysics, Vol. 162, p. 913-930.

VITA

Ece Karadeniz was born on December 3, 1979, in Izmir, Turkey. She received her Bachelor's degree in Geological Engineering from Dokuz Eylul University, Izmir, Turkey in May 2001. She continued her education in University of Texas at Arlington in ELI program and received LAC Master Student Runner-up Scholarship and Hardest Working Student Awards for Fall 2002. She received her M.S. degree in Geological Engineering from Missouri University of Science and Technology, Missouri, USA in December 2008. During the course of her study she worked as a Graduate Research Assistant & Graduate Teaching Assistant and she taught Geology for Engineers. She is a member of Association of Engineering and Environmental Geologists.